Memoria de tesis doctoral presentada para optar al título de Doctor por la Universidad de Cantabria en el Programa de Doctorado en Ingeniería Química y de Procesos

UNIVERSIDAD DE CANTABRIA

Escuela Técnica Superior de Ingenieros Industriales y de Telecomunicación

Departamento de Ingenierías Química y Biomolecular

PROGRESS IN THE REACTIVITY OF ADVANCED OXIDATION MEDIA. APPLICATION TO THE FENTON TREATMENT OF 2-CHLOROPHENOL SOLUTIONS

AVANCES EN LA DETERMINACIÓN DE LA REACTIVIDAD DE MEDIOS DE OXIDACIÓN AVANZADA. APLICACIÓN A LA OXIDACIÓN FENTON DE DISOLUCIONES DE 2-CLOROFENOL

Doctoral advisors:

Prof. Dr. Inmaculada Ortiz Uribe

Dr. Mª Fresnedo San Román San Emeterio

Santander, 2017

Pablo Fernández Castro

Universidad de Cantabria

Escuela Técnica Superior de Ingenieros Industriales y de Telecomunicación

Departamento de Ingenierías Química y Biomolecular

PROGRESS IN THE REACTIVITY OF ADVANCED OXIDATION MEDIA. APPLICATION TO THE FENTON TREATMENT OF 2-CHLOROPHENOL SOLUTIONS

"Avances en la determinación de la reactividad de medios de oxidación avanzada. Aplicación a la oxidación Fenton de disoluciones de 2-clorofenol"

Memoria de tesis doctoral presentada para optar al título de
Doctor por la Universidad de Cantabria. Programa Oficial de Doctorado
en Ingeniería Química y de Procesos.

Pablo Fernández Castro

Directores de tesis:

Prof. Dr. Inmaculada Ortiz Uribe

Dr. Mª Fresnedo San Román San Emeterio

Santander, 2017

Programa Oficial de Doctorado en Ingeniería Química y de Procesos (BOE núm. 36, de 10 de febrero de 2010. RUCT: 5311209) con Mención hacia la Excelencia (BOE núm. 253, de 20 de Octubre de 2011. Referencia: MEE2011-0031)

Este trabajo se ha realizado gracias a la financiación recibida por parte del Ministerio de Economía y Competitividad de España y El Fondo Europeo de Desarrollo Regional (FEDER) a través de los proyectos del plan nacional de I+D+i: CTQ2011-25262, "Evolución de la concentración de PCDD/FS en los tratamientos de oxidación avanzada de lixiviados de vertedero"; y CTM2014-58029-R, "Identificación y cuantificación de las variables responsables de la potencial formación de PCDD/Fs en procesos de oxidación avanzada."

Pablo Fernández Castro ha disfrutado de una beca de Formación de Personal Investigador (F.P.I.) del Ministerio de Economía y Competitividad (MINECO, Ref.: BES-2012-054790) para la realización de esta Tesis Doctoral. Asimismo, el autor del presente trabajo ha disfrutado de una ayuda económica a la movilidad predoctoral del MINECO (Ref.: EEBB-I-16-11256) para la realización de una estancia breve de investigación de 4 meses de duración en el *Fire Safety & Combustion Kinetics Lab* de la Universidad de Murdoch (Perth, Australia) bajo la supervisión del Prof. Dr. Bogdan Dlugogorski y el Dr. Mohammednoor Altarawneh.

¡Gracias!

Agradecimientos

Me gustaría agradecer sinceramente a las directoras de la presente tesis doctoral, la Prof. Dr. Inmaculada Ortiz Uribe y la Dr. María Fresnedo San Román San Emeterio, por darme la oportunidad de iniciar mi carrera investigadora bajo su supervisión y apoyo, que me ha permitido llegar con éxito al final de esta etapa gracias a sus consejos e inestimable ayuda. Sin duda, la realización de esta tesis no hubiera sido posible sin vuestra confianza.

I would like to acknowledge Prof. Bogdan Dlugogorski and Dr. Mohammednoor Altarawneh the chance to work with them and their team at *Fire Safety & Combustion Kinetics Lab* of Murdoch University (Perth, Australia); it was an unforgettable professional and personal experience. I would especially like to thank Kuba for his patience, help and fellowship; you really made it easy to me! Many thanks to Sand and the people of the staff room, I am very happy to have had the opportunity to know worthy people like you.

Agradecer de igual manera el apoyo y amabilidad recibida por parte del profesorado del Departamento de Ingenierías Química y Biomolecular así como el personal técnico y administrativo, y muy especialmente a Gema que siempre ha estado dispuesta a echarme una mano cuando lo he necesitado (¡y con la mejor de las sonrisas!). Extender mi agradecimiento a todos los compañeros con los que he compartido tanto tiempo estos años, muy especialmente a Marta, Sonia y Claudia con quien he tenido la oportunidad de trabajar mano a mano, ¡vosotros le ponéis alma a los laboratorios! Me siento afortunado de haber formado parte de este equipo. Y, por supuesto, estoy encantado de haber compartido esta vivencia con los chicos/as S458, ¡sois geniales!

Especial mención a los que habéis sido mi bastón, ojos y corazón durante esta etapa: Ana, Andrés, Azucena, Carolina, Gabriel, Germán, Esther, Isabel y Sara. Son

muchos momentos y viajes compartidos que siempre llevaré conmigo. Pero sin duda mi mayor agradecimiento y admiración es para Mariana, que más que una compañera ha sido una gran amiga, y más que una amiga una hermana. No todo el mundo puede presumir de llevar 25 años compartiendo tantas experiencias, disfrutando de tu apoyo incondicional y tus consejos. ¡Las palabras se quedan cortas para vosotros!

A mi familia, quienes siempre han apostado y depositado su confianza en mí, inculcándome el buen hacer desde el respeto, comprendiéndome esos días que ni yo podía aguantarme, siempre presentes en las buenas y en las malas. El sólo hecho de estar aquí ya es motivo para agradeceros, pero los años de dedicación y amor son otro motivo enorme para hacerlo.

Por último, no quiero olvidarme de "mi gente de Torre", quienes han sido un apoyo fundamental no sólo durante esta etapa, sino día a día desde hace ya muchos años. Los amigos, al igual que los grandes logros de la vida, se hacen de a pocos, pasito a paso, a fuego lento. Gracias por crear esto conmigo.

¡MUCHAS GRACIAS!

Table of contents

Summary/Resumen **xi**

Chapter 1. Introduction **1**

1.1. Water contamination: a matter of increasing concern 5

1.2. Fenton oxidation 8

1.2.1. Fundamentals and state of the art 8

1.2.2. Challenges in the application of Fenton oxidation processes 13

1.3. Reactivity of oxidizing media 14

1.4. State of the art of the formation and destruction of PCDD/Fs in liquid phase 20

1.4.1. Polychlorinated dibenzo-p-dioxins and dibenzofurans (PCDD/Fs) 20

1.4.2. Oxidation of organic containing PCDD/Fs or their parent compounds by AOPs 30

1.4.3. Background on computational chemistry: application to the mechanisms of PCDD/Fs formation from precursors 34

1.5. Background, thesis scope and outline 38

References 40

Chapter 2. Materials and Methods **53**

2.1. Chemical reagents 57

2.2. Fenton oxidation experiments 59

2.3. Analytical measurements 60

2.3.1. Analysis of hydrogen peroxide 60

2.3.2. Analysis of chemical oxygen demand 61

2.3.3. Analysis of total organic carbon 62

2.3.4. Analysis of inorganic ions and organic acids 63

2.3.5. Analysis of 2-chlorophenol and related aromatic compounds 64

2.3.6. Qualitative screening of organics in the advanced oxidation of 2-CP 65

2.3.7. Analysis of the hydroxyl radical concentration by means of DMSO probe 66

2.3.8. Analysis of radical species by EPR analysis 67

2.3.9. FTIR-ATR 72

2.3.10. Analysis of PCDD/Fs 72

2.3.11. Quality control and quality assurance (QC/QA) in the analysis of PCDD/Fs 77

2.4. Computational calculations 78

2.4.1. Electrophilic halogenation of phenolic compounds in aqueous and gas phase 78

2.4.2. Study of the solvation effect and reaction with H_2O during PCDD/Fs from 2-CP as precursor 79

References 80

Chapter 3. Assessment of PCDD/Fs formation during the Fenton oxidation of 2-chlorophenol **83**

3.1. Characterization of the oxidation medium 87

3.1.1. Assessment of DMSO as molecular probe for the identification of ·OH 87

3.1.2. Evaluation of DMPO as spin-trap for the identification of inorganic and organic radicals 97

3.2. Fenton oxidation of 2-chlorophenol solutions 119

3.2.1. Influence of the presence of chloride ions in the aqueous solution 120

3.2.2. Influence of the iron dose 123

3.2.3. Effect of addition of a copper salt to the oxidation medium 132

3.3. Generation of PCDD/Fs from 2-chlorophenol oxidation 136

3.3.1. Influence of the operation variables 136

3.3.2. Comparative analysis of the influence of operation variables 153

3.4. Contribution to the scientific knowledge and open questions 156

References 158

Chapter 4. Mechanistic study in the oxidation of the PCDD/Fs precursor 2-chlorophenol **169**

4.1. Application of computational chemistry to the study of phenolic 173

4.1.1. Electrophilic chlorination of chlorophenolic family 176

4.1.2. Electrophilic hydroxylation of 2-CP 182

4.2. Mechanistic proposal for the formation of PCDD/Fs from 2-CP based on previous theoretical studies 186

4.2.1. Study of the mechanisms of PCDD/Fs formation from the radical-radical pathway 188

4.2.2. Study of the solvation effect and reaction with H_2O during PCDD/Fs from 2-CP as precursor 199

4.3. Contribution to the scientific knowledge and open questions 205

References 206

Chapter 5. Conclusions and Challenges for future research 213

5.1. Conclusions 217

5.2. Challenges for future research 221

5.3. Conclusiones 223

5.4. Desafíos futuros 227

Annexes 231

Annex I- Nomenclature 233

Annex II- Specific Nomenclature for PCDD/Fs 235

Annex III- General features of the probes employed in the determination of radical ·OH, $O_2^{-\bullet}$/$HO_2^{\bullet}$ and $^1O_2$ 236

Annex IV- PCDD/Fs concentration in labelled and native standards 252

Annex V- Quality control and quality assurance (QC/QA) in the analysis of PCDD/Fs 255

Annex VI- Characterization of the oxidation medium: Assessment of DMSO as molecular probe for the identification of ·OH in the electrochemical oxidation 258

Annex VII- List of scientific contributions 261

References 264

Summary

The concern about water pollution has augmented during the last few years due to the increasing domestic and industrial activities together with growing population. Among the possible compounds found in wastewaters, chlorinated organic compounds include some of the most toxic and largest groups of hazardous chemicals. Chlorophenols (CPs) comprise a group of organic compounds that can be found in the environment as consequence of their widespread and long-term use in industry and daily life. Owing to their high toxicity and low biodegradability, CPs have been listed by the U.S. EPA and by the European Commission as priority pollutants. Furthermore, CPs are known to be precursors of the highly toxic polychlorodibenzo-p-dioxins and polychlorodibenzofurans (PCDD/Fs) that are also considered as priority pollutants. Among the 210 possible congeners of PCDD/Fs, the 17 congeners having the positions 2,3,7,8 chlorinated have received the greatest attention owing to the fact that the human exposure is related with different diseases and cancer, as it has been considered by the U.S. EPA in the case of 2,3,7,8-TCDD that is the most toxic congener.

As a result of their low solubility in water almost all the studies regarding PCDD/Fs formation and degradation are focused on gas phase. However, the wide use of compounds such as CPs in insecticides, biocides, etc. has resulted in the increase in the presence of these pollutants in aqueous streams, whose treatment may result in the generation of PCDD/Fs. Both CPs and PCDD/Fs are characterized by their resistance towards chemical and biological degradation, so more effective technologies are needed. Advanced oxidation processes (AOPs) postulate as viable technologies to treat recalcitrant wastewaters by means of generating reactive oxygen species (ROS). Hydroxyl radical (·OH) is the most powerful ROS, which is non-selective and reacts rapidly with organic/inorganic pollutants. Among different AOPs, Fenton oxidation is proposed as a feasible technology to convert a broad range of contaminants to harmless or biodegradable products, or even to mineralize

them, by using relatively non-expensive reagents which are easy to handle and environmentally safe. Nonetheless, it has been observed that the partial mineralization of organic pollutants may lead to the formation of oxidation byproducts with higher toxicity than their parent compounds. In this sense, the incomplete treatment of chlorophenols causes the formation of polychlorinated dibenzo-*p*-dioxins and dibenzofurans (PCDD/Fs), as it has been previously observed during the application of AOPs by the Advanced Separation Processes research group of the University of Cantabria.

In light of these facts, this thesis aims at acquiring new knowledge on the generation of PCDD/Fs during the advanced oxidation treatment of pollutants that serve as precursors of PCDD/Fs, particularized for the Fenton oxidation of 2-chlorophenol.

Firstly, in Chapter 1, an overview of the fundaments of advanced oxidation processes and, specifically, of Fenton oxidation is presented, as well as the summary of the current methods for the identification of reactive oxygen species. Additionally, the main features of PCDD/Fs and chlorophenols as precursors during the application of AOPs are briefly explained. On the other hand, the employment of computational chemistry for the study of the PCDD/Fs formation mechanisms from precursors is put in context.

The chemical reagents, experimental set-up, analytical methods and techniques together with the computational calculations details are included in Chapter 2.

With the aim of studying in depth what is happening in the Fenton system, Chapter 3 presents the results obtained when two different methods widely used in bibliography, based on DMSO-HPLC (dimethyl sulfoxide - high performance liquid chromatography) and DMPO-EPR (5,5-dimethyl-1-pyrroline N-oxide – electron paramagnetic resonance spectroscopy), were tested for the identification and quantification not only of reactive oxygen species but also organic radicals produced as a consequence of the Fenton oxidation of 2-CP. A more detailed study was carried

out in relation with the effect of chloride ions, iron dose and copper dose on the reduction of 2-CP concentration, chemical oxygen demand and total organic carbon, as well as on the formation of oxidation byproducts. One group of oxidation products that are expected during the Fenton treatment are the unwanted PCDD/Fs, which have been quantified during the development of this thesis. For the first time, results regarding the concentration distribution of unchlorinated and low-chlorinated DD/Fs (from mono- to tri-CDD/Fs) have been quantified during the application of advanced oxidation processes. A summary of the influence of the experimental variables on the Fenton oxidation of 2-CP as well as on the PCDD/Fs generation is gathered in this chapter too.

On the one hand, Chapter 4 includes theoretical calculations carried out to study the electrophilic chlorination of phenol and hydroxylation of 2-chlorophenol that have been really useful to describe the experimental product distribution observed in literature and throughout the Chapter 3. On the other hand, the research performed in the course of this thesis enabled the observation of semiquinone radicals (by means of EPR spectroscopy) that can be also related to the presence of chlorophenoxy radicals which, among others, are responsible of the formation of PCDD/Fs as it is described in Chapter 4. Although there are several works dealing with the description of the mechanisms involved in the formation of PCDD/Fs from precursors such as phenols and chlorophenols, most of the information is only available for gas phase. As a result, this thesis gathers for the first time a complete mechanistic proposal for the formation of PCDD/Fs from chlorophenol in aqueous phase, based on the data already published for gas phase and compared with the concentrations of dioxins and furans experimentally obtained and specified in Chapter 3. Furthermore, computational calculations were performed in order to study how the water affects the thermodynamics of the reactions leading to PCDD/Fs in those stages characterized by higher activation energies according to bibliography.

This thesis reports novel results regarding the effectiveness of some molecular probes to measure the presence of radical species that are responsible of the oxidation of organic pollutants and the formation of other unwanted byproducts, which may result in higher toxicity of the aqueous matrix. Besides, new progress on the quantification and mechanisms involved in the generation of PCDD/Fs during the advanced oxidation treatment of 2-CP aqueous solutions is also offered.

Resumen

La preocupación acerca de la contaminación de las aguas ha aumentado durante los últimos años debido al incremento de las actividades domésticas e industriales, así como al aumento de la población. Entre los posibles compuestos encontrados en las aguas residuales, los compuestos orgánicos clorados incluyen alguno de los químicos más tóxicos y peligrosos. Los clorofenoles (CPs) comprenden un grupo de compuestos orgánicos que se pueden encontrar en el medioambiente como consecuencia de su amplio y largo uso en la industria y vida diaria. Debido a su elevada toxicidad y baja biodegradabilidad, los CPs han sido listados por la U.S. EPA y la Comisión Europea como contaminantes prioritarios. Además, estos compuestos son conocidos por actuar como precursores de los compuestos de mayor toxicidad policlorodibenzo-p-dioxinas y policlorodibenzofuranos (PCDD/Fs), los cuales son considerados a su vez contaminantes prioritarios. Entre los 210 congéneres posibles de PCDD/Fs, los 17 conteniendo las posiciones 2,3,7,8 cloradas han recibido mayor atención ya que la exposición humana a estas especies está relacionada con diferentes enfermedades y cáncer, tal y como ocurre especialmente con 2,3,7,8-TCDD, considerado como el más tóxico por la U.S. EPA.

Como consecuencia de su baja solubilidad en agua, la mayoría de los estudios referentes a la generación y degradación de PCDD/Fs se ha centrado en fase gas. Sin embargo, el amplio uso de compuestos como el CP en la elaboración de insecticidas, biocidas, etc. ha dado lugar al incremento de la presencia de estas sustancias en

corrientes acuosas, cuyo tratamiento puede resultar en la generación de PCDD/Fs. Tanto los CPs como las PCDD/Fs se caracterizan por su alta resistencia a la degradación química y biológica, lo que implica la necesidad de emplear tecnologías más efectivas en su eliminación. Los procesos de oxidación avanzada (POAs) se postulan como tecnologías viables en el tratamiento de aguas residuales recalcitrantes mediante la generación de especies reactivas de oxígeno (ROS de sus siglas en inglés- reactive oxygen species). El radical hidroxilo (·OH) es el ROS más poderoso, siendo no selectivo y reaccionando rápidamente con los contaminantes orgánicos/inorgánicos. Entre los diferentes POAs, la oxidación Fenton se propone como una tecnología factible para convertir un amplio rango de contaminantes en productos menos dañinos o biodegradables, o incluso mineralizarlos, mediante el empleo de reactivos relativamente baratos, fáciles de manejar y seguros medioambientalmente. Sin embargo, se ha observado que la mineralización parcial de los contaminantes orgánicos puede dar lugar a la formación de subproductos de oxidación con mayor toxicidad que el compuesto original. En este sentido, el tratamiento incompleto de los clorofenoles provoca la formación de PCDD/Fs, tal y como ha sido descrito previamente durante la aplicación de POAs por el grupo de investigación de Procesos Avanzados de Separación de la Universidad de Cantabria.

A la luz de estos resultados, esta tesis tiene como objetivo adquirir nuevos conocimientos sobre la generación de PCDD/Fs durante el tratamiento de oxidación avanzada de contaminantes que actúan como precursores de PCDD/Fs, particularizado en la oxidación Fenton de 2-CP.

En primer lugar, en el Capítulo 1, se presenta una visión general de los fundamentos de los procesos de oxidación avanzada y, específicamente, de la oxidación Fenton, así como un resumen de los métodos que actualmente se emplean en la identificación de las especies reactivas de oxígeno. Además, se explican las principales características de las PCDD/Fs y los clorofenoles como precursores durante la aplicación de POAs. Por otro lado, se contextualiza el empleo de cálculos

químicos computacionales para el estudio los mecanismos de formación de PCDD/Fs.

El Capítulo 2 incluye los reactivos químicos empleados, el montaje experimental, los métodos y técnicas analíticas utilizadas, y los detalles relacionados con los cálculos computacionales.

Con el objetivo de estudiar en profundidad qué ocurre en el sistema Fenton, el Capítulo 3 presenta los resultados obtenidos cuando dos métodos diferentes y ampliamente utilizados en bibliografía, basados en DMSO-HPLC (dimetilsulfóxido – cromatografía líquida de alta resolución) y DMPO-EPR (5,5-dimetil-1-pirrolina N-óxido – espectroscopia de resonancia electroparamagnética), se utilizan en la identificación y cuantificación no solo de las especies reactivas de oxígeno sino también de los radicales orgánicos producidos como consecuencia de la oxidación Fenton de 2-CP. Se ha realizado un estudio más detallado relativo al efecto de los iones cloruro, la dosis de hierro y la dosis de cobre sobre la reducción de la concentración de 2-CP, la demanda química de oxígeno y el carbono orgánico total, así como sobre la formación de subproductos de oxidación. Dentro del grupo de subproductos no deseados están las PCDD/Fs, que han sido cuantificadas durante el desarrollo de esta tesis doctoral. Por primera vez, se han cuantificado las concentraciones de dioxinas y furanos no clorados y de bajo grado de cloración (desde mono a tri-CDD/Fs) durante la aplicación de procesos de oxidación avanzada en fase líquida. Se ha incluido, además, un resumen acerca de la influencia de las variables experimentales características del proceso Fenton en la oxidación de 2-CP y en la generación de PCDD/Fs.

Por un lado, el Capítulo 4 incluye los cálculos teóricos llevados a cabo para estudiar la cloración electrofílica de fenol y la hidroxilación de 2-clorofenol, lo que ha permitido describir la distribución de productos observada en literatura y a lo largo del Capítulo 3. Por otro lado, las labores de investigación realizadas en el transcurso de la presente tesis permitieron observar la generación de radicales semiquinona (por medio de espectroscopia EPR) que están relacionados con la

presencia de radicales clorofenoxi los cuales, entre otros, son los responsables de la formación de PCDD/Fs tal y como se describe en el Capítulo 4. Aunque hay trabajos relativos a la descripción de los mecanismos involucrados en la formación de PCDD/Fs a partir de precursores como el fenol y los clorofenoles, la mayor parte de la información se refiere a fase gas. Por lo tanto, esta tesis reúne por primera vez una propuesta completa de los mecanismos de formación de PCDD/Fs a partir de una disolución acuosa de clorofenol, tomando como base los datos disponibles en fase gas y comparándolos con las concentraciones de dioxinas y furanos observados experimentalmente y que se especifican en el Capítulo 3. Además, en esta tesis se ha realizado cálculos computacionales adicionales con el objetivo de estudiar cómo afecta el agua a la termodinámica de las reacciones que dan lugar a la formación de PCDD/Fs en aquellas etapas caracterizadas por mayores valores de la energía de activación de acuerdo a la bibliografía.

Por tanto, esta tesis presenta resultados novedosos en relación a la eficacia de los sensores moleculares en la determinación de la presencia de especies radicalarias que son responsables de la oxidación de contaminantes orgánicos y de la formación de otros subproductos no deseados, que pueden resultar en una mayor toxicidad de la matriz acuosa. Además, se muestran avances en la cuantificación y en la definición de los mecanismos involucrados en la generación de PCDD/Fs durante el tratamiento de oxidación avanzado de disoluciones acuosas conteniendo 2-clorofenol.

Chapter 1

Introduction

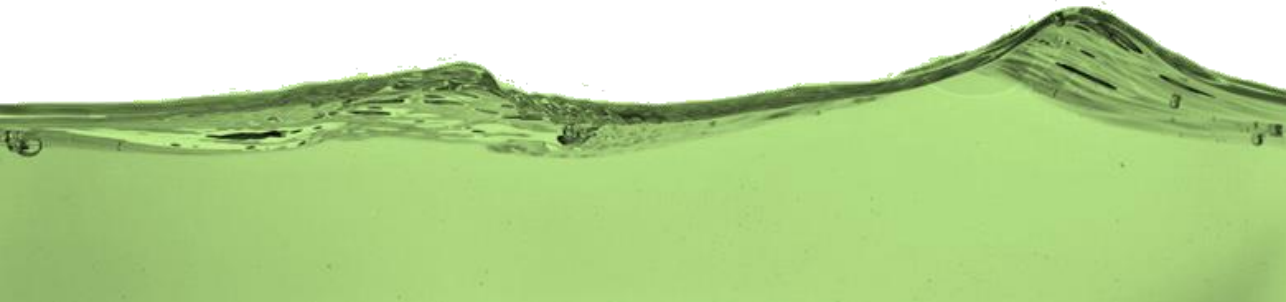

Chapter 1

Introduction

Abstract

During the last decades, the presence of new pollutants recalcitrant to conventional biological and chemical processes has aroused social concern that legislation has become stricter due to the adverse effect of these contaminants, as it is the case of polychlorinated dibenzo-*p*-dioxins and dibenzofurans (PCDD/Fs). It is of relevant importance to identify if dioxins and furans are present in aquatic streams because they affect the environment and living organisms, causing serious health issues such as cancer. These toxic and refractory pollutants are unintentionally produced and are released to aquatic environment from contaminated soils, sediments, leaching of landfill or even during the treatment of wastewaters containing other pollutants that act as precursors. Owing to their resistance towards chemical and biological degradation, more effective technologies are needed. In this sense, advanced oxidation processes (AOPs) are posed as attractive alternative technologies. Consequently, in this introductory chapter, the reader will find an overview of the fundamentals of AOPs applied to the wastewater treatment focusing on Fenton oxidation. Then, a summary of the current methods to identify the reactive oxygen species, which are responsible for the oxidation of the target compounds, is described. Afterwards, the main features of PCDD/Fs and their potential formation during the application of advanced oxidation treatment of precursors are described, paying special attention to the group of chlorophenols. Furthermore, a brief notion about theoretical computational calculations and their contribution to the study of the generation of PCDD/Fs from precursors is offered. Finally, the background, scope and outline of this thesis are summarized.

1.1. Water contamination: a matter of increasing concern

Wastewater may be defined as water containing pollutants, which means it cannot be used like pure water and should not be disposed of in a manner dangerous to humans, living organisms, and the environment.[1] Concern about the growth of surface and underground water contamination has increased over the years at the same time that the quality requirements of treated waters are more stringent.[2] Conventionally, biological, physical and chemical methods have been applied to treat wastewaters. Nevertheless, they sometimes are inefficient and exhibit certain disadvantages.[1,3] For instance, chlorination leads to the formation of by-products with potential adverse health effects. On the other hand, precipitation, chemical coagulation and flocculation require large amounts of chemicals and produce large quantities of sludge.[1] The use of adsorption and membrane technologies is usually associated to operational difficulties and high capital costs.[1] Regarding biological methods, the microorganisms utilized are not capable in many cases of oxidizing all the organic matter owing to the increase of recalcitrant contaminants characterized by high chemical stability and low biodegradability, so it is necessary to adopt reactive systems much more effective and capable of mineralizing these compounds.[4] Therefore, one of the great challenges of modern society is to guarantee adequate water resources with a desirable quality by exploring new treatment technologies that can be also combined with the currently available technologies.[5] Advanced oxidation processes (AOPs) have arisen as feasible technological alternatives.

AOPs are processes that usually operate near ambient temperature and normal pressure, and they are based on the generation of reactive oxygen species (ROS) such as hydroxyl radical (·OH or HO·), superoxide radical ($O_2^{-\bullet}$), hydroperoxyl radical ($HO_2^{\bullet}$), singlet oxygen ($^1O_2$) and hydrogen peroxide (H_2O_2).[2,4-7] Hydroxyl radicals are the most powerful oxidants after fluorine (Table 1.1) and they play an important role in the degradation of organic compounds in natural waters owing to its high and non-specific reactivity, with second-order rate constants in the range 10^7–10^{10} M^{-1} s^{-1}.[8,10] Hence, the main objective of AOPs is to generate hydroxyl

radicals in sufficient quantities to be able to oxidize the majority of the complex chemicals present in wastewaters to carbon dioxide, water and inorganic compounds or, at least, achieve their transformation into harmless products.[4,7,11,12]

Table 1.1. Standard reduction potential of various reactive species.

Reactive Species	Potential (V)
Fluorine (F_2)	3.06
Hydroxyl radical (·OH)	2.80
Ozone (O_3)	2.08
Hydrogen peroxide (H_2O_2)	1.78
Potassium permanganate ($KMnO_4$)	1.70
Hypochlorous acid (HClO)	1.49
Chlorine (Cl_2)	1.36
Oxygen (O_2)	1.23

AOPs have been successfully applied to the treatment of recalcitrant compounds present in actual wastewaters[13] from the chemical industry (including fine chemical, pulp and paper, petrochemical, and pharmaceutical industry);[14-16] textile and tannery industry;[17,18] food and agro-industry;[19,20] drinking water, landfill leachate and urban wastewater;[21-25] and emerging pollutants.[12,26-28] The mentioned examples are only the tip of the iceberg of a set of numerous studies in which the viability of AOPs as feasible alternatives for the treatment of wastewater is assessed. AOPs consist of a group of different technologies which may be grouped into the following categories: (i) Fenton processes that include conventional Fenton, Fenton-like, photo-Fenton and electro-Fenton; (ii) photolytic and photocatalytic systems; (iii) electrochemical technologies that take into consideration electro-oxidation, photoelectro-oxidation and photoelectrocatalytic processes, and electrical discharges; (iv) technologies based on ultrasounds such as sonolysis, sonocatalysis and hydrodynamic cavitation; and (v) γ-radiolysis and heavy ions (Figure 1.1).[2]

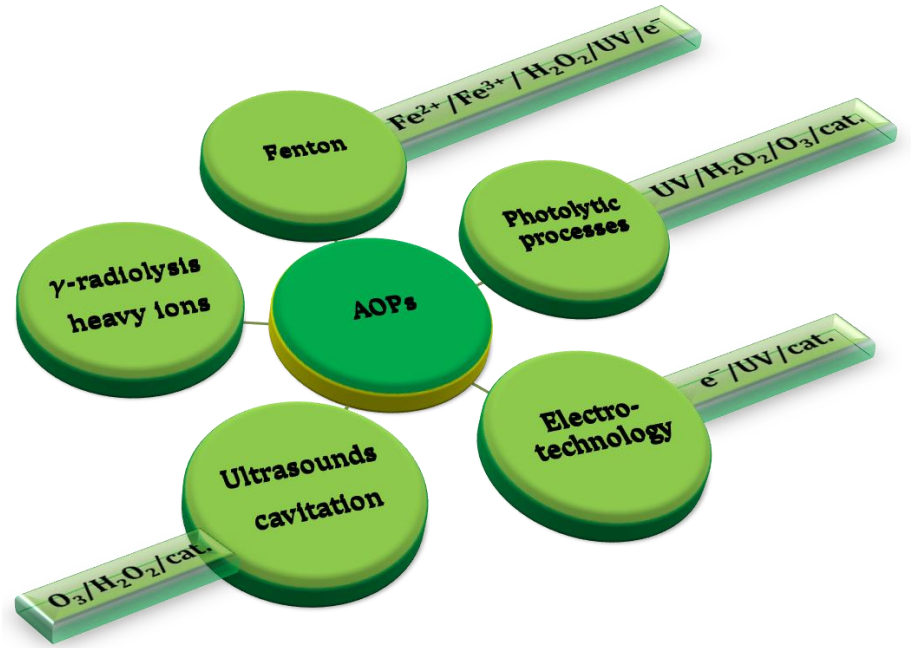

Figure 1.1. Classification of Advanced Oxidation Processes. Cat.: catalyst.

By and large, the main advantages of the AOPs can be summarized as follows: (i) potentiality to remove high organic carbon charges; (ii) capacity to act over complex matrices; (iii) the pollutant is not transferred to another phase; and (iv) refractory pollutants are converted into compounds that are easily biodegradable. Nevertheless, AOPs have certain disadvantages that they have to face depending on the type of treatment: (i) energy intensive in many cases leading to high costs, e.g., electrochemical and photocatalytic oxidation; (ii) costs of the reagents, e.g., H_2O_2 in Fenton reaction; and (iii) the presence of catalysts or oxidants in the final product may increase the toxicity, e.g., photocatalysis and Fenton.[3] In this sense, the viable application of AOPs is dependent on the organic content and the flow rate of the stream to be treated, but also on the typology of the pollutants.[3,5,29] In any case, the use of AOPs is advised for streams with a total organic carbon (TOC) concentration up to 1 g L^{-1}, as it can be seen in Figure 1.2 that depicts the application range of different oxidation technologies.[3,5,29]

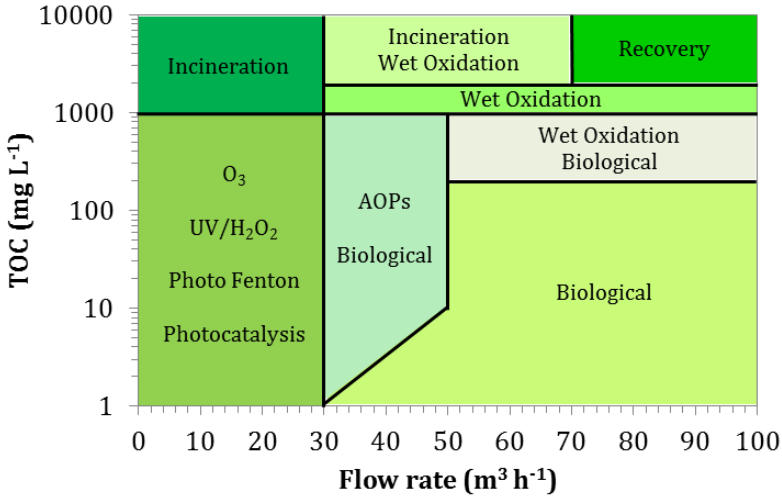

Figure 1.2. Application range of different oxidation technologies.[3,5,29]

In terms of chemical oxygen demand (COD), AOPs are usually recommended up to 5 g O_2 L^{-1} when working with medium flow rates. As a consequence of the limitations of AOPs mainly related to the costs of the reagents and energy, the concept of hybrid processes has aroused in the last few years, which basically consist of a combination of different treatment alternatives such as photocatalysis-membrane separations, AOPs-biological treatment, etc.[5] The integration of different processes results in cost-effective alternatives that have been already tested at laboratory scale and implemented in real industrial processes, especially the combination AOPs-biological treatment.[3,5,20]

1.2. Fenton oxidation

1.2.1. Fundamentals and state of the art

One of the most effective technologies to remove organic pollutants from aqueous solutions is the Fenton oxidation treatment. In 1876, H.J.H. Fenton published his first note on the oxidation of tartaric acid where he observed the interaction of tartaric acid with certain oxidizing agents in presence of a trace of ferrous salt, but it was not until 1893 when he reported that he had isolated the

oxidation product of tartaric acid and determined its empirical formula.[30,31] Basically, his work was focused on the reaction of carboxylic acids with iron (II) and H_2O_2.

The catalytic decomposition of H_2O_2 by ferrous and ferric salts occurs by means of chain and radical reactions.[32] When the initial iron salt is in the form of ferrous salt, the Fenton oxidation is initiated by the generation of $HO^{\bullet}$ according to the classical Fenton's reaction (Reaction 1.1).[33] Through the reaction between Fe(III) and H_2O_2, Fe(II) may be regenerated (Fenton-like reaction, Reaction 1.2).[34-37] However, the latter is considered as the limiting step in the Fenton oxidation (lower second-order kinetic constant, k).

$$Fe^{2+} + H_2O_2 \rightarrow Fe^{3+} + HO^{\bullet} + HO^{-} \qquad k = 76\ M^{-1}s^{-1} \tag{1.1}$$

$$Fe^{3+} + H_2O_2 \rightarrow Fe^{2+} + HO_2^{\bullet} + H^{+} \qquad k = 0.01\ M^{-1}s^{-1} \tag{1.2}$$

The reaction between $HO^{\bullet}$ and organic compounds (represented by RH, Reaction 1.3) is very fast (10^7–10^{10} M^{-1} s^{-1}), leading to the formation of organic radicals as transient intermediates whose further reaction results in the generation of more stable products (Reaction 1.4), other radical species (Reaction 1.5), or even the complete mineralization to CO_2 and H_2O.[9,38] Some organic compounds and radicals may participate in the reduction from ferric to ferrous ion and, thus, increasing the regeneration rate of the catalyst (Reaction 1.6).[39]

$$RH + HO^{\bullet} \rightarrow R^{\bullet} + H_2O \tag{1.3}$$

$$R^{\bullet} + H_2O_2 \rightarrow ROH + HO^{\bullet} \tag{1.4}$$

$$R^{\bullet} + O_2 \rightarrow ROO^{\bullet} \tag{1.5}$$

$$R^{\bullet} + Fe^{3+} \rightarrow R^{+} + Fe^{2+} \tag{1.6}$$

However, the oxidation process can be negatively affected by competitive reactions in which the Fenton reagents and radical species generated act as scavengers of $HO^{\bullet}$ (Reactions 1.7-1.10).[9,17,40]

$$Fe^{2+} + HO^{\bullet} \rightarrow Fe^{3+} + HO^{-} \qquad k = 3.2 \cdot 10^{8}\ M^{-1}s^{-1} \qquad (1.7)$$

$$H_2O_2 + HO^{\bullet} \rightarrow HO_2^{\bullet} + H_2O \qquad k = 2.7 \cdot 10^{7}\ M^{-1}s^{-1} \qquad (1.8)$$

$$HO_2^{\bullet} + HO^{\bullet} \rightarrow H_2O + O_2 \qquad k = 7.1 \cdot 10^{9}\ M^{-1}s^{-1} \qquad (1.9)$$

$$HO^{\bullet} + HO^{\bullet} \rightarrow H_2O_2 \qquad k = 5.2 \cdot 10^{9}\ M^{-1}s^{-1} \qquad (1.10)$$

Regarding the attack of organic compounds by HO•, it can occur by H-abstraction (Reaction 1.3), addition to the aromatic ring (Reaction 1.11) and addition to the C-C unsaturated bonds (Reaction 1.12), leading to the formation of organic radicals.[35,38]

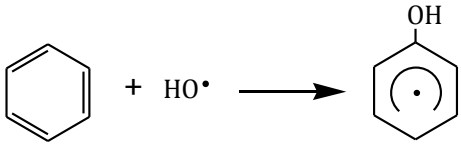

(1.11)

$$HO^{\bullet} + H_2C = CH_2 \rightarrow HO - CH_2 - CH_2^{\bullet} \qquad (1.12)$$

During the Fenton treatment some aspects have to be taken into account, i.e., pH, temperature, H_2O_2 dose, Fe(II) dose and the presence of some organic and inorganic substrates. The pH of the oxidation medium affects the predominance of certain reactions. It has been proved that in the majority of the cases the optimum pH is 3-4.[11,41] pH values under 2.5 result in i) the formation of $(Fe(II)(H_2O))^{2+}$ that reacts more slowly with H_2O_2 to produce HO•, ii) the scavenging of HO• by the excess of H^+, producing H_2O after gaining an electron from Fe(II), and iii) the formation of $H_3O_2^+$ that hinders the reaction between Fe(III) and H_2O_2.[38,41-44] At pH above 4, the oxidation potential of HO• decreases owing to i) the formation of Fe(II) complexes $[Fe(II)(H_2O)_6]^{2+}$, ii) the formation of ferric oxyhydroxides and their precipitation is favored and, therefore, the availability of iron decreases, and iii) the presence of HO^- favors the decomposition of H_2O_2 to oxygen (Reactions 1.13 and 1.14).[38,41-45]

$$H_2O_2 + HO^{-} \rightarrow HO_2^{-} + H_2O \qquad (1.13)$$

$$H_2O_2 + HO_2^{-} \rightarrow H_2O + O_2 + HO^{-} \qquad (1.14)$$

The increase of temperature is associated with the enhancement of the oxidation process and the degree of mineralization, allowing the reduction of the Fenton reagent dose.[42,46] However, temperatures above 40 ºC lead to a diminishment on the effectiveness of the hydrogen peroxide utilization owing to the fact that the decomposition of H_2O_2 into H_2O and O_2 is favored.[11]

The concentration of hydrogen peroxide plays a key role, affecting to the overall degradation efficacy.[11] The dosage of H_2O_2 must be enough to allow the degradation of pollutants, but an excess must be avoided due to its contribution to the final COD of the treated effluent; its risk and toxicity for many microorganisms when Fenton oxidation is integrated with biological treatment; large quantities of H_2O_2 cause $HO^{\bullet}$ scavenging (Reaction 1.8); the O_2 off-gassing provoked by the autodecomposition of excess H_2O_2 may result in iron sludge flotation; the cost of the Fenton treatment may increase as a consequence of higher H_2O_2 doses.[11,38,47] A theoretical mass ratio for removable COD has been defined as H_2O_2/COD equal to 2.12: 470.6 mg L^{-1} COD require around 1000 mg L^{-1} H_2O_2 (2 mol H_2O_2 per mol of COD).[33,47]

With respect to the iron dose, as a general rule, the degradation rate increases as ferrous concentration rises until a certain value in which higher concentrations do not result in the improvement of the oxidation treatment.[11] Moreover, high quantities of iron ions contribute to the total dissolved solids content that is usually controlled and contemplated by legislation, as well as to the amount of iron requiring treatment and whose maximum allowable discharge limit is stablished at 10 mg L^{-1} in Spain.[48] Furthermore, an excess of ferrous ion results in scavenging of $HO^{\bullet}$ (Reaction 1.7).[11,33,38] The iron dose is usually referred to hydrogen peroxide (Fe(II)/H_2O_2). Three different ratios have been defined: i) Fe(II)/H_2O_2≥ 2, where iron acts as reagent instead of catalyst consuming $HO^{\bullet}$; ii) Fe(II)/H_2O_2<< 1, which corresponds to the situation leading to higher availability of $HO^{\bullet}$; and iii) Fe(II)/H_2O_2≈ 1, which leads to an underperformance of iron compared to case ii) where ferrous ion is continuously regenerated.[49,50] With the aim of obtaining a reasonable generation of $HO^{\bullet}$ avoiding their scavenging by H_2O_2, it is widely accepted that the optimum H_2O_2/Fe(II) ratio is within the range 5-25 (wt/wt).[11,33,51]

Finally, the presence of organic and inorganic compounds may affect the overall effectiveness of the process. In this sense, the presence of chloride in the reaction medium results in the reduction of the oxidation rate because it acts as $HO^{\bullet}$ scavenger, or even, at high concentrations, chloride could inhibit the Fenton oxidation due to the complexation of iron.[43,52] Phosphate, sulfate, organosulfonate, fluoride and bromide are other examples of inorganic compounds affecting the Fenton treatment.[35] Regarding the organic compounds, there are two opposite possibilities: i) compounds such as acetic acid, acetone, carbon tetrachloride, n-paraffins, maleic acid, malonic acid and oxalic acid among others are refractory towards Fenton's reagent; ii) organic species such as quinones and semiquinones participate in the reduction of iron from Fe(III) to Fe(II).[11,35,39,53,54]

Fenton oxidation has been applied to a wide variety of synthetic and real effluents i) from industrial wastewaters such as chemical, pharmaceutical, textile, paper pulp, etc.; ii) from sludge and from contaminated soils, leading to toxicity reduction, biodegradability improvements, color and odor removal.[17] The main advantages of the Fenton treatment are related to the low energetic requirement because the oxidation process is carried out at ambient temperature and pressure, and it can be enhanced by solar light; the Fenton reagents are easy to handle and store, readily available and environmentally benign; the plant design and construction is simple; because the reactions take place in an homogeneous phase, there are not limitations regarding mass transport.[17,35,36] On the other hand, as it will be mentioned later, the low operational and investment costs make Fenton oxidation competitive when compared to other AOPs.[55]

Regarding the costs associated to the Fenton oxidation, according to the thorough study carried out by Cañizares et al. (2009), Fenton seems to be really competitive with other AOPs such as electrochemical oxidation and ozonation process.[55] The estimated operation costs are 0.7-3.0 € kg^{-1} equivalent O_2 for Fenton, 2.4-4.0 € kg^{-1} equivalent O_2 for conductive-diamond electrochemical oxidation and 8.5-10.0 € kg^{-1} equivalent O_2 for ozonation, although they may vary depending on the nature of the contaminant to be treated. In terms of investment costs, Fenton

has the lowest once although electrochemical oxidation can compete with Fenton treatment in those situations in which the formation of refractory products that require additional treatments occurs. Hence, the low costs of Fenton compared to other AOPs make it suitable for its application in the treatment of polluted waters.

1.2.2. Challenges in the application of Fenton oxidation processes

There are some limitations that Fenton oxidation has to overcome, mainly associated to post-treatment of the final stream. Initially, the pH must be controlled to the optimal acidic condition but, after the treatment, the pH has to be readjusted to neutral values. As a consequence of the Fenton oxidation and the neutralization step, the production of iron oxide sludge appears as an important drawback making an additional separation stage necessary prior to the discharge of the treated water.[17,35,36] However, the sludge generation in Fenton oxidation is expected to be minimal compared to the conventional biological treatment, easy to handle and with good settleability and dewaterability.[38] On the other hand, another factor to take into account, as it was mentioned previously, is the presence of inorganic and organic species that may affect the overall effectiveness of the process, for instance, some chemicals such as acetic and oxalic acids are recalcitrant to Fenton oxidation.[56]

The major weaknesses raised for the Fenton treatment may be solved by means of process integration. Commonly, Fenton oxidation has been proposed as a pretreatment stage in which non-biodegradable and recalcitrant compounds are oxidized to yield short chain oxidation products that are suitable to be treated by means of conventional biological treatments.[35] Oxidation byproducts such as oxalic, maleic and acetic acid, which are resistant to Fenton oxidation and form stable complexes with iron, are readily treated in biological systems at considerable lower cost.[36] On the other hand, attractive alternatives such as photo-Fenton and electro-Fenton may intensify the performance of the conventional Fenton treatment, for example, working in presence of light facilitates the mineralization of the organic acids by Fe(III)-catalyzed photoreactions, and Fe(III) is reduced to Fe(II) via

photolysis allowing the reduction of the iron dose and, consequently, the final sludge volume.[57]

1.3. Reactivity of oxidizing media

As it has been mentioned in the previous section, AOPs are viable technologies for environmental remediation of wastewaters containing non-biodegradable compounds. These technologies are based on the generation of ROS that are radical and non-radical species with the ability to participate in the mineralization of pollutants that are not degradable by means of conventional treatments, taking advantage of their non-selective character and their rapid reactions rates.[2] Hydroxyl radical (·OH), superoxide radical ($O_2^{-\bullet}$), hydroperoxyl radical ($HO_2^{\bullet}$), singlet oxygen ($^1O_2$) and hydrogen peroxide (H_2O_2) are the main examples of ROS.

Different methods for the analysis of ROS have arisen with the aim of assessing the effectiveness of each AOP, evaluating what species are generated and, therefore, deepening on the mechanisms involved during the application of advanced oxidation treatments. Direct methods can not be directly applied due to the short lifetime of the ROS (10^{-10} s for ·OH), so indirect methods based on the use of molecular probes or scavengers to selectively detect ROS have been developed.[58-62] In theory, these methods involve the use of a compound that reacts selectively, sensitively and unambiguously with the ROS under study and, then, ROS are quantified by means of the loss of a reagent or the accumulation of a product.[63,64] Important aspects to take into account when selecting an analytical method to determine ROS include: i) sensitivity; ii) selectivity and specificity towards the analyte of interest; iii) measurements with enough fast time resolution; and iv) stability of the probe and its reaction products.[9,65,66] Other relevant considerations are the availability, robustness and cost of the instrumentation and probe molecules, as well as the selection of proper operating conditions, such as the probe concentration, to avoid the reaction of ROS with themselves or prevent further reaction of the product and, therefore, underestimate the ROS concentration.

The indirect methods applied in the determination of ROS can be summarized in the following categories: (i) absorbance (UV/vis) probing methods, based on either the absorbance loss of the probe or the increasing absorbance of the product; (ii) fluorescence probing methods, where the reaction between the probe and the ROS leads to the formation of products showing strong fluorescence when they are excited at a specific wavelength; (iii) chemiluminescence probing methods, based on the reaction of a chemiluminogenic probe with ROS to yield a chemiluminescent product that irradiates light without being externally excited; (iv) spin-trapping methods, where the spin-trap agent reacts with the unpaired electron of the free radical; (v) electrochemical analysis based on cyclic voltammetry (CV), chronoamperometry (CA) and electrochemical detection (ED).[63,67-69]

Table 1.2 contains for each ROS a summary of the analytical methods and molecular probes employed during the application of AOPs in the quantification of ·OH, $O_2^{-\bullet}/HO_2^{\bullet}$ and $^1O_2$, as well as the main strengths and drawbacks of each method. Further information can be found in Annex III (Tables III.1-III.3) and in an exhaustive review previously published in the framework of this thesis (Fernández-Castro, 2015).[2] In general, there are some points in common for the different probes and methods that have to be contemplated, such as the addition of enough probe concentration to trap all the radicals generated and the attention to other species present in the reactive system which may act as scavengers of the ROS. Most of the works developed in bibliography focus on the identification of hydroxyl radical due to its high reactivity and its fundamental role as oxidant ($E^{o}_{NHE,pH7}(\cdot OH,H^+/H_2O)$= 2.18 V); second-order rate constants in the range 10^7-10^{10} M^{-1} s^{-1}).[8,9] Almost all the probes used to quantify ·OH are selective towards this radical and the analytical methods for its determination are simple regardless of the method followed, being the absorbance and spin-trapping the commonest methods, whereas the electrochemical is not enough developed and requires the comparison with other methods. The employment of dimethyl sulfoxide (DMSO), salicylic acid (SA), terephthalic acid/sodium terephthalate (TA/NaTA) and 5,5-Dimethyl-1-pyrroline N-oxide (DMPO) is widely extended for the different AOPs. One of the major issues

that arises during the hydroxyl radical identification is the further oxidation of the hydroxylation products which may result in an underestimation of ·OH concentration (Table 1.2 and Table III.1- Annex III). Furthermore, sometimes more than one oxidation product is generated, which is not advisable, as it is the case of benzoic acids, coumarin-3-carboxylic acid, phenolic-type compounds, etc.

Less is known about superoxide and hydroperoxide radicals (Reactions 1.2 and 1.8) that usually are produced from side reactions. $O_2^{-\bullet}$ may be produced as a result of the donation of an electron to oxygen and its protonation leads to $HO_2^{\bullet}$.[70] Though $O_2^{-\bullet}$ is relatively inactive by itself owing to resonance stabilization, in aqueous media at neutral pH protons promote a rapid reaction leading to H_2O_2 (Reaction 1.15, with a high equilibrium constant).[63,71]

$$2\,O_2^{-\bullet} + 2\,H^+ \rightarrow H_2O_2 + O_2 \qquad K_{pH\,7} = 4 \cdot 10^{20} \qquad (1.15)$$

Its standard potential, $E°(O_2^{-\bullet},H^+/H_2O_2)$= 0.95 V vs. NHE at pH= 7, is less than half of the corresponding to ·OH. The second-order rate constants are not as high as in the case of ·OH reaction, but they can reach the range 10^7-10^{10} M^{-1} s^{-1} when $O_2^{-\bullet}$ reacts with luminol, superoxide dismutase (SOD), different quinones, etc.[40] The presence of complexing agents and salts in the solution, pH and type of solvents influence the half-life time of $O_2^{-\bullet}/HO_2^{\bullet}$.[72]

The most used probe for the quantitative determination of $O_2^{-\bullet}$ is luminol, whose reaction leads to the generation of chemiluminescent product (Table 1.2 and Table III.2- Annex III). Nevertheless, luminol presents important weaknesses as its non-selectivity towards $O_2^{-\bullet}$ and the background noise during the luminescence analyses which restricts its use to alkaline pH.[73] Alternatively, when DMPO is added to the solution, the different signals obtained after its reaction with ·OH or $O_2^{-\bullet}/HO_2^{\bullet}$ allow the discrimination of each radical DMPO-·OH or DMPO-·OOH. However, DMPO-·OOH adducts are unstable and decay to DMPO-·OH which results in a misinterpretation of the generation of ·OH and ·OOH radicals.[74,75]

With regard to singlet oxygen, it can be easily generated in solution by energy transfer from excited photosensitizers or chemically.[63,76-78] $^1O_2$ has a standard potential $E°(^1O_2/O_2^{-\bullet})$= 0.65 V vs. NHE at pH= 7 and its lifetime in aqueous solution depends on the presence of scavengers, being 4 μs in pure water.[76,77] On the one hand, $^1O_2$ can be directly measured through the luminescence emitted at 1270 nm, although sometimes the weak signal recorded hinders the application of this direct analytical method.[79,80] On the other hand, indirect methods have been also developed with the aim of taking a step further towards improving its quantitative determination. Mainly, these indirect methods are based on the addition of a probe which after reacting with $^1O_2$ leads to the formation of a fluorescent or luminescent product (Table 1.2 and Table III.3-Annex III) Nowadays, most of the molecular probes used have been synthetized in the laboratory although other such as Singlet Oxygen Sensor Green (SOSG) and 2,2,6,6-tetramethylpiperidine (TEMP) are commercially available.

Table 1.2. General features of the probes employed in the determination of the radicals (Rad.) ·OH, $O_2^{-\bullet}/HO_2^{\bullet}$ and $^1O_2$.

Rad.	Method	Molecular probes*	Main strengths	Main weaknesses
·OH	Absorbance UV/vis	BA, Benzene, 4-CP, DMSO, 4-HBA, CH_3OH, NPG, n-propanol, OPDA, p-CBA, phenylalanine, quinoline RhB, RNO, SA, TA and NaTA	· Selectivity towards ·OH · Reproducibility and accuracy · Reaction products are stable · Simplicity and commercial availability	· Further oxidation of reaction products. Product distribution
	Fluorescence	BA, 3-CCA, coumarin, DMSO, DPCI, ninhydrin, SA, TA and NaTA	· Selectivity towards ·OH · Reproducibility, sensitivity and accuracy · Simple methods · Commercial availability	· Fluorescence is pH dependent · Further oxidation of reaction products. Product distribution · Filter effect and fluorescence quenching
	Luminescence	IBG, Phth	· Selectivity towards ·OH · Reproducibility, sensitivity and accuracy	· Chemiluminescence is pH dependent · Further oxidation of reaction products. Product distribution · Difference in luminescence emission between products
	Spin-trapping	3-carboxyproxyl, DMPO, FDMPO, nitrone	· Simplicity and sensitivity · Short analysis time · It is not affected by suspensions	· Reaction with other ROS · Stability of the hydroxylation product
	Electrochemical	4-HBA, catechol, $Ru(NH_3)_6^{3+}$, SA	· Selectivity towards ·OH	· Generation of different oxidation products · Usually require testing by other methods

* BA: benzoic acid; 4-CP: 4-chlorophenol; 3-CCA: coumarin-3-carboxylic acid; DMPO: 5,5-Dimethyl-1-pyrroline N-oxide; DMSO: dimethyl sulfoxide; DPCI: 1,5-Diphenylcarbohydrazide; FDMPO: 4-hydroxy-5,5,dimethyl-2-trifluoromethylpyrroline-1-oxide; IBG: indoxyl-β- glucuronide; NPG: N,N′-(5-nitro-1,3-phenylene)bisglutaramide; OPDA: o-phenylene diamine; p-CBA: p-chlorobenzoic acid; Phth: phthalic hydrazide; RhB: [9-(2-carboxyphenyl)-6-diethylamino-3-xanthenylidene]-diethylammonium chloride; RNO: N,N-dimethyl-4-nitrosoaniline; SA: salicylic acid; TA: terephthalic acid; NaTA: sodium terephthalate.

Table 1.2. General features of the probes employed in the determination of the radicals (Rad.) ·OH, $O_2^{-\bullet}/HO_2^{\bullet}$ and $^1O_2$ (continuation).

Rad.	Method	Molecular probes*	Main strengths	Main weaknesses
$O_2^{-\bullet}/HO_2^{\bullet}$	Absorbance UV/vis	FC. NBD-Cl, NBT, XTT	· Selectivity	· Solubility of the probes
	Fluorescence	BA, NaTA	· Sensitivity	· The signal is pH dependent · Formation of numerous products
	Luminescence	Luminol, MCLA	· Sensitivity	· Background chemiluminescence
	Spin-trapping	DMPO	· Sensitivity	· Selectivity · Stability of the adduct
$^1O_2$	Direct analysis	$^1O_2$ phosphorescence	· Direct measurement	· Under N_2 environments, the concentration of $^1O_2$ decreases · Stability
	Fluorescence	AAPD, DMAX, DPAX, MTTA-Eu^{3+}, Naphthoxazole based, SOSG, TTF, TTFA	· Selectivity towards $^1O_2$ · Sensitivity	· Usually synthesized in the laboratory
	Luminescence	PATA-Tb^{3+}, Re(I) complex, SVE, TTF, TTFA	· Selectivity towards $^1O_2$ · Initial probe hardly emits luminescence	· Synthesis in the laboratory
	Spin-trapping	TEMP	· Selectivity towards $^1O_2$	

* AAPD: anthryl-appended porphyrin dyad; BA: benzoic acid; DMAX: 9-[2-(3-carboxy-9,10-dimethyl)anthryl]-6-hydroxy-3H-xanthen-3-one; DPAX: 9-[2-(3-carboxy-9,10-diphenyl)anthryl]-6-hydroxy-3H-xanthen-3-one; DMPO: 5,5-Dimethyl-1-pyrroline N-oxide; FC: ferrocytochrome C; MCLA: methoxy cypiridina luciferin analog; MTTA-Eu^{3+}: 4′-(10-methyl-9-anthryl)-2,2′:6′,2′′-terpyridine-6,6′′-diyl]bis(methylenenitrilo)tetrakis (acetate)-Eu^{3+}; NBD-Cl: 7-chloro-4-nitrobenzo-2-oxa-1,3-diazole; NaTA: sodium terephthalate; NBT: nitroblue tetrazolium salt; XTT: 2,3-bis(2-methoxy-4-nitro-5-sulfophenyl)-2Htetrazolium-5-carboxanilide; SOSG: Singlet Oxygen Sensor Green reagent; TEMP: 2,2,6,6-tetramethylpiperidine; TTF: 4,5-dimethylthio-4′-[2-(9-anthryloxy)ethylthio]tetrathiafulvalene; TTFA: tetrathiafulvalene-anthracene dyad.

1.4. State of the art of the formation and destruction of PCDD/Fs in liquid phase

1.4.1. Polychlorinated dibenzo-p-dioxins and dibenzofurans (PCDD/Fs)

Plychlorinated dibenzo-*p*-dioxins and dibenzofurans (PCDD/Fs, generally called dioxins) are a group of almost planar tricyclic aromatic compounds with similar structures, chemical and physical properties.[81-83] There are as many homologues groups as number of chlorine atoms in the PCDD/F structure, where each homologues group is formed by a different number of congeners depending on the possible number of isomers, resulting in a total of 75 PCDDs and 135 PCDFs (Table 1.3). Dioxins are characterized by their low vapor pressure, extremely low solubility in water, solubility in organic/fatty matrices and their preference to bind to organic matter in soil and sediments, i.e., lipophilic character.[84]

Table 1.3. PCDD and PCDF structural formula and number of chlorinated congeners per homologue group.

PCDDs		PCDFs	
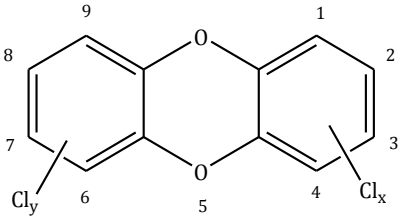		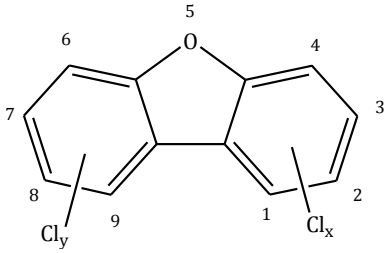	
No. of chlorines	No. of congeners	No. of chlorines	No. of congeners
1	2	1	4
2	10	2	16
3	14	3	28
4	22	4	38
5	14	5	28
6	10	6	16
7	2	7	4
8	1	8	1
Total	75	Total	135

Dioxins are considered persistent organic pollutants (POPs) owing to their physical, chemical and biological stability, long-range transport and persistence character. Commonly, those PCDD/Fs, with four or more chlorine atoms in their structure, having the positions 2, 3, 7 and 8 chlorinated (a total of 17 congeners) have received the greatest attention because of their higher toxicity and extreme resistance to chemical and biological degradation processes.[85,86] In 1997, the International Agency for Research on Cancer (IARC) classified the most toxic congener 2,3,7,8-TCDD as carcinogenic to humans.[84] Usually, PCDD/Fs appear as a mixture of the most toxic 2,3,7,8-PCDD/Fs congeners and other isomers. With the aim of facilitating the risk assessment and regulation of these compounds, the concepts of toxic equivalency factor (TEF) and toxic equivalents (TEQ) were defined.[81,84] TEF is based on the relative toxicity of dioxin-like compounds in relation to 2,3,7,8-TCDD congener determined from *in vitro* and *in vivo* studies. The sum of the product of each 2,3,7,8-PCDD/F concentration and each TEF results in the TEQ (first two terms of Equation 1.1). Two different TEF have been defined, (i) the international TEFs (I-TEFs) which are a result of cooperative effort of the Committee on the Challenges of Modern Society from North Atlantic Treaty Organization (NATO/CCMS); and (ii) the World Health Organization TEFs (WHO-TEFs). The latter not only included re-evaluated values of the TEFs but it also took into consideration the toxicity associated to the dioxin-like compounds polychlorinated biphenyl (PCB, Equation 1.1).[87,88] The proposed TEFs are summarized in Table 1.4, and they should be updated periodically as the availability of toxicity data increases.

$$\mathrm{TEQ} = \sum_{i}(\mathrm{PCDD}_i \cdot \mathrm{TEF}_i) + \sum_{j}(\mathrm{PCDF}_j \cdot \mathrm{TEF}_j) + \sum_{k}(\mathrm{PCB}_k \cdot \mathrm{TEF}_k) \qquad \text{(Eq. 1.1)}$$

Table 1.4. Toxic equivalency factors for the 17 2,3,7,8-PCDD/Fs congeners.

Congener	I-TEF	WHO-TEF
2,3,7,8-TCDD	1	1
1,2,3,7,8-PeCDD	0.5	1
1,2,3,4,7,8-HxCDD	0.1	0.1
1,2,3,6,7,8-HxCDD	0.1	0.1
1,2,3,7,8,9-HxCDD	0.1	0.1
1,2,3,4,6,7,8-HpCDD	0.01	0.01
OCDD	0.001	0.0003
2,3,7,8-TCDF	0.1	0.1
1,2,3,7,8-PeCDF	0.05	0.03
2,3,4,7,8-PeCDF	0.5	0.3
1,2,3,4,7,8-HxCDF	0.1	0.1
1,2,3,6,7,8-HxCDF	0.1	0.1
1,2,3,7,8,9-HxCDF	0.1	0.1
2,3,4,6,7,8-HxCDF	0.1	0.1
1,2,3,4,6,7,8-HpCDF	0.01	0.01
1,2,3,4,7,8,9-HpCDF	0.01	0.01
OCDF	0.001	0.0003

Sources of PCDD/Fs

PCDD/Fs can be formed naturally as a consequence of the incomplete combustion of forest fires, volcanic activity or even biologically from chlorinated precursors.[84,89] However, in most of the cases, they are unintentionally produced as trace contaminants in many industrial and thermal processes. Primary sources of dioxins include i) production and use of chloroorganic chemicals, ii) chlorine bleaching of pulp and paper, iii) chlorine-alkali plants using graphite electrodes, iv) metals smelting and refining, v) waste incineration, vi) fuel combustion, vii) other high-temperature processes such as cement kilns.[81,84,86,89-93] Secondary sources (reservoirs) are sewage sludge, composts, landfills and contaminated soils and sediments where PCDD/Fs are already present and may re-enter into the environment (Figure 1.3).

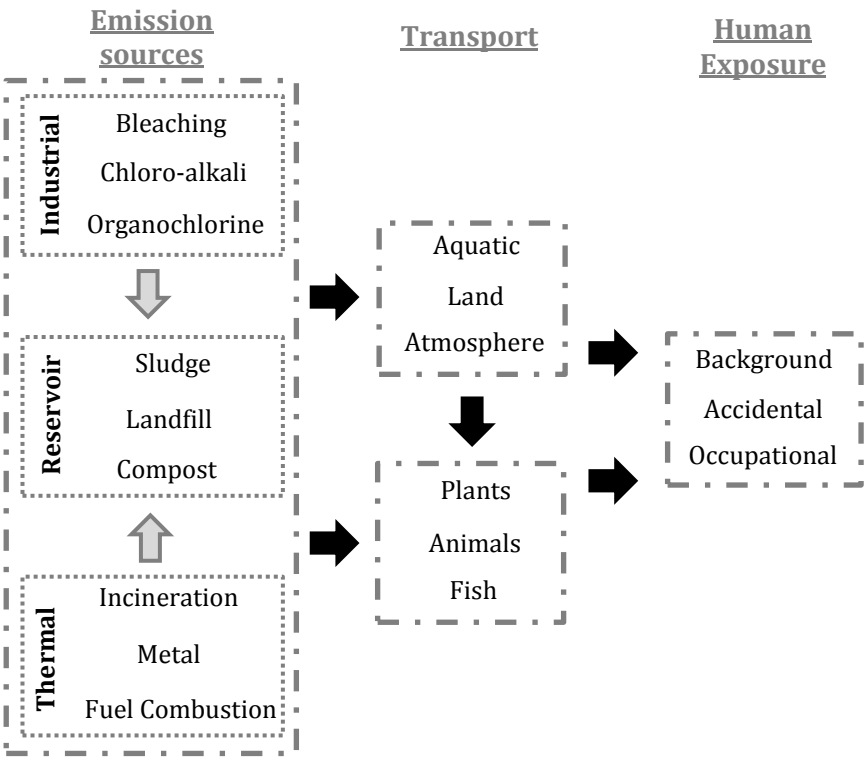

Figure 1.3. Sources, transport and human exposure to PCDD/Fs (adapted).[94]

The generation of PCDD/Fs throughout the production and use of chloroorganic compounds (aromatic and aliphatic) as well as inorganic chlorinated chemicals is positively affected by high temperatures, alkaline media and UV-light.[95] Nowadays, thermal processes are the main source of dioxins that may come from PCDD/Fs already present in the incoming waste, formed from related chlorinated precursors or produced via oxidation and chlorination of any unburned carbon in the particles (*de novo* synthesis).[94,96] The temperature and the presence of catalysts are relevant factors influencing the formation of PCDD/Fs during the application of thermal processes.

As it was stated above, PCDD/Fs are characterized by their extremely low solubility in water and, perhaps, that was the reason why almost the majority of the studies were focused on gas phase. Nevertheless, PCDD/Fs may be transported from

contaminated sites to groundwaters in the presence of certain substances such as dissolved organic matter, directly released to aquatic environments from chemical and bleaching industries as well as agricultural activities, and transferred from atmosphere by means of diffusive absorption and dry deposition.[94,97,98] On the other hand, recent studies have shown that these POPs can be formed during the treatment of wastewaters containing other compounds that act as precursors, for instance, during the treatment of chloroderivatives of phenol in the presence of peroxidase enzymes, and throughout the application of advanced oxidation processes to landfill seepage waters and waters containing phenolic/chlorophenolic compounds in the presence/absence of chloride in the medium.[28,99]

According to the available data from the Spanish Pollutant Release and Transfer Register (PRTR) in 2015, around 36 and 238 g TEQ yr^{-1} were emitted to the atmosphere and water, respectively.[100] This information corresponds only to the activities of companies that emit more than 1 g yr^{-1}. País Vasco and Cataluña are the Autonomous Communities releasing higher amounts of PCDD/Fs to the atmosphere, 41.3% and 28.5%, respectively (Figure 1.4), whereas Cantabria emits 13.5% of the total emission. Regarding the discharges in aquatic systems, the majority corresponds to Murcia region (petroleum refining).

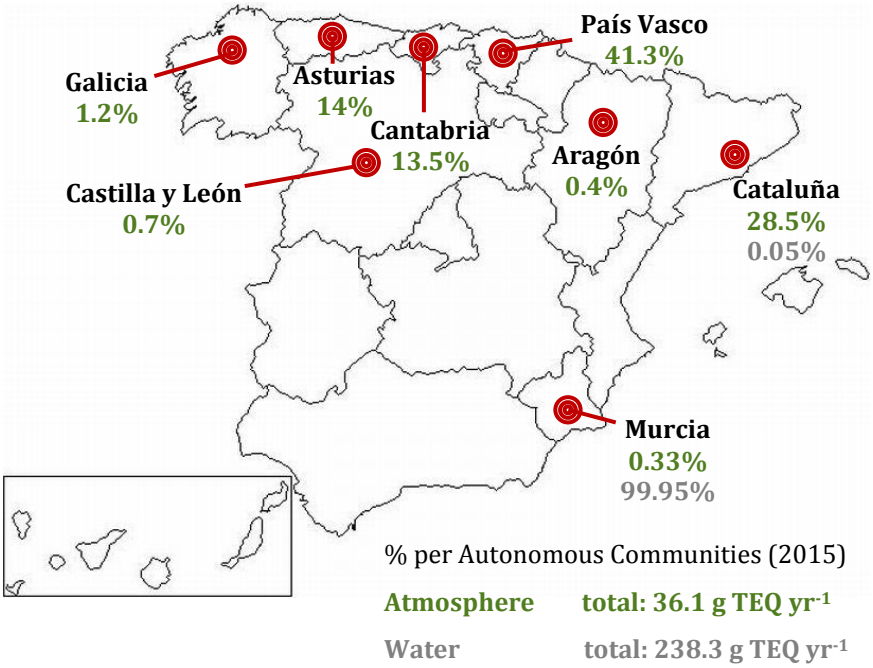

Figure 1.4. Total amount of PCDD/Fs emitted to atmospheric and aquatic environments in Spain: distribution between different Autonomous Communities. Data from Comunidad Valenciana are being reviewed.[100]

In terms of activities, metal industries together with the production of oxygenated hydrocarbons are responsible for more than 98% of PCDD/Fs emitted to the atmosphere while more than 99.8% of the PCDD/Fs released to waters come from petroleum refining (Figure 1.5). In the case of Cantabria region, all the PCDD/Fs released have their origin in the metal melting industry.

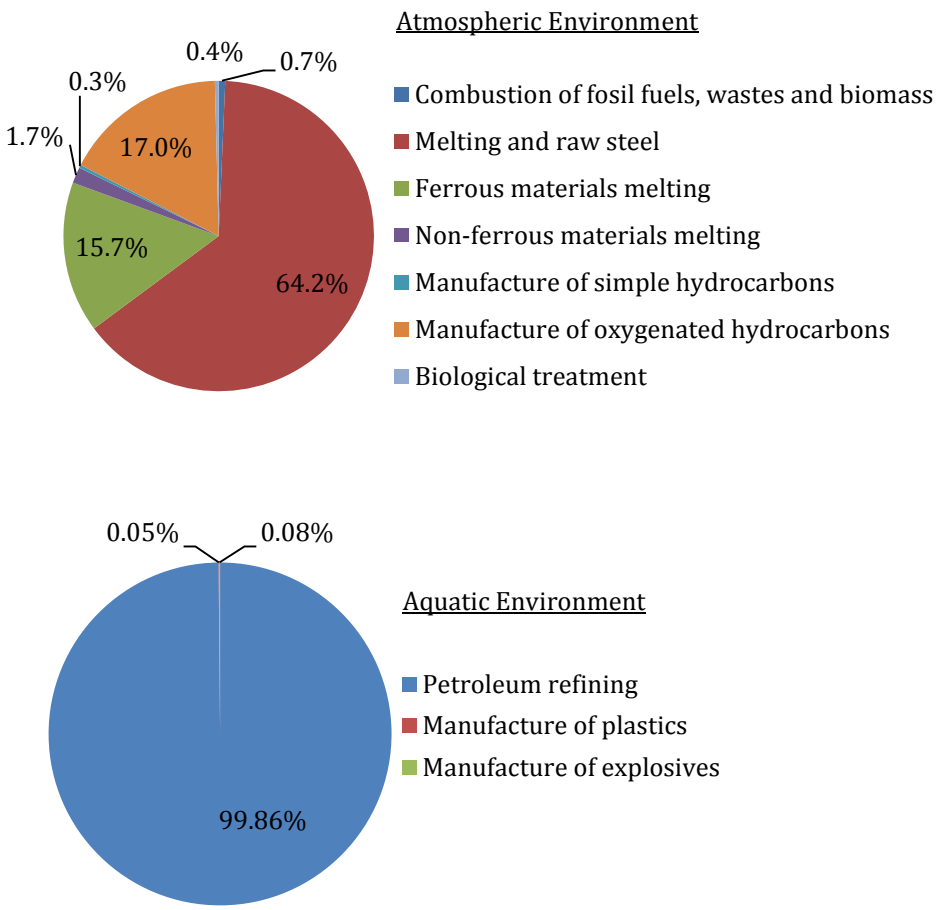

Figure 1.5. Releases of PCDD/Fs in Spain categorized in different industrial activities: data for atmospheric and aquatic environments. Data from Comunidad Valenciana are being reviewed.[100]

It should be noted that in spite of the low solubility of PCDD/Fs in water, most of the amounts registered in the Spanish PRTR are released to the aquatic environment, this may be due to the high content of organics present in the aqueous streams of the petroleum refining that facilitate the solution of PCDD/Fs, and the high activity of this type of industry.

Health effects of PCDD/Fs

There are three different ways in which humans can be exposed to PCDD/Fs (Figure 1.3). Background exposure constitutes the main pathway and takes place mainly through the contamination of the food, i.e., accumulation in the food chain caused by PCDD/Fs deposition.[101] Other background human exposure routes are inhalation of air and dermal adsorption.[84] The second exposure pathway is related to accidents as it was the case of the explosion of 2,4,5-trichlorophenol (2,4,5-triCP) factory at Seveso (Italy).[85] Finally, the occupational exposure has special relevance at waste incineration and chloroorganics manufacture plants. The effects of PCDD/Fs on the human health will depend on the exposure dose, duration, personal traits and habits, and interactions with other chemicals present.

In vivo assays have shown carcinogenic and non-carcinogenic effects caused by PCDD/Fs such as endometriosis, developmental neurobehavioral effects, developmental reproductive effects, immunotoxic effects, tumors, alterations of thyroid hormone, etc.[81,84,102] The effects in humans are not well known and in most cases the information comes from industrial accidents or high exposures, mainly dermatological (chloracne) and endocrinological problems. Although epidemiological studies support the relation between high levels of PCDD/Fs exposure and cancer, due to the lack of available data, only 2,3,7,8-TCDD have been classified as human carcinogenic, whereas there is limited evidence for the carcinogenicity in experimental animals of other 2,3,7,8-PCDD/Fs. It is believed that biological effects of the different 2,3,7,8-PCDD/Fs is dependent of their ability to interact with the cytosolic aryl (aromatic)hydrocarbon receptor, which would activate the response of the genes.[81,89]

Legislation and regulations

In the European Water framework Directive, PCDD/Fs were not considered as priority pollutants until 29 April 2004 when the Regulation (EC) 850/2004 on persistent organic pollutants was presented (Table 1.5).[85] This regulation ratified the international agreement obtained in the Stockholm Convention held in Sweden

in 2001, with the objective of eliminating and restricting the production and use of POPs.[103] By 1st May 2011, 173 parties were integrated in this organization, with 132 of them developing national implementation plans. The aim of this Convention is the protection of the human health and environment from POPs highlighting the toxicity and hazards of these pollutants, measures to reduce or remove their releases from intentional/unintentional production as well as from stockpiles and wastes, register of specific exemptions, and implementation plans.[104] Initially, only 12 compounds were considered in POPs list, including PCDD, PCDF and PCB. In 2009, nine compounds/groups of compounds were added to the list, whereas in the meeting in 2011 another one was included.[105] Continuing with the protecting policy in the European Union, the European Regulation 166/2006, concerning the establishment of a European Pollutant Release and Transfer Register, was published. This regulation states that any activity exceeding the applicable threshold of 0.0001 kg TEQ yr^{-1} (PCDD+PCDF, atmospheric, aqueous and/or soil emissions) shall report the amounts released annually to its competent authority. It was in the Directive 2013/39/EU when the European Parliament and the Council of the European Union included environmental quality standards (EQS) for dioxins and dioxin-like compounds that includes 7 PCDDs (2,3,7,8-chlorinated congeners), 10 PCDFs (2,3,7,8-chlorinated congeners) and 12 dioxin-like polychlorinated biphenyls (PCB-DL).[106] However, in the case of these pollutants an average annual or maximum allowable concentration in water was not defined, so the only EQS available is the one corresponding to the content PCDD+PCDF+PCB-DL in biota with a maximum value of 0.0065 μg TEQ kg^{-1} wet weight, taking as reference the WHO-TEFs defined in Table 1.4.[88]

Table 1.5. European aquatic policy timeline related to organochlorines and PCDD/Fs.

Directive	Remarks
75/440/EEC[107] (1975)	Characteristics of surface water intended for the abstraction of drinking water including limits for phenols, polycyclic aromatic hydrocarbons (PAH), and total pesticides, among others.
76/464/EEC[108] (1976)	Pollution caused by certain dangerous substances discharged into the aquatic environment including organohalogen compounds. Repealed by 2006/11/EC.
80/68/EEC[109] (1980)	Protection of groundwater against pollution caused by certain dangerous substances such as organohalogen compounds and substances which may form them in the waters. Repealed by Directive 2000/60/EEC.
80/778/EC[110] (1980)	Quality of water intended for human consumption: guide levels and maximum admissible concentration for phenols, pesticides, organochlorine compounds and PAH, among others.
84/491/EEC[111] (1984)	Limit values and quality objectives for discharges of hexachlorocyclohexane. Repealed by 2008/105/EC.
86/280/EEC[112] (1986)	Limit values and quality objectives for discharge of certain dangerous substances included in 76/464/EEC. Groundwater is excluded from this Directive. It provides limit values for pentachlorophenol and hexachlorobenzene, among others. Amended by Directives 88/347/EEC, 90/415/EEC, 91/692/EEC, 2008/105/EC. Repealed by 2008/105/EC.
2000/60/EC[113] (2000)	Establishment of a framework for Community action in the field of water policy. Priority substances are not indicated but it considered their proposition after the evaluation period. Amended by Directives 2008/105/EC and 2013/39/EU.
2455/2001/EC [114] (2001)	List of priority substances in the field of water policy (2000/60/EC). Hexachlorobenzene, hexachlorocyclohexane, pentachlorobenzene and pentachlorophenol, among others, are included.
850/2004/EC[115] (2004)	The Community signed on the Stockholm Convention on POPs related to the prohibition, restriction, placing and minimization of substances such as PCDD/Fs.
2006/11/EC[116] (2006)	Pollution caused by certain dangerous substances discharged into the aquatic environment. Definition of two lists of families and groups of substances, including organohalogen compounds and substances that possess carcinogenic properties. Amended by 2008/105/EC.
2006/118/EC[117] (2006)	Protection of groundwater: guidelines for the establishment of threshold values.
2006/166/EC[118] (2006)	Establishment of a European Pollutant Release and Transfer Register. Applicable threshold of 0.0001 kg TEQ yr^{-1} for PCDD/Fs.
2008/105/EC[119] (2008)	Environmental quality standards in the field of water policy: priority pollutants and certain other pollutants such as benzene, hexachloro-benzene/-cyclohexane, pentachloro-benzene/-phenol, trichlorobenzene, etc. Proposal of substances subject to review for possible identification as priority substances includes PCDD/Fs. Amended by 2013/39/EU.
2013/39/EU[106] (2013)	Priority substances in the field of water policy. Inclusion of PCDD/Fs and related compounds as priority substances.

With respect to the Spanish regulations, the Spanish Government ratified the agreement reached in the Stockholm Convention through the national Reglamento 850/2004.[120] Additional measures have been adapted from the directives approved in the European Council. The Spanish Government transposed the European Regulation 166/2006 into the Real Decreto 508/2007 keeping that any activity exceeding the applicable threshold of 0.0001 kg TEQ yr^{-1} (PCDD+PCDF, atmospheric, aqueous and/or soil emissions) shall report the amounts released annually.[118,121] Later on, through the Real Decreto 817/2015 the Directive 2013/39/EU was transposed, maintaining the EQS value 0.0065 μg TEQ kg^{-1} wet weight in biota.[106,122]

Regarding the water regulations in the United States, the Environmental Protection Agency (EPA) stablished in 1974 a maximum contaminant level goal in drinking water for dioxins (2,3,7,8) of zero, although based on this value an enforceable maximum contaminant level of 30 pg L^{-1} was set.[123]

1.4.2. Oxidation of organic containing PCDD/Fs or their parent compounds by AOPs

Although AOPs have been successfully applied in the elimination of recalcitrant compounds, many times, owing to the incomplete oxidation of the starting organic pollutants, other organic contaminants are unintentionally generated, which can be even more dangerous than the parent compound.[28] As a consequence, it is of special relevance the selection of a technology capable of mineralizing the target contaminants or that transforms them into innocuous products, which can be oxidize by other technologies such as biological treatments. Benzenes, phenols, cyclohexanes and their products of chlorination, among many other compounds, form an important group of substances that act as precursors of the highly toxic PCDD/Fs. However, little is known about the potential and mechanisms of these precursors in aqueous samples to form PCDD/Fs, especially when AOPs are applied. In this sense, in a previous work developed in the Department of Chemical and Biomolecular Engineering of the University of Cantabria, Vallejo et al. (2015) summarized the main substances acting as precursors of PCDD/Fs when photolytic,

Fenton and electrochemical based processes were employed.[28] Chlorophenols (CPs), chloronitrobenzene and triclosan (5-chloro-2-(2,4-dichlorophenoxy)phenol) are examples of compounds described in bibliography whose oxidation reactions under certain conditions favor the generation of PCDD/Fs, especially when an additional source of chlorine is present in solution (e.g., landfill leachates with high content in chlorides) and when working in default of oxidizing agent (Fenton oxidation).[28]

On the other hand, although the number of studies about both PCDD/Fs formation and destruction in aqueous phase is scarce, there is a higher number of those dealing with the degradation of PCDD/Fs based not only on photolytic, Fenton and electrochemical processes, but also on ozone and sonolytic processes.[28] The effectiveness in the removal will depend on the oxidation technology selected and the conditions applied. For instance, Vallejo et al. (2014) observed the generation of PCDD/Fs during the Fenton oxidation of 2-CP when only 20% of the theoretical stoichiometric amount of hydrogen peroxide required to completely mineralized the initial concentration of 2-CP was used.[124] However, as soon as the concentration of H_2O_2 was increased up to 100% of the theoretical stoichiometric amount, the concentration of PCDD/Fs was undetectable. This is a good example that shows the initial oxidation reactions leading to condensation byproducts which are further oxidized after selection of the proper reaction conditions. Another good example is a work developed also by Vallejo et al. (2013) in which the electrochemical oxidation of 2-CP was carried out with the aim of assessing the influence of the electrolyte type (Na_2SO_4 or NaCl) and, therefore, the influence of chloride in the generation of PCDD/Fs.[27] The results displayed interesting information in terms of the byproducts obtained: i) when working with chloride di-CPs and tri-CPs were the main aromatics obtained, whereas working with sulfate the main aromatic byproducts were non-chlorinated organics; ii) working with sulfate as electrolyte the most toxic PCDD/Fs congeners were not obtained as oxidation byproducts while using chloride the concentrations of 2,3,7,8-PCDD/Fs were in the range of ng L^{-1}.[125] Henceforth, the information will focus on chlorophenols owing to the fact that they are considered the main precursors of PCDD/Fs and, especially, on 2-CP. Chlorophenols constitute

an important group of organic substances (nineteen possible chlorinated phenols containing between 1 and 5 chlorines, Figure 1.6) characterized by low biodegradability, bactericidal activity, strong odor, phototoxicity and bioaccumulation ability in organisms.[126-128] All the CPs, are solid except for the 2-CP.

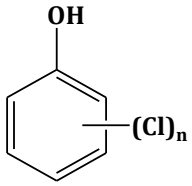

Figure 1.6. Scheme of chlorinated phenols where n=1-5. There are 19 different combinations.

Sources and treatment methods of chlorophenols

Chlorophenols can be found in a wide variety of environments as a consequence of their production, use or the degradation of other products. Not all the CPs are synthetized for industrial purposes: only monoCPs, 2,4-diCP, 2,4,6-triCP, 2,4,5-triCP, 2,3,4,5-tetraCP, 2,3,4,6-tetraCP and pentaCP.[99] These compounds find application in the preparation of herbicides, fungicides, bactericides, insecticides, wood and leather preservatives, pharmaceuticals, and dyes.[51,99,128-130] However, CPs have not only be found in industrial wastewaters, but also in ground and drinking waters as a consequence of the agricultural runoff, breakdown of the biocides, chlorination of water for disinfection and production of paper.

Consequently, the treatment of the effluents containing these pollutants is a matter of relevant and increasing concern due to their high production, fairly stable at 100 kt yr^{-1}, and because their degradation in aquatic streams does not occur in a natural way.[51] Microorganisms are not able to break down chlorophenols' structure that are present in water, soil and sediments even when they are at low concentrations or the biodegradation reactions occurs very slowly, with half-life of days or weeks.[99,131] Additionally, other possible pathway in which they could be naturally degraded in aquatic environment is by means of photolytic processes involving direct photolysis of CP and formation of ROS, which attack the chlorophenolic molecule. However, the photodegration occurs only in the upper

surface layer and depends on the season of the year, e.g., the half-life of 2,4-diCP varies from summer to winter (0.8 and 3 h, respectively). Furthermore, CPs are resistant to direct oxidation by oxygen dissolved in water. Finally, thermal treatments may result in the generation of other hazardous compounds. Therefore, alternative technologies able to remediate wastewaters polluted with this family of compounds (including their chemical products with a real application) are required. As it was previously mentioned, AOPs postulate as feasible technologies near ambient conditions to battle against the persistent and recalcitrant character of CPs as long as other toxic products are avoided.[126]

Health effects of chlorophenols

Toxicity of chlorophenol is given by the chlorination degree as well as the position of chlorine atoms.[99] The higher the number of chlorine substituents, the higher the toxicity. CPs with *meta* position substituted present higher toxicity than *para*- and *ortho*-CPs. They can affect the fauna and flora owing to their bactericidal activity, phytotoxicity and lipophilic character.[129] Some of the immediate effects observed in humans include irritation of nose, eyes, respiratory tract and skin.[130] Severe pathological modifications in the gastrointestinal tract, lungs, spleen, liver, kidneys, hepatic and cardiovascular systems have been found and they can cause dermatoses.[131] Experiments in rats confirmed that the exposure to some CPs showed an increase on carcinogenicity whereas cohort studies of people exposed to chlorophenols and phenoxy herbicides displayed higher levels of cancer mortality, respiratory cancer, ischemic heart diseases and so on.[99]

Legislation and regulations for chlorophenols

Even if the initial regulations from the European Economic Community (EEC) were generic in terms of the definition of pollutants, in 1976 the EEC published a directive regarding the pollution caused by certain dangerous substances discharges into aquatic system including organohalogen compounds (Table 1.5).[108] Afterwards, in 1980, the EEC stablished guide levels and maximum admissible concentration (MAC) in water intended for human consumption for phenols (MAC,

0.5 μg L^{-1}), and pesticides and related products (MAC, 0.1-0.5 μg L^{-1}), among others.[109] Pentachlorophenol was firstly included in the Directive 86/280/EEC.[112] It was in 2008 when European Commission (EC) started to talk about priority pollutants and they stablished environmental quality standards.[119] The most recent MAC-EQS values are gathered in the Directive 2013/39/EU, being 1 μg L^{-1} for pentaCP in inland and other surface waters and stablishing an annual average EQS of 0.4 μg L^{-1}.[106] Regarding the Spanish legislation, the values approved by the European Union for pentaCP have been ratified by the Spanish Ministry of Agriculture, Food and Environment by means of the Real Decreto 817/2015.[122]

With regard to the U.S. EPA regulations, they have developed two lists: a list of toxic pollutants and a list of priority pollutants. The Priority Pollutant List makes the list of toxic pollutants more usable, i.e., it is more practical for testing and for regulation and the chemicals are described by their individual chemical names, whereas the list of toxic pollutants, in contrast, contains open-ended groups of pollutants in which there is no test for the group as a whole, nor it is practical to regulate or test for all the compounds. The list of toxic pollutants includes 2-CP, 2,4-diCP, pentaCP and other chlorinated phenols.[132] 2,4,6-triCP has been listed as priority pollutant by the U.S. EPA together with the previously mentioned.[133] In the case of pentaCP a maximum contaminant level goal of 1 μg L^{-1} has been stablished with a public health goal of zero. Regarding the World Health Organization, they established guideline values for 2,4,6-triCP (200 μg L^{-1}) and pentaCP (9 μg L^{-1}) in drinking waters.[127]

1.4.3. Background on computational chemistry: application to the mechanisms of PCDD/Fs formation from precursors

Over the last decade, computer advances and the development of more sophisticated commercial packages have permitted the implementation of computational methods and basis sets to obtain high-accuracy molecular orbital calculations.[134] The computational chemistry allows researchers to investigate different parameters such as molecular geometry; energy of the molecules and

transition states; IR, UV and NMR spectra, the interaction of a substrate with an enzyme, the physical properties of substances; among others.[135] Therefore, the molecular modelling can provide enormous value not only to the organic, inorganic and analytical chemistry but also to the biochemistry.[136] Furthermore, the use of computational chemistry leads to faster results than experiments and it is environmentally safer. Computational studies may be carried out by means of different tools:[135-138]

i. Molecular mechanics is based on a model of a molecule as a collection of atoms held together by bonds. It is a fast calculation.
ii. *Ab initio* calculations (*from first principles*) are based on the Schrödinger equation (Equation 1.2) and, therefore, on the behavior of the electrons in a molecule, giving the energy of the molecule and the electronic distribution through the wave function which is not measurable or observable. These calculations are relatively slow.

$$\nabla^2\psi + \frac{8 \cdot \pi^2 \cdot m}{h^2} \cdot (E - V) \cdot \psi = 0 \qquad \text{(Eq. 1.2)}$$

where,

∇^2: Laplacian operator (Equation 1.3)

Ψ^2: probability density function (Equation 1.4)

m: mass of the particle

h: Planck's constant

E: total energy

V: potential energy

$$\nabla^2 = \frac{\partial^2}{\partial x^2} + \frac{\partial^2}{\partial y^2} + \frac{\partial^2}{\partial z^2} \qquad \text{(Eq. 1.3)}$$

$$\mathrm{Prob}(V) = \int_V \psi^2 \cdot dx \cdot dy \cdot dz \qquad \text{(Eq. 1.4)}$$

where,

P(V): probability of finding the particle somewhere in a volume V

iii. Semiempirical calculations are based on the Schrödinger equation as well. This method is parameterized with experimental values although it usually fits well even if there are not results for the specific system being calculated. It is faster than *ab initio* methods but slower than molecular quantum mechanics. The results are not as accurate as *ab initio* and density functional calculations.

iv. Density functional theory (DFT) is relatively new (1980's) and is based on the Schrödinger equation. Nevertheless, the electron distribution is calculated directly without determining the wave function, i.e., it is based on the charge or electron density which is a measurable value (electron diffraction or X-ray diffraction). This method is faster than *ab initio* but slower than Semiempirical calculations.

v. Molecular dynamics calculations are related to the laws of motion to molecules, finding application in the motion between enzyme-substrate and water molecules around a molecule of solute.

In general, *ab initio* and DFT calculations are recommended for the study of novel molecules that are not too big whereas semiempirical methods are adequate for larger molecules.[135,137] Molecular mechanics enable the calculation of geometries and energies of very large molecules such as proteins and nucleic acids although this method does not provide information about the electronic properties (Table 1.6).

Table 1.6. Features of the computational methods based on the works of Lewards (2010) and Irikura et al. (1998).[135,137]

Method	Applicability	Cost	Reliability
Molecular mechanics	Common organic; 100,000 atoms	Software: + Computer: -	Mean errors: +++; Maximum errors: ++
Semiempirical	Organic, some inorganic; 500 atoms	Software: + Computer: +	Mean errors: ++; Maximum errors: ++
Ab initio	All; 20 atoms	Software: +++ Computer: +++	Mean errors: ++; Maximum errors: +
DFT	All; 50 atoms	Software: +++ Computer: ++	Mean errors: ++; Maximum errors: +

Generally, *ab initio* and DFT methods are employed for quantum chemical calculations leading to good values of reliability. On the one hand, DFT calculations require lower computational time than advanced *ab initio* methods achieving the same accuracy. On the other hand, the use of bigger basis sets in the case of *ab initio* methods lead to more precise solutions whereas in the case of DFT the use of larger sets does not have big changes.[138] Both theories can be applied to obtain information about bond energies, ideal-gas thermochemistry, adsorption, solvation, reaction kinetics, properties of materials and analytical information. In order to obtain accurate results, it is especially important the correct selection of the basis sets, where methods such as MP2 (Møller–Plesset perturbation theory) and B3LYP (Becke, three-parameter, Lee-Yang-Parr exchange-correlation functional) are usually less demanding and enough satisfactory for structural optimizations. In the case of thermochemical calculations, with the aim of obtaining better accuracy, higher level methods are usually employed although in the case of PCDD/Fs it not practical.

Because of the high toxicity of PCDD/Fs and the complex reactions involved in their formation from precursors through the generation of transient species, some authors propose their theoretical study and the subsequent experimental validation.[138] As a consequence, there are many theoretical works published that study the most likely pathways in the formation of PCDD/Fs taking into account the energetic barriers when they are generated from precursors such as phenol, chlorophenols (single molecules or combination of different chlorophenols), catechol, chlorobenzenes, etc.[45,138-142] However, all the works published are referred to homogeneous or heterogeneous gas phase whereas studies for aqueous phase are lacking.

1.5. Background, thesis scope and outline

This thesis has as a starting point an earlier work developed at the Advanced Separation Process (ASP) group of the University of Cantabria. Vallejo et al. (2014) studied the generation and destruction of PCDD/Fs when AOPs were applied with the aim of treating model solutions of 2-CP (a known precursor of dioxins and furans) and real wastewaters from municipal solid waste landfill leachates.[143] Parameters such as total organic carbon, chemical oxygen demand and the identification of other intermediate products formed during the treatment process were evaluated. In this sense, the application of Fenton and electrochemical oxidation were assessed for both aqueous matrices. On the one hand, with regard to the model solution of 2-CP, it was observed that 2-CP is removed from the solution by means of Fenton and electrochemical oxidation, but the values of TOC and COD showed that it is not directly mineralized and, therefore, the generation of other organic oxidation intermediary and by-products is taking place. One of those products is the group of highly toxic PCDD/Fs, whose formation is more important in presence of chloride medium (Fenton and electrochemical oxidation) and when working under substoichiometric conditions (Fenton oxidation). Stronger oxidation conditions displace the reaction towards CO_2 and H_2O. On the other hand, regarding the treatment of landfill leachate both electrochemical and Fenton oxidation contribute to the diminishment of the initial TOC and COD. However, there was a different behavior in terms of PCDD/Fs, where electrochemical oxidation had a positive effect in their destruction. The Fenton process resulted in an increase with the treatment time likely due to the simultaneous presence of Fe^{2+}, Fe^{3+} and potential precursors of PCDD/Fs that may appear in the oxidation pathway.

Based on the previous results, the main goal of this thesis is to deepen in knowledge of the fundamentals that lead to the generation of PCDD/Fs working with 2-CP as precursor. Among different AOPs, Fenton oxidation has been applied as it is considered one of the most applied methods for the treatment of wastewaters containing recalcitrant compounds.[143-145] In order to further understand and complete the studies developed by the research group, the influence of the iron dose

has been assessed. Furthermore, whereas studies about the formation of PCDD/Fs in wastewaters are scarce and they are focused on homologue groups from tetra- to octa-PCDD/Fs, this thesis deepens in the formation of non-chlorinated and low-chlorinated DD/Fs (from mon- to tri-) to assist the identification of the reaction pathway that leads to PCDD/Fs in aqueous phase oxidation media. Additionally, due to the absence of mechanistic studies with regard to the formation of PCDD/Fs in aqueous samples, a mechanism proposal during the Fenton oxidation has been included based on the published computational studies applied to combustion and pyrolysis of 2-CP. Moreover, a brief notion about the theoretical study of the chlorination pathway of phenol and chlorophenols, together with the evaluation of how the solvation effect can affect the theoretical results regarding the energetic requirements in the formation of PCDD/Fs from 2-CP will be displayed.

On the other hand, the design and development of methods trying to rigorously identify and quantify radical species, including organic and inorganic such as reactive oxygen species, have been intensified as a consequence of the increasing use of AOPs in order to comprehend which are the main reactive species generated during the application of each AOP and how they can participate in the oxidation of the pollutants. In this sense, two different wide extended methods that are able not only to identify ROS but also organic radicals have been assessed, which may result in an added value to describe the formation of PCDD/Fs.

References

1. Muruganandham M, Suri RPS, Jafari S, Sillanpää M, Lee G-J, Wu JJ, Swaminathan M. Recent developments in homogeneous advanced oxidation processes for water and wastewater treatment. Int. J. Photoenergy 2014 (2014) Article ID 821674, 21 pages.

2. Fernández-Castro P, Vallejo M, San Román MF, Ortiz I. Insight on the fundamentals of advanced oxidation processes: Role and review of the determination methods of reactive oxygen species. J. Chem. Technol. Biotechnol. 90: 796-820 (2015).

3. Sanz J, Lombraña JI, De Luis A. State of art in advanced oxidation application to industrial effluents: New developments and future trends. Afinidad 70: 24-32 (2013).

4. Andreozzi R, Caprio V, Insola A, Marotta R. Advanced oxidation processes (AOP) for water purification and recovery. Catal. Today 53: 51-59 (1999).

5. Ortiz I, Mosquera-Corral A, Rodicio JL, Esplugas S. Advanced technologies for water treatment and reuse. AIChE J. 61: 3146-3158 (2015).

6. Oturan MA, Aaron J-J. Advanced oxidation processes in water/wastewater treatment: Principles and applications. A review. Crit. Rev. Environ. Sci. Technol. 44: 2577-2641 (2014).

7. Glaze WH, Kang J, Chapin DH. The chemistry of water treatment processes involving ozone, hydrogen peroxide and ultraviolet radiation. Ozone-Sci. Eng. 9: 335-352 (1987).

8. Yang X-J, Xu X-M, Xu J, Han Y-F. Iron oxychloride (FeOCl): An efficient Fenton-like catalyst for producing hydroxyl radicals in degradation of organic contaminants. J. Am. Chem. Soc. 135: 16058-16061 (2013).

9. Buxton GV, Greenstock CL, Helman WP, Ross AB. Critical review of rate constants for reactions of hydrated electrons, hydrogen atoms and hydroxyl radicals ($\cdot OH/\cdot O^-$) in aqueous solution. J. Phys. Chem. Ref. Data. 17: 513-886 (1988).

10. Munter R. Advanced oxidation processes–current status and prospects. Proc. Estonian Acad. Sci. Chem. 50: 59-80 (2001).

11. Gogate PR, Pandit AB. A review of imperative technologies for wastewater treatment I: Oxidation technologies at ambient conditions. Adv. Environ. Res. 8: 501-51 (2004).

12. Ribeiro AR, Nunes OC, Pereira MFR, Silva AMT. An overview on the advanced oxidation processes applied for the treatment of water pollutants defined in the recently launched Directive 2013/39/EU. Environ. Int. 75: 33-51 (2015).

13. Anglada Á, Urtiaga A, Ortiz I. Contributions of electrochemical oxidation to waste-water treatment: Fundamentals and review of applications. J. Chem. Technol. Biotechnol. 84: 1747-1755 (2009).

14. Munoz M, De Pedro ZM, Casas JA, Rodriguez JJ. Triclosan breakdown by Fenton-like oxidation. Chem. Eng. J. 198: 275-281 (2012).

15. Feng L, van Hullebusch ED, Rodrigo MA, Esposito G, Oturan MA. Removal of residual anti-inflammatory and analgesic pharmaceuticals from aqueous systems by electrochemical advanced oxidation processes. A review. Chem. Eng. J. 228: 944-964 (2013).

16. Urtiaga A, Fernandez-Castro P, Gómez P, Ortiz I. Remediation of wastewaters containing tetrahydrofuran. study of the electrochemical mineralization on BDD electrodes. Chem. Eng. J. 239: 341-350 (2014).

17. Bautista P, Mohedano AF, Casas JA, Zazo JA, Rodriguez JJ. An overview of the application of Fenton oxidation to industrial wastewaters treatment. J. Chem. Technol. Biotechnol. 83: 1323-1338 (2008).

18. Konstantinou IK, Albanis TA. TiO_2-assisted photocatalytic degradation of azo dyes in aqueous solution: Kinetic and mechanistic investigations: A review. Appl. Catal. B- Environ. 49: 1-14 (2004).

19. Cañizares P, Lobato J, Paz R, Rodrigo MA, Sáez C. Advanced oxidation processes for the treatment of olive-oil mills wastewater. Chemosphere 67: 832-838 (2007).

20. Oller I, Malato S, Sánchez-Pérez JA. Combination of advanced oxidation processes and biological treatments for wastewater decontamination—A review. Sci. Total Environ. 409: 4141-4166 (2011).

21. Zhou Q, Li W, Hua T. Removal of organic matter from landfill leachate by advanced oxidation processes: A review. Int. J. Chem. Eng. 2010 (2010) Article ID 270532, 10 pages.

22. Rizzo L. Bioassays as a tool for evaluating advanced oxidation processes in water and wastewater treatment. Water Res. 45: 4311-4340 (2011).

23. Primo O, Rivero MJ, Ortiz I. Photo-Fenton process as an efficient alternative to the treatment of landfill leachates. J. Hazard. Mater. 153: 834-842 (2008).

24. Anglada Á, Urtiaga AM, Ortiz I. Laboratory and pilot plant scale study on the electrochemical oxidation of landfill leachate. J. Hazard. Mater. 181: 729-735 (2010).

25. Pérez G, Saiz J, Ibañez R, Urtiaga AM, Ortiz I. Assessment of the formation of inorganic oxidation by-products during the electrocatalytic treatment of ammonium from landfill leachates. Water Res. 46: 2579-2590 (2012).

26. Tobajas M, Belver C, Rodriguez JJ. Degradation of emerging pollutants in water under solar irradiation using novel TiO_2-ZnO/clay nanoarchitectures. Chem. Eng. J. 309: 596-606 (2017).

27. Vallejo M, San Román MF, Irabien A, Ortiz I. Comparative study of the destruction of polychlorinated dibenzo-p-dioxins and dibenzofurans during Fenton and electrochemical oxidation of landfill leachates. Chemosphere 90: 132-138 (2013).

28. Vallejo M, Fresnedo San Román M, Ortiz I, Irabien A. Overview of the PCDD/Fs degradation potential and formation risk in the application of advanced oxidation processes (AOPs) to wastewater treatment. Chemosphere 118: 44-56 (2015).

29. Hancock FE. Catalytic strategies for industrial water re-use. Catal. Today 53: 3-9 (1999).

30. Fenton HJH. LXXIII.- oxidation of tartaric acid in presence of iron. J. Chem. Soc., T. 65: 899-910 (1894).

31. Koppenol WH. The centennial of the Fenton reaction. Free Radic. Biol. Med. 15: 645-651 (1993).

32. Haber F, Weiss J. The catalytic decomposition of hydrogen peroxide by iron salts. P. R. Soc. Lond. A-Conta. 147: 332-351 (1934).

33. Perez-Moya M, Graells M, del Valle LJ, Centelles E, Mansilla HD. Fenton and photo-Fenton degradation of 2-chlorophenol: Multivariate analysis and toxicity monitoring. Catal. Today 124: 163-171 (2007).

34. Bishop D, Stern G, Fleischman M, Marshall L. Hydrogen peroxide catalytic oxidation of refractory organics in municipal waste waters. Ind Eng Chem Proc DD. 7: 110-117 (1968).

35. Pignatello JJ, Oliveros E, MacKay A. Advanced oxidation processes for organic contaminant destruction based on the Fenton reaction and related chemistry. Crit. Rev. Environ. Sci. Technol. 36: 1-84 (2006).

36. Pliego G, Zazo JA, Garcia-Muñoz P, Munoz M, Casas JA, Rodriguez JJ. Trends in the intensification of the Fenton process for wastewater treatment: An overview. Crit. Rev. Environ. Sci. Technol. 45: 2611-2692 (2015).

37. Walling C. Fenton's reagent revisited. Acc. Chem. Res. 8: 125-131 (1975).

38. Diya'uddeen BH, Aziz AA, Daud W. On the limitation of Fenton oxidation operational parameters: A review. Int. J. Chem. React. Eng. 10: 1542-1580 (2012).

39. Chen R, Pignatello JJ. Role of quinone intermediates as electron shuttles in Fenton and photoassisted Fenton oxidations of aromatic compounds. Environ. Sci. Technol. 31: 2399-2406 (1997).

40. Bielski BHJ, Cabelli DE, Arudi RL, Ross AB. Reactivity of HO_2/O^{-}_2 radicals in aqueous solution. J. Phys. Chem. Ref. Data 14: 1041-1100 (1985).

41. Duesterberg CK, Waite TD. Process optimization of Fenton oxidation using kinetic modeling. Environ. Sci. Technol. 40: 4189-4195 (2006).

42. Venny, Gan S, Ng HK. Current status and prospects of fenton oxidation for the decontamination of persistent organic pollutants (POPs) in soils. Chem. Eng. J. 213: 295-317 (2012).

43. Lu M-C, Chang Y-F, Chen I-M, Huang Y-Y. Effect of chloride ions on the oxidation of aniline by Fenton's reagent. J. Environ. Manage. 75: 177-182 (2005).

44. Tang W, Huang C. 2, 4-dichlorophenol oxidation kinetics by Fenton's reagent. Environ. Technol. 17: 1371-1378 (1996).

45. Zhang H, Heung JC, Huang C. Optimization of Fenton process for the treatment of landfill leachate. J. Hazard. Mater. 125: 166-174 (2005).

46. Zazo JA, Pliego G, Blasco S, Casas JA, Rodriguez JJ. Intensification of the Fenton process by increasing the temperature. Ind. Eng. Chem. Res. 50: 866-870 (2011).

47. Deng Y, Englehardt JD. Treatment of landfill leachate by the Fenton process. Water Res. 40: 3683-3694 (2006).

48. Ruza J, Bordas M, Espinosa G, Puig A. Manual para la gestión de vertidos: Autorización de vertido. Ministerio de Medio Ambiente, Madrid (2007).

49. Yoon J, Lee Y, Kim S. Investigation of the reaction pathway of OH radicals produced by Fenton oxidation in the conditions of wastewater treatment. Water Sci. Technol. 44: 15-21 (2001).

50. Neyens E, Baeyens J. A review of classic Fenton's peroxidation as an advanced oxidation technique. J. Hazard. Mater. 98: 33-50 (2003).

51. Pera-Titus M, Garcıa-Molina V, Baños MA, Giménez J, Esplugas S. Degradation of chlorophenols by means of advanced oxidation processes: A general review. Appl. Catal. B-Environ. 47: 219-256 (2004).

52. De Laat J, Le TG. Effects of chloride ions on the iron(III)-catalyzed decomposition of hydrogen peroxide and on the efficiency of the Fenton-like oxidation process. Appl. Catal. B-Environ 66: 137-146 (2006).

53. Zuo Y, Holgne J. Formation of hydrogen peroxide and depletion of oxalic acid in atmospheric water by photolysis of iron(III)-oxalato complexes. Environ. Sci. Technol. 26: 1014-1022 (1992).

54. Nakagawa H, Yamaguchi E. Influence of oxalic acid formed on the degradation of phenol by Fenton reagent. Chemosphere 88: 183-187 (2012).

55. Canizares P, Paz R, Sáez C, Rodrigo MA. Costs of the electrochemical oxidation of wastewaters: A comparison with ozonation and Fenton oxidation processes. J. Environ. Manage. 90: 410-420 (2009).

56. Hermosilla D, Cortijo M, Huang C. The role of iron on the degradation and mineralization of organic compounds using conventional Fenton and photo-Fenton processes. Chem. Eng. J. 155: 637-646 (2009).

57. Umar M, Aziz HA, Yusoff MS. Trends in the use of Fenton, electro-Fenton and photo-Fenton for the treatment of landfill leachate. Waste Manage. 30: 2113-2121 (2010).

58. Tung C, Chang J, Hsieh Y, Hsu J, Ellis AV, Liu W, Yan R. Comparison of hydroxyl radical yields between photo-and electro-catalyzed water treatments. J. Taiwan Inst. Chem. E. 45: 1649-1654 (2014).

59. Gualandi I, Tonelli D. A new electrochemical sensor for OH radicals detection. Talanta 115: 779-786 (2013).

60. Bubacz K, Kusiak-Nejman E, Tryba B, Morawski A. Investigation of OH radicals formation on the surface of TiO_2/N photocatalyst at the presence of terephthalic acid solution. estimation of optimal conditions. J. Photochem. Photobiol. A 261: 7-11 (2013).

61. Hu Y, Lu Y, Zhou G, Xia X. A simple electrochemical method for the determination of hydroxyl free radicals without separation process. Talanta 74: 760-765 (2008).

62. Rivas FJ, Beltran FJ, Frades J, Buxeda P. Oxidation of p-hydroxybenzoic acid by Fenton's reagent. Water. Res. 35: 387-396 (2001).

63. Burns JM, Cooper WJ, Ferry JL, King DW, DiMento BP, McNeill K, Miller CJ, Miller WL, Peake BM, Rusak SA. Methods for reactive oxygen species (ROS) detection in aqueous environments. Aquat. Sci. 74: 683-734 (2012).

64. Page SE, Arnold WA, McNeill K. Terephthalate as a probe for photochemically generated hydroxyl radical. J. Environ. Monitor. 12: 1658-1665 (2010).

65. Bartosz G. Use of spectroscopic probes for detection of reactive oxygen species. Clin. Chim. Acta 368: 53-76 (2006).

66. Gomes A, Fernandes E, Lima JL. Fluorescence probes used for detection of reactive oxygen species. J. Biochem. Biophys. Meth. 65: 45-80 (2005).

67. Zhang B, Li-Xia Z, Jin-Ming L. Study on superoxide and hydroxyl radicals generated in indirect electrochemical oxidation by chemiluminescence and UV-visible spectra. J. Environ. Sci. 20: 1006-1011 (2008).

68. Newton GL, Milligan JR. Fluorescence detection of hydroxyl radicals. Radiat. Phys. Chem. 75: 473-478 (2006).

69. Nosaka, Y. and Nosaka, A. Y. (2013) Identification and Roles of the Active Species Generated on Various Photocatalysts. In Photocatalysis and Water Purification: From Fundamentals to Recent Applications (pp 3-24), Wiley-VCH Verlag GmbH & Co. KGaA, Weinheim, Germany.

70. Lu C, Song G, Lin J. Reactive oxygen species and their chemiluminescence-detection methods. TrAC-Trend Anal. Chem. 25: 985-995 (2006).

71. Sawyer DT, Valentine JS. How super is superoxide? Acc. Chem. Res. 14: 393-400 (1981).

72. Heller M, Croot P. Application of a superoxide (O^{2-}) thermal source (SOTS-1) for the determination and calibration of O^{2-} fluxes in seawater. Anal. Chim. Acta 667: 1-13 (2010).

73. Wu X, Lingyue M, Akiyama K. Chemiluminescence study of active oxygen species produced by TiO_2 photocatalytic reaction. Luminescence 20: 36-40 (2005).

74. He W, Liu Y, Wamer WG, Yin J. Electron spin resonance spectroscopy for the study of nanomaterial-mediated generation of reactive oxygen species. J. Food Drug Anal. 22: 49-63 (2014).

75. Shi H, Timmins G, Monske M, Burdick A, Kalyanaraman B, Liu Y, Clément J, Burchiel S, Liu KJ. Evaluation of spin trapping agents and trapping conditions for detection of cell-generated reactive oxygen species. Arch. Biochem. Biophys. 437: 59-68 (2005).

76. Adam W, Kazakov DV, Kazakov VP. Singlet-oxygen chemiluminescence in peroxide reactions. Chem. Rev. 105: 3371-3387 (2005).

77. Wu H, Song Q, Ran G, Lu X, Xu B. Recent developments in the detection of singlet oxygen with molecular spectroscopic methods. TrAC-Trend Anal. Chem. 30: 133-411 (2011).

78. DeRosa MC, Crutchley RJ. Photosensitized singlet oxygen and its applications. Coord. Chem. Rev. 233: 351-371 (2002).

79. Baier J, Fuß T, Pöllmann C, Wiesmann C, Pindl K, Engl R, Baumer D, Maier M, Landthaler M, Bäumler W. Theoretical and experimental analysis of the luminescence signal of singlet oxygen for different photosensitizers. J. Photochem. Photobio. B 87: 163-173 (2007).

80. Schweitzer C, Schmidt R. Physical mechanisms of generation and deactivation of singlet oxygen. Chem. Rev. 103: 1685-758 (2003).

81. World Health Organization. Air quality guidelines: global update 2005: particulate matter, ozone, nitrogen dioxide, and sulfur dioxide (2006).

82. Cederberg TL Assessment of dietary intake of dioxins and related PCBs by the population of EU Member States. European Commission (2000).

83. IARC Working Group on the Evaluation of Carcinogenic Risks to Humans, World Health Organization, & International Agency for Research on Cancer. Polychlorinated dibenzo-para-dioxins and polychlorinated dibenzofurans (Vol. 69). World Health Organization (1997).

84. Fiedler H Dioxins and furans (PCDD/PCDF). In Persistent Organic Pollutants (pp. 123-201). Springer Berlin Heidelberg (2003).

85. Esposito M, Tiernan T, Dryden F. Dioxins. US environmental protection agency. Cincinnati, OH (1980).

86. Shields WJ, Tondeur Y, Benton L, Edwards MR. 14 dioxins and furans. In Environmental Forensics: Contaminant Specific Guide, 293 (2010).

87. Kutz FW, Barnes DG, Bottimore DP, Greim H, Bretthauer EW. The international toxicity equivalency factor (I-TEF) method of risk assessment for complex mixtures of dioxins and related compounds. Chemosphere 20: 751-757 (1990).

88. Van den Berg M, Birnbaum LS, Denison M, De Vito M, Farland W, Feeley M, Fiedler H, Hakansson H, Hanberg A, Haws L, Rose M, Safe S, Schrenk D, Tohyama C, Tritscher A, Tuomisto J, Tysklind M, Walker N, Peterson RE. The 2005 world health organization reevaluation of human and mammalian toxic equivalency factors for dioxins and dioxin-like compounds. Toxicol. Sci. 93: 223-241 (2006).

89. Chemicals U. Dioxin and furan inventories: National and regional emissions of PCDD/PCDF. Geneva. UNEP Chemicals :22-23 (1999).

90. Kulkarni PS, Crespo JG, Afonso CA. Dioxins sources and current remediation technologies—a review. Environ. Int. 34: 139-153 (2008).

91. Dimmel DR, Riggs KB, Pitts G, White J, Lucas S. Formation mechanisms of polychlorinated dibenzo-p-dioxins and dibenzofurans during pulp chlorination. Environ. Sci. Technol. 27: 2553-2558 (1993).

92. Wang X, Ni Y, Zhang H, Zhang X, Chen J. Formation and emission of PCDD/Fs in chinese non-wood pulp and paper mills. Environ. Sci. Technol. 46: 12234-12240 (2012).

93. Holt E, Weber R, Stevenson G, Gaus C. Formation of dioxins during exposure of pesticide formulations to sunlight. Chemosphere 88: 364-370 (2012).

94. Weber R, Gaus C, Tysklind M, Johnston P, Forter M, Hollert H, Heinisch E, Holoubek I, Lloyd-Smith M, Masunaga S. Dioxin-and POP-contaminated sites—contemporary and future relevance and challenges. Environ. Sci. Pollut. Res. 15: 363-393 (2008).

95. Fiedler H, Hutzinger O, Welsch-Pausch K, Schmiedinger A, Umlauf G. Evaluation of the occurrence of PCDD/PCDF and POPs in wastes and their potential to enter the foodchain. Final Report. University of Bayreuth, Bayreuth (2000).

96. McKay G. Dioxin characterisation, formation and minimisation during municipal solid waste (MSW) incineration: Review. Chem. Eng. J. 86: 343-368 (2002).

97. Morales L, Dachs J, Fernández-Pinos M, Berrojalbiz N, Mompean C, González-Gaya B, Jiménez B, Bode A, Ábalos M, Abad E. Oceanic sink and biogeochemical controls on the accumulation of polychlorinated dibenzo-p-dioxins, dibenzofurans, and biphenyls in plankton. Environ. Sci. Technol. 49: 13853-13861 (2015).

98. Fernández J, Arjol MA, Cacho C. POP-contaminated sites from HCH production in Sabiñánigo, Spain. Environ Sci Pollut Res 20 :1937-50 (2013).

99. Czaplicka M. Sources and transformations of chlorophenols in the natural environment. Sci. Total Environ. 322: 21-39 (2004).

100. Ministerio de Agricultura, Alimentación y Medio Ambiente, Gobierno de España. Registro estatal de emisiones y fuentes contaminantes (PRTR). http://www.prtr-es.es/informes/pollutant.aspx (visited 18/11/2016).

101. Cederberg, TL. Assessment of dietary intake of dioxins and related PCBs by the population of EU Member States. European Commission. Brussel, Belgium (2000).

102. van Leeuwen FR, Younes M. Assessment of the health risks of dioxins: Re-evaluation of the tolerable daily intake (TDI). Food Addit. Contam. 17: 223-369 (2000).

103. Stockholm convention clearing house: Http://chm.pops.int/Implementation/PublicAwareness/10thAnniversary/tabid/2231/Default.aspx (consulted 18/11/2016).

104. Stockholm Convention. Stockholm convention on persistent organic pollutants (POPs) as amended in 2009: http://www.wipo.int/edocs/trtdocs/en/unep-pop/trt_unep_pop_2.pdf (consulted 18/11/2016).

105. Fiedler H, Abad E, van Bavel B, De Boer J, Bogdal C, Malisch R. The need for capacity building and first results for the Stockholm Convention global monitoring plan. TrAC-Trend Anal. Chem. 46: 72-84 (2013).

106. European Union. Directive 2013/39/EU of the European Parliament and of the Council of 12 August 2013 amending Directives 2000/60/EC and 2008/105/EC as regards priority substances in the field of water policy. Official Journal of the European Union (2013).

107. European Economic Community. Council Directive 75/440/EEC of 16 june 1975 concerning the quality required of surface water intended for the abstraction of drinking water in the member states as amended by Council Directive 79/869/EEC (further amended by Council Directive 81/855/EEC and Council Regulation 807/2003/EC) and both amended by Council Directive 91/692/EEC (further amended by Regulation 1882/2003/EC) (1975).

108. European Economic Community. Council Directive 76/464/EEC of 4 may 1976 on pollution caused by certain dangerous substances discharged into the aquatic environment of the community. Official Journal L 129: 23-29 (1976).

109. European Economic Community. Council Directive 80/68/EEC of 17 december 1979 on the protection of groundwater against pollution caused by certain dangerous substances. Official Journal 20: 43-48 (1980).

110. European Commission. Directive 80/778/EC relating to the quality of water intended for human consumption. Official Journal 229: 11-29 (1980).

111. European Economic Community. Council Directive 84/491/EEC of 9 october 1984 on limit values and quality objectives for discharges of hexachlorocyclohexane (1984).

112. European Economic Community. 86/280/EEC of 12 june 1986 on limit values and quality objectives for discharges of certain dangerous substances included in list I of the annex to directive 76/464/EEC. Official Journal L 181 (1986).

113. European Commission. Directive 2000/60/EC of the european parliament and of the council establishing a framework for the community action in the field of water policy (2000).

114. European Commission. Directive 2455/2001/EC of the european parliament and of the council of 20 november 2001 establishing the list of priority substances in the field of water policy and amending Directive 2000/60/EC. Official Journal 15: 1-5 (2001).

115. European Commission. Regulation (EC) no 850/2004 of the european parliament and of the council of 29 april 2004 on persistent organic pollutants and amending directive 79/117/EEC. Official Journal 158 (2004).

116. European Commission. Directive 2006/11/EC of the european parliament and of the council of 15 february 2006 on pollution caused by certain dangerous substances discharged into the aquatic environment of the community. Official Journal 64: 52-59 (2006).

117. European Commission. Directive 2006/118/EC of the European Parliament and of the Council of 12 december 2006 on the protection of groundwater against pollution and deterioration. Official Journal L 372: 19-31 (2006).

118. European Commission. Regulation (EC) no 166/2006 of the European Parliament and of the Council of 18 january 2006 concerning the establishment of a European pollutant release and transfer register and amending council directives 91/689/EEC and 96/61/EC text with EEA relevance. Official Journal 33: 1-17 (2006).

119. European Commission. Directive 2008/105/EC of the European Parliament and of the Council of 16 december 2008 on environmental quality standards in the field of water policy, amending and subsequently repealing. Official Journal 348: 84-97 (2008).

120. Subdirección General de Calidad del Aire y Prevención de Riesgos del Ministerio del Medio Ambiente, Gobierno de España. Plan nacional de aplicación del Convenio de Estocolmo y el Reglamento 850/2004, sobre contaminantes orgánicos persistentes (2004): http://www.pops.int/documents/implementation/nips/submissions/nip_spain.pdf (consulted 20/11/2016)

121. Ministerio de Medio Ambiente, Gobierno de España. Real decreto 508/2007, de 20 de abril, por el que se regula el suministro de información sobre emisiones del reglamento E-PRTR y de las autorizaciones ambientales integradas (BOE-A-2007-8351). 96: 17686-17703 (2007).

122. Ministerio de Agricultura, Alimentación y Medio Ambiente, Gobierno de España. Real decreto 817/2015, de 11 de septiembre, por el que se establecen los criterios de seguimiento y evaluación del estado de las aguas superficiales y las normas de calidad ambiental (BOE-A-2015-9806). 219: 80582-80677 (2015).

123. U.S. EPA. U.S. EPA 811-F-95-003C. National primary drinking water regulations: Contaminant specific fact sheets, synthetic organic chemicals. 1-62 (1995).

124. Vallejo M, San Román MF, Ortiz I, Irabien A. The critical role of the operating conditions on the Fenton oxidation of 2-chlorophenol: Assessment of PCDD/Fs formation. J. Hazard. Mater. 279: 579-585 (2014).

125. Vallejo M, San Román MF, Ortiz I. Quantitative assessment of the formation of polychlorinated derivatives, PCDD/Fs, in the electrochemical oxidation of 2-chlorophenol as function of the electrolyte type. Environ. Sci. Technol. 47:12400- 12408 (2013).

126. Detomaso A, Lopez A, Lovecchio G, Mascolo G, Curci R. Practical applications of the Fenton reaction to the removal of chlorinated aromatic pollutants. Environ. Sci. Pollut. Res. 10: 379-384 (2003).

127. World Health Organization. Guidelines for drinking-water quality. WHO Chron 38: 104-108 (2011).

128. Pizarro AH, Molina CB, Monsalvo VM, Mohedano AF, Rodríguez JJ. Biodegradabilidad de efluentes resultantes del tratamiento de clorofenoles mediante hidrodecloración catalítica. Ingeniería química 507: 56-60 (2012).

129. Muller F, Caillard L. Chlorophenols. Ullmann's encyclopedia of industrial chemistry (1986), Willey Online Library.

130. Desmurs J, Ratton S. Chlorophenols. kirk-othmer encyclopedia of chemical technology. 4th Edition (1993).

131. US Department of Health and Human Services. Toxicological profile for chlorophenols. Sciences International, Inc.: Research Triangle Institute, NC (1999).

132. U.S. EPA. Section 401.15 - toxic pollutants. Title 40- protection of environment.Chapter I- environmental protection agency (continued). Subchapter N- effluent guidelines and standards. Part 401- general provisions. https://www.gpo.gov/fdsys/pkg/CFR-2014-title40-vol29/xml/CFR-2014-title40-vol29-sec401-15.xml (consulted 29/11/2016).

133. U.S. EPA. Appendix A to part 423- 126 priority pollutants. Title 40- protection of environment. Chapter I- environmental protection agency (continued). subchapter N- effluent guidelines and standards. Part 423- steam electric power generating point source category. https://www.gpo.gov/fdsys/pkg/CFR-2014-title40-vol29/xml/CFR-2014-title40-vol29-part423-appA.xml (consulted 29/11/2016).

134. Omar S, Palomar J, Gómez-Sainero LM, Álvarez-Montero MA, Martin-Martinez M, Rodriguez JJ. Density functional theory analysis of dichloromethane and hydrogen interaction with Pd clusters: First step to simulate catalytic hydrodechlorination. J. Phys. Chem. C 115: 14180-14192 (2011).

135. Lewars EG. Computational chemistry: Introduction to the theory and applications of molecular and quantum mechanics. Springer Netherlands, 2nd Edition (2011).

136. Levine IN. Quantum chemistry (2000). Allyn Bacon, New York, USA..

137. Irikura KK, Frurip DJ. Computational thermochemistry. Washington, DC: American Chemical Society. 677: pp 212 (1998)

138. Altarawneh M, Dlugogorski BZ, Kennedy EM, Mackie JC. Mechanisms for formation, chlorination, dechlorination and destruction of polychlorinated dibenzo-p-dioxins and dibenzofurans (PCDD/Fs). Prog. Energy Combust. Sci. 35: 245-274 (2009).

139. Xu F, Yu W, Gao R, Zhou Q, Zhang Q, Wang W. Dioxin formations from the radical/radical cross-condensation of phenoxy radicals with 2-chlorophenoxy radicals and 2,4,6-trichlorophenoxy radicals. Environ. Sci. Technol. 44: 6745-6751 (2010).

140. Briois C, Ryan S, Tabor D, Touati A, Gullett BK. Formation of polychlorinated dibenzo-p-dioxins and dibenzofurans from a mixture of chlorophenols over fly ash: Influence of water vapor. Environ. Sci. Technol. 41: 850-856 (2007).

141. Mosallanejad S, Dlugogorski BZ, Kennedy EM, Stockenhuber M, Lomnicki SM, Assaf NW, Altarawneh M. Formation of PCDD/Fs in oxidation of 2-chlorophenol on neat silica surface. Environ. Sci. Technol. 50: 1412-1418 (2016).

142. Altarawneh M, Dlugogorski BZ. Formation of dibenzofuran, dibenzo-p-dioxin and their hydroxylated derivatives from catechol. Phys. Chem. Chem. Phys. 17: 1822-1830 (2015).

143. Vallejo Montes M. Assessment of polychlorinated dibenzo-p-dioxins and dibenzofurans, PCDD/Fs, in the application of advanced oxidation processes. Doctoral Thesis, University of Cantabria, Santander (2014).

144. Alonso Solana E. Contribución al tratamiento de lixiviados de vertedero de residuos sólidos urbanos mediante procesos de oxidación avanzada. Doctoral Thesis, University of Cantabria, Santander (2013).

145. Primo Martínez O. Mejoras en el tratamiento de lixiviados de vertedero de RSU mediante procesos de oxidación avanzada. Doctoral Thesis, University of Cantabria, Santander (2009).

Chapter 2

Materials & Methods

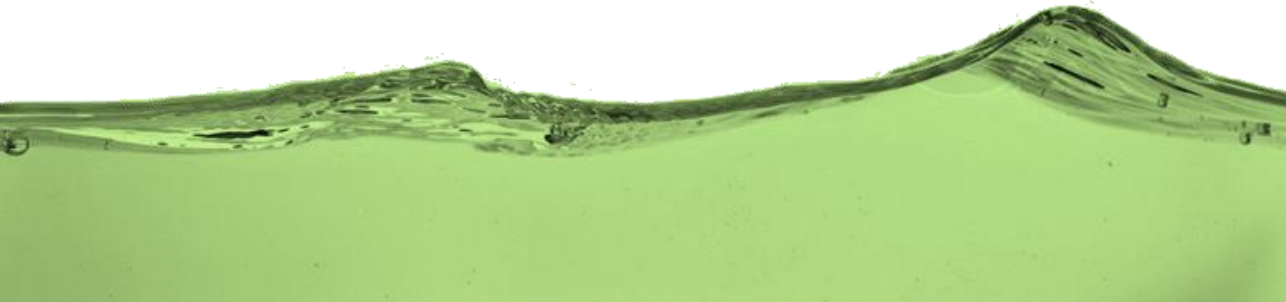

Chapter 2

Materials and Methods

Abstract

This chapter contains the characteristics of the chemicals employed during the development of the experimental part of present doctoral thesis, the procedure followed during the Fenton oxidation experiments as well as the analytical methods followed for the different analysis carried out such as total organic carbon and chemical oxygen demand measurements, identification of oxidation byproducts, quantification of PCDD/Fs and analysis of the radical species. The computational methods used during the theoretical calculations for the electrophilic halogenation of phenolic compounds and the study of the solvation effect in the generation of PCDD/Fs from 2-CP as precursor, are described in this section.

2.1. Chemical Reagents

Table 2.1 summarizes the chemicals used in the Fenton experiments as well as the standards utilized for the analytical measurements. The specific reagents applied for PCDD/Fs analysis are detailed in Table 2.2.

Table 2.1. List of the chemicals used in this thesis.

Name	Chemical Formula	Purity	Supplier
Acetic acid	$C_2H_4O_2$	100%	Merck
Acetonitrile	C_2H_3N	99.9%	Panreac
Ammonium Iron (II) sulfate (FAS)	$(NH_4)_2Fe(SO_4)_2{\cdot}6H_2O$	25%	Panreac
Ammonium molibdate	$(NH_4)_6Mo_7O_{24}{\cdot}4H_2O$	98%	Panreac
Benzoquinone	$C_6H_4O_2$	98%	Merck
Buffer solution pH 4	H_3PO_4-NaH_2PO_4		Panreac
Catechol	$C_6H_6O_2$	98%	Merck
2-Chlorobenzoquinone	$C_6H_3ClO_2$	95%	Sigma-Aldrich
3-Chlorocatechol	$C_6H_5ClO_2$	1 g L^{-1}	Spex Certiprep
2-Chlorophenol	C_6H_5ClO	99%	Sigma-Aldrich
2-Chlororesorcinol	$C_6H_5ClO_2$	97%	Sigma-Aldrich
2,4-Dichlorophenol	$C_6H_4Cl_2O$	99%	Sigma-Aldrich
2,6-Dichlorobenzoquinone	$C_6H_4Cl_2O$	99%	Sigma-Aldrich
Derquim MC Chromic Mixture			Panreac
5,5-Dimethyl-1-Pyrroline-N-Oxide	$C_6H_{11}NO$	>97%	Sigma-Aldrich Cayman Chem.
Dimethyl sulfoxide	C_2H_6SO	99.8%	Scharlau
2,4-dinitrophenylhidrazine	$C_6H_6N_4O_4$	99%	Sigma-Aldrich
DPD free chlorine	$(C_2H_5)_2NC_6H_4NH_2$		HACH
Ferroin	$C_{36}H_{24}FeN_6^{2+}$	0.025 M	Panreac
Formaldehyde	CH_2O	37-38%	Panreac
Formic acid	CH_2O_2	98%	Panreac
Fumaric acid	$C_4H_4O_4$	99%	Panreac
Hydrogen peroxide	H_2O_2	30%	Merck/Scharlab
Hydroquinone	$C_6H_6O_2$	99%	Panreac
Inorganic Carbon (IC) standard	Na_2CO_3 + $NaHCO_3$	0.5 g L^{-1}	Panreac

Table 2.1. List of the chemicals used in this thesis (continuation).

Name	Chemical Formula	Purity	Supplier
Inorganic anions	Cl^-, SO_4^{2-}	1 g L^{-1}	Merck
Iron sulfate 7-hydrate	$FeSO_4 \cdot 7H_2O$	99.5%	Panreac
Maleic acid	$C_4H_4O_4$	99%	Sigma-Aldrich
Malonic acid	$C_3H_4O_4$	99%	Merck
Methanol	CH_4O	Suprasolv	Merck
Methyl benzoate	$C_8H_8O_2$	99%	Alfa Aesar
Nitric acid	HNO_3	65%	Scharlau
Oxalic acid	$C_2H_2O_4$	99%	Panreac
Phenol	C_6H_6O	99%	Panreac
Phosphoric acid	H_3PO_4	85%	Panreac
Potassium dichromate	$K_2Cr_2O_7$	0.1 N	Merck
Potassium hydrogen phthalate	$C_8H_3KO_4$		Nacalai Tesque
Potassium iodide	KI	99%	Panreac
Silver sulfate solution	Ag_2SO_4	10 g L^{-1}	Panreac
Sodium bisulfite	$NaHSO_3$	40% w/v	Panreac
Sodium chloride	NaCl	99.5%	Panreac
Sodium hydroxide	NaOH	32% w/v	Panreac
Sodium thiosulfate	$Na_2S_2O_3$	0.1 N	Panreac
Sodium sulfate	Na_2SO_4	99%	Merck
Starch Solution		1%	Panreac
Sulfuric acid (Emsure)	H_2SO_4	98%	Merck-Millipore
2,3,6-trichlorophenol	$C_6H_3Cl_3O$	98%	Sigma-Aldrich
Total organic carbon standard	$C_8H_5O_4K$	1 g L^{-1}	Panreac

Table 2.2. Summary of the chemical reagents utilized for PCDD/Fs analysis.

Reagent	Supplier
Acetone (Suprasolv)	Merck-Millipore
Dichloromethane (Unisolv)	Merck-Millipore
Ethyl acetate(Pestinorm)	VWR Chemicals
Toluene (Unisolv)	Merck-Millipore
EPA 1613 CSL-CS5: calibration standard solutions	Wellington Lab.
EPA 1613 ISS: internal standard spiking solution	Wellington Lab.
EPA 1613 LCS: labelled compound stock solution	Wellington Lab.
EPA 1613 PAR: precision and recovery stock solution	Wellington Lab.
DDF-MDT: native PCDD/PCDF solution/mixture	Wellington Lab.
MDDF-MDT: mass-labelled PCDD/PCDF solution/mixture	Wellington Lab.

2.2. Fenton oxidation experiments

All experiments were conducted in a batch glass reactor under air pressure and magnetically stirred (700 rpm) with temperature control (RET basic IKA safety control, Figure 2.1). Iron sulfate heptahydrate ($FeSO_4 \cdot 7H_2O$) was added to the solution up to the desired Fe^{2+} dose and the Fenton reactions were carried out adjusting the initial pH of the solutions to 3.0 with nitric acid and sodium hydroxide. The experiments were initiated by adding the hydrogen peroxide dose of interest to the solution. Samples were periodically withdrawn and quenched with sodium bisulfite ($NaHSO_3$) to avoid further reactions.

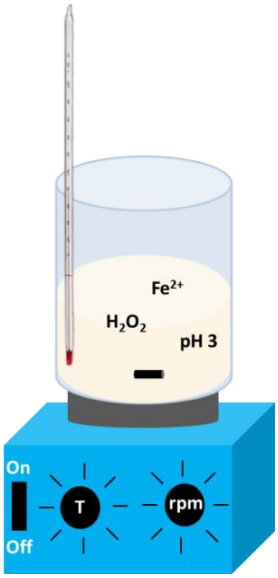

Figure 2.1. Experimental set-up scheme employed in Fenton oxidation.

2.3. Analytical measurements

2.3.1. Analysis of hydrogen peroxide

H_2O_2 was instantaneously measured just after the sample withdrawn by iodometric titration employing sodium thiosulfate.[1] A known volume of the sample is added to an Erlenmeyer flask containing 10 mL of a KI aqueous solution (1% w/v) and 10 mL of an acidic solution that is prepared by adding 0.18 g L^{-1} of $(NH_4)_6Mo_7O_{24}{\cdot}4H_2O$ to a 20% H_2SO_4 – 80% water (v/v) solution. The color of the solution turns yellowness and then, two/three drops of a starch solution are spiked acquiring a dark color. Afterwards, the solution is stirred and titrated with Na_2SO_3 until the color disappears. The concentration of H_2O_2 is calculated according to Equation 2.1.

$$C_{H_2O_2} = \frac{V_{Na_2S_2O_3} \cdot N_{Na_2S_2O_3}}{V_{sample}} \cdot \frac{MW_{H_2O_2}}{2} \qquad \text{(Eq. 2.1)}$$

where

C= concentration (mg L^{-1})

V= volume (mL)

N= normality (N)

MW= molecular weight (mg mol^{-1})

2.3.2. Analysis of chemical oxygen demand

Chemical oxygen demand (COD) was analyzed following a closed reflux titrimetric method.[2] The procedure consists of adding 1.5 mL of $K_2Cr_2O_7$ (0.04 M) and 3.5 mL of Ag_2SO_4 (10 g L^{-1}) to sulphuric acid into a vial together with 2.5 mL of sample. In the case of the blank solution, 2.5 mL of ultrapure (UP) water are added instead of the sample. Each solution is shacked until complete mixing and, then, it is digested (Thermoreactor TR300, Merck) at 150 ºC during 2 h (Figure 2.2). After the digestion and cooling down to room temperature, a ferroin indicator solution is added to every solution (including blank solution) and, afterwards, they are titrated with standard ferrous ammonium sulfate titrant (FAS, 0.02 M) freshly prepared everyday. The value of COD is obtained by Equation 2.2.

$$\text{COD as mg } O_2\ L^{-1} = \frac{(A - B) \cdot M \cdot 8000}{\text{mL sample}} \qquad \text{(Eq. 2.2)}$$

where

A= mL FAS used for blank

B= mL FAS used for sample

M= molarity of FAS, and

8000= milliequivalent weight of oxygen x 1000 mL L^{-1}

Figure 2.2. Digestion reactor (Thermoreaktor TR300, Merck).

2.3.3. Analysis of total organic carbon

Total organic carbon (TOC) was measured using a TOC analyzer Shimadzu TOC-V CPH with auto-sampler ASI-V (Figure 2.3). TOC is obtained subtracting inorganic carbon (IC) to total carbon (TC, Equation 2.3). The procedure followed by the analyzer for TC analysis consists on the introduction of 50 µL of sample into the TC combustion tube, where it is burned (680 ºC) and converted to carbon dioxide (CO_2). The sample is then transported by a carrier gas, which flows at a rate of 150 mL min^{-1}, to an electronic dehumidifier, a halogen scrubber and, finally, to the cell of a non-dispersive infrared (NDIR) gas analyzer, where the CO_2 is analyzed. The NDIR provides an analogue detection signal that forms a peak proportional to the TC concentration of the sample. The IC analysis is carried out by acidifying the sample with a small amount of hydrochloric acid to obtain a pH less than 3, where all carbonates are converted to carbon dioxide and detected by the NDIR. The equipment is configured to carry out 3 measurements and if the standard deviation is lower than 0.2, it provides the average TOC concentration. If not, it carries out two additional measurements and selects the three values with lower deviation. The calibration curve was made with TOC (500 mg L^{-1}) and IC standard solutions (50 mg L^{-1}).

$$\text{TOC (mg L}^{-1}) = \text{TC (mg L}^{-1}) - \text{IC (mg L}^{-1}) \qquad \text{(Eq. 2.3)}$$

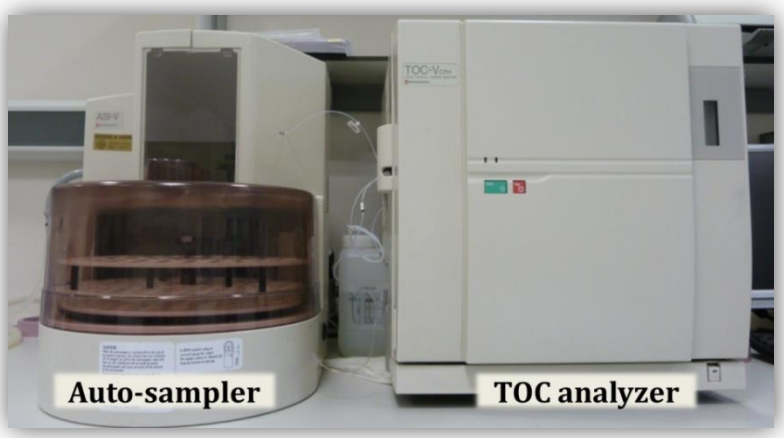

Figure 2.3. TOC analyzer Shimadzu TOC-V CPH with auto-sampler ASI-V.

2.3.4. Analysis of inorganic ions and organic acids

The analysis of chloride (Cl^-), chlorate (ClO_3^-) and aliphatic organic acids including acetic, formic, malonic, maleic, oxalic and fumaric acids were carried out by ion chromatography with anionic suppression using the chromatograph Dionex ICS-1100 with a conductivity cell detector (ASR-ULTRA model) (Figure 2.4). The system was run using a 25 µL sampling loop. The ions separation occurred on an IonPac AS9-HC 4 mm anion separation column at 30 °C. The suppressing system eliminates the conductivity due to the produced anions from the mobile phase using a column model P/N 53946. The samples were supplied to the system by means of a Dionex AS40 auto-sampler. The eluent was a 9 mM Na_2CO_3 solution at 1 mL min^{-1}. Anions were retained in the column and eluted at different retention times being registered in the detector. The signal from the detector was transformed into concentration by means of the calibration curves (in the range of 0.5 to 100 mg L^{-1}) of the measured compounds. The entire system was controlled by Chromeleon 6.8 software.

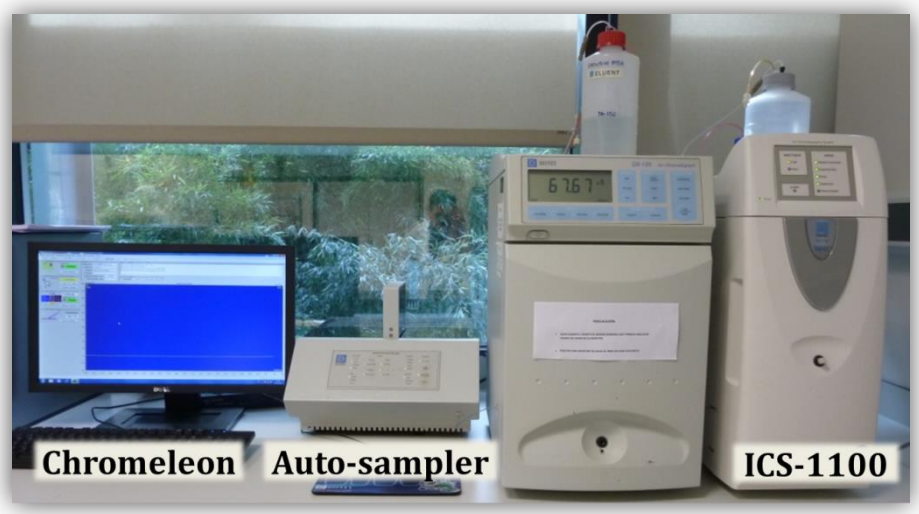

Figure 2.4. Ion chromatograph Dionex ICS-1100 equipped with a conductivity cell detector (ASR-ULTRA model).

2.3.5 Analysis of 2-chlorophenol and related aromatic compounds

2-CP and related aromatic compounds were analyzed by means of high performance liquid chromatography (HPLC) using a Waters 2690 HPLC coupled to a Waters 996 photo diode array (PDA) detector (Figure 2.5). The separation of CP, phenol, benzoic acid, catechol, chlorocatechol, hydroquinone, chlorohydroquinone, p-benzoquinone, 2-chloro-p-benzoquinone, 2,6-dichloro-p-benzoquinone, resorcinol, 2- and 4-chlororesorcinol took place on a Gemini C-18 separation column (L= 150 mm; $Ø_i$= 3 mm) using 4 mM H_2SO_4 as mobile phase with a flowrate of 1 mL min^{-1}. The selected wavelengths were 210 and 245 nm and the column temperature was kept at 50 ºC. Alternatively, the separation of 2,4- and 2,6-dichlorophenol, and 2,3,6-trichlorophenol occurred using 20% acetonitrile- 80% H_3PO_4 0.01 M as mobile phase at 1 mL min^{-1} with a flow gradient up to 80% acetonitrile- 20% H_3PO_4 in 2.5 min. The selected wavelengths were 210, 254 and 280 nm and the column temperature was 30 ºC. The signal from the detector was transformed into concentration by means of the calibration curves (in the range of 0.1 to 200 mg L^{-1}) of the measured compounds.

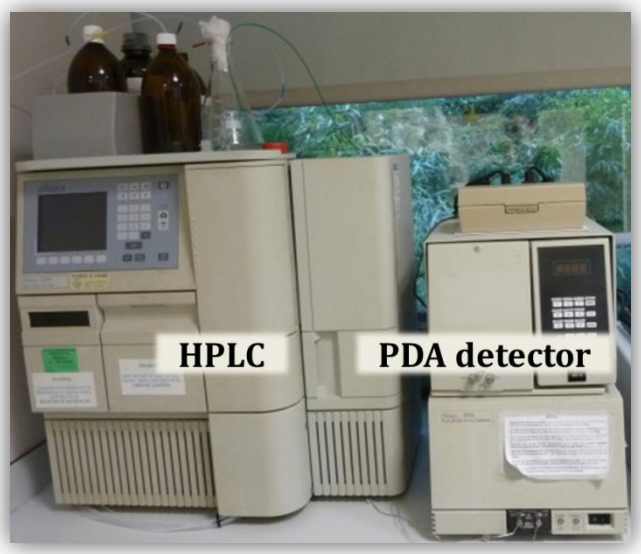

Figure 2.5. Waters 2690 HPLC coupled to a Waters 996 photo diode array (PDA) detector.

2.3.6. Qualitative screening of organics in the advanced oxidation of 2-CP

Qualitative screening (non-target analysis) for intermediate organic compounds formed during the Fenton oxidation of 2-chlorophenol solutions was performed by gas chromatography-mass spectrometry (GC-MS).[3] Samples (100 mL) were extracted twice with 50 ml of dichloromethane using a separatory funnel. The organic extract was concentrated up to 1 mL using a rotatory evaporator in a first step (Laborota 4000) and a N_2 stream in a second step. Finally, the concentrated extract was analyzed using a GC-MS Shimadzu QP2010 equipped with an auto-injector AOC-20i (Figure 2.6). The analytes were separated using a HP5 MS column (L= 30 m; Øi= 0.25 mm) with a film thickness of 0.1 mm. The temperature program of the GC–MS oven was 60 ºC, hold 3 min, rate 10 ºC min^{-1} to 270 ºC, hold 2.5 min. Helium was used as a carrier gas at a flow rate of 1 mL min^{-1}. A volume sample of 2 µL was injected in splitless mode and the injector temperature was set at 285 ºC. The mass spectrometer was operated in the electron impact ionization mode (70 eV). The transfer line and ion source temperatures were 290 and 230 ºC, respectively. Data acquisition was in full scan mode with a range from m/z 35 to 400. Confirmation of all structural assignments for the identified compounds was made using the NIST08 spectra library.

Figure 2.6. GC-MS Shimadzu QP2010 equipped with an auto-injector AOC-20i.

Additionally, a qualitative screening without an extraction process was carried out. 200 µL of the sample were flushed to a total volume of 10 mL with methanol and then analyzed by GC-MS. The main difference regarding the analysis of the organic extract is that a range from m/z 50 to 350 was selected to avoid the interference of H_2O, N_2, CO_2 with a corresponding m/z values of 18, 28 and 44, respectively. Furthermore, the volume sample injected was 2.5 µL instead of the 2 µL injected when the final Fenton sample was extracted with dichloromethane.

2.3.7. Analysis of the hydroxyl radical concentration by means of DMSO probe

The analysis of the concentration of hydroxyl radicals was performed according to Tai et al. (2004)[4] and U.S. EPA method 8315 A (1996)[5]. This method is based on a set of chain reactions that are initiated by the reaction between 2 mol of dimethyl sulfoxide (DMSO) and 2 mol of HO•, leading finally to 1 mol of formaldehyde (Reactions 2.1-2.3). Then, a derivatization procedure with 2,4-dinitrophenylhydrazine (DNPH) is carried out to produce the corresponding adduct formaldehyde-2,4-dinitrophenylhydrazine, HCHO-DNPH (Reaction 2.4), which is finally analyzed by HPLC-PDA. To evaluate the generation of ·OH in AOPs, the initial solution contains 0.267 M of DMSO in UP water.

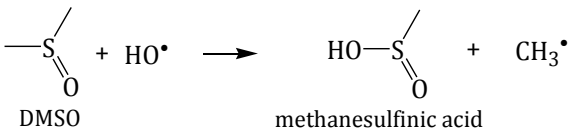

(2.1)

$$CH_3^{\bullet} + O_2 \longrightarrow CH_3OO\bullet \qquad (2.2)$$

$$2\ CH_3OO^{\bullet} \longrightarrow HCHO + CH_3OH + O_2 \qquad (2.3)$$

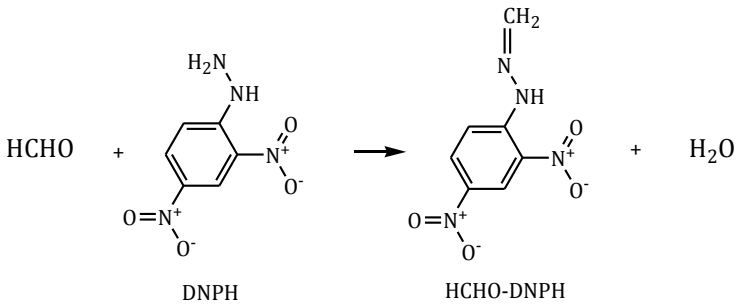

(2.4)

Standard solutions were prepared through the derivatization of formaldehyde solutions with known concentration: 2 mL of formaldehyde solution (or reaction sample) are mixed with 2.5 mL of pH 4.0 H_3PO_4-NaH_2PO_4 buffer solution, 0.2 mL of a 6 mM DNPH solution and is flushed to 5 mL with UP water. The mixture was maintained at room temperature for 30 min and analyzed using a Waters 2690 HPLC coupled to a Waters 996 PDA detector (Figure 2.5). Separation occurred with a XBridge C18 (5 µm, 4,6 mm x 250 mm) analytical column using a methanol/water mixture (60:40 v/v) as mobile phase with a flow-rate of 0.6 mL min^{-1}. The detection wavelength was 355 nm. The signal from the detector was transformed into concentration by means of the calibration curve obtained with formaldehyde standards (in the range 0.1-15 mg L^{-1}).

2.3.8. Analysis of radical species by EPR analysis

Inorganic and organic radicals have been identified by means of electroparamagnetic resonance spectrometry (EPR). EPR measurements were carried out on a Bruker EMX-X Band spectrometer at 100 kHz field modulation at room temperature (Figure 2.7a). Figure 2.7b depicts the scheme of an X-band EPR spectrometer. General instrument settings such as microwave power, modulation amplitude, receiver gain, etc. were modified between different experiments, so these values will be defined along the results section. The EPR spectra were obtained using a 2 mm thin wall precision quartz tube (Wilmad Labglasse 704-PQ-100 M). Approximately a sample of 18 µL was withdrawn at different oxidation times. 5,5-Dimethyl-1-pyrroline N-oxide (DMPO) was selected as spin trap owing to the fact

that it is one of the most common probes, it is cheaper and more commercially available than other spin traps. Different experiments in presence and absence of DMPO were conducted to assess the generation of inorganic and organic radical species during Fenton oxidation of 2-CP. Absolute measurements, in which the absolute EPR signal intensity is directly converted to a concentration without the need of a reference sample, were conducted based on the integrated intensity of the EPR absorption signal (two integrations). Bis Diphenyl Allyl-Benzene Complex (BDPA) was used to calibrate the spectrometer's signal channel reference phase and modulation amplitude in order to obtain maximum sensitivity, minimum distortion, and quantitatively reproducible measurements.

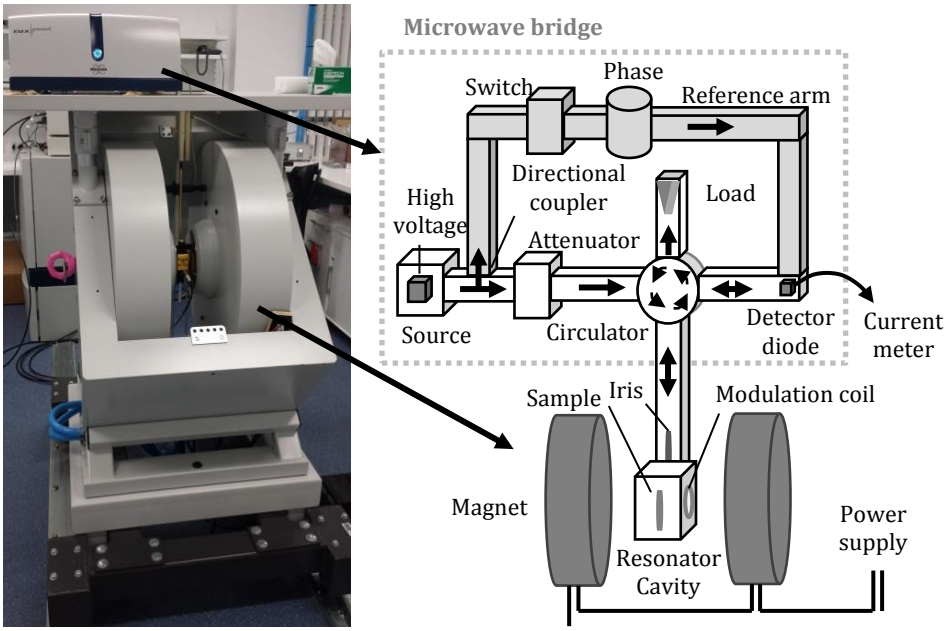

(a) (b)

Figure 2.7. (a) Bruker EMX-X band spectrometer; (b) Scheme of an X-band EPR spectrometer according to Hagen (2008).[6]

The energy differences in EPR spectroscopy are predominantly due to the interaction of unpaired electrons with a magnetic field (Zeeman effect), resulting in a magnetic moment with the highest and lowest energy when the electron moment

is aligned with or against the magnetic field, respectively.[7,8] One of the characteristics parameters is the g-factor which indicates the energy between the two spin levels as a function of the magnetic field applied, and whose value is approximately equal to 2 for most samples (Equation 2.4).

$$\Delta E = h \cdot \nu = g \cdot \beta \cdot B_0 \qquad \text{(Eq. 2.4)}$$

where

h= Planck constant: $6.626 \cdot 10^{-34}$ J s

ν = frequency of the radiation (MHz)

β = constant Bohr magneton: $9.274 \cdot 10^{-28}$ J G^{-1}, and

B_0= magnetic field (Gauss, G)

The unpaired electron is very sensitive to its local surroundings, i.e., the electron may be affected by a local magnetic field produced by the nuclei of the atoms and molecules, which is called hyperfine interaction.[7, 8] For nuclei, the number of lines (n) of the EPR signal due to the local magnetic field of a nearby nucleus is equal to 2I+1, where 'I' represents the spin quantum of the nucleus (Figure 2.8). The distance between the peaks is known as the hyperfine splitting constant or hyperfine splitting (a).

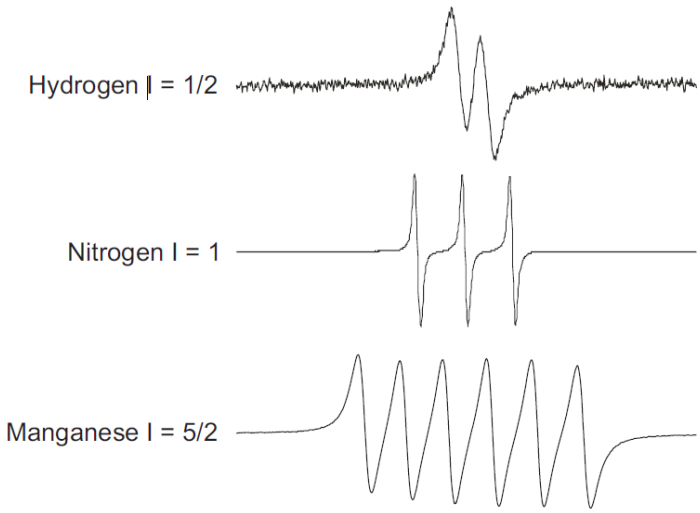

Figure 2.8. Number of lines as a function of the spin quantum number.[7]

Taking as an example DMPO-·OH, the construction of the hyperfine pattern would be represented by Figure 2.9.

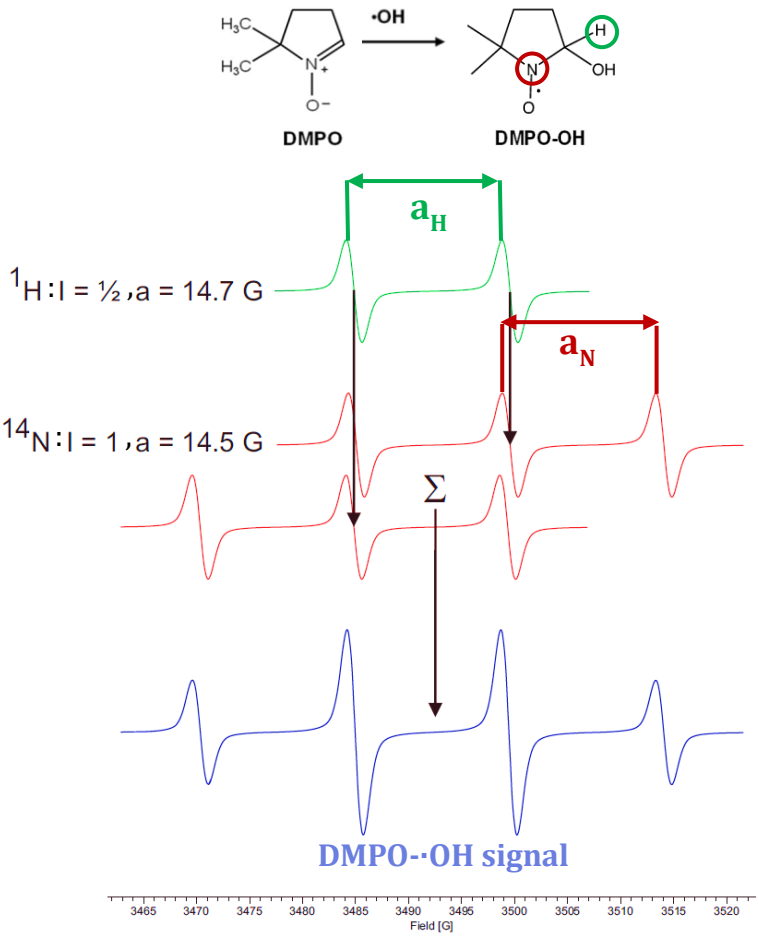

Figure 2.9. Construction of the hyperfine pattern of the DMPO-OH adduct.[7]

This figure represents in green the doublet corresponding to the β proton (I= 1/2, n= 2) and the distance between both peaks is the hyperfine splitting (a_H= 14.7 G). That doublet signal is further split into two triplets (I= 1, n= 3) by the nitroxide nitrogen, with a distance between signals a_N= 14.5 G, which would lead to 6 signals. However, because the hyperfine splitting's a_H and a_N are almost the same, when all the peaks are summed, a signal of 4 peaks with an intensity ratio 1:2:2:1 is obtained.[7,8]

Stopped-flow experiments

A SFM-3000 stopped flow equipment (Biologic) was used to conduct Fenton experiments and analyze the generation of radical species immediately after the addition of the Fenton reagents (Figure 2.10).

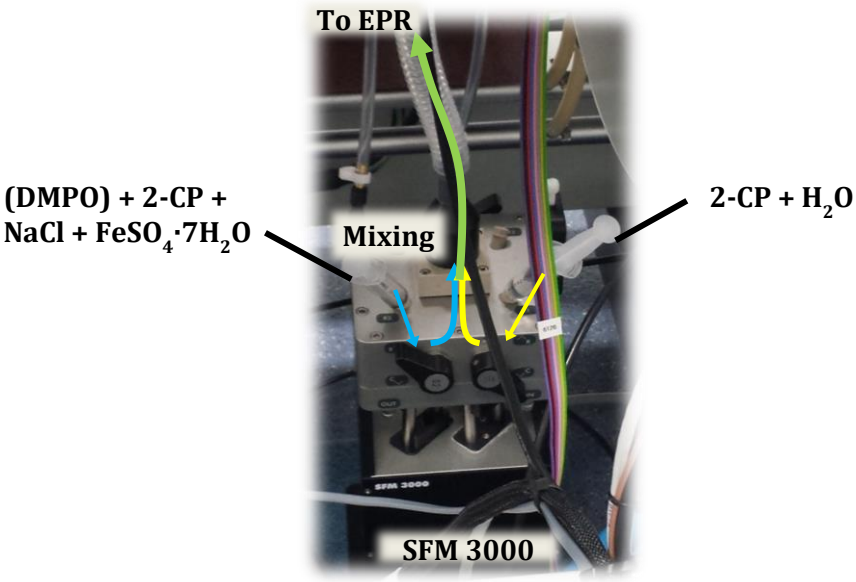

Figure 2.10. Stopped flow SFM-3000 connected to a Bruker EMX spectrometer.

Although this equipment is commonly used for kinetic studies, it was used to favor mixing. Two different solutions were prepared and dosed in the syringes, one containing the iron salt and 2-CP, and the other one containing H_2O_2, 2-CP, NaCl and DMPO. The concentrations used will be described in the results section. The Biokine software controlled the MPS-70/3 unit, which includes the syringes operation, i.e., mixing ratio, total volume/shot and total flow rate. A special fitting was designed to connect the multi-mixer (SFM-3000), located next to the EPR, to a Blaubrand® Intramark 7087 33 Green capillary tube with an internal diameter of 0.43 mm. This capillary tube was introduced in the resonator cavity (active volume 23 mm long, Figure 2.7b) resulting in a sample analysis volume of 3.34 µL. A volume of 754 µL per shot was selected to ensure that the reaction solution reached the EPR tube, keeping the ratio between both streams 1:1 and a total flow rate equal to 2 mL s^{-1}.

2.3.9. FTIR-ATR

Attenuated total reflection used in conjunction with Fourier transform infrared (FTIR-ATR) spectroscopy enables samples to be analyzed directly in the liquid or solid state without additional preparation. A Pike GladiATR coupled to a Cary 670 FTIR (Agilent technologies, Figure 2.11) was used during the application of Fenton oxidation to characterize the type of bonds present in the aqueous solution, working with two different types of detectors: i) DLaTGS (deuterated L-alanine doped triglycine sulfate), and ii) MCT (mercury cadmium telluride), having the latter higher sensitivity when IR yield is low or higher analysis rates are required. Samples were withdrawn at 0 s, 10 s and each 3 min 20 s, and one drop of the Fenton solution was placed in the detector prior to each analysis (60 scans, MIR source 4 cm^{-1} at 4000 cm^{-1}).

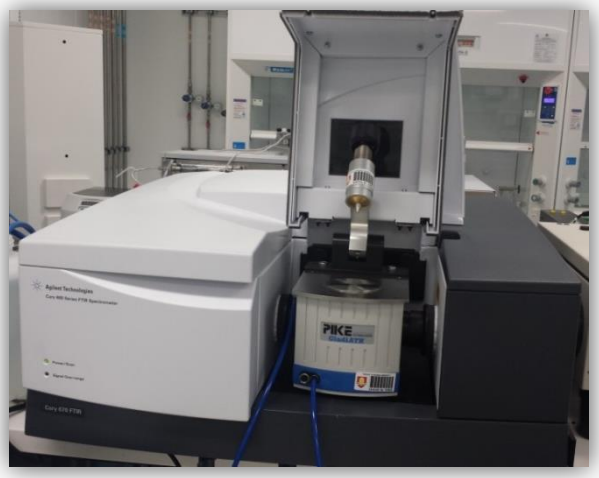

Figure 2.11. Pike GladiATR coupled to a Cary 670 FTIR (Agilent Technologies).

2.3.10. Analysis of PCDD/Fs

PCDD/Fs were determined according to the Standard Method U.S. EPA 1613 (1994)[9] by isotope dilution and high resolution gas chromatography/high resolution mass spectrometry (HRGC-HRMS). All the steps are briefly summarized in Figure 2.12 and fully described below.

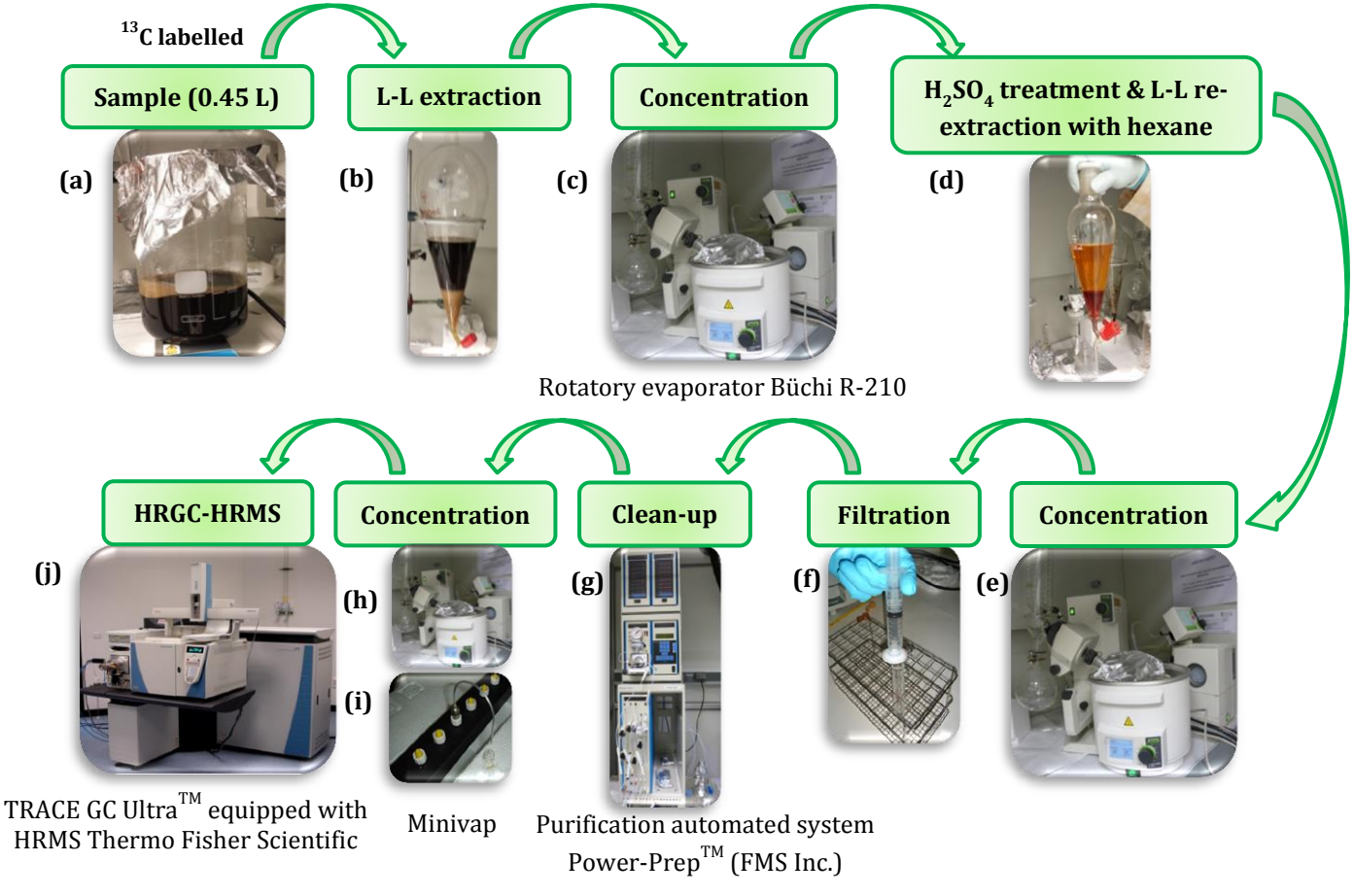

Figure 2.12. Analytical methodology scheme for the determination of PCDD/Fs.

This method consisted of a set of stages that requires a rigorous follow up of each step: extraction, concentration and purification steps prior to the analysis by high resolution gas chromatography coupled to high resolution mass spectrometry (HRGC-HRMS). Different standard solutions have been employed during the quantification and quality assurance in the analysis of PCDD/Fs: labelled compound solution, LCS; precision and recovery solution, PAR; and internal standard solution, ISS.

Extraction of PCDD/Fs

Samples (0.45 L) were spiked with 10 µL of a 15 ^{13}C-labelled PCDD/Fs solution (EPA 1613 LCS, from TCDD/Fs to OCDD/Fs; Table IV.1, Annex IV) and 5 µL of mass-labelled PCDD/Fs standard, prepared from the 100-times dilution of the commercial MDDF-MDT standard (unchlorinated and from mono- to tri-CDD/Fs, Table IV.2, Annex IV), dissolved in acetone and mixed by carefully shaking with a stirrer (Vortex 2x^3, Velp scientifica). Original labelled standards were in nonane solution, so their solution in acetone let their subsequent solution in water in such a way that the whole preparation process was the same for both native PCDD/Fs generated during the experiments and the added mass-labelled PCDD/Fs (Figure 2.12a). Labelled standards have been used in order to know the recovery after the preparation of the sample and the analysis, which allowed re-calculating the concentration of the native PCDD/Fs present in the solution by comparison between the same compounds labelled or not. The vial that contains the labelled PCDD/Fs solution was washed three times with dichloromethane and added to the aqueous sample of interest. Then, PCDD/Fs were extracted from aqueous phase with three portions of 60 mL and 1 portion of 30 mL aliquots of dichloromethane using a 2 L separatory funnel (Figure 2.12b).

Concentration

The organic extract (dichloromethane) was concentrated in a rotatory evaporator Büchi R-210 (Figure 2.12c) near to dryness at T= 34 ºC and P= 750-600

mbar. Afterwards, the extract is rinsed with dichloromethane and concentrated again near to dryness. This procedure was carried out three times.

H_2SO_4 treatment

Samples with high quantity of co-extracted organic matter (those that were not clear) were treated with H_2SO_4. In these situations, the evaporated extracts were transferred to n-hexane, treated with 50 mL of H_2SO_4 and extracted with 75 mL of n-hexane (Figure 2.12d). This procedure was realized twice. If hexane extractions had still co-extracted organic matter, an additional H_2SO_4 treatment was done (20-30 mL). The organic phase was then dried with Na_2SO_4.

Concentration

The organic phase (n-hexane) was concentrated in the rotatory evaporator at T= 35 ºC and P= 600-300 mbar (Figure 2.12e). Next, the extract was rinsed with n-hexane and concentrated again near to dryness in triplicate. The later rinsed process was concentrated to approximately 1-2 mL.

Filtration

The concentrated extract was filtered through a 0.45 µm PTFE filter and transferred to 12 mL of n-hexane (Figure 2.12f).

Extract clean-up

A solid-liquid adsorption chromatography using the automated system Power-Prep™ (Fluid Management Systems Inc., Waltham) was implemented to purify the extract (Figure 2.12g). Power-Prep is based on the sequential use of multilayer silica, basic alumina and PX-21 carbon adsorbents. The extract was pumped from the vial through the columns using next solvents and their mixtures: n-hexane, n-hexane/dichloromethane (98/2 v/v), n-hexane/dichloromethane (50/50 v/v), toluene/ethyl acetate (50/50 v/v) and toluene. The purified extract was collected in 75 mL of toluene.

Concentration and drying

Toluene was evaporated in the rotatory evaporator at T= 50 ºC and P= 150-85 mbar near to dryness (Figure 2.12h). Next, the extract was rinsed with toluene and evaporated again near to dryness in triplicate. Then, it was transferred into a vial to be concentrated to dryness under a nitrogen stream in a minivap unit (Figure 2.12i).

HRGC-HRMS analysis

Purified samples were analyzed by the Chromatography Service (SERCROM) of the University of Cantabria. Before the chromatographic analysis, internal syringe standards (EPA 1613 ISS; Table IV.1, Annex IV) were added to the sample. The analysis realized by HRGC-HRMS on a Trace Ultra™ gas chromatograph equipped with a split/splitless injector (Figure 2.12j, Thermo Electron S.p.A.) and a DB-5 MS fused silica capillary column (J&W Scientific). The initial temperature of the column, 120 ºC, was kept constant for 2 min and then it was increased sequentially in 3 steps to (i) 210 ºC, 230 ºC and 310 ºC at 15, 1 and 3 ºC min^{-1}, respectively, for the analysis from tetra- to octa-CDD/Fs; and to (ii) 212, 232 and 233 ºC at 6, 1 and 0.5 ºC min^{-1} for the analysis of non-chlorinated DD/F and from mono- to tri-CDD/Fs. The column was connected through a heated transfer line kept at 270 ºC to a DFS high-resolution magnetic sector mass spectrometer with a BE geometry (Figure 2.12j). A positive electron ionization (EI+) mode with ionization energy of 45 eV was used in the source and its temperature was set at 270 ºC. The mass spectrometer was operated in the SIM mode at 10,000 resolution power (10% valley definition). Detection limits were calculated as the concentration values that gave instrumental responses within a signal-to-noise ratio of 3. Quantitative determination was carried out by the isotopic dilution method. Relative response factors (RRFs), obtained from the calibration curve by analyzing 1613CSL and 1613CS-1–CS-4 (Table IV.3, Annex IV) standard solution mixtures for tetra- to octa-PCDD/Fs and the dilutions prepared from the DDF-MDT (in the range 0.5-200 ng mL^{-1}; Table IV.2, Annex IV) for non-chlorinated and mono- to tri-CDD/Fs, were used to determine the target compounds concentration in the samples. The recoveries of labelled standards were

calculated using a mixture of two labelled PCDD/Fs included in the ISS that are added to the samples before the chromatographic analysis.

2.3.11. Quality control and quality assurance (QC/QA) in the analysis of PCDD/Fs

The main objective of the QC/QA was the verification of the accuracy, recoveries and the absence of contamination during the analysis. Several precision and recovery experiments were performed using UP water spiked with PCDD/Fs isotopically labelled, 1-2 ng EPA 1613 LCS (Table V.1, Annex V), and native PCDD/Fs, 20-200 pg EPA 1613 PAR (Table V.1, Annex V). Furthermore, blank experiments were carried out with UP water spiked with LCS standard (1-2 ng).

The relative standard deviations (RSD) in the analyses of UP water spiked with a known amount of native PCDD/Fs were in the range 10.7-17.5% for OCDF and 1,2,3,7,8,9-HxCDD (Table V.1, Annex V), respectively. In addition, the recoveries of labelled PCDD/Fs ranged from 75.6 to 93% for 2,3,7,8-TCDF^{13}C and 1,2,3,7,8-PeCDD^{13}C (Table V.2 Annex V), respectively, all within the limits stablished by EPA method (Table V.3, Annex V). Hence, acceptable precision and recoveries in the analysis of PCDD/Fs were achieved.

The results from the blank experiments showed that the concentrations of native PCDD/Fs were in most cases below the detection limit (Table V.1, Annex V) indicating the absence of contamination. On the other hand, average recoveries of labelled PCDD/Fs were in the range 76.8-91.2% for 2,3,7,8-TCDF^{13}C and 1,2,3,4,7,8,9-HpCDF^{13}C, respectively (Table V.2, Annex V). Consequently, the analytical methodology setup fulfils the acceptance criteria stablished by EPA 1613 Method (Table V.3, Annex V).[9] Likewise, the recoveries obtained during the Fenton oxidation experiments were inside the range proposed by EPA 1613 Method.

2.4. Computational calculations

2.4.1. Electrophilic halogenation of phenolic compounds in aqueous and gas phase

Density functional theory (DFT) calculations have been performed using DMol[3] implemented in Materials Studio 8.0.[10] As it was previously mentioned in the introductory section, DFT methods lead to good values of reliability and are recommended for molecules that are not too big, requiring lower computational time than *ab initio* calculations. Geometry optimization was conducted using the Generalized Gradient Approximation (GGA) level and Perdew and Wang's 1991 gradient-corrected correlation functional (PW91), with the double numerical plus *d*-functions (DND) basis set. In order to provide a benchmark of accuracy for obtained GGA properties, obtained Hirshfeld charge distributions and Fukui indices of electrophilic attack, $f^{-1}(\vec{r})$ for unsubstituted phenol, were contrasted with analogous values evaluated with the more timely consuming Becke-Lee-Yang-Parr (BLYP) correlation functional (Figure 2.13).[11] Fukui indices have been applied for assessing the chemical reactivity of a compound, where the higher electrophilic Fukui value for one atom in a molecule implies higher probability of that atom to be halogenated; whereas Hirshfeld is one of the methods for computing atomic charges.[12,13] Fine quality with a convergence tolerance of $1 \cdot 10^{-5}$ Ha has been selected. For the calculations in aqueous phase, the solvation model has been used and the conductor-like screening model (COSMO) has been selected to assess the solvation effect.

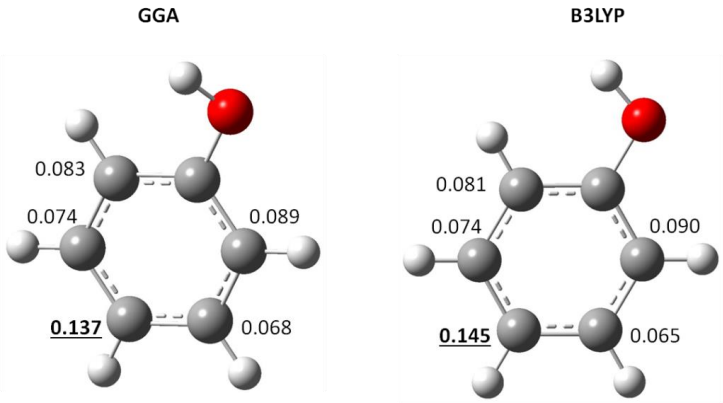

Figure 2.13. Fukui indices of electrophilic attack, f^{-1} (r), predicted by GGA and B3LYP functional.

2.4.2. Study of the solvation effect and reaction with H_2O during PCDD/Fs from 2-CP as precursor

As in the previous section, DFT calculations implemented in Materials Studio 8.0 were carried out. Geometry and energy optimization together with transition state searching were conducted using a GGA/PW91 level with the DND basis set. The energy results for gas phase were compared with those presented by Altarawneh et al. (2007), which were calculated by means of the software Gaussian 03 through DFT calculations selecting B3LYP/6-311+G(3df,2p) level of theory for the geometry or B3LYP/6-31G(d) for energy calculations, prior to the study of the solvation effect, and the effect of H_2O as reactant in gaseous phase, leading to comparable values with an acceptable deviation of ± 2 kcal mol^{-1}.[14] Additionally, in that calculations in which the obtained values were far from the already published with regard to gas phase, the software Gaussian 09 with the functional M062X (based on GGA approximation) and 6-311G(d,p) level of theory was employed. Owing to the higher time consumption of the latter, a supercomputer belonging to the National Computational Infrastructure of Australia was used for the quantum calculations.

References

1. Primo Martínez O. Mejoras en el tratamiento de lixiviados de vertedero de RSU mediante procesos de oxidación avanzada. Doctoral Thesis, University of Cantabria, Santander (2009).

2. APHA, AWWA, WEF, American Public Health Association/Water Environment Federation. Standard Methods for Examination of Water and Wastewater. Washington, DC, USA. 20th ed. (1998).

3. Vallejo Montes M. Assessment of polychlorinated dibenzo-p-dioxins and dibenzofurans, PCDD/Fs, in the application of advanced oxidation processes. Doctoral Thesis, University of Cantabria, Santander (2014).

4. Tai C, Peng J, Liu J, Jiang G, Zou H. Determination of hydroxyl radicals in advanced oxidation processes with dimethyl sulfoxide trapping and liquid chromatography. Anal. Chim. Acta 527: 73-80 (2004).

5. EPA Method 8315A (SW-846). Determination of carbonyl compounds by high performance liquid chromatography (HPLC). revision 1 (1996).

6. Hagen WR. Biomolecular EPR spectroscopy. CRC press. Boca Raton, FL (2008).

7. Ralph T. Weber. Xenon User's guide: Manual version 1.3. (2011).

8. Weil JA, Bolton JR. Electron paramagnetic resonance: Elementary theory and practical applications. John Wiley & Sons, Hoboken, NJ. 2nd Edition (2007).

9. EPA Method 1613. Tetra-trough octa-chlorinated dioxins and furans by isotope dilution HRGC-HRMS. U.S. Environmental Protection Agency. Office of water. engineering and analysis division (4303). Washington, DC (1994)

10. Delley B. From molecules to solids with the $DMol^3$ approach. J. Chem. Phys. 113: 7756-7764 (2000).

11. Perdew JP, Chevary JA, Vosko SH, Jackson KA, Pederson MR, Singh DJ, Fiolhais C. Atoms, molecules, solids, and surfaces: Applications of the generalized gradient approximation for exchange and correlation. Phys. Rev. B 46: 6671-6687 (1992).

12. Altarawneh M, Dlugogorski BZ. Formation and chlorination of carbazole, phenoxazine, and phenazine. Environ. Sci. Technol. 49: 2215-2221 (2015).

13. Thanikaivelan P, Padmanabhan J, Subramanian V, Ramasami T. Chemical reactivity and selectivity using Fukui functions: Basis set and population scheme dependence in the framework of B3LYP theory. Theor. Chem. Acc. 107: 326-335 (2002).

14. Altarawneh M, Dlugogorski BZ, Kennedy EM, Mackie JC. Quantum chemical investigation of formation of polychlorodibenzo-p-dioxins and dibenzofurans from oxidation and pyrolysis of 2-chlorophenol. J. Phys. Chem. A 111: 2563-2573 (2007).

Chapter 3

Assessment of PCDD/Fs formation during the Fenton oxidation of 2-chlorophenol

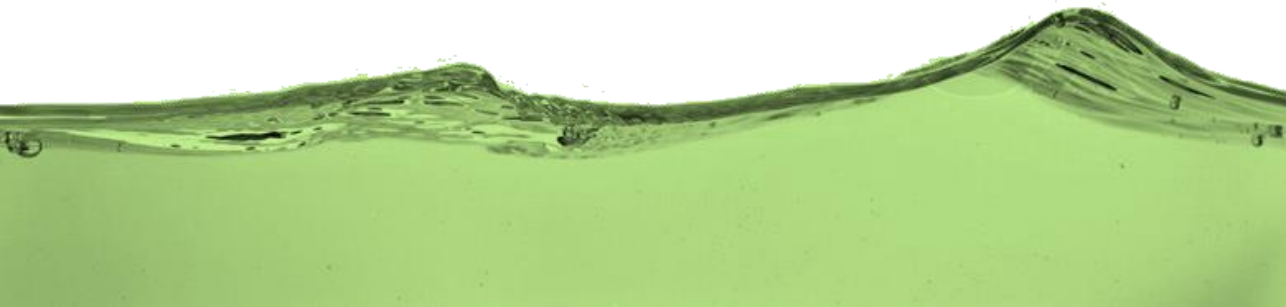

Chapter 3

Assessment of PCDD/Fs formation during the Fenton oxidation of 2-chlorophenol

Abstract

Owing to the fact that reactive oxygen species (ROS) play a fundamental role during the application of advanced oxidation processes, a section covering the experimental study of several indirect methods to identify and quantify the generation of ROS based on the use of dimethyl sulfoxide (DMSO) and 5,5-Dimethyl-1-pyrroline N-oxide (DMPO) as molecular probes has been included. The Fenton oxidation of 2-CP aqueous solutions has been studied in terms of the removal yield of the target compound, the abatement of TOC and COD, and the identification of the main byproducts generated during the advanced treatment. In this sense, the influence of different operational variables such as chloride ions, iron dose as well as addition of a copper salt has been assessed. Then, the effect that these operating parameters together with the treatment time have on the formation PCDD/Fs during the Fenton treatment of 2-CP will be described. Finally, the results obtained along the present thesis and those obtained previously by the Advanced Separation Process research group will be compared.

3.1. Characterization of the oxidation medium

Advanced oxidation processes are based on the generation of powerful oxidant species. The identification and quantification of the main radicals generated during AOPs may help to understand what is happening in the reaction media. As it has been previously mentioned, hydroxyl radicals (·OH) are the most reactive ROS, and they have been more widely studied as the variety of methods available for their identification reflects.[1] On the other hand, regarding superoxide/hydroperoxyl radical ($O_2^{-\bullet}/HO_2^{\bullet}$) and singlet oxygen ($^1O_2$), their generation is usually more characteristic of photocatalytic and photosensitization reactions, respectively. In this sense, because this thesis is focused on the application of Fenton oxidation, the assessment of the generation of radical species will be centered mainly on the analysis of ·OH radicals by means of the reaction with the molecular probes DMSO and DMPO. In the case of DMSO, additional results when electrochemical oxidation is applied are gathered in Annex VI. With regard to DMPO, it allowed the identification of ·OH and other radical species when Fenton oxidation is conducted, as it will be reported later.

3.1.1. Assessment of DMSO as molecular probe for the identification of ·OH

The use of dimethyl sulfoxide as molecular probe to identify and quantify ·OH reports certain advantages such as the good selectivity of the reaction between DMSO-·OH, simplicity and sensitivity of the method, or presence of only one quantitative product (Table III.1, Annex III).[1] However, it has some weaknesses such as the derivatization time needed before the analysis or even the fact that both DMSO and HCHO (the quantitative product) may be degraded by UV/H_2O_2. Along this point, the results obtained in Fenton oxidation will be displayed.

Fenton oxidation

The first step consisted in the repetition of the original methodology to check its reproducibility, i.e., to check whether the methodology presented by Tai et al. (2004) was replicable.[2] That work assessed the generation of hydroxyl radicals by

means of Fenton and Fenton-like reactions (Reactions 3.1 and 3.2), carrying out their indirect measurement with DMSO as molecular probe (Reactions 3.3 and 3.4).

$$Fe^{2+} + H_2O_2 \rightarrow Fe^{3+} + HO^{\bullet} + HO^{-} \qquad k = 76\ M^{-1}s^{-1} \tag{3.1}$$

$$Fe^{3+} + H_2O_2 \rightarrow Fe^{2+} + HO_2^{\bullet} + H^{+} \qquad k = 0.01\ M^{-1}s^{-1} \tag{3.2}$$

$$2\ DMSO + 2\ HO\cdot \rightarrow HCHO \tag{3.3}$$

$$HCHO + DNPH \xrightarrow{derivatization} HCHO - DNPH \tag{3.4}$$

As it has been explained in the "Materials and Methods" section, the Fenton experiments carried out in this thesis were conducted in a glass reactor magnetically stirred adding initially DMSO, iron salt and hydrogen peroxide (Figure 3.1a). Figure 3.1b presents the results obtained by Tai et al. (2004) working with 267 mM DMSO, 8 mM H_2O_2 and 0.2 mM $(NH_4)_2Fe(SO_4)_2{\cdot}6H_2O$, those obtained in the laboratory under the same conditions, and the results varying the iron source ($FeSO_4{\cdot}7H_2O$).

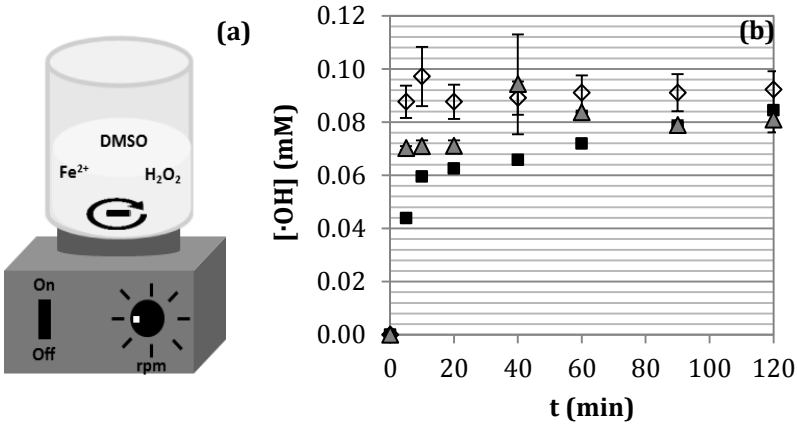

Figure 3.1. (a) Scheme of the Fenton oxidation system; (b) $[\cdot OH]_{generated}$ during the Fenton oxidation of 267 mM DMSO, 8 mM H_2O_2 and 0.2 mM Fe^{2+}. ■ $(NH_4)_2Fe(SO_4)_2{\cdot}6H_2O$, Tai et al. (2004);[2] △ $(NH_4)_2Fe(SO_4)_2{\cdot}6H_2O$, laboratory; and ◇ $FeSO_4{\cdot}7H_2O$, laboratory. Common experimental conditions: V_t, 0.1 L; pH_0, 3; T ambient; stirring rate, 300 rpm.

The results obtained in the laboratory were very similar to those published previously by Tai et al. (2004) when the same iron salt was employed, $(NH_4)_2Fe(SO_4)_2{\cdot}6H_2O$, so it can be concluded that the methodology is reproducible (Figure 3.1b). On the other hand, instead of $(NH_4)_2Fe(SO_4)_2{\cdot}6H_2O$ as iron source $FeSO_4{\cdot}7H_2O$ was tested, leading to similar results and, therefore, showing that there is no influence of the tested iron source for these two iron salts (Figure 3.1b).

As it was previously mentioned in the "Materials and Methods" section, sodium bisulfite was added to quench the residual H_2O_2 present in the samples withdrawn from Fenton experiments. Nonetheless, the interference of $NaHSO_3$ in the HPLC analysis was found due to the reaction of bisulfite with HCHO, which is the product employed to quantify the ·OH generated (Reactions 3.1 and 3.3).[3-5] Hence, the procedure followed consisted on mixing the reaction sample with the pH 4.0 buffer solution and the DNPH solution (Reaction 3.4).

Once confirmed the reproducibility of the method followed by Tai et al. (2004), the next step consisted on its application to the experimental conditions of interest that will be employed for the Fenton oxidation of 2-CP, in a way that the concentration of hydroxyl radicals generated may help to understand and describe the change in general parameters such as 2-CP, COD, TOC and the formation of PCDD/Fs. As a consequence, the H_2O_2 dose was raised to 40.44 mM while the iron dose was varied in the range 0.09-1.44 mM, which are the conditions applied during the Fenton treatment of 2-CP solution. The Fenton oxidation of a solution containing the molecular probe leads to the cumulated concentration of ·OH displayed in Figure 3.2.

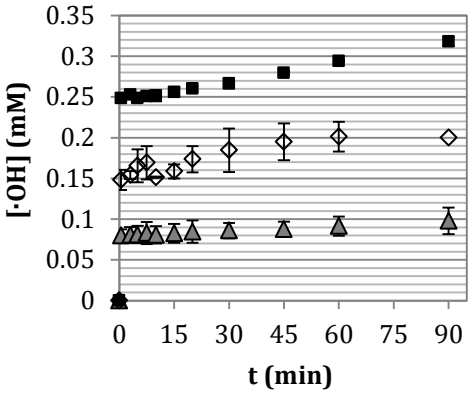

Figure 3.2. Generation of hydroxyl radical employing different iron doses: △ 0.09 mM, ◇ 0.18 mM and ■ 0.36 mM $FeSO_4 \cdot 7H_2O$. Common experimental conditions: $[DMSO]_0$, 267 mM; $[H_2O_2]_0$, 40.44 mM; $[NaCl]_0$, 56.3 mM; V_t, 1 L; pH_0, 3; T ambient; stirring rate, 700 rpm.

The higher the iron dose, the higher the hydroxyl radicals concentration. However, their concentration did not follow a significant increase after the initial measurement at 30 s, especially for the lowest iron dose. In addition, the concentrations observed are in the range 0.1-0.32 mM, far from the maximum concentration theoretically expected taking into account the Reaction 3.1, i.e., starting from 40.44 mM H_2O_2 it could be expected a maximum of 40.44 mM ·OH without considering side reactions or the regeneration from ferric to ferrous salt (Reaction 3.2); with reference to the maximum potential concentration the obtained yield was in the range 0.26-0.79%.

Afterwards, with the aim of ascertaining what was happening in the reaction system, the concentration of hydrogen peroxide was followed when 0.18 mM Fe(II) and 1.44 mM Fe(II) were employed. Figure 3.3 depicts the monitoring of H_2O_2 concentration during the Fenton reaction of different solutions containing the Fenton reagents, DMSO and/or chloride (used also during the Fenton oxidation of 2-CP) for both iron doses.

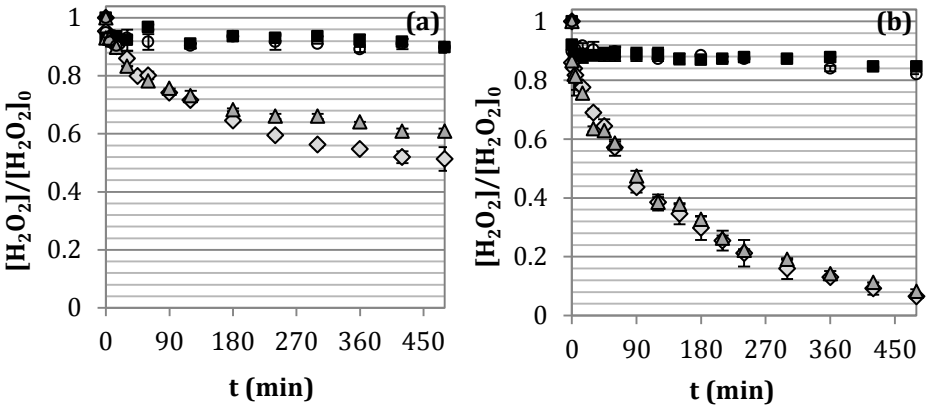

Figure 3.3. Monitoring of H_2O_2 concentration during the Fenton oxidation employing (a) 0.18 mM or (b) 1.44 mM $FeSO_4 \cdot 7H_2O$ under the following conditions: ◇ 40.44 mM H_2O_2; ■ 40.44 mM H_2O_2 + 267 mM DMSO; △ 40.44 mM H_2O_2 + 56.3 mM NaCl; and ○ 40.44 mM H_2O_2 + 267 mM DMSO + 56.3 mM NaCl. Common experimental conditions: V_t, 1 L; pH_0, 3; T ambient; stirring rate, 700 rpm.

It can be observed (Figure 3.3a) that under the presence of DMSO or DMSO + Cl^-, the concentration of H_2O_2 had a slight initial decrease and, then, kept invariable during at least 8 hours. However, when the system was composed only by the Fenton reagents (H_2O_2 + Fe(II)) or the Fenton reagents and chloride, the decomposition of H_2O_2 took place following the typical profile (Figure 3.3a).[6,7] Additionally, the same experiments were carried out but increasing the iron dose up to 1.44 mM, which showed the same behavior in terms of H_2O_2 depletion (Figure 3.3b): i) no change in H_2O_2 concentration when DMSO is present in the solution and ii) depletion of H_2O_2 in absence of DMSO. The influence of the iron salt can be clearly appreciated in Figure 3.4, in which the decreasing trend of H_2O_2 was represented for different solutions containing (or not) DMSO and/or chloride.

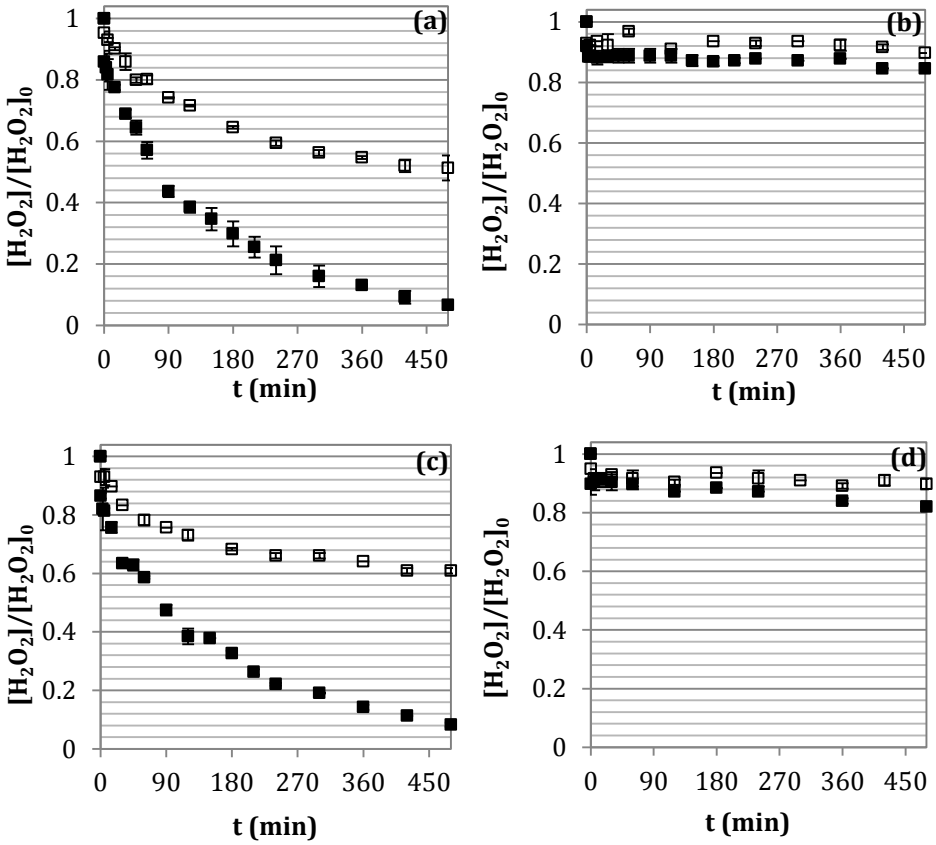

Figure 3.4. Comparison of the H_2O_2 depletion working with 0.18 mM Fe_2SO_4 (empty symbols) or 1.44 mM Fe_2SO_4 (filled symbols). (a) 40.44 mM H_2O_2, (b) 40.44 mM H_2O_2 + 267 mM DMSO, (c) 40.44 mM H_2O_2 + 56.3 mM NaCl, and (d) 40.44 mM H_2O_2 + 267 mM DMSO + 56.3 mM NaCl. Common experimental conditions: V_t, 1 L; pH_0, 3; T ambient; stirring rate, 700 rpm.

In those experiments in which DMSO was added, slight variations were observed that may be due to the error associated with the analysis (Figure 3.4b and d). Nevertheless, as it could be expected, increasing the concentration of the catalyst in the absence of DMSO the decomposition rate of H_2O_2 is also augmented (Figure 3.4a and c).

From the results obtained and presented along this point, it can be inferred that DMSO or an immediate oxidation product is interacting with iron in a way that it hinders the catalysis of the hydrogen peroxide decomposition and, therefore, the

generation of hydroxyl radicals that would react with DMSO to yield formaldehyde. Previous studies on the oxidation of DMSO by means of the Fenton reagent showed its almost complete degradation but only when working with iron concentrations higher than the corresponding to DMSO.[8-10] In those cases in which the iron dose is lower than the concentration of DMSO, the latter decreased as a function of the Fe(II) employed.[9-11] Some of the literature related to Fenton oxidation showed that there is a plateau region in the oxidation of DMSO, which coincides with the plateau region in the concentration of H_2O_2 displayed in Figures 3.3 and 3.4 for 0.18 mM Fe(II), but there is no explanation for the phenomena involved in the reaction system other than postulating higher efficiency when iron dose is increased.[9-11]

Matira et al. in a recent paper published in 2015 followed the presence of iron in the oxidation state Fe(II) during the Fenton oxidation of DMSO, and observed that after the initial reaction time it was not present anymore.[8] The results obtained by Matira et al. (2015) could be explained taking into account that the regeneration from Fe(III) to Fe(II) is slow (Reactions 3.1 and 3.2) and once Fe(II) is regenerated it is back consumed, but also taking into consideration that the complexation of Fe(III) with DMSO or with an oxidation product may be also occurring. The maximum concentration of ·OH depicted in Figure 3.2 shows similar values to the corresponding initial concentration of Fe(II), obtaining one mole of ·OH per mole of Fe(II). Although in this thesis the unavailability of Fe(II) has not been assessed, it seems that once Fe(II) is oxidized to Fe(III) the Fenton reaction stops. According to the experimental data (Figure 3.4a and c), the inhibition of the Fenton oxidation is not caused by the formation of inorganic complexes between iron-oxygenated species or iron-chlorine species since the hydrogen peroxide keeps reacting. However, according to the data published in literature, there are some organics such as oxalic acid that have the ability to complex iron, thus preventing the redox cycle Fe^{2+}/Fe^{3+}.[12,13] With regard to the oxidation of DMSO, the oxidation products formerly described have been methanesulfinate, methanesulfonate and formate along with formaldehyde, although there is no available information about their possible role as complexation agents for iron (II or III).[8,14] In this sense, the only

published data with regard to DMSO complexes is related to the formation of complexes like $[Fe(DMSO)_6](ClO_4)_3 \cdot DMSO$ and $FeCl_3 \cdot 2DMSO$ that are characterized by a yellow-green and yellow color, respectively.[15,16] A good example of the changes taking place in the reactor is given in Figure 3.5 that compares the coloration before and after starting the Fenton oxidation, which could indicate the formation of organometallic complexes of iron.

(a) **(b)**

Figure 3.5. Coloration of the Fenton system (a) before and (b) after the addition of 40.4 mM H_2O_2. Experimental conditions: $[DMSO]_0$, 267 mM; $[FeSO_4 \cdot 7H_2O]_0$, 1.44 mM; $[NaCl]_0$, 56.3 mM; V_t, 1 L; pH_0, 3; T, ambient; stirring rate, 700 rpm.

Additional experiments were developed increasing the temperature up to 70 ºC. Figure 3.6 displays the results obtained by increasing the temperature from 20 to 70 ºC, assessing the influence of adding DMSO and chloride to the reaction medium.

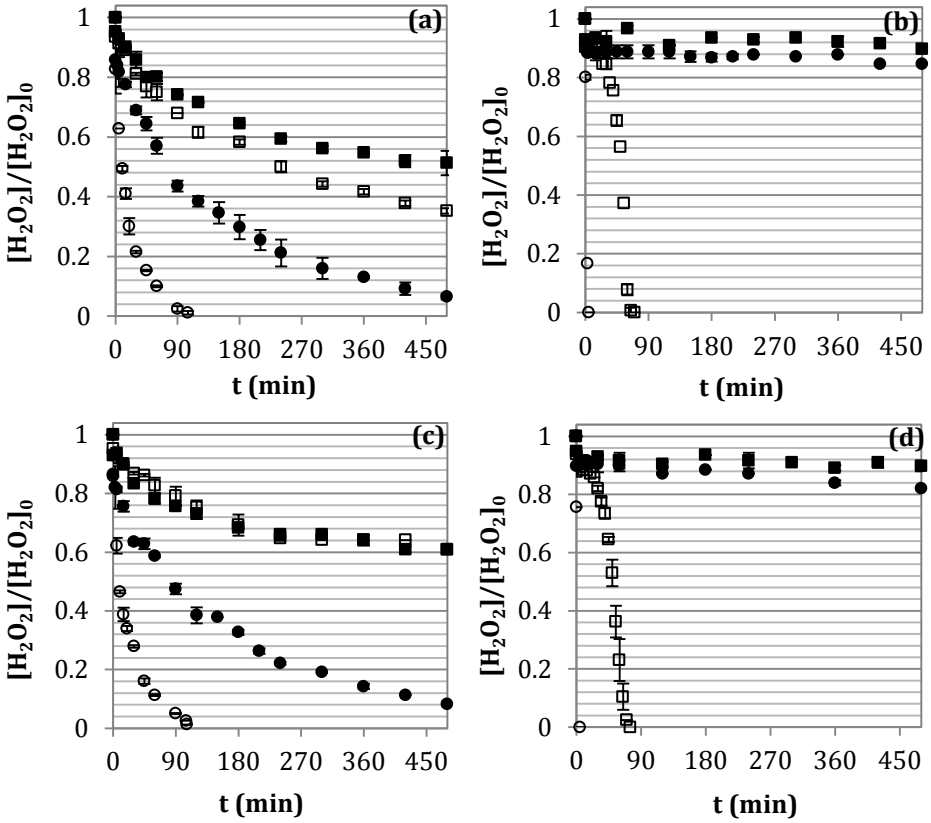

Figure 3.6. Comparison of the H_2O_2 depletion working with 0.18 mM Fe_2SO_4 (square) or 1.44 mM Fe_2SO_4 (circle) at 20 ºC (filled) and 70 ºC (empty). (a) 40.44 mM H_2O_2, (b) 40.44 mM H_2O_2 + 267 mM DMSO, (c) 40.44 mM H_2O_2 + 56.3 mM NaCl, and (d) 40.44 mM H_2O_2 + 267 mM DMSO + 56.3 mM NaCl. V_t: 1 L, pH_0: 3, stirring rate: 700 rpm.

Experiments carried out with a solution of only H_2O_2 at 70 ºC did not show any change in its concentration for 3 h (not represented in Figure 3.6). Through the variation of the temperature it was observed an increase in the hydrogen peroxide decomposition rate working with both iron doses (Figure 3.6a and c), 0.18 and 1.44 mM, which can be explained due to the enhancement of the iron catalyzed H_2O_2 decomposition.[17] Furthermore, there is a change in the behavior of H_2O_2 decomposition as the temperature increases when the solution contained DMSO (Figure 3.6b and d). The concentration of hydrogen peroxide at 20 ºC kept constant,

whereas the increase up to 70 ºC enabled the decomposition of H_2O_2, that in the case of 1.44 mM Fe(II) resulted in a fast and complete depletion of H_2O_2 after 5 min. The increase in the temperature had not only effect on H_2O_2 decomposition, but also in the hydroxyl radical formation as it is displayed in Figure 3.7.

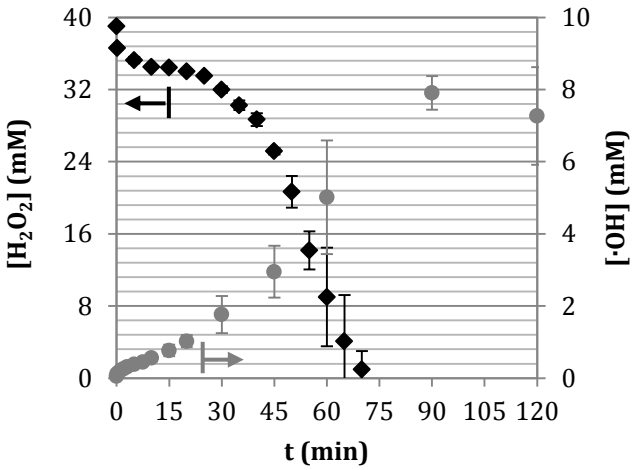

Figure 3.7. (♦) Consumption of H_2O_2 and (●) cumulative concentration of ·OH generated during the Fenton reaction. $[DMSO]_0$: 267 mM, $[H_2O_2]_0$: 40.44 mM, $[FeSO_4{\cdot}7H_2O]_0$: 0.18 mM, $[NaCl]_0$: 56.3 mM, V_t: 1 L, pH_0: 3, T: 70 ºC, stirring rate: 700 rpm.

A maximum cumulative concentration of hydroxyl radicals of 8 mM was obtained at 90 min increasing the temperature, whereas working at 20 ºC and 0.18 mM Fe(II) the maximum concentration of hydroxyl radicals was 0.2 mM (Figure 3.2). The results displayed a plateau region between 5 min and 25 min (Figure 3.7), which could be related with the formation of an organic-iron complex that is thermally decomposed afterwards in a similar way to the formation of the ferric oxalate.[17,18] Hence, DMSO does not seem to be the proper molecular probe to quantify the generation of ·OH during the Fenton treatment owing to the fact that the probe itself interfers in the analysis.

3.1.2. Evaluation of DMPO as spin-trap for the identification of inorganic and organic radicals

a) Viability of the use of DMPO as spin-trap in Fenton oxidation

Identification of the proper DMPO/Fenton reagents ratio

Unlike the method developed for the analysis of ·OH by means of HPLC-UV using DMSO as molecular probe, in the case of DMPO as spin-trap and EPR analysis there is not consensus about the proper concentrations of the spin-trap (Table 3.1). One of the main differences between DMPO and DMSO is the more expensive price of DMPO. In this sense, different concentrations of DMPO have been employed depending on the AOP applied.

Table 3.1. Identification of ROS during the application of AOPs using DMPO as spin-trap.

AOPs	V_{exp}	[DMPO]	Ref.
Sonolysis	20 ml	1 mM	19, 20
Catalytic decomposition of H_2O_2	20 mL	58 mM	21
Photoelectrocatalysis	50 mL	?	22
Photocatalysis	50 µL	0.35 - 150 mM	23
Sonolysis	5 mL	90 mM	24
Fenton-like	20 mL	100 mM	25
Electrochemical oxidation	?	?	26
Fenton and electrolysis	?	10 mM	27
Fenton	2 mL	4.25 mM	28
Photocatalysis	0.5 mL	30 mM	29
Photolysis	?	0.2 mM	30
Radiolysis	?	0.15 - 2 mM	31
Fenton	200 µL	100 mM	32
Fenton	37 µL	40.5 – 43.8 mM	33
CuO/silica particles	200 µL	150 mM	34
Photolysis H_2O_2	400 µL	25 mM	35
Gamma irradiation	?	200 mM	36

DMPO is one of the molecular probes most widely used allowing the identification of both inorganic and organic radicals. In a first stage, the research has been restricted to aqueous solutions containing DMPO as the only organic substance. The experiments were performed with 5-10 mL of total volume and 100 mM DMPO due to the fact that the EPR signals corresponding to the generated radical species were not visible for concentrations lower than 70 mM, so an additional amount of DMPO was added to work with excess. Regarding the reaction volume, it was reduced to 0.01-0.005 L^{-1} (compared to DMSO and 2-CP experiments) owing to the higher price of DMPO.

In a first attempt, the experimental conditions of interest were selected, as it was explained before for the studies with DMSO. Initially, the Fenton solution was composed of 100 mM DMPO, 40.44 mM H_2O_2, 1.44 mM $FeSO_4 \cdot 7H_2O$, 56.34 mM NaCl, pH_0= 3, ambient temperature and the stirring rate was 700 rpm. The main signal expected would be the corresponding to the adduct DMPO-·OH, which is characterized by 4 peaks with a ratio 1:2:2:1, hyperfine constants a_N= a_H= 14.9 G and g-value= 2.0055 (Figure 3.8).

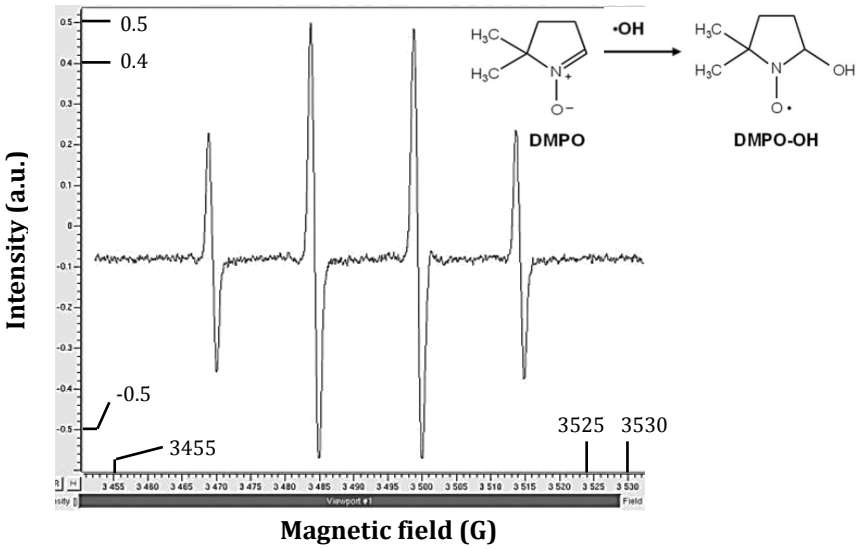

Figure 3.8. Formation of the DMPO-·OH adduct after the reaction of ·OH with DMPO and its EPR spectra.

Throughout the Fenton process under the conditions described above, the EPR spectra were more complex and additional peaks other than DMPO-·OH were recognized in the EPR spectra together with a change in the coloration of the sample from yellowish to intense violet. Figure 3.9 represents the spectrum obtained when a sample was withdrawn at $t_{sampling}$= 30 s and analyzed at $t_{analysis}$= 53 min 53 s ($t_{total,analysis}$= 55 min 33 s).

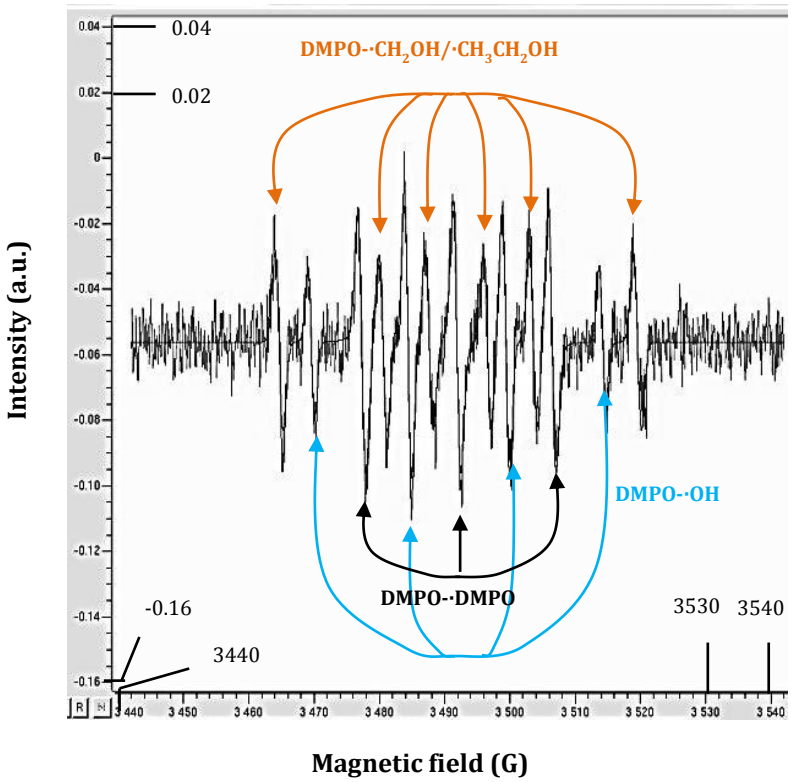

Figure 3.9. EPR spectra during the Fenton oxidation at $t_{sampling}$= 30 s and $t_{analysis}$= 53 min 53 s without quenching the reaction. Orange arrows: DMPO-·CH_2OH/·CH_2CH_2OH, blue arrows: DMPO-·OH, black arrows: DMPO-·DMPO. $[DMPO]_0$: 100 mM, $[H_2O_2]_0$: 40.44 mM, $[FeSO_4{\cdot}7H_2O]_0$: 1.44 mM, V_t: 0.01 L, pH_0: 3, T: ambient, stirring rate: 700 rpm. Microwave power: 5.024 mW, microwave frequency: 9.8 GHz, modulation frequency: 100 kHz, modulation amplitude: 0.1 G, center field: 3492 G, sweep width: 100 G, sweep time: 99.9 s, time constant: 81.92 ms, receiver gain: 80 dB, power attenuation: 16 dB.

The library contained in the Bruker software allowed identifying one of the signals as DMPO-·CH_2OH. However, according to the spin trap data base of the National Institute of Environmental Health Sciences (NIH) of the United States (http://tools.niehs.nih.gov/stdb/) both methoxy and ethoxy have almost identical values of a_N= 16 G, a_H= 23 G, g-value= 2.0055, with a ratio 1:1:1:1:1:1. On the other hand, Andersen and Skibsted (1998) found a similar spectrum during the Fenton oxidation of beer, identifying these radicals as 1-hydroxyethyl.[37]

Secondly, a triplet, with a signal ratio 1:1:1, was identified and characterized by a hyperfine splitting a_N= 15.1 G and g-factor= 2.0056 G. This signal was previously found by Lipczynska-Kochany et al. (1991) during the direct photolysis of 4-CP in the presence of DMPO and by Fontmorin et al. (2016) during the Fenton reaction of DMPO, being identified as the dimerization product of DMPO (Figure 3.9, Scheme 3.1).[38,39]

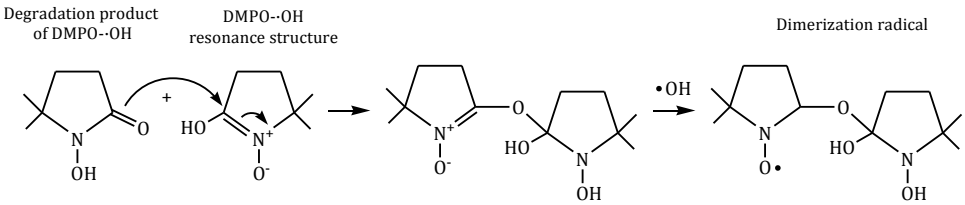

Scheme 3.1. Dimerization of DMPO by the reaction of the degradation product of DMPO-·OH with DMPO-·OH.[38]

Figure 3.10 displays the intensity of the radical signals of a sample withdrawn 30 s after starting the Fenton experiment, placed in the EPR cell and analyzed continuously from 1 min 37 s to 53 min 53 s. Red and purple colors in the density plot represent strong maximum and minimum intensities. Each signal has been identified with the corresponding radical. The intensity of DMPO-·OH and DMPO-·alcohol diminished whereas the corresponding to the dimerization increased with time. The diminishment of the signals is related with the stability of the adducts that in the case of DMPO-·OH, has a half-life between 2-60 min (up to 2.6 h described in bibliography depending on the operational conditions).[21,23,36,38,40]

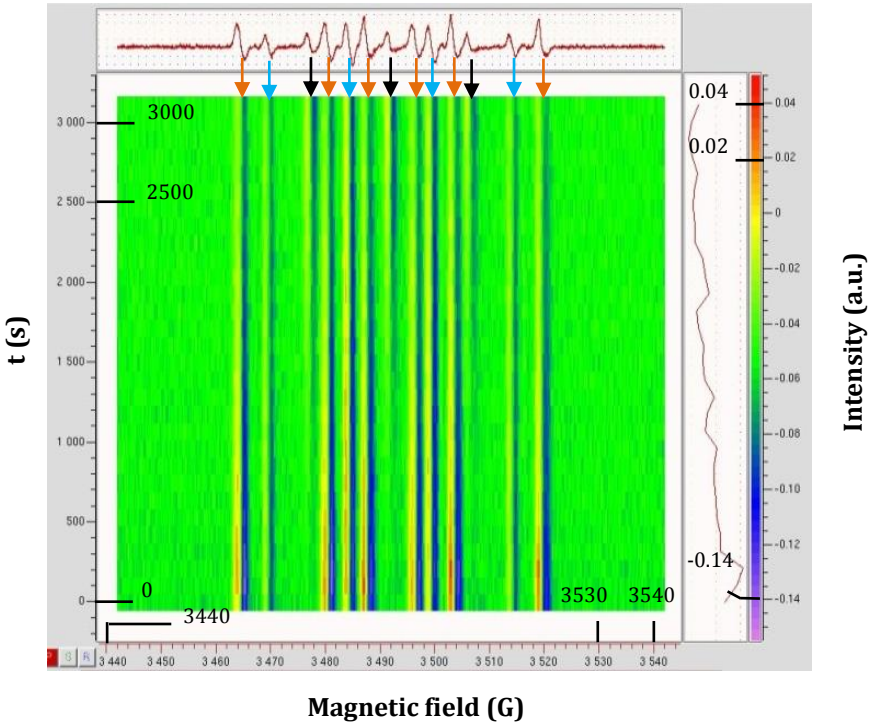

Figure 3.10. Density plot of the Fenton oxidation at $t_{sampling}$= 30 s and $t_{analysis}$= 1 min 37 s - 53 min 53 s without quenching the reaction (30 successive analysis). Orange arrows: DMPO-·CH_2OH/·CH_2CH_2OH, blue arrows: DMPO-·OH, black arrows: DMPO-·DMPO. The experimental conditions and the EPR analysis parameters were the same as in Figure 3.9.

Once the hyperfine splitting constants, the g-factor and the intensities were known, the quantification of the spin number was carried out by the software leading to the concentrations shown in Figure 3.11. As in the case in which the intensities were represented (Figure 3.10), there is a decrease in all the concentrations with the exception of the dimerization product of DMPO. There is some scattering in the results of methoxy radical, but it may be explained taking into consideration the similarities in the hyperfine constants and g-value for the shortest chain alcohols.

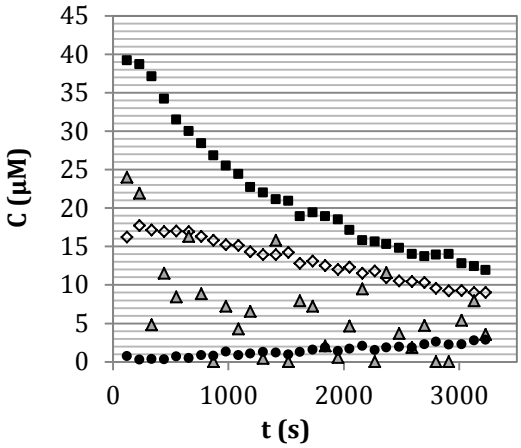

Figure 3.11. Concentration of the radical species generated during the Fenton reaction in presence of DMPO at $t_{sampling}$= 30 s and $t_{analysis}$= 1 min 37 s - 53 min 53 s without quenching the reaction (30 successive analysis). ■ DMPO-·CH_2CH_2OH, ◇ DMPO-·OH, △ DMPO-·CH_2OH, ● DMPO-·DMPO. The experimental conditions and the EPR analysis parameters were the same as in Figure 3.9.

Finally, another important aspect to consider is the change in the coloration once the oxidation reactions started. Precisely, the first step in the discovery of the Fenton reaction was the observation of a color change towards violet when a solution of tartaric acid and iron sulfate was mixed with an oxidizing agent (H_2O_2) yielding glycolaldehyde (Scheme 3.2a).[41,42]

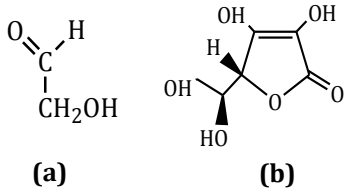

Scheme 3.2. Structures of (a) glycolaldehyde and (b) ascorbic acid.

Yao et al. (2015) observed the formation of glycolaldehyde during the oxidation of other organics such as ascorbic acid.[43] Both DMPO (Figure 3.8) and ascorbic acid (Scheme 3.2b) are composed by 5 atoms in the cyclic structure, one of them is an heteroatom, so this could be a possible pathway for the formation of glycolaldehyde.

On the other hand, a second pathway would be its generation through the reaction of $\cdot CH_2OH$ radicals, which has been identified during the experiment previously presented (Figures 3.9-3.11).[44] Anyway, further analysis of this sample would be necessary to confirm that glycolaldehyde is one of the oxidation products generated.

What is clear from the results presented until now is that the oxidation of DMPO-·OH occurs as DMPO was the only organic present in the aqueous solution, which implies an underestimation of the ·OH concentration. As a consequence, owing to the fact that the main purpose is to quantify the ·OH generated along the application of Fenton and to avoid the degradation of DMPO-·OH (underestimation of ·OH, Scheme 3.1), the conditions were modified by means of the Fenton reagent, reducing the concentrations of hydrogen peroxide and iron to 4.044 mM and 9 μM, respectively. Under these conditions, the change in the color of the reaction solution was not observed and the only radical specie identified was hydroxyl radical. The sample was also analyzed by attenuated total reflection (FTIR-ATR) spectroscopy with a MCT detector (mercury cadmium telluride). The absorbance data are presented in Figure 3.12 and the comparison was carried out considering the size of the peaks for the different samples since the correction with a baseline was not possible due to the interference of the signals corresponding to water.

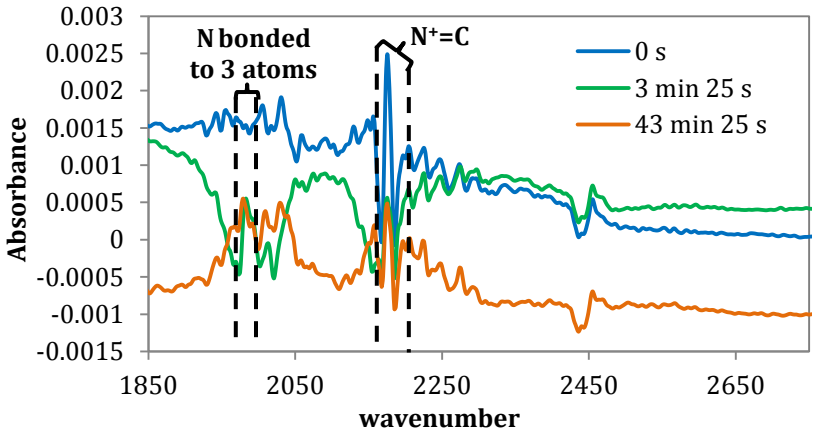

Figure 3.12. FTIR-ATR spectra at different reaction times. MCT detector, 60 scans, MIR source 4 cm^{-1} at 4000 cm^{-1}. $[DMPO]_0$: 100 mM, $[H_2O_2]_0$: 4.044 mM, $[FeSO_4 \cdot 7H_2O]_0$: 9 μM.

The results depicted in Figure 3.12 portray a diminishment in the absorbance at the characteristic wavelength for nitrogen double bonded to carbon atom (characteristic of DMPO), whereas the signal corresponding to nitrogen bonded to three different atoms (corresponding to DMPO-·OH) increased and, hence, supporting the reaction from DMPO to DMPO-·OH.

Therefore, it is fundamental the selection of proper ratios between the concentration of the molecular probe and the Fenton reagents. In the framework of this thesis, higher concentrations of DMPO would be needed to develop a deep evaluation of the influence of the operational conditions such as temperature, hydrogen peroxide or iron dose. These experiments are a preliminary study developed at the Fire Safety and Combustion Kinetics Laboratory of the University of Murdoch (Australia) by the PhD candidate that should be broaden in the future.

Influence of the use of $NaHSO_3$ as H_2O_2 quencher

During the Fenton oxidation carried out with DMPO in aqueous solution, some tests were performed by adding sodium bisulfite to quench the residual hydrogen peroxide. After its addition to the sample withdrawn from the reactor, in that case in which the solution had turned to a violet color, it recovers again the initial yellowish color, which implies that some type of reaction is occurring between the bisulfite and the unknown oxidation product responsible of the coloration (proposed previously to be glycolaldehyde); this is similar to what happened when working with DMSO as molecular probe with the disappearance of formaldehyde leading to the formation of adducts aldehyde-bisulfite. Reactions 3.5 and 3.6 display two examples of the reaction of formaldehyde and benzaldehyde with bisulfite.[3-5]

$$HCHO + HSO_3 \rightarrow HOCH_2 \cdot SO_3^- \tag{3.5}$$

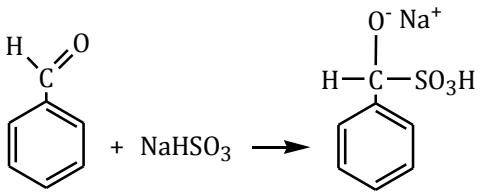

(3.6)

On the other hand, Figure 3.13 depicts the results obtained by EPR spectroscopy when adding bisulfite, showing a completely different spectrum to that displayed in Figure 3.9, characterized by a g-factor= 2.0055 , a_N= 14.6 G, and a_H= 16.1 G.

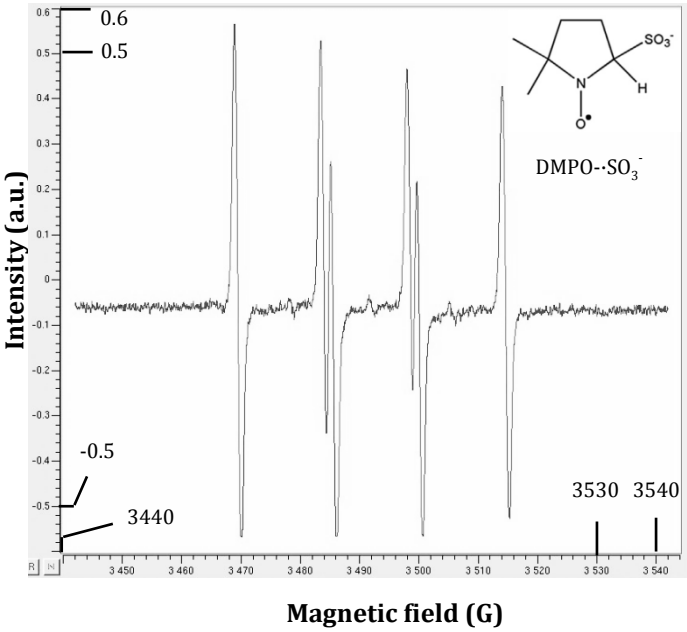

Figure 3.13. EPR spectra during the Fenton oxidation at $t_{sampling}$= 3 s and $t_{analysis}$= 2 min adding $NaHSO_3$. $[DMPO]_0$: 100 mM, $[H_2O_2]_0$: 40.44 mM, $[FeSO_4{\cdot}7H_2O]_0$: 1.44 mM, V_t: 0.01 L, pH_0: 3, T: ambient, stirring rate: 700 rpm. The EPR analysis parameters were the same as in Figure 3.9.

The spectrum displayed in Figure 3.13 corresponds to DMPO-·SO_3^- that has been previously observed and it is a consequence of the reaction of DMPO-·OH with bisulfite according to Reaction 3.7 and the generation of ·SO_3^- that reacts with DMPO (Reaction 3.8).[38,45] Consequently, no reagents to quench the hydrogen peroxide have been added in the next experiments, and the samples were immediately analyzed. Additionally, some results obtained with a stopped-flow equipment coupled to the EPR will be presented later.

$$\mathrm{DMPO-{\cdot}OH} + \mathrm{SO_3^{2-}} \rightarrow \mathrm{DMPO-{\cdot}SO_3^{-}} + \mathrm{HO^-} \qquad (3.7)$$

$$H_2O_2 + 2\ SO_3^{2-} \rightarrow 2\ \cdot SO_3^- \xrightarrow{2\ DMPO} 2\ DMPO - \cdot SO_3^- \qquad (3.8)$$

Influence of the analysis procedure on the radical concentration profile

Three different tests were carried out to assess the influence of the sampling and analysis time. These tests consisted on i) multiple scans of a sample withdrawn from the reactor 10 s after starting the experiment and analyzed at 2 min 2 s ($t_{0,analysis}$= 2 min 2 s), ii) five scans per withdrawn sample (t_{sample}= 10 s, 10 min 15 s, 21 min 50 s, and 29 min; $t_{0,analysis}$= 1 min 49 s, 12 min 38 s, 22 min 49 s, and 31 min 18 s; respectively), and iii) one scan per sample withdrawn from the reactor (t_{sample}= 10 s, 5 min 15 s, 10 min 45 s, 17 min 30 s, 21 min 35 s, and 25 min 45 s; $t_{0,analysis}$= 3 min, 8 min 9 s, 13 min 17 s, 19 min 23 s, 23 min 47 s, and 28 min 10 s; respectively). Figure 3.14 presents the concentration of DMPO-·OH obtained following the three procedures at different Fenton reaction times.

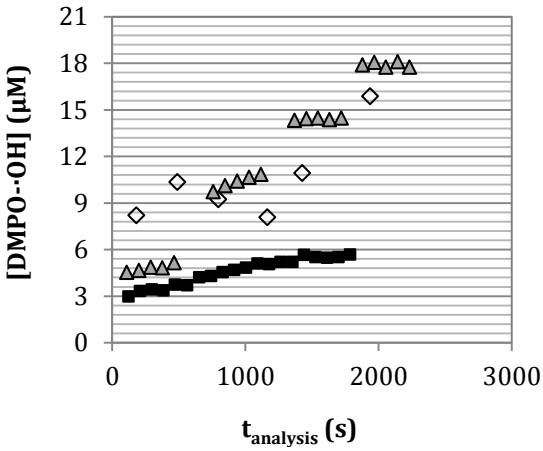

Figure 3.14. Generation of ·OH during the Fenton oxidation of DMPO and 2-CP. ■ multiple scans for a sample withdrawn 10 s after starting the experiment; △ five scans per withdrawn sample; and ◇ one scan per sample. $[DMPO]_0$: 100 mM, [2-CP]: 31.12 mM, $[H_2O_2]_0$: 40.44 mM, $[FeSO_4 \cdot 7H_2O]_0$: 1.44 mM, $[NaCl]_0$: 56.34 mM, V_t: 0.005 L, pH_0: 3, T: ambient, stirring rate: 700 rpm. The EPR analysis parameters were the same as in Figure 3.9.

Significant differences were observed in terms of hydroxyl radical concentration. When the procedure followed was multiple scans of the same sample, there was a

slight gradual increase in the concentration of ·OH in the EPR cell that is likely due to mass transfer limitations as the solution is not being stirred inside the resonator cavity. In the procedure (ii), the concentrations of DMPO-·OH followed a step shape where the main changes arise in the time lag that occurred between the sample was withdrawn from the reactor and analyzed rather than between multiple scans, ratifying the limitations in the mass transfer. Lastly, following the procedure (iii), it can be observed that, with some scattering in the results, the concentration of DMPO-·OH is in the range of the initial results of each sample withdrawn according to the procedure (ii). Therefore, in order to properly quantify the concentration of radicals, it is essential to withdraw the sample from the reactor avoiding death times between sampling and analysis according to procedure (iii).

Consequently, as it has been analyzed in this section, the quantification of radical species during the application of Fenton oxidation by means of DMPO utilization and EPR spectroscopy is not a trivial procedure and it will depend on the conditions applied. The use of a DMPO/H_2O_2 molar ratio over 25, prevents the oxidation of DMPO-·OH adduct. Furthermore, the sampling method is of special relevance since (i) the addition of other reagents such as bisulfite may interfere in the EPR analysis; (ii) the death time between sampling and analysis results in the distortion of the real radicals concentration.

<u>b) Identification of inorganic and organic radicals during the Fenton oxidation of 2-chlorophenol</u>

The next step consisted on the addition of 2-chlorophenol to the reaction system. The starting point was selected at the same conditions that will be employed in the assessment of PCDD/Fs formation during the Fenton oxidation of 2-CP ([DMPO]: 100 mM, [2-CP]: 15.56 mM, [H_2O_2]: 40.44 mM; [Fe(II)]: 0.09 mM: [NaCl]: 56.34 mM). The EPR spectra and concentration profile obtained during the Fenton oxidation of 15.56 mM 2-CP are presented in Figure 3.15.

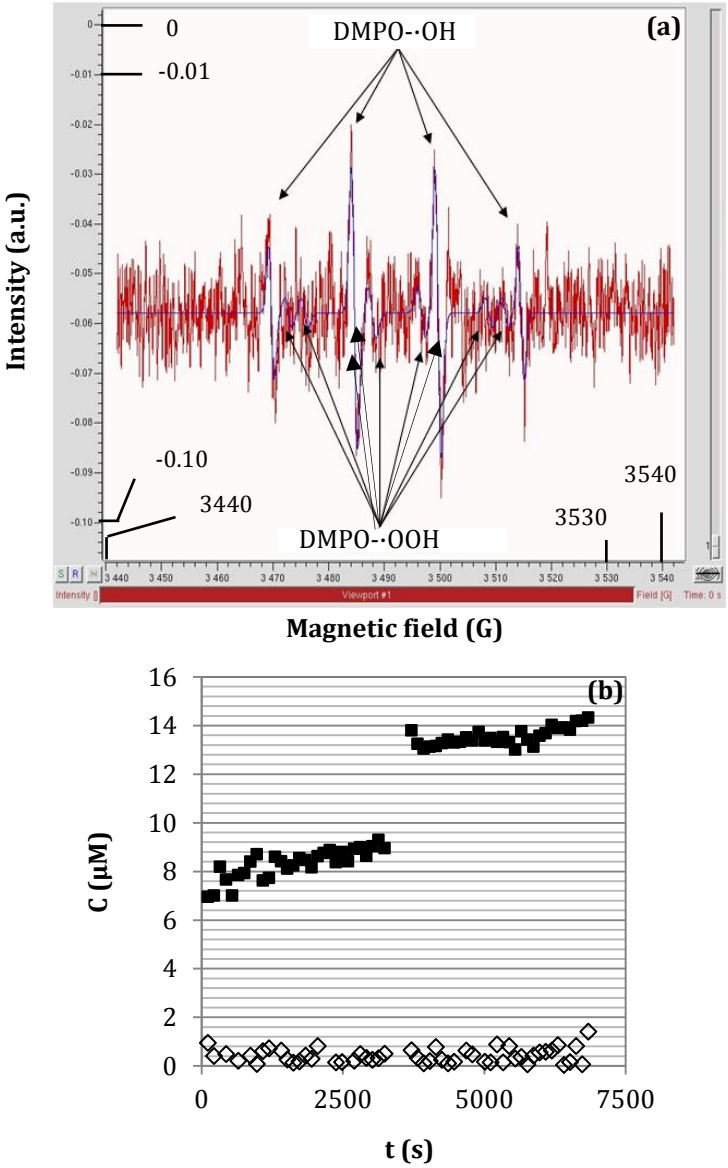

Figure 3.15. (a) EPR spectra during the Fenton oxidation at $t_{sampling}$= 15 s and $t_{analysis}$= 2 min; and (b) ROS concentrations for samples withdrawn at $t_{sampling}$= 15 s and 60 min, and continuously analyzed for 1 h in both cases: ■ DMPO-·OH and ◇ DMPO-·OOH. $[DMPO]_0$: 100 mM, $[2\text{-}CP]_0$: 15.56 mM, $[H_2O_2]_0$: 40.44 mM, $[FeSO_4{\cdot}7H_2O]_0$: 0.09 mM, $[NaCl]_0$: 56.34 mM, V_t: 0.005 L, pH_0: 3, T: ambient, stirring rate: 700 rpm. The EPR analysis parameters were the same as in Figure 3.9.

Under these experimental conditions, only ·OH and ·OOH (ratio 1:1:2:2:2:2:1:1, hyperfine constants a_N= 11.822, $a_{H,1}$= 12.3305 G, and $a_{H,2}$= 2.91126 G and g-value= 2.0053) were identified, and no organic radicals from the decomposition of DMPO or from the oxidation of 2-CP were observed (Figure 3.15a). The concentration of ·OH was in the range 7-14 μM while the concentration of ·OOH was in the range 0.03-0.94 μM and with a relatively higher dispersion likely due to the proximity to the detection limit. Figure 3.15b shows the concentrations of both radical species for samples withdrawn at t_0= 15 s and t_1= 60 min, introduced to the EPR cell and continuously analyzed. As it was commented previously (Figure 3.14), there are quantitative differences for DMPO-·OH concentrations when a sample has been continuously stirred or kept inside the EPR cell (Figure 3.15b). In the case of DMPO-·OOH concentrations, this difference between two samples was not outstanding likely due to the lower concentrations and the proximity to the detection limit. The gradual increase of ·OH radicals during the Fenton oxidation may be explained taking into account the reaction of Fe(II) with the H_2O_2 present in the aqueous medium, as it can be inferred from Figure 3.3a in absence of any organic and from the work developed by Vallejo et al. (2015) in presence of 2-CP.[46] On the other hand, whereas working only with 2-CP the solution changes the color from colorless to a dark brown, in the case of the DMPO and 2-CP mixture the change from yellowish (given by DMPO) to brownish (given by oxidation byproducts from 2-CP) occurred after one hour which could be explained considering that competition reactions between both organics are taking place ($k_{2\text{-}CP,\cdot OH}$= $1.2\cdot10^{10}$ M-1 s^{-1} and $k_{DMPO,\cdot OH}$= $4.3\cdot10^{9}$ M^{-1} s^{-1}).[47]

The increase of iron concentration up to 1.44 mM keeping the rest of operational conditions constant, resulted in an instantaneous change in the color of the solution as a consequence of the superior availability of ·OH due to the higher concentration of catalyst. In this sense, Figure 3.16 compares the concentration of the adduct DMPO-·OH working with 0.09 and 1.44 mM Fe(II) as time passes when a sample withdrawn at 15 s is subject to successive analysis

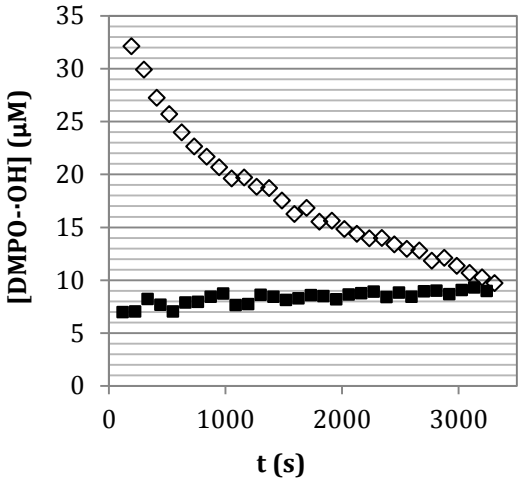

Figure 3.16. Generation of ·OH during the Fenton oxidation of DMPO and 2-CP. ■ 0.09 mM Fe(II), ◇ 1.44 mM Fe(II). The experimental conditions and the EPR analysis parameters were the same as in Figure 3.15.

From the information obtained by EPR analysis, only hydroxyl radicals were identified. At the lowest concentration of Fe^{2+} (0.09 mM) the DMPO-·OH concentration gradually increased because of the availability of hydrogen peroxide in the system according to the results published in Fernández-Castro et al. (2016), but working with 1.44 mM Fe(II) a diminishment was observed as a consequence of the likely depletion of H_2O_2 and the stability of DMPO-·OH, which resulted in the lack of radical signals when a sample after 1 h of Fenton reaction was analyzed.[48]

With the aim of deepening in the generation of organic radicals from 2-CP that could explain the formation of condensation byproducts such as PCDD/Fs, the iron dose was maintained at 0.09 mM but the concentration of 2-CP was doubled (31.12 mM). Figure 3.17 displays the comparison of DMPO-·OH concentration working with both 2-CP concentrations: 15.56 and 31.12 mM.

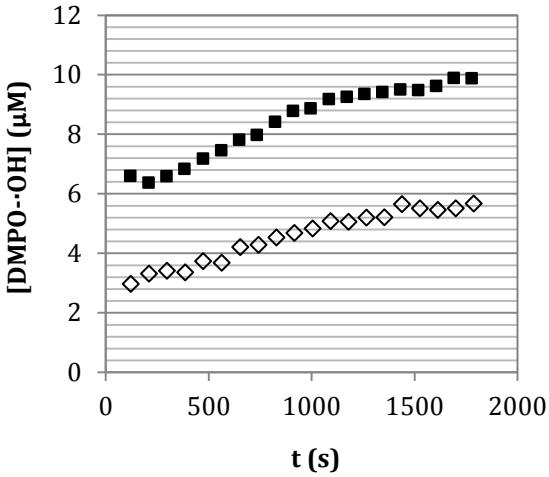

Figure 3.17. Generation of ·OH during the Fenton oxidation of DMPO and 2-CP. ■ 15.56 mM 2-CP, ◇ 31.12 mM 2-CP. $[DMPO]_0$: 100 mM, $[H_2O_2]_0$: 40.44 mM, $[FeSO_4 \cdot 7H_2O]_0$: 0.09 mM, $[NaCl]_0$: 56.34 mM. V_t: 0.005 L, pH_0: 3, T: ambient, stirring rate: 700 rpm. The EPR analysis parameters were the same as in Figure 3.9.

Again, the only radical specie observed was ·OH but an increase in the 2-CP concentration resulted in lower concentration of the adduct DMPO-·OH that is understandable considering the competition reaction of the hydroxyl radical with DMPO, 2-CP and other possible compounds present in the solution as a consequence of the oxidation reactions.

In a final attempt, and owing to the possibility of having organic radicals in concentrations lower than the limit of detection, the concentration of 2-CP was raised up to 10 times (155.6 mM). The Fenton reagents doses were also increased keeping the ratio H_2O_2:Fe(II), but the hydrogen peroxide dose was 10% of the theoretical stoichiometric amount required to completely mineralize 2-CP (instead of the previous 20%, Reaction 3.9), trying to preserve the reaction process in the initial oxidation radicals/intermediates and avoiding, therefore, additional oxidation reactions that increase the complexity and product distribution.

$$C_6H_5OCl + 13\ H_2O_2 \rightarrow 6\ CO_2 + 15\ H_2O + HCl \qquad (3.9)$$

With this modified conditions, three different signals were identified corresponding to DMPO-·OH, DMPO-·DMPO, and a new one that seems to be overlapped by DMPO-·OH that, as it will be explained below, will correspond to semiquinone type radical (Figure 3.18).

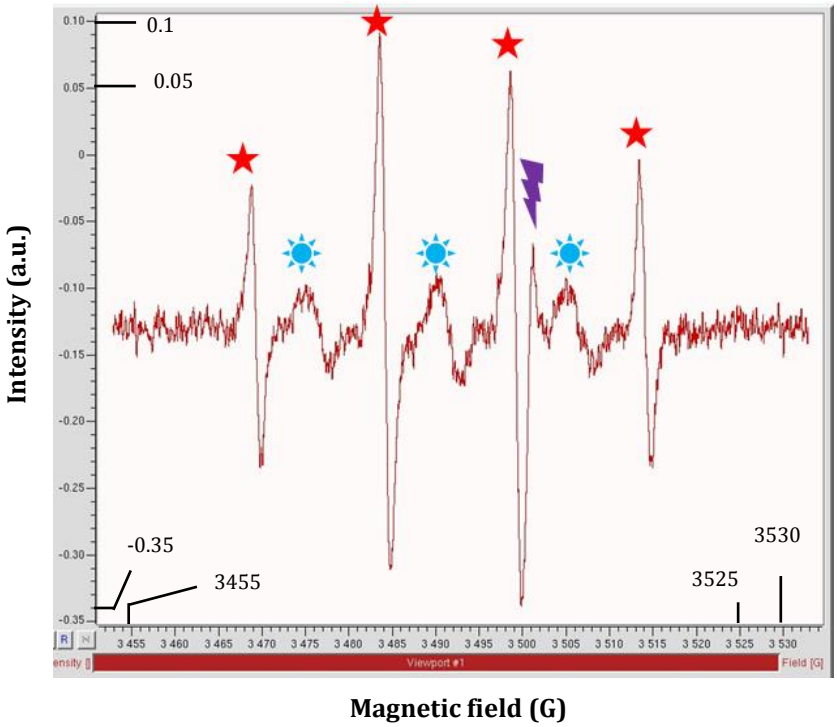

Figure 3.18. EPR spectra during the Fenton oxidation of DMPO and 2-CP at $t_{sampling}$= 26 min 30 s and $t_{analysis}$= 35 min: ★ DMPO-·OH, ☀ DMPO-·DMPO, ⚡ semiquinones type. $[DMPO]_0$: 100 mM, $[2\text{-}CP]_0$: 155.6 mM, $[H_2O_2]_0$: 202.22 mM, $[FeSO_4 \cdot 7H_2O]_0$: 7.22 mM, $[NaCl]_0$: 56.34 mM. V_t: 0.005 L, pH_0: 3, T: ambient, stirring rate: 700 rpm. Microwave power: 63.25 mW, microwave frequency: 9.8 GHz, modulation frequency: 100 kHz, modulation amplitude: 1 G, center field: 3492.85 G, sweep width: 80 G, sweep time: 80 s, time constant: 81.92 ms, receiver gain: 80 dB, power attenuation: 5 dB.

Deepening in the identification of the unknown signal, which as it was mentioned in Figure 3.18 will correspond to semiquinones type radical, an additional test without adding DMPO was carried out keeping the other experimental conditions constant to check if that signal is a consequence of a DMPO adduct. During this test

the signal was recognized again but displaying two peaks (Figure 3.19), which demonstrates that, first, it was not associated to a DMPO adduct and, second, it was overlapped by the signal of DMPO-·OH (Figure 3.18). Paying attention to the g-factor (g-factor= 2), the shape of the peak, and comparing with the data gathered in bibliography, this signal has been associated with semiquinone-type radicals that in many cases are related to humic acids.[49-51]

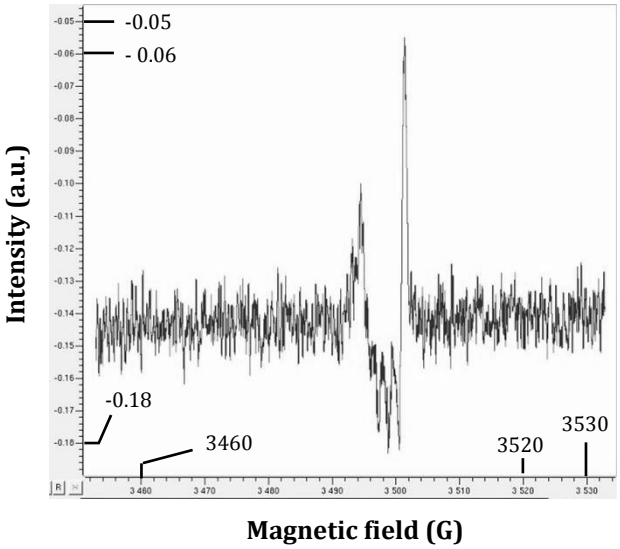

Figure 3.19. EPR spectra during the Fenton oxidation of 2-CP. $[2\text{-CP}]_0$: 155.6 mM, $[H_2O_2]_0$: 202.22 mM, $[FeSO_4{\cdot}7H_2O]_0$: 7.22 mM, $[NaCl]_0$: 56.34 mM. V_t: 0.005 L, pH_0: 3, T: ambient, stirring rate: 700 rpm. The EPR analysis parameters were the same as in Figure 3.18.

Semiquinone radicals may be formed from hydrogen abstraction or hydroxylation of a phenolic compound (Reactions 3.10 and 3.11, respectively), oxidation of phenolic compounds with ferric ion (Reaction 3.12) or oxidation of benzoquinones by other radical species (Reaction 3.13).[52-55]

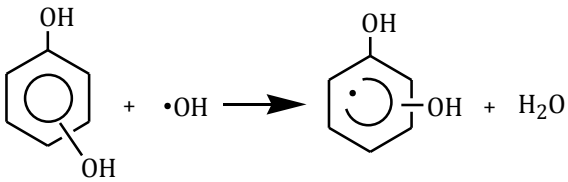

(3.10)

phenolic semiquinone radical

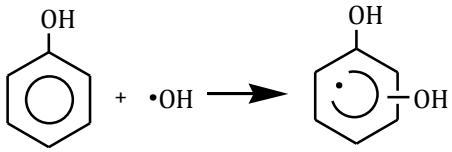

$k = 7.3 \cdot 10^{9}\ M^{-1}\ s^{-1}$ (3.11)

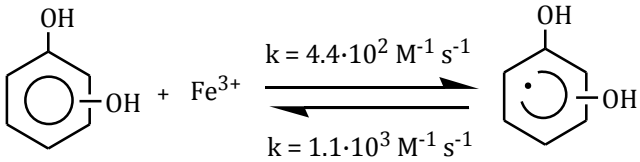

(3.12)

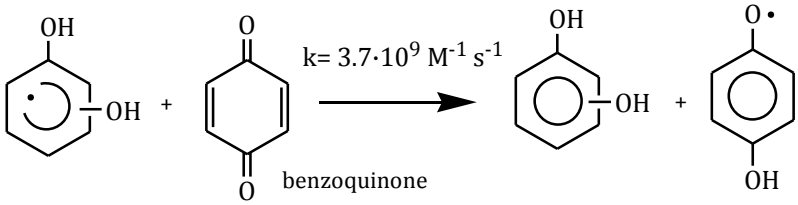

(3.13)

On the other hand, benzoquinone may be formed from the reaction of phenyl (Reaction 3.14) and phenoxy (Reaction 3.15) radical with molecular oxygen.[56-58] Both radicals have been identified as important precursors in the generation of PCDD/Fs as it would be explained later in the mechanisms proposal (Chapter 4).[59-61] At the same time, phenoxy type radical may be generated from semiquinone type radical (Reaction 3.16).[55]

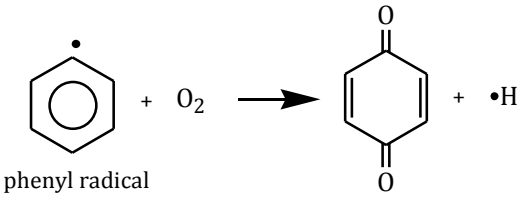

(3.14)

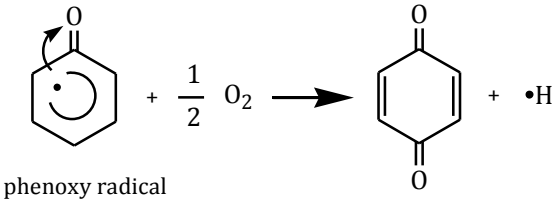

(3.15)

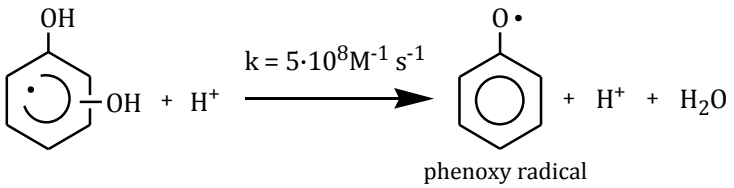

(3.16)

Under the last experimental conditions and increasing the center field and sweep width, another signal with a very broaden spectrum was identified as it is depicted in Figure 3.20.

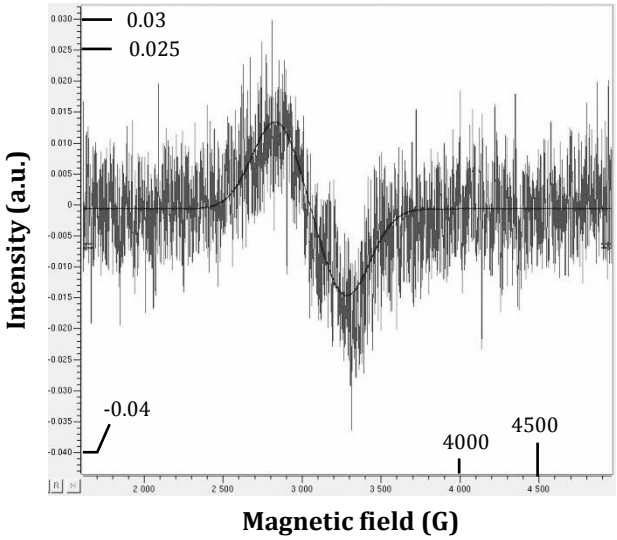

Figure 3.20. EPR spectra during the Fenton oxidation of 2-CP. $[2\text{-CP}]_0$: 155.6 mM, $[H_2O_2]_0$: 202.22 mM, $[FeSO_4{\cdot}7H_2O]_0$: 7.22 mM, $[NaCl]_0$: 56.34 mM. V_t: 0.005 L, pH_0: 3, T: ambient, stirring rate: 700 rpm. Microwave power: 63.25 mW, microwave frequency: 9.8 GHz, modulation frequency: 100 kHz, modulation amplitude: 1 G, center field: 2500 G, sweep width: 5000 G, sweep time: 250 s, time constant: 81.92 ms, receiver gain: 80 dB, power attenuation: 5 dB.

The signal observed is related to the presence of iron in the likely form of organic-ferric complexes (g-factor= 2.3140) as iron precipitates were observed.[62] The integration of the observed signal leads to a concentration of 4.2 mM. Therefore, when working with 7.22 mM of iron the formation of iron precipitates occurred, which can not only justify the identification of Fe(III) by EPR spectroscopy but also that 4.2 mM of the 7.22 mM are in the form of ferric species.

Stopped-flow Fenton oxidation coupled to EPR spectrometer

A stopped-flow apparatus was employed to conduct the Fenton experiments and directly analyze the generation of radical species by means of EPR spectroscopy (Chapter 2). Two different solutions were prepared, one of them containing the iron salt (14.44 mM), DMPO (0 or 200 mM), sodium chloride (112.68 mM) and 2-CP (155.56 mM) and the second one containing hydrogen peroxide (404.44 mM) and 2-CP (155.56 mM). Each solution was loaded in a different chamber to prevent the Fenton reaction (Figure 2.10, Chapter 2). A ratio 1:1 between both lines, a total volume shot of 754 μL with a total flowrate of 2 mL s^{-1} was selected in order to keep the experimental conditions of the batch Fenton ($[2\text{-CP}]_0$: 155.6 mM, $[H_2O_2]_0$: 202.22 mM, $[FeSO_4{\cdot}7H_2O]_0$: 7.22 mM, $[NaCl]_0$: 56.34 mM) and provide enough solution to fill the EPR cell. With the stopped-flow configuration, the dead time between the sample withdrawal and analysis is eliminated and, therefore, it can allow the identification of possible radical species generated at initial times. Figure 3.21 portrays the monitoring of the signal area for DMPO-·OH under the operational conditions described above for the stopped flow experiment.

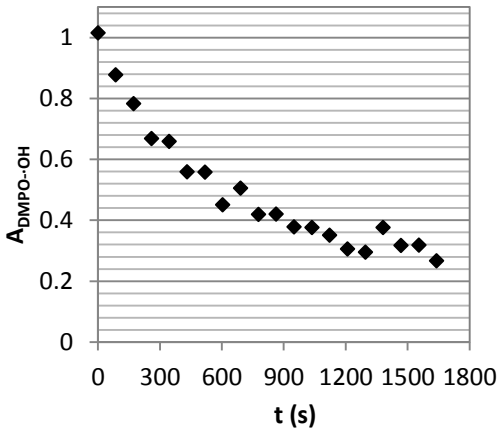

Figure 3.21. EPR signal area for DMPO-·OH obtained during the stopped-flow Fenton oxidation of DMPO and 2-CP. $[DMPO]_0$: 100 mM, $[2\text{-CP}]_0$: 155.6 mM, $[H_2O_2]_0$: 202.22 mM, $[FeSO_4{\cdot}7H_2O]_0$: 7.22 mM, $[NaCl]_0$: 56.34 mM. V_t: 0.005 L, pH_0: 3, T: ambient, stirring rate: 700 rpm. The EPR analysis parameters were the same as in Figure 3.20.

During the Fenton oxidation of DMPO and 2-CP, the DMPO-·OH adduct was the only radical observed in the EPR spectrum, whose signal area diminished with the time as a consequence of the stability of the adduct (Figure 3.21). In this case and different from the Fenton experiments without stopped-flow apparatus (Figure 3.18), the absence of other radical species in the EPR spectra may be explained by different reasons: i) the volume analyzed was 3.34 μL instead of 18 μL (without stopped-flow) that can have influence on the sensitivity of the analysis; ii) the sample was analyzed immediately after the mixing of the Fenton reagents and the generation of other radical species previously identified might require longer reaction times; and iii) after the initial injection, the sample is affected by mass transfer limitations that could affect the formation of the other radical species. Alternatively, Figure 3.22 displays the EPR obtained when DMPO was not added to the reaction medium.

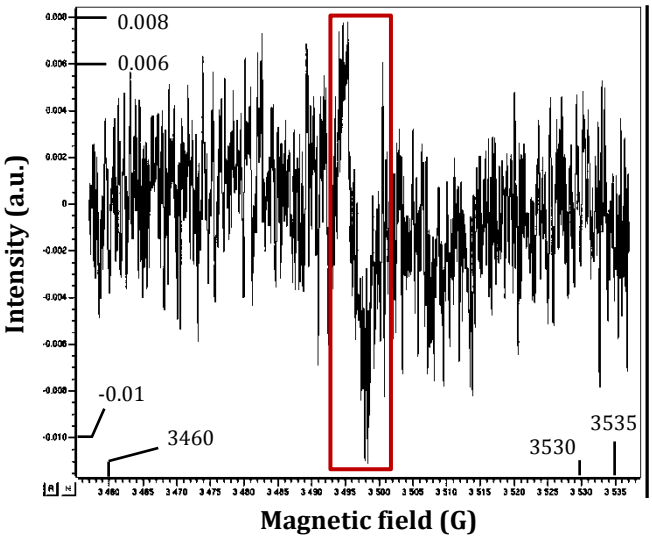

Figure 3.22. EPR spectra during the stopped-flow Fenton oxidation of 2-CP. $[2\text{-CP}]_0$: 155.6 mM, $[H_2O_2]_0$: 202.22 mM, $[FeSO_4{\cdot}7H_2O]_0$: 7.22 mM, $[NaCl]_0$: 56.34 mM. V_t: 0.005 L, pH_0: 3, T: ambient, stirring rate: 700 rpm. Microwave power: 63.25 mW, microwave frequency: 9.8 GHz, modulation frequency: 100 kHz, modulation amplitude: 1 G, center field: 3497 G, sweep width: 80 G, sweep time: 80 s, time constant: 81.92 ms, receiver gain: 40 dB, power attenuation: 5 dB.

When DMPO was not added to the reaction medium, the signal corresponding to semiquinone type radical was observed. Nevertheless, it cannot be clearly appreciated as when the stopped-flow apparatus was not used (Figure 3.19), supporting the idea of the lack of sensitivity at that concentration levels of the radical specie. Therefore, the EPR cell of higher volume should be coupled to the stopped-flow system with the aim of obtaining enough radicals concentration to overcome the limit of detection and to improve the resolution of the signals in the spectrum.

Summarizing the information explained along this section, EPR spectroscopy is a viable technique to identify the generation of both inorganic and organic radicals. As it was mentioned in the previous section, the proper conditions must be considered in order to avoid the oxidation of DMPO or DMPO adducts resulting in underestimation of the radical species of interest. For the specific study of Fenton oxidation of 2-CP, although 2-chlorophenoxy radicals were expected, it is likely that they were in concentrations lower than the limit of detection and, therefore, their identification was not possible. However, semiquinone radicals were observed in the EPR spectra even in the absence of DMPO as a consequence of their high stability compared to ·OH, and these radicals are deeply related to 2-CP and 2-chlorophenoxy radicals. Thus, this section constitutes an advanced step in the study of Fenton oxidation and, mainly, in the identification of transient species during the oxidation of the organic pollutants, especially of those species participating in the formation of PCDD/Fs. The connection of a stopped flow equipment with the EPR spectrometer allows the analysis of a sample at the initial reaction time although an improvement based on the increase of the EPR cell volume must be made to provide enough spin concentration to overcome the limit of detection.

3.2. Fenton oxidation of 2-chlorophenol solutions

In the following sub-sections the treatment of 2-chlorophenol solutions will be addressed not only because of its wide use in the preparation of large number of chemicals (herbicides, insecticides, among others), but also because it is provided of a toxic and carcinogenic character and may act as precursor of PCDD/Fs, which are even more toxic than the parent contaminant. Continuing with the research work developed by Vallejo et al. (2014), an initial concentration of 2-CP equal to 15.56 mM was selected (2000 mg L^{-1}) for the experimental work.[63] This concentration is relatively high compared to the concentration reported in industrial effluents and municipal waste discharges, typically containing CPs concentrations from 1 to 21 mg L^{-1}.[64] However, higher concentrations of phenolic compounds have been found in wastewaters from oil refineries and cocking plants or even up to 10,000 mg L^{-1} in olive oil mills wastewaters.[65,66] On the other hand, the selection of larger initial concentrations will allow the correct evaluation of the byproducts formed during the Fenton oxidation.[67,68]

The starting point lies in the work developed by the Advanced Separation Processes research group on the Fenton oxidation of 2-CP aqueous solutions, in which the influence of H_2O_2 dose and temperature were assessed. Both parameters had a fundamental importance in the reduction of COD and TOC, as well as in the intermediate oxidation byproducts generated and their concentration. It was observed that under substoichiometric hydrogen peroxide doses (20%) and at room temperature, the reduction of COD and TOC was hardly affected, and some aromatic compounds were detected as oxidation byproducts. In the present chapter, through the different sections, the influence of variables such as the presence of chloride ions, the iron dose and the addition of a copper salt will be evaluated. Furthermore, a complete comparison with previous results of the Advanced Separation Processes research group will be carried out. This section will be focused on the effect of the Fenton reaction on the abatement of 2-CP, COD, TOC and the generation of major oxidation byproducts, taking as reference point the use of substoichiometric hydrogen peroxide dose (20%) as it enables to remove almost all the initial 2-CP.

3.2.1. Influence of the presence of chloride ions in the aqueous solution

Wastewaters are usually characterized by the presence of inorganic salts being chlorine salts group the most frequently encountered.[69] High concentrations of chloride have been found in wastewaters from the manufacture of pesticides and herbicides, organic peroxides, pharmaceutics or even from landfill leachates, among others.[69,70] The treatment of aqueous solutions containing organochlorine compounds leads also to the release of chloride to the aqueous medium as a consequence of the mineralization reactions.[63] It is well known that chloride may act as scavenger of ·OH radicals, reducing their availability to react with the target pollutant.[1] As a consequence, this section aims to study the effect of chloride presence on the reaction medium throughout the application of Fenton oxidation to a 2-CP aqueous solution. A maximum concentration of 2000 mg L^{-1} has been selected and two different H_2O_2 doses have been studied (20 and 100% of the stoichiometric amount, Reaction 3.9). Figure 3.23 portrays the effect of chloride working under both H_2O_2 doses on the diminishment of 2-CP concentration, COD and TOC. The ratio H_2O_2/Fe(II) was kept to the values previously used by the research group, i.e., 0.18 mM Fe(II) when 40.44 mM H_2O_2 was employed (20% stoichiometry) and 7.22 mM Fe(II) when 202.22 mM H_2O_2 was used (100% stoichiometry).

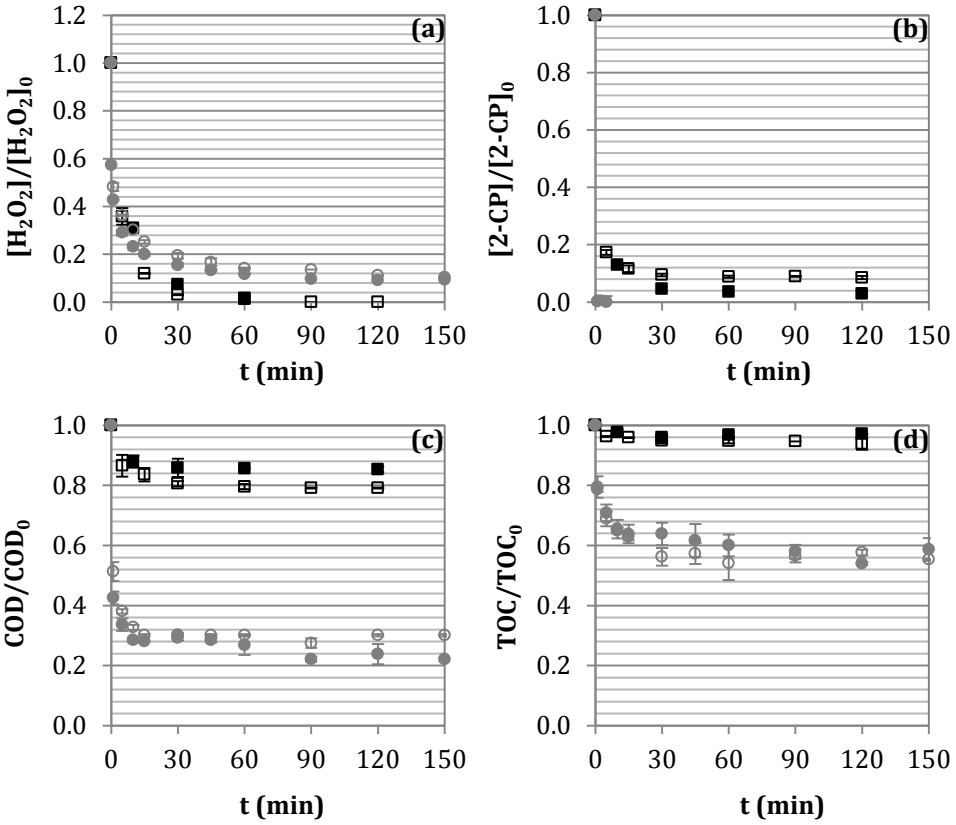

Figure 3.23. Effect of chloride on the (a) depletion of H_2O_2, (b) reduction of 2-CP, (c) diminishment of COD, and (d) decrease of TOC during the Fenton oxidation of 2-CP aqueous solutions. Filled symbols: 0 mM Cl^-, empty symbols: 56.34 mM Cl^-. ■ $[H_2O_2]$= 40.44 mM, $[Fe^{2+}]$= 0.18 mM; ● $[H_2O_2]_0$= 202.2 mM, $[Fe^{2+}]$= 7.22 mM. Common experimental conditions: $[2\text{-CP}]_0$= 15.56 mM, 20 ºC, pH_0= 3, V_0= 1 L.

As it can be seen in Figure 3.23, the presence of chloride did not have any remarkable influence on the profiles of H_2O_2, 2-CP, COD or TOC concentrations under the experimental conditions analyzed. Although free chlorine could not be measured in these experiments due to the brownish color of the solution that hinders its quantification by means of a colorimetric method, it is well known that the chloride present in the aqueous medium unselectively reacts with the generated ·OH radicals (k, $4.3\cdot10^9$ L mol^{-1} s^{-1}) leading to the formation of free chlorine species:

Cl_2 (pH≤ 3, Reactions 3.17-3.19), HClO (pH< 7.5, Reaction 3.20) and ClO^- (Reaction 3.21).[47,71-73]

$$HO\cdot + Cl^- \rightarrow ClOH^{\cdot -} \tag{3.17}$$

$$\cdot ClOH^- + H^+ \rightarrow \cdot Cl + H_2O \tag{3.18}$$

$$\cdot Cl + \cdot Cl \rightarrow Cl_2 \tag{3.19}$$

$$Cl_2 + H_2O \rightarrow HOCl + H^+ + Cl^- \tag{3.20}$$

$$HOCl \rightarrow OCl^- + H^+ \tag{3.21}$$

Usually, ·Cl radical is less reactive than ·OH, but in its reactions with organic compounds the magnitude of the rate constants for ·Cl are comparable to those for ·OH.[73] According to Pignatello et al. (1992), the scavenging effect of ·OH radicals by chloride is noticeable above 10 mM Cl^- (pH= 2.8) which is lower than the concentration employed in this thesis (56.34 mM).[74] On the other hand, concentrations of Cl^- over 200 mM result in the formation of ferric chlorocomplexes that hinders the regeneration of Fe^{2+}.[75] However, at the selected conditions no solids derived from complexation reactions were observed after the Fenton oxidation; and even if free chlorine is produced, it took part in the oxidation reactions as almost identical COD and TOC profiles were obtained (Figure 3.23c and d). What it is clear from Figure 3.23 is the relevance of the hydrogen peroxide dose, which resulted in a major oxidation degree owing to the higher availability of ·OH as it was previously explained by Vallejo et al. (2014).[63,76] 2-CP was completely removed after 5 minutes of treatment under 100% H_2O_2, whereas under substoichiometric concentrations there was around 5% of 2-CP left once the hydrogen peroxide was depleted. In terms of COD and TOC, the increase of the hydrogen peroxide dose resulted in an increase in their reduction yield from 13% to 74% and from 10% to 40%, respectively.

3.2.2. Influence of the iron dose

The effect of different concentrations of the catalyst, Fe^{2+}, on the Fenton oxidation of 2-CP has been studied. The Fe^{2+} concentration was selected at catalytic ratios ($Fe^{2+}/H_2O_2 << 1$) to avoid ·OH recombination and ·OH scavenging by Fe^{2+} (Reactions 1.7-1.10, Chapter 1) as well as to prevent any coagulation effect ($Fe^{2+}/H_2O_2 > 2$).[77-79] In this sense, five Fe(II) concentrations (0.09, 0.18, 0.36, 1.44 and 2.88 mM) were selected maintaining the H_2O_2 dose corresponding to 20% (40.44 mM) of the theoretical stoichiometric amount to mineralize 2-CP (Reaction 3.9). The selection of that concentration of hydrogen peroxide is related to the results previously observed in the research group, which corresponded to the almost complete degradation of the pollutant (90% of the initial 2-CP was oxidized) and the generation of higher concentrations of PCDD/Fs. Figure 3.24 presents the results obtained in terms of H_2O_2 depletion, decrease of 2-CP concentration, COD and TOC; by applying Fenton oxidation to a solution initially containing 2-CP, working with different iron doses under substoichiometric H_2O_2 dose.

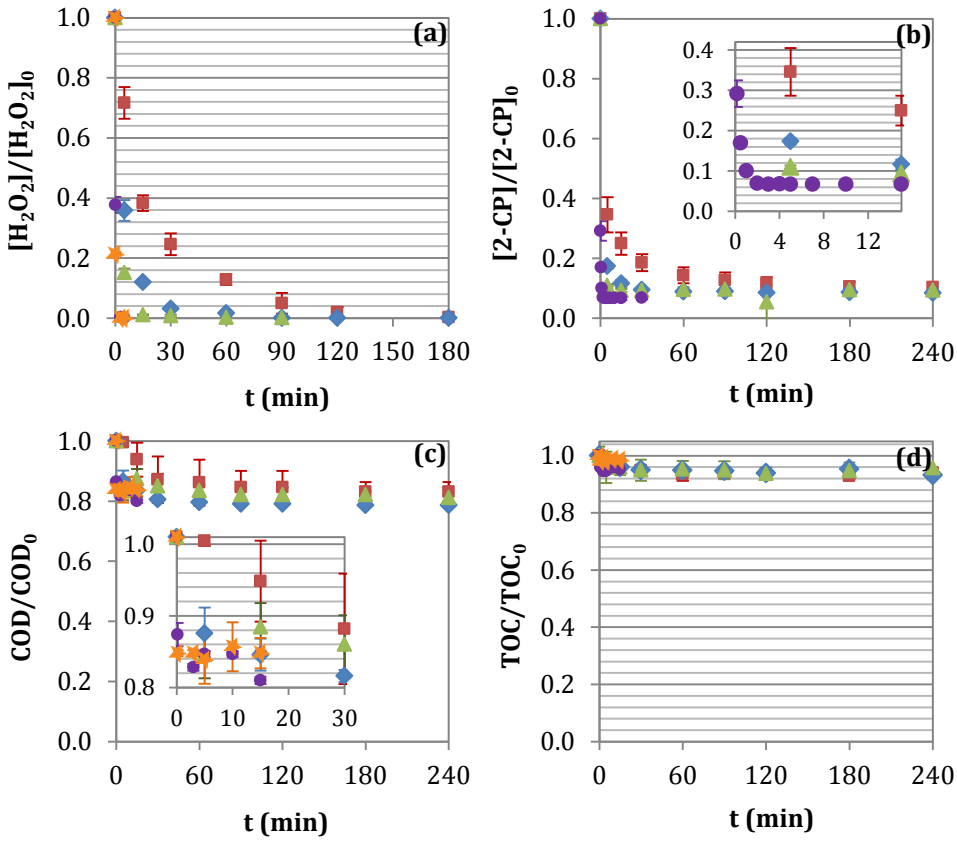

Figure 3.24. Effect of iron dose on the (a) depletion of H_2O_2, (b) reduction of 2-CP, (c) diminishment of COD, and (d) decrease of TOC during the Fenton oxidation of 2-CP aqueous solutions. $FeSO_4 \cdot 7H_2O$: ■ 0.09 mM, ◆ 0.18 mM, ▲ 0.36 mM, ★ 1.44 mM, and ● 2.88 mM. Common experimental conditions: $[H_2O_2]_0$= 40.44 mM, $[2\text{-CP}]_0$= 15.56 mM, [NaCl]= 56.34 mM, 20 ºC, pH_0= 3, V_0= 1 L.

Experiments were carried out for 4 hours although it was observed that after the H_2O_2 was depleted there was no change in the concentration of the measured parameters (Figure 3.24a). At a H_2O_2 concentration of 20% of the stoichiometric dose, a maximum of 90% of 2-CP was oxidized within the first 15 min of treatment for all Fe^{2+} doses tested with the exception of 0.09 mM that required at least 60 min (Figure 3.24b). As previously reported, the concentration of the Fe^{2+} catalyst is important for the reaction kinetics.[80] Indeed, the rate of 2-CP conversion augmented

with the increase in the concentration of ferrous ions (Figure 3.24b) due to a faster decomposition of H_2O_2 and, consequently, higher availability of ·OH. However, such increase in the removal rate was less noticeable for concentrations above 0.18 mM of Fe^{2+}, which could be explained by the faster H_2O_2 decomposition leading to higher concentrations of ·OH and ·OOH and auto-scavenging reactions that decrease ·OH availability (Reactions 1.7-1.10).[81,82] In contrast, changes in iron concentration had not influence on the final COD decrease and mineralization degree (Figure 3.24c and d), which were far from being completed under the operating conditions used in this work. As it happened with 2-CP diminishment (Figure 3.24b), an increase in COD removal was not appreciated working above 0.18 mM Fe(II). There was a larger decrease in COD compared to TOC, indicating that although organic matter was partially oxidized, only around 5% was transformed into CO_2. Given that 90% of 2-CP was removed, the COD and TOC profiles suggest the formation and presence of non-degraded organic matter remaining in the reaction medium.

Analysis of the oxidation byproducts generated in the Fenton oxidation of 2-CP

In order to identify the oxidation products formed during the application of the Fenton reaction to 2-CP aqueous solutions, samples collected during the Fenton treatment of 2-CP at different iron doses were analyzed by HPLC and ion chromatography according to the methods described in Chapter 2. Three aromatic intermediate products, 2-chlorobenzoquinone, 3-chlorocatechol and catechol, were identified during the treatment (Scheme 3.3), whose concentration during the Fenton treatment is portrayed in Figure 3.25.

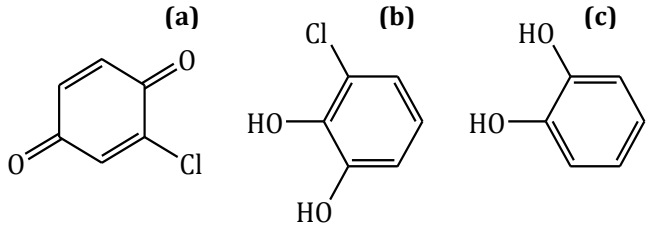

Scheme 3.3. Main aromatic byproducts from Fenton oxidation of 2-CP: a) 2-chlorobenzoquinone, b) 3-chlorocatechol and c) catechol.

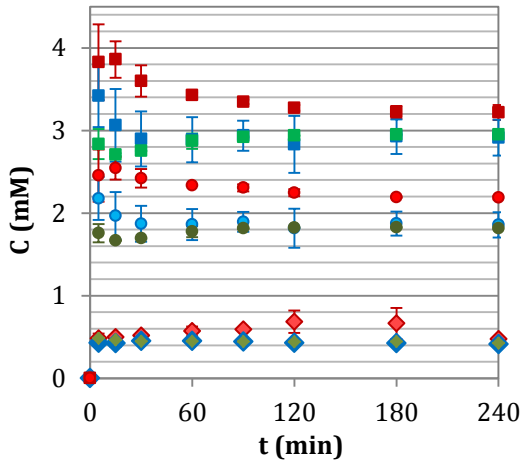

Figure 3.25. Effect of the iron dose on the generation of ■ 2-chlorobenzoquinone; ● 3-chlorocatechol; and ◆ catechol. Symbols color: red, 0.09 mM Fe(II); blue, 0.18 mM Fe(II); and green, 0.36 mM Fe(II). Common experimental conditions: $[H_2O_2]_0$= 40.44 mM, $[2\text{-CP}]_0$= 15.56 mM, [NaCl]= 56.34 mM, 20 ºC, pH_0= 3, V_0= 1 L.

The lower dose of Fe^{2+} resulted in higher maximum yields of 2-chlorobenzoquinone and 3-chlorocatechol, which are the initial byproducts, and slower degradation of these compounds in agreement with a slower H_2O_2 consumption (Figure 3.24a) and consequently lower ·OH availability. As in the case of 2-CP, the effect of the iron dose on the removal of the reaction intermediates was less pronounced at concentrations higher than 0.18 mM. In contrast, there was no significant effect of the iron concentration on the concentrations of catechol over the treatment time, which was detected at considerably lower concentration values than 2-chlorobenzoquinone.

Chen and Pignatello (1997) stated that aromatics such as catechol, hydroquinone and benzoquinone led to the formation of semiquinone radicals during the Fenton reaction that participate in the Fe(II)/Fe(III) cycle by means of oxidation and reduction reactions (Reactions 3.12, 3.22 and 3.23).[55] Precisely, these radicals were identified by EPR as it was displayed in Figure 3.19.

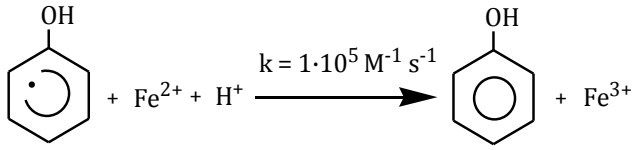

(3.22)

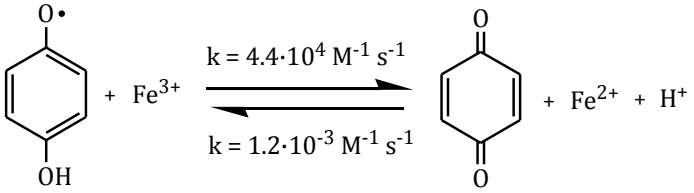

(3.23)

Figure 3.26 displays the decrease of hydrogen peroxide when the Fenton oxidation is carried out in the presence of 2-CP or without any organic compound in the reaction medium.

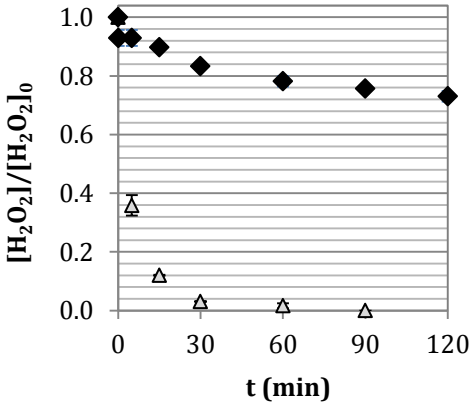

Figure 3.26. Depletion of H_2O_2 during the Fenton oxidation in the ◆ absence and △ presence of 15.56 mM 2-CP. $[Fe(II)]_0$= 0.18 mM, $[H_2O_2]_0$= 40.44 mM, [NaCl]= 56.34 mM, 20 ºC, pH_0= 3, V_0= 1 L.

A faster hydrogen peroxide decomposition was observed when chlorophenol was added to the reaction medium compared to the solution having only the Fenton reagents (absence of 2-CP, Figure 3.26). This fact can be explained considering the Reactions 3.12 and 3.23, especially the latter reaction that takes into account the reaction of the semiquinone type radicals, which were identified in the EPR analysis during the Fenton oxidation of 2-CP, with Fe(III). Precisely, the regeneration step from Fe(III) to Fe(II) is the limiting step in the Fenton reaction (Reactions 3.1 and

3.2). Consequently, the availability of Fe(III) is higher than the corresponding to Fe(II) so Reactions 3.12 and 3.23 shift to the right.[8]

Together with the aromatic oxidation byproducts, two aliphatic carboxylic acids, oxalic and formic acids, were also detected at low concentrations as a result of the cleavage of the aromatic ring (Scheme 3.4), whereas fumaric acid was only found working with an iron concentration of 0.18 mM.

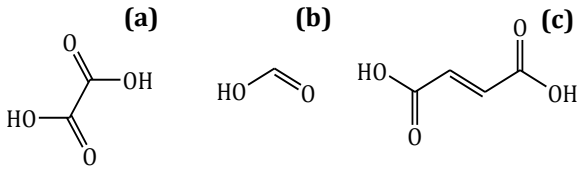

Scheme 3.4. Main aliphatic acids generated in the Fenton oxidation of 2-CP: a) oxalic acid, b) formic acid and c) fumaric acid.

Figure 3.27 shows the concentration profile for oxalic and formic acid during the Fenton oxidation employing different concentrations of iron.

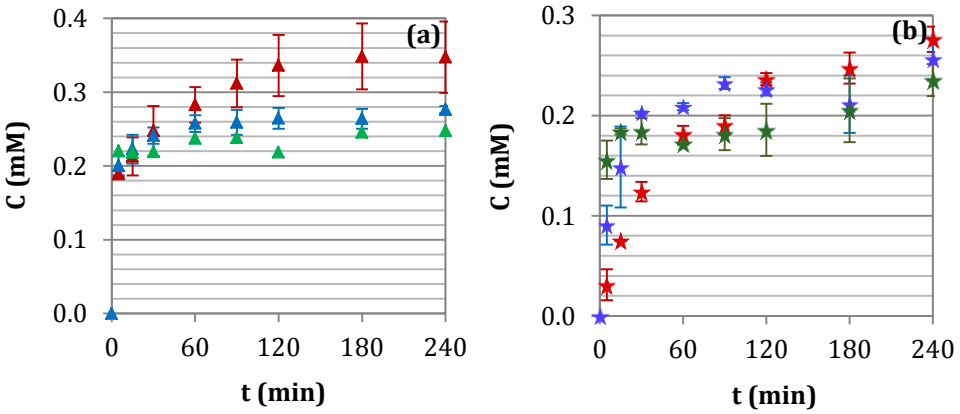

Figure 3.27. Effect of iron dose on the generation of ▲ formic acid; and ★ oxalic acid. Symbols color: red, 0.09 mM Fe(II); blue, 0.18 mM Fe(II); and green, 0.36 mM Fe(II). Common experimental conditions: $[H_2O_2]_0$= 40.44 mM, $[2\text{-CP}]_0$= 15.56 mM, [NaCl]= 56.34 mM, 20 ºC, pH_0= 3, V_0= 1 L.

With respect to the formic acid formation, there was no influence of the iron concentration in the first minutes of treatment; however, after 90 min, slightly

higher concentrations of formic acid were observed for lower iron doses (Figure 3.27a). Regarding the oxalic acid concentration, the higher iron concentration employed led to a faster aromatic ring cleavage as it was shown for 2-chlorobenzoquinone and 3-chlorocatechol, due to the higher ·OH availability, and thus rapid conversion of the organic matter into oxalic acid during the first minutes of the reaction (Figure 3.27b). Contrary to quinone type compounds, oxalic acid is known to act as suppressor of the ferric ion reduction due to its complexation with Fe(III) and, thus, terminating the Fenton reaction.[83] Additionally, concentrations up to 0.08 mM of fumaric acid were quantified when 0.18 mM Fe(II) was employed.

Influence of iron dose on TOC and chlorine balances

Theoretical TOC values were calculated considering the carbon content of the identified intermediate products together with that of the remaining concentration of 2-CP and compared to experimentally measured TOC data, which allowed to determine the percentage of unidentified TOC for the different iron doses tested. Figure 3.28 displays the percentage of TOC and chlorine that remained unidentified during the Fenton oxidation of 2-CP in aqueous solution.

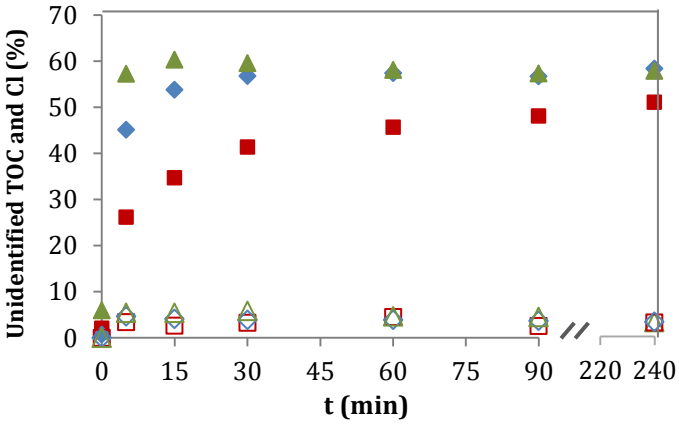

Figure 3.28. Unidentified TOC (filled symbols) and chlorine (empty symbols) during the Fenton oxidation of 2-CP aqueous solutions for different iron doses: ■ 0.09 mM, ◆ 0.18 mM, and ▲ 0.36 mM. Common experimental conditions: $[H_2O_2]_0$= 40.44 mM, $[2\text{-CP}]_0$= 15.56 mM, [NaCl]= 56.34 mM, 20 ºC, pH_0= 3, V_0= 1 L.

As can be observed in Figure 3.28, working with the lowest dose of iron, 0.09 mM, the percentage of unidentified TOC and, therefore, the unidentified oxidation intermediates was lower than the observed at higher iron concentrations, which could be explained by the slower conversion of 2-CP and higher concentrations of the identified aromatics and aliphatic acids displayed in Figures 3.26 and 3.27. After 4 h, 50% of TOC in the lowest iron concentration treatment remained unidentified whereas this value was 57% for both 0.18 and 0.36 mM Fe(II). The increase in the percentage of unidentified TOC during the first 15 min was larger for 0.36 mM Fe(II) treatment compared to the 0.18 mM Fe(II), which corresponded to a high removal rate of 2-CP (Figure 3.24b). After 30 min, there was no difference in the unidentified fraction of TOC between those iron doses. It is important to consider that the only organic compound present at t_0 is 2-chlorophenol. At initial reaction time, the aromatic byproducts 2-chlorobenzoquinone, 3-chlorocatechol and catechol were formed, resulting in more than 90% of TOC content identified. As the reaction proceeds the product distribution increases, making difficult to identify and quantify all of them.

The unselective reaction of ·OH together with their high reactivity and low H_2O_2 dose could explain differences between measured and theoretical TOC values, leading to the generation of numerous compounds low in concentration. The qualitative analyses carried out by GC-MS confirmed the formation of aromatic and condensation species, such as 2-chloro-1,4-benzenediol, 4-chloro-1,2-benzenediol, 4-chloro-1,3-benzenediol, and 5-chloro-1,3-benzodioxole (Scheme 3.5), inter alia, but they were not identified by HPLC suggesting low formation yields. Furthermore, some byproducts with dioxin-like structure were formed, including 2,4'-dichloro-5-hydroxydiphenyl ether, 4,4'-dichloro-1,1'-biphenyl-3,3'-diol and 4-chloro-2-[(5-chloro-2-hydroxyphenyl)methyl]phenol, which gather a higher number of carbon atoms than 2-CP.

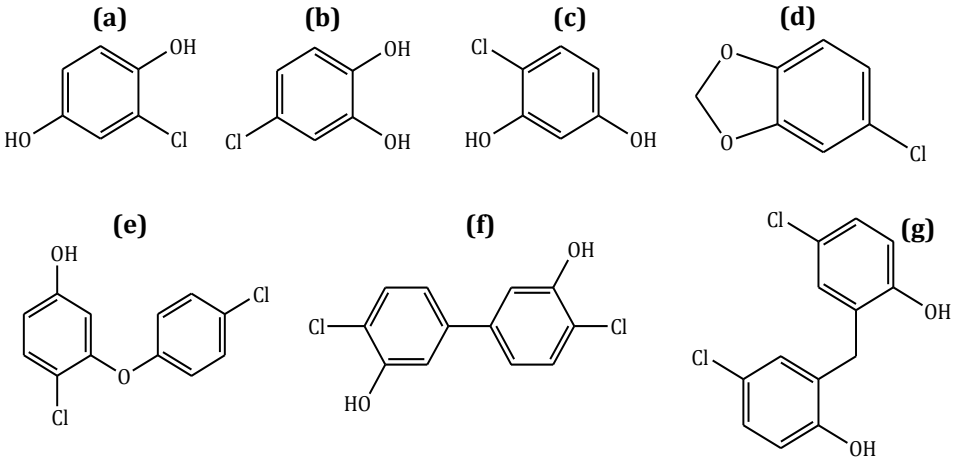

Scheme 3.5. Byproducts identified by GC-MS from Fenton oxidation of 2-CP: a) 2-chloro-1,4-benzenediol, b) 4-chloro-1,2-benzenediol, c) 4-chloro-1,3-benzenediol, d) 5-chloro-1,3-benzodioxole, e) 2,4'-dichloro-5-hydroxydiphenyl ether, f) 4,4'-dichloro-1,1'-biphenyl-3,3'-diol and g) 4-chloro-2-[(5-chloro-2-hydroxyphenyl)methyl]phenol.

In the literature, the observed differences between the measured and the calculated TOC have been frequently explained by the formation of coupling-reaction between aromatic species, which confer a dark brownish color to the reaction medium.[84,85] Some of these condensation substances, such as chlorinated biphenyl, chlorinated phenoxyphenols, chlorinated diphenyl ethers and chlorinated dioxins and furans have been identified by GC-MS during Fenton and Fenton-like treatments of solutions containing CPs at substoichiometric conditions.[67,68,76,86,87] Nevertheless, there is still lack understanding of the formation and identification of reaction products that occur at substoichiometric H_2O_2 to CP molar ratios.[68] Anyway, such unidentified byproducts have been shown to be susceptible to oxidation under more severe conditions such as the increase of the temperature and hydrogen peroxide dose.[76,85]

The percentage of unidentified chlorine was determined by accounting for the chlorine content of the identified species, 2-CP, 2-chlorobenzoquinone and 3-chlorocatechol, and analytically determined chloride that is present in the aqueous

solution. As it can be seen in Figure 3.28, there was no influence of the iron dose on the chlorine balance and 3% of chlorine remained unidentified for the three iron quantities used. According to Pignatello (1992), chlorine radicals can be formed from the reaction between ·OH and chloride and could contribute to the formation of chlorinated organic compounds.[74] As a result, some of the non-identified organic compounds may also have chlorine atoms in their structure. Though PCDD/Fs have been quantified, as it will be presented later, the concentration was really very low and not enough to completely justify the chlorine balance. On the other hand, as it was stated above, qualitative analyses of withdrawn samples displayed the formation of aromatic and condensation byproducts which also contain chlorine in their structure. Consequently, the sum of their concentrations, the concentration of many other organochlorinated compounds which have not been identified in this work, the concentration of free chlorine species that could be formed through hydroxylation of chloride ions together with the concentration of the possible iron(III)-chlorocomplexes, may explain the unidentified remaining percentage of chlorine.[53]

3.2.3. Effect of addition of a copper salt to the oxidation medium

As it was previously mentioned, wastewaters are usually characterized by the presence of inorganic salts that can include heavy metals to a greater or lesser extent depending on the origin of the sewage. For instance, there is variability between the composition of different landfill leachates as a consequence of the type of residues, age of the landfill, etc. The amount of chloride used in this thesis has been 2000 mg L^{-1}, which is in the average value of those reported in different studies where the concentration of Cl^- ranged from 10 to 5700 mg L^{-1}, reaching values up to 11375 mg L^{-1}.[88-92] Regarding iron, values between 0.2 and 28 mg L^{-1} have been found, or even values up to 42000 mg L^{-1} (in this thesis the concentration used was commonly 5-20 mg L^{-1} Fe^{2+}). On the other hand, this type of aqueous streams contains many other heavy metals such as copper, which can reach values between 0.01-43 mg L^{-1} depending on the type of the materials landfilled. Copper has been employed some times in Fenton-like studies, mainly in electro-Fenton and

photo-Fenton processes as well as heterogeneous catalysis.[21,93] In gas phase, it has been observed that copper promotes the formation of PCDD/Fs during pyrolysis and combustion processes from precursors and/or carbonaceous matrixes.[94-98] As a result, taking into consideration that copper could be present in the wastewater and its possible effect on the yield of Fenton oxidation as well as its potential role in the generation of PCDD/Fs, its influence throughout the Fenton treatment of 2-CP solution has been assessed.

Experiments adding 1 and 50 mg L^{-1} $CuSO_4 \cdot 5H_2O$ (0.016 and 0.787 mM, respectively) to the 2-CP (15.56 mM) aqueous solution in the presence (1.44 mM) and absence of Fe(II) were carried out and compared to that situation in which the copper salt was not added. In this sense, Figure 3.29 presents the changes in H_2O_2, 2-CP and TOC when working under substoichiometric hydrogen peroxide dose.

The trend in the hydrogen peroxide consumption in the conventional Fenton and adding the two different copper concentrations was the same, resulting in the complete depletion of H_2O_2 after 3 min (Figure 3.29a). However, when copper was the only metal present in the solution, there is not variation in the hydrogen peroxide concentration regarding the initial one, which means that the Fenton-like reaction is not taking place. With respect to the 2-CP analysis, a similar situation is occurring, i.e., in all experiments containing the iron salt 2-CP removal reached around 93% (Figure 3.29b), but not in the absence of iron that is responsible for the generation of ·OH through the Fenton-like oxidation. Furthermore, it can be confirmed that the decomposition of 2-CP by copper is not happening. Finally, with regard to TOC, the absence of oxidation reactions in the aqueous system results in the preservation of TOC (experiment containing only the copper salt), whereas there was no influence of the addition of the copper salt to the Fenton solution (Figure 3.29c).

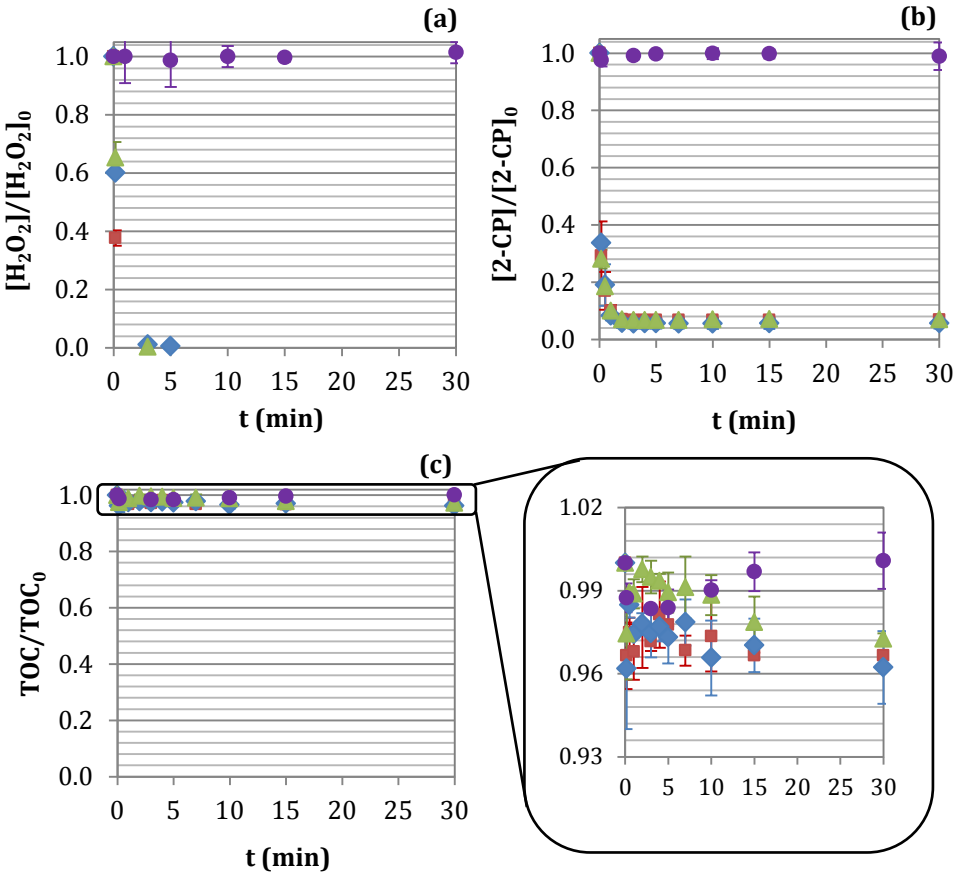

Figure 3.29. Effect of copper dose on the (a) depletion of H_2O_2, (b) reduction of 2-CP, and (c) decrease of TOC during the Fenton oxidation of 2-CP aqueous solutions. ■ $FeSO_4 \cdot 7H_2O$: 1.44 mM, $CuSO_4 \cdot 5H_2O$: 0 mM; ◆ $FeSO_4 \cdot 7H_2O$: 1.44 mM, $CuSO_4 \cdot 5H_2O$: 0.016 mM; ▲ $FeSO_4 \cdot 7H_2O$: 1.44 mM, $CuSO_4 \cdot 5H_2O$: 0.787 mM; and ● $FeSO_4 \cdot 7H_2O$: 0 mM, $CuSO_4 \cdot 5H_2O$: 0.787 mM. Common experimental conditions: 20 ºC, pH_0= 3, V_0= 1 L.

In some way, the real effect of copper, when both metals were added, could not be identified owing to the experimental conditions used in this study that resulted in a very fast removal of 2-CP and a slight reduction in TOC, small enough to see the variation between the experiments since the average values are inside the standard deviation.

These results are in line with those observed by Friedrich et al. (2012) during the Fenton oxidation of 10 mM phenol employing 0.5 mM Cu(II) and 200 mM H_2O_2, where TOC kept constant in absence of added Fe(II).[99] The addition of 0.5 mM Cu(II) in that work led to a reduction of TOC from 40 to 50%, although they used 143% of the stoichiometric amount of H_2O_2 needed for the complete mineralization of phenol while the results in Figure 3.29 display the behavior working at 20% and, therefore, in the initial steps of oxidation (low TOC decrease). During the application of solar photolysis and photoelectro-Fenton to oxalic and oxamic acid solutions, Garcia-Segura et al. (2016) and Pagano et al. (2011) achieved higher yields in their removal working with iron as catalyst although a combination of both copper and iron had a positive effect in the removal of these acids (Reactions 3.24 and 3.25).[93,100] Alternatively, other studies showed the effect of the addition of coper salt when the Fenton reaction was carried out by heterogeneous catalysis with Fe(II) or nano-scale zero-valent iron, displaying a positive effect during the oxidation of chlorobenzene and trichloroethylene, respectively.[100,101] In the case of the Fenton-like oxidation of trichloroethylene with nano-scale zero-valent iron, the increase in the removal yield comes with an increase of the iron concentration in the solution that may directly participate in the Fenton oxidation (Reactions 3.26-3.28).[100,101]

$$Cu^{+} + H_2O_2 \rightarrow Cu^{2+} + \cdot OH + OH^{-} \tag{3.24}$$

$$Fe^{3+} + Cu^{+} \rightarrow Fe^{2+} + Cu^{2+} \qquad \Delta E^0 = 0.618\ V \tag{3.25}$$

$$Fe^{0} + H_2O_2 \rightarrow Fe^{2+} + 2\ OH^{-} \tag{3.26}$$

$$Fe^{0} + 2\ Fe^{3+} \rightarrow 3\ Fe^{2+} \qquad \Delta E^0 = 1.211\ V \tag{3.27}$$

$$Fe^{0} + Cu^{2+} \rightarrow Fe^{2+} + Cu^{0} \qquad \Delta E^0 = 0.777\ V \quad K = 1.9 \cdot 10^{26} \tag{3.28}$$

3.3. Generation of PCDD/Fs from 2-chlorophenol oxidation

3.3.1. Influence of the operation variables

In this point, the generation of PCDD/Fs from the application of Fenton treatment to an aqueous solution of 2-CP is assessed. Most of the information presented corresponds to dioxins and furans of high chlorination degree (from tetra- to octa-) that comprise the most toxic congeners 2,3,7,8-PCDD/Fs. Once again, almost all the data have been obtained working with substoichiometric hydrogen peroxide doses that, in spite of enabling the almost complete degradation of 2-CP, favors PCDD/Fs formation as a result of the initial oxidation steps in which the TOC remained almost constant.[63]

Influence of the oxidation time

Initially, the generation of PCDD/Fs has been followed considering two different times for the Fenton reaction: 1 and 4 h. Stoichiometric hydrogen peroxide dose was selected (202.2 mM) as there was H_2O_2 left after one hour working under substoichiometric conditions, allowing further reaction of the oxidation byproducts formed from 2-CP (Figure 3.23). Figure 3.30 depicts how the treatment time affects the formation of PCDD/Fs in terms of total concentration of the homologues and concentration of the most toxic congeners (2,3,7,8-PCDD/Fs).

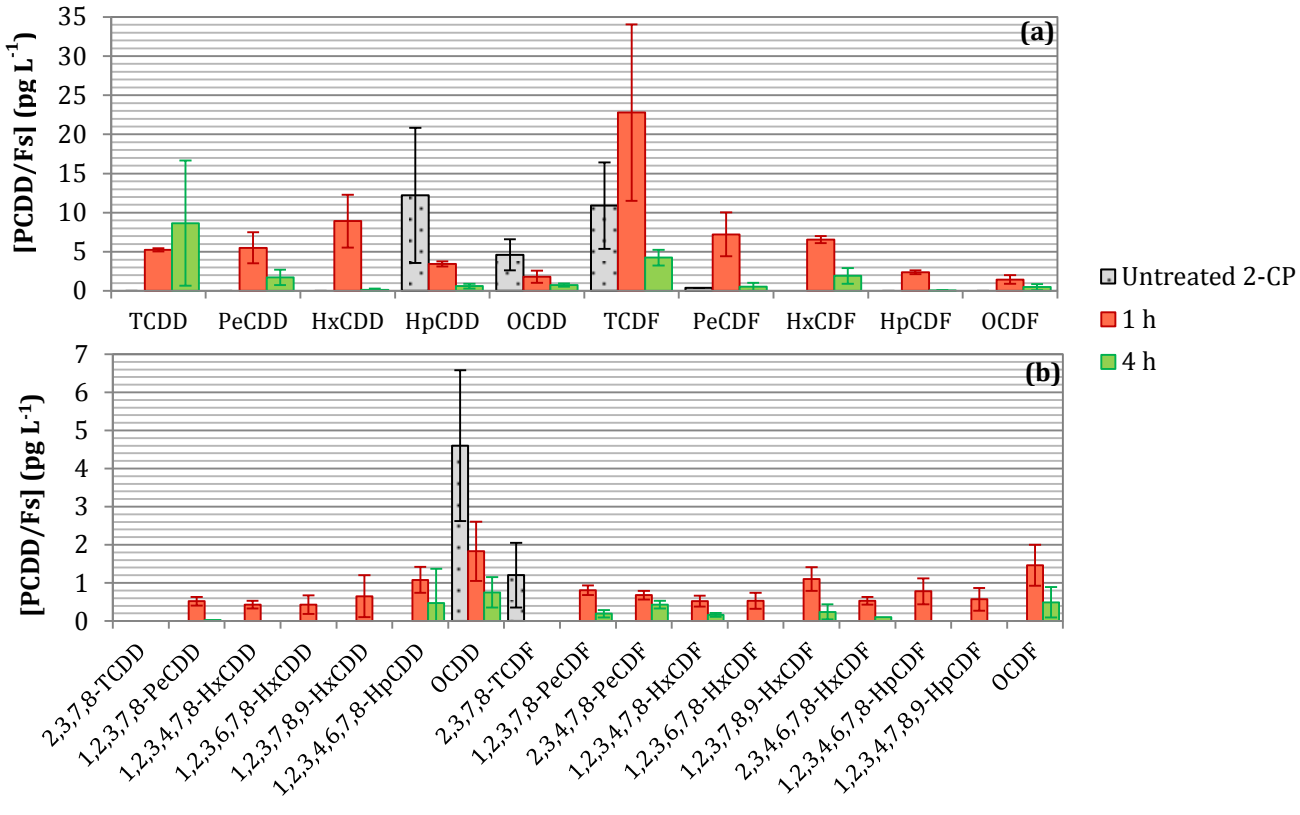

Figure 3.30. Effect of treatment time on the generation of PCDD/Fs during the Fenton oxidation of 2-CP: (a) homologue profile, (b) 2,3,7,8-PCDD/Fs. $[2\text{-CP}]_0$= 15.56 mM, $[H_2O_2]_0$= 202.2mM, $[Fe^{2+}]$= 7.22 mM, 20 ºC, pH_0= 3, V_0= 1 L.

Firstly, it can be observed that the solution of 2-CP alone in UP water had a small concentration of PCDD/Fs that was likely associated to its manufacture process.[102] The solution containing 2-CP was characterized by 17.7 pg L^{-1} PCDD/Fs, 5.8 pg L^{-1} 2,3,7,8-PCDD/Fs and 0.12 pg WHO-TEQ L^{-1}, being TCDF the dominant homologue (11.5 pg L^{-1}, 65%). When the Fenton reagents were added to the aqueous system, an increase in PCDD/Fs concentration from 17.7 to 65.4 pg L^{-1} was observed after 1 h of reaction as a consequence of the oxidation of 2-CP (Figure 3.30a). The major concentration corresponded to TCDF, whereas the initial HpCDD and OCDD present in the 2-CP solution had disappeared almost completely. On the other hand, an increase in the concentration of the most toxic congeners (2,3,7,8-PCDD/Fs) was also identified although they kept under 2.0 pg L^{-1} (a total of 11.9 pg L^{-1} and 1.2 pg WHO-TEQ L^{-1}, Figure 3.30b). Allowing the reaction to continue for 3 more hours ($t_{reaction}$= 4 h), there was a diminishment in all concentrations (a total of 19.1 pg L^{-1}) with the exception of TCDD (an increase from 5.2 to 8.7 pg L^{-1}), which could be related to the experimental error. With regard to 2,3,7,8-PCDD/Fs, their concentration diminished likely due to their removal through Fenton oxidation from 1 h to 4 h (from 11.9 to 2.9 pg L^{-1}). Therefore, in spite of obtaining low values of PCDD/Fs, Figure 3.30 displays the importance of PCDD/Fs generation mainly at initial Fenton treatment times, whose concentration will decrease if enough oxidizing agent is provided.

Influence of chloride ions concentration

The analyses of PCDD/Fs were performed after the complete depletion of H_2O_2, commonly keeping the solution for 4 h. The effect of the addition of chloride (56.34 mM) to the Fenton solution has been assessed for the two hydrogen peroxide doses studied, i.e., 20% and 100% of the stoichiometric amount (40.44 and 202.2 mM, respectively). Figure 3.31 portrays the comparison regarding the concentration of total homologue and 2,3,7,8-PCDD/Fs for both H_2O_2 doses in presence and absence of chloride in the aqueous solution.

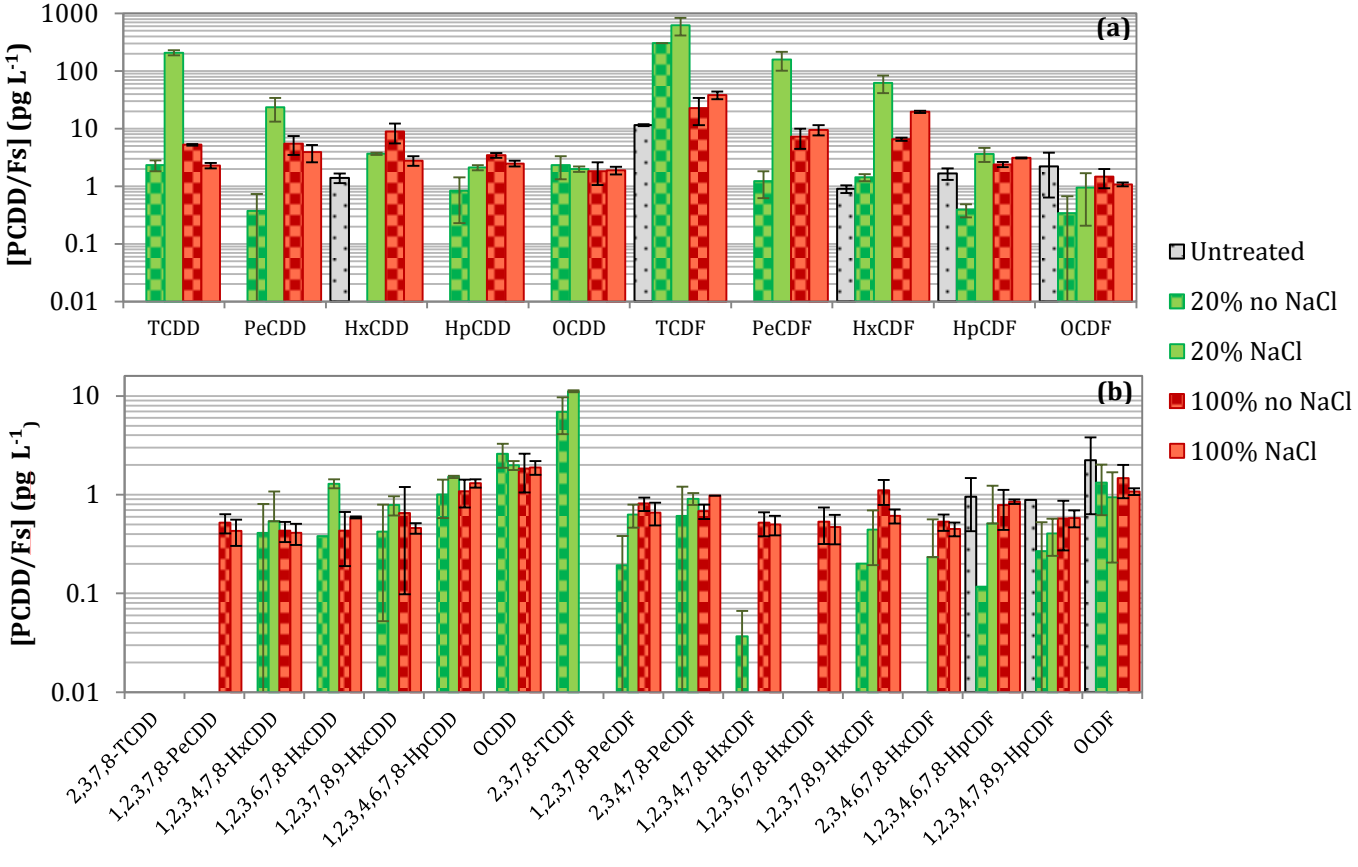

Figure 3.31. Effect of chloride on the generation of PCDD/Fs during the Fenton oxidation of 2-CP (15.56 mM): (a) homologue profile, (b) 2,3,7,8-PCDD/Fs. 20% H_2O_2: 40.44 mM H_2O_2, $[Fe^{2+}]$= 0.18 mM; 100% H_2O_2: $[H_2O_2]_0$= 202.2mM, $[Fe^{2+}]$= 7.22 mM. [NaCl]= 56.3 mM, 20 ºC, pH_0= 3, V_0= 1 L.

The application of Fenton oxidation under substoichiometric H_2O_2 dose (20%) without adding chloride compared to the untreated solution, resulted in an increase of the total PCDD/Fs concentration (1013.4 pg L^{-1}), 2,3,7,8-PCDD/Fs concentration (14.42 pg L^{-1}), and TEQ (1.04 pg WHO-TEQ L^{-1}). The concentration profile of the homologue groups displays a predominance of TCDF (303.6 pg L^{-1}) that corresponds to the 30% of the total amount of PCDD/Fs from tetra- to octa-chlorinated derivatives (Figure 3.31a). New groups of homologues such as TCDD, PeCDD, HpCDD, OCDD and PeCDF appeared as a consequence of the Fenton treatment compared to the untreated solution. These results demonstrated the potential of 2-CP as precursor of PCDD/Fs. The observation of HxCDD-OCDD, which were not present in the initial 2-CP solution, involves that chlorination reactions were occurring in the reaction system from the release of chlorine of the initial 2-CP, as it was the only source of chlorine, leading to the formation of reactive free chlorine (Reactions 3.17-3.21). With regard to 2,3,7,8-PCDD/Fs congeners (Figure 3.31b), which lead to a WHO-TEQ= 1.04 pg L^{-1}), most of them were at concentrations below 1 pg L^{-1} and furans were predominant, especially 2,3,7,8-TCDF (6.9 pg L^{-1}, 47.9% of total 2,3,7,8-PCDD/Fs).

When NaCl was added to the reaction medium, the concentration of total PCDD/Fs augmented 3.7 times compared to the Fenton treatment without chloride (3795.1 pg L^{-1}). Higher concentrations were obtained for all the homologue PCDD/Fs (Figure 3.31a), where the major differences were produced in the formation of TCDD and TCDF (from 2 to 208 pg L^{-1}, and from 303 to 628 pg L^{-1}, respectively). Under the mentioned conditions, it can be observed an increase in the homologue concentration from TCDD to OCDD and from TCDF to OCDF that may explain the chain of chlorination reactions. Although no differences in terms of H_2O_2, 2-CP, COD and TOC diminishment were observed with and without the addition of Cl^- (Figure 3.23), it is clear that part of the hydroxyl radicals generated in the Fenton reaction were consumed by chloride to produce chlorine radical according to Reactions 3.17 and 3.18; this radical takes part in the chlorination reaction towards PCDD/Fs of higher chlorination degree. In terms of 2,3,7,8-PCDD/Fs, 21.4 pg L^{-1}

were quantified (1.5 times higher than without chloride, Figure 3.31b), although big differences were not observed between both conditions taking into consideration the error bars. The toxic equivalency was 1.76, which is also lower than the enforceable maximum contaminant level of 30 pg L^{-1} stablished by the EPA.[103]

In general, the presence of PCDD/Fs in the final solution can be prevented by augmenting the dose of hydrogen peroxide (Figure 3.31). As it was represented in Figure 3.23, an increase in the concentration of H_2O_2 resulted in a faster degradation of 2-CP and higher COD and TOC removal, which is related to the displacement of the reagent towards simpler oxidation products (short chain byproducts and CO_2).[71] In this sense, dioxins and furans are probably formed at initial times and then, due to the availability of ·OH, they are degraded. When theoretical stoichiometric amounts of H_2O_2 were used, the total concentration of PCDD/Fs was 65.4 and 85.1 pg L^{-1} (without and with NaCl, respectively), but similar concentrations were obtained comparing the values and errors for each homologue group and the most toxic congeners (Figure 3.31), different from the results obtained under substoichiometric H_2O_2 in which the presence of chloride resulted in a 3.7 times increase of the total PCDD/Fs concentration. Once again, the maximum concentration corresponded to TCDF: 58.7% and 45.0% of total PCDD/Fs (Figure 3.31a) that in the case of substoichiometric H_2O_2 concentration were 30% and 17% (without and with NaCl, respectively). With regard to the 2,3,7,8-PCDD/Fs, stoichiometric H_2O_2 dose led to similar final concentrations: 11.9 and 11.3 pg L^{-1} in the absence and presence of chloride, respectively, with WHO-TEQ equal to 1.19 and 1.12 pg L^{-1}.

Although a detailed analysis of the proposed mechanisms for the formation of PCDD/Fs from 2-CP will be discussed in Chapter 4, a brief notion will be explained here to understand how the chlorine specie participates in their generation. 2-CP only has one chlorine atom, so direct condensation reaction of 2-CP molecules would lead to the formation of a dioxin with a maximum of two chlorine atoms. However, as it is depicted in Figure 3.30, dioxins of higher chlorination degree were identified, i.e., further chlorination of the precursors and/or dioxins was happening.

In gas phase reactions (combustion and pyrolysis), an increase in PCDD/Fs concentration was observed increasing the amount of active chlorine during *de novo* formation from fly ashes: chlorine participates in the formation of PCDD/Fs by chlorinating the carbon matrix and breaking the bonds between the aromatic rings.[94,104,105] The reaction in gas phase between chlorine and PCDD/Fs precursors such as chlorophenols can lead to the formation of (chloro)phenyl radicals throughout the H abstraction, radicals whose condensation reactions may produce PCDD/Fs.[94,106] A positive effect of chlorine on the formation of PCDD/Fs was also observed during the non-wood pulp bleaching, where the active chlorine may contribute to the rupture of lignin chains that afterwards continue the reactive process towards PCDD/Fs.[107]

Influence of the iron dose

In spite of the fact that there were not differences in terms of final 2-CP, COD and TOC removal between the various iron doses applied working under substoichiometric Fenton conditions, the effect of the initial ferrous concentration on the formation of dioxins and furans has been assessed. Whereas previous studies related to the generation of PCDD/Fs in wastewaters were focused on the identification of homologue groups from tetra- to octa-PCDD/Fs, this section deepens in the formation of non-chlorinated (DD/Fs) and low chlorinated CDD/Fs (from mono- to tri-) to assist the identification of the reaction pathway that leads to PCDD/Fs in aqueous phase oxidation media (Chapter 4), as they can serve as precursors of PCDD/Fs of higher chlorination degree when there is a source of chlorine. In this sense, the conditions selected are those that led to higher PCDD/Fs generation: substoichiometric H_2O_2 and chloride presence in the aqueous solution.

<u>a) Formation of low chlorinated PCDD/F</u>

Figure 3.32 displays the concentrations of DD/Fs and low chlorinated DD/DFs working with different Fe^{2+} doses during the Fenton oxidation of 15.56 mM 2-CP, in the presence of 56.34 mM NaCl and adding only the 20% of the stoichiometric H_2O_2 dose (40.44 mM).

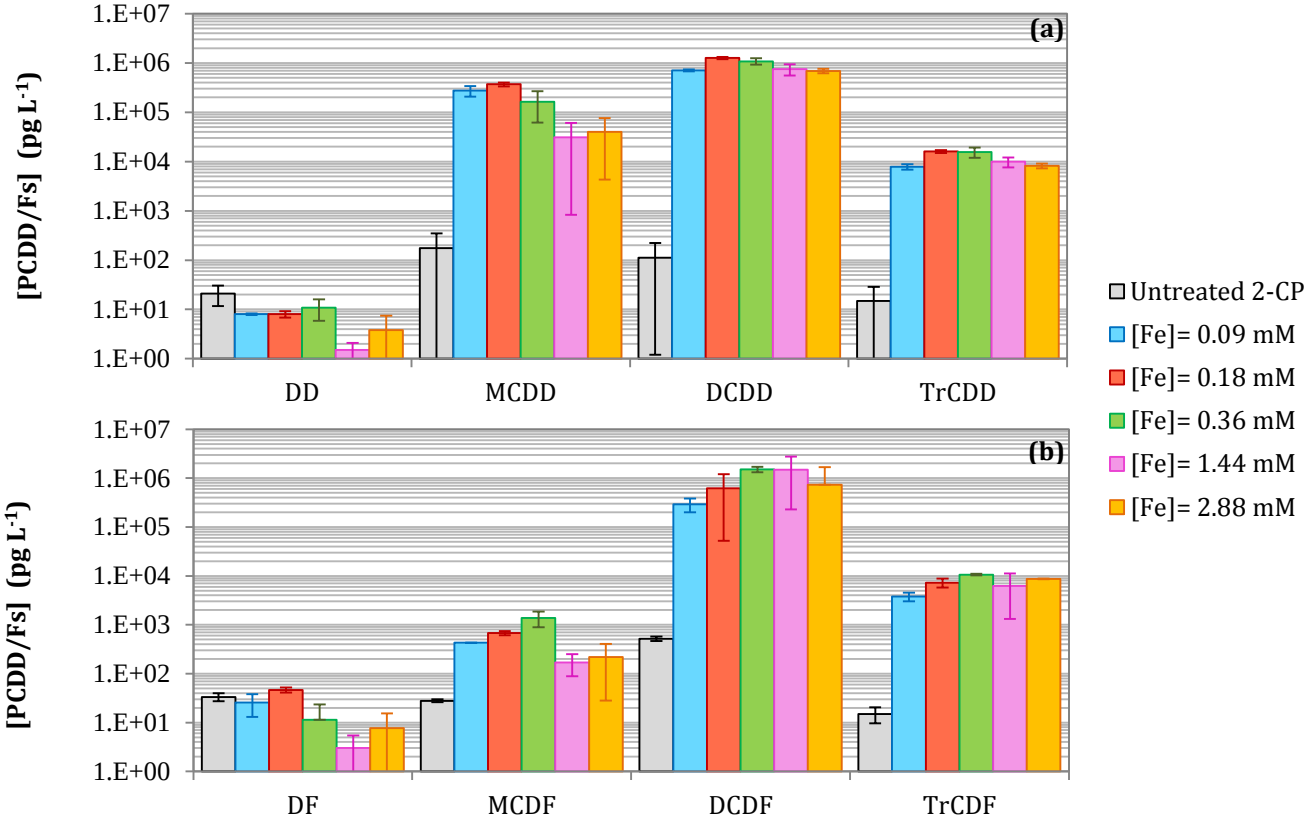

Figure 3.32. Effect of the iron dose on the generation of non-chlorinated and low chlorinated, form mono- to tri- (a) dioxins and (b) furans during the Fenton oxidation of 2-CP. $[2\text{-CP}]_0$= 15.56 mM, $[H_2O_2]_0$= 40.44 mM, [NaCl]= 56.34 mM, 20 ºC, pH_0= 3, V_0= 1 L.

Although the initial 2-CP solution contains PCDD/Fs, a notorious increase has been observed in all the homologue groups with the exception of the non-chlorinated species that maintained the initial concentration or they were slightly reduced during the Fenton oxidation. Taking into account the standard deviation, a consistent conclusion about the influence of the iron dose in the formation of PCDD/Fs cannot be elucidated and a general rule cannot be stablished as it seems that dioxins reached their maximum concentration working with 0.18 mM Fe^{2+} while the maximum furans concentration would be reached working with 0.36 mM Fe^{2+}.

The average total concentration of dioxins and furans considering the results of the experiments with different iron doses was 1085±376 and 938±490 ng L^{-1}, respectively, which corresponded to an increase of more than 2200 times in the initial concentration. In the case of dioxins, MCDD and DCDD were the major groups with an average concentration of 176 and 898 ng L^{-1} representing 16.2 and 82.7%, respectively, of the total dioxin concentration evaluated in this section. DCDF constituted the main low-chlorinated DF in the Fenton oxidation of 2-CP with an average concentration of 930 ng L^{-1} that corresponds to 99.2% of the total furan concentration analyzed in this section. By and large, DCDD and DCDF were the species with higher yield and represent 44.4 and 46.0%, respectively, of total PCDD/Fs concentrations analyzed in this section followed by MCDD (8.7%), adding all together 99%. The concentrations of TrCDD and TrCDF were around two orders of magnitude lower than DCDD/Fs, with average values of 11 and 7 ng L^{-1} each.

b) Formation of high chlorinated PCDD/F

Figure 3.33 presents the comparison of the concentration profile of dioxins and furans of higher chlorination degree for different iron doses employed during the Fenton oxidation of 2-CP, working under substoichiometric hydrogen peroxide doses.

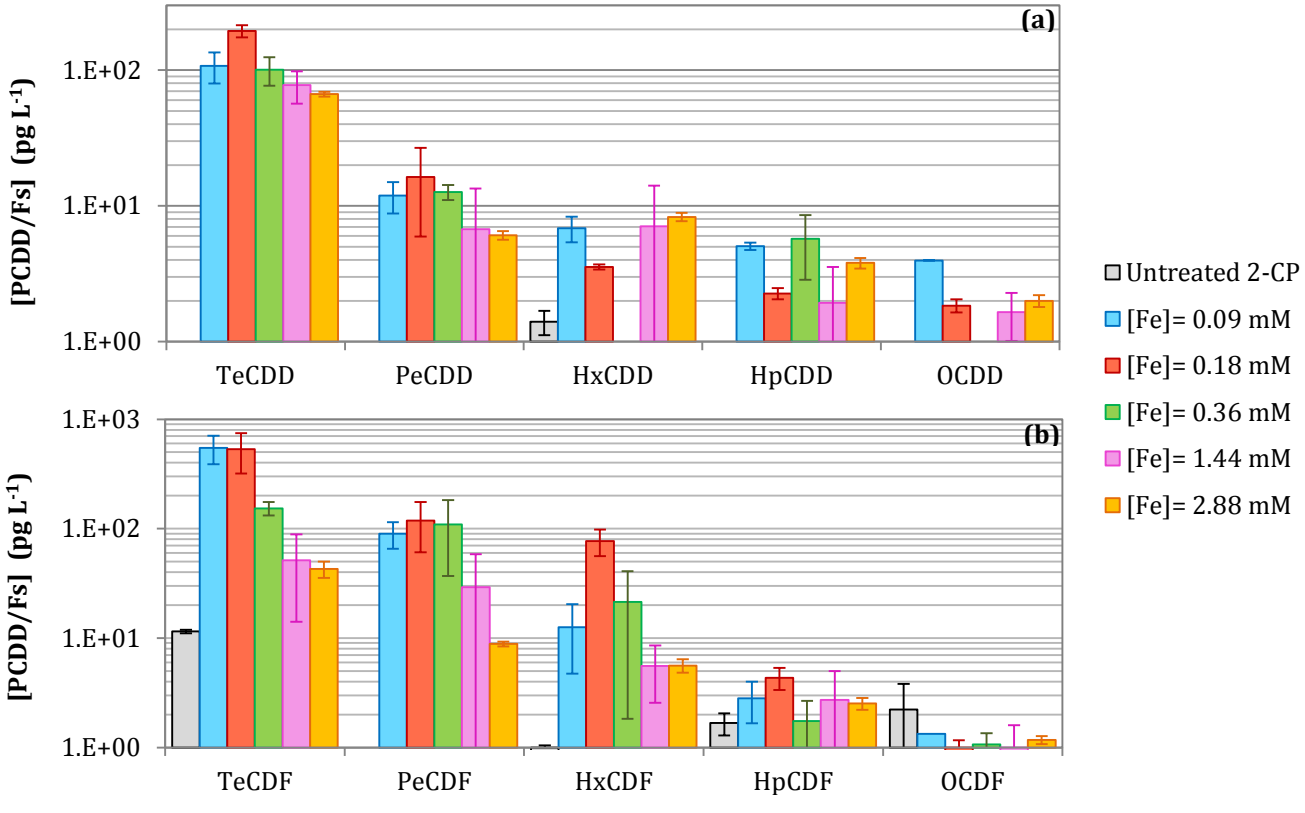

Figure 3.33. Effect of the iron dose on the generation of high chlorinated, form tetra- to octa- (a) dioxins and (b) furans during the Fenton oxidation of 2-CP. $[2\text{-CP}]_0$= 15.56 mM, $[H_2O_2]_0$= 40.44 mM, [NaCl]= 56.34 mM, 20 ºC, pH_0= 3, V_0= 1 L.

First of all, it is of special relevance to highlight the differences in the scale of concentrations between the low and high chlorination PCDD/Fs (10^6 pg L^{-1} for DCDD/F against 10^2 for TeCDD/F), i.e., TCCD/F-OCDD/F have been observed during the Fenton oxidation of 2-CP although at lower concentrations than the low chlorinated homologue groups. Though in some cases the standard deviation between duplicate results was considerable, taking into consideration the average concentration of each homologue for all the iron doses studied, the distribution of dioxins was TCDD, 82.1 pg L^{-1}; PeCDD, 9.5 pg L^{-1}; HxCDD, 5.8 pg L^{-1}; HpCDD, 3.7 pg L^{-1}; and OCDD, 1.7 pg L^{-1} (Figure 3.33). With regard to the distribution of furans, the average concentrations obtained were TCDF, 207.5 pg L^{-1}; PeCDF, 58.2 pg L^{-1}; HxCDF, 16.3 pg L^{-1}; HpCDF, 2.5 pg L^{-1}; and OCDF, 1.0 pg L^{-1}. In this sense, the increase of high chlorinated PCDD/Fs was around 28 times compared to the initial solution containing only 2-CP, unlike low-chlorinated DD/Fs (2200 times higher). The total average concentration of tetra-octaCDD/Fs by using 0.18 mM Fe(II) was 1094 pg L^{-1}, superior than the corresponding one to 0.09 mM Fe(II) (789 pg L^{-1}), but further iron addition resulted in a decrease of tetra-octaCDD/Fs (down to 147.6 pg L^{-1} in the presence of 2.88 mM Fe(II)).

Considering the global distribution of PCDD/Fs from non-chlorinated to octa-chlorinated, maximum concentrations were obtained for DCDD/F and a general trend can be deduced from Figures 3.32 and 3.33 that predicts a decrease in the PCDD/F homologue concentration as the chlorination degree increases, particularly from DCDD/F to PeCDD/F. Given the set of all the homologue groups, the average concentration of DCDD and DCDF constituted 44.4 and 46.0% of the total PCDD/Fs concentration indicating the low weight of high chlorinated PCDD/Fs in the total count. On the other hand, as mentioned in the preceding section, a final conclusion about the influence of iron concentration cannot be evidenced (Figures 3.32 and 3.33). What it is clear is that it is especially important to consider the generation of low chlorinated DD/Fs since they may act as precursors of the high chlorinated derivatives and, as a result, of 2,3,7,8-PCDD/Fs, as it will be explained later in Chapter 4.

Figure 3.34 shows the profile of 2,3,7,8-PCDD/Fs generated as a result of the Fenton oxidation of 2-CP using different Fe(II) doses and under the same conditions described in Figures 3.32 and 3.33. 2,3,7,8-PCDD/Fs have been detected at very low concentrations, within the range 3.5-21.4 pg L^{-1}, thus the formation of less toxic PCDD/Fs (other than 2,3,7,8-PCDD/Fs) was favored under the operating conditions used in this thesis. The most significant result was related to the formation of 2,3,7,8-TCDF that reach a concentration of 11.1 pg L^{-1} at an iron concentration of 0.18 mM but was not found at higher doses. Consequently, WHO-TEQ values were low, ranging from 0.2 to 1.8 pg WHO-TEQ L^{-1}, and lower than the maximum level for drinking water (30 pg L^{-1} of 2,3,7,8-TEQ; U.S. EPA). It should be noted that low PCDD/Fs concentrations do not eliminate threats, as these pollutants are highly persistent in the environment, lipophilic and toxic even at very low concentrations.

Therefore, under the iron doses selected in this thesis, no relevant differences in terms of PCDD/Fs generation have been observed. It is important to highlight that in all the cases catalytic concentrations of Fe(II) were used (Fe(II)/H_2O_2<< 1), which only had influence on the kinetics of H_2O_2 decomposition to generate ·OH, leading in all the Fe(II)/H_2O_2 evaluated ratios to similar final 2-CP concentrations, COD, TOC, and PCDD/Fs. The influence of iron on the formation of PCDD/Fs has been more thoroughly studied in combustion processes. In this sense, the presence of metallic compounds such as iron and copper is known to be important for the formation of PCDD/Fs in the postcombustion zone in an incinerator.[108,109] Iron is a redox active metal and the most abundant transition metal in fly ash, contributing to the formation of surface-associated phenoxyl radicals, which undergo further reactions to yield PCDD/Fs.[110] In addition to combustion processes, some studies have provided evidence of the OCDD formation when the precursor molecule pentachlorophenol was mixed at environmental conditions with a Fe(III)-montmorillonite clay mineral catalyst.[111] The formation of OCDD as photodegradation product of pentachlorophenol (PCP) in aqueous solutions containing Fe(III) at pH 3 and 5 was also detected likely resulting from dimerization via radical coupling of the intermediates from PCP.[112]

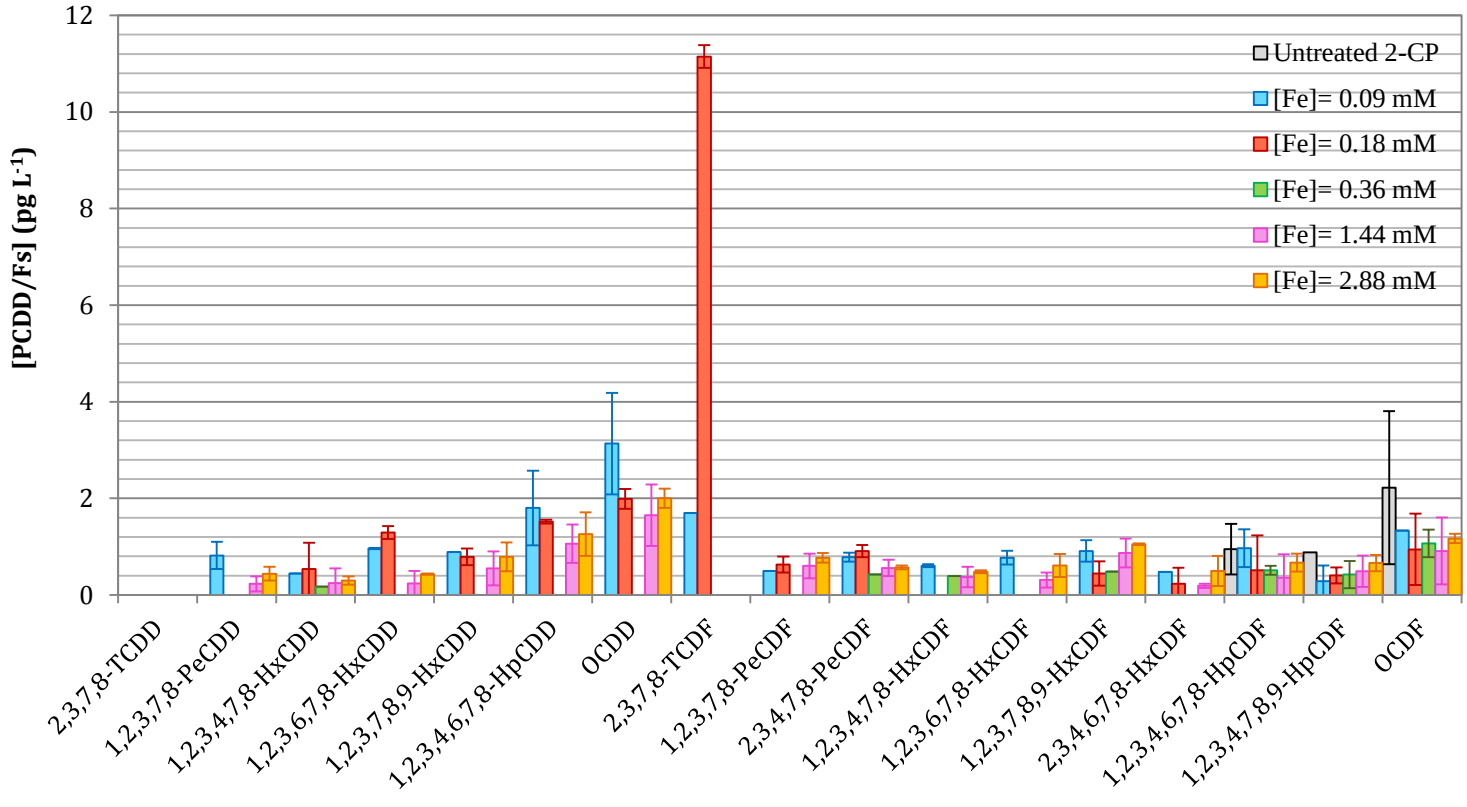

Figure 3.34. Effect of the iron dose on the generation of 2,3,7,8-PCDD/Fs during the Fenton oxidation of 2-CP. $[2\text{-CP}]_0$= 15.56 mM, $[H_2O_2]_0$= 40.44 mM, [NaCl]= 56.34 mM, 20 ºC, pH_0= 3, V_0= 1 L.

Effect of addition of copper salt to the oxidation medium

The generation of PCDD/Fs was compared during the Fenton oxidation of 2-CP in absence of copper and adding 50 mg L^{-1} of $CuSO_4 \cdot 5H_2O$ (0.79 mM). These results are portrayed in Figure 3.35, taking as reference the Fenton experiments in which 1.44 mM Fe(II) and 40.44 mM H_2O_2 were used in the presence of 56.34 mM NaCl. In terms of total concentration of the homologues groups, the major difference between adding or not the copper salt was observed for MCDD (0.6 *vs* 1.2 μg L^{-1}), DCDD (2.3 *vs* 4.0 μg L^{-1}) and MCDF (4.5 *vs* 6.6 μg L^{-1}). However, the differences between the total concentrations between both experiments are inside the error range, and, therefore, it is not easy to discriminate the real effect of copper in the generation of PCDD/Fs. The trend in the concentration profile was the same as presented without copper in which DCDD and DCDF were the main homologues generated. Considering also that the results for derivatives from tetra- to octa-DD/Fs were almost equal (Figure 3.35), it could be assumed that the generation of PCDD/Fs is independent of the copper presence in solution for the experimental conditions studied. The results presented here could serve as preliminary data that should be further confirmed and completed in the future broadening the parameters of study.

Regarding the formation of the most toxic congeners, which are presented in Figure 3.36, slightly higher concentrations were found during the Fenton experiments with Cu(II) although considering the error bars it cannot be ensured that copper had any positive effect on the formation of 2,3,7,8-PCDD/Fs.

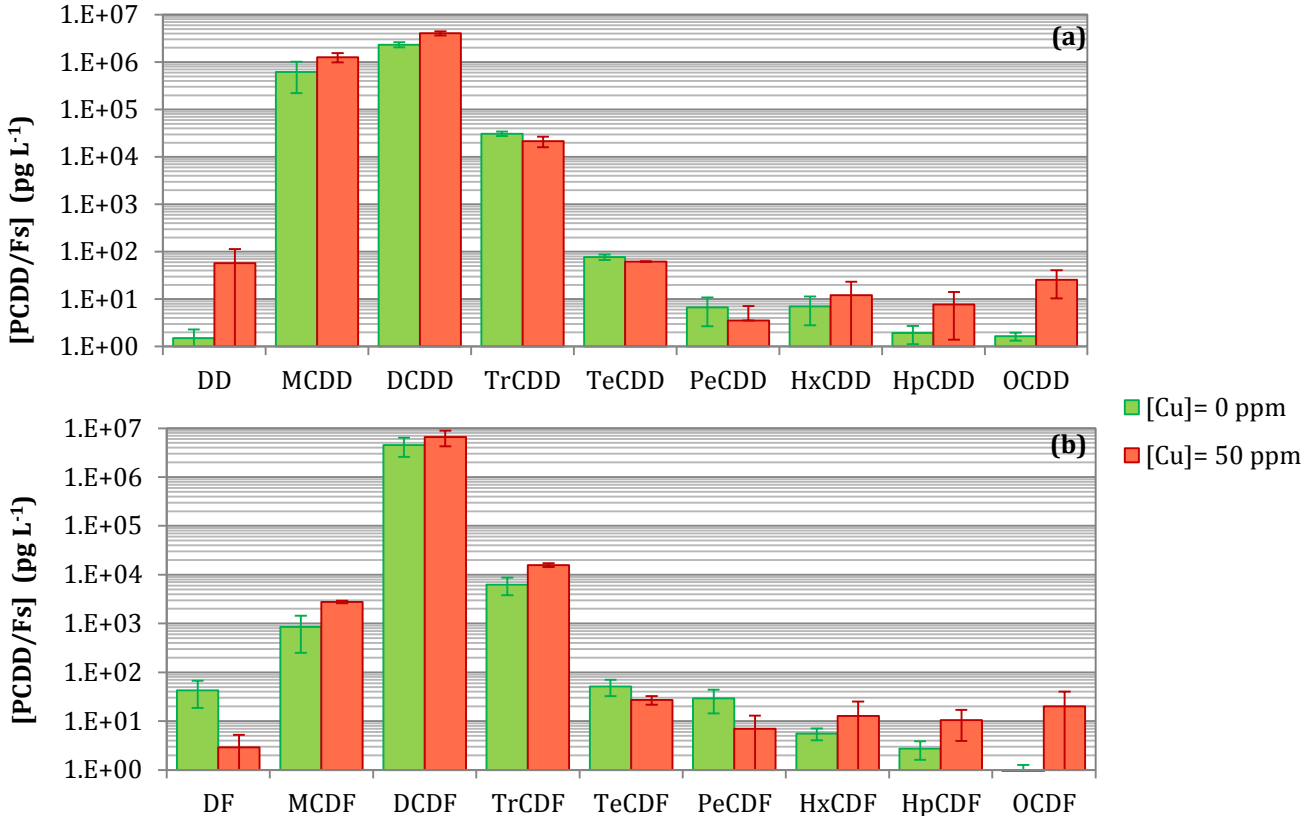

Figure 3.35. Effect of copper salt on the generation of (a) PCDDs and (b) PCDFs during the Fenton oxidation of 2-CP. $[2\text{-CP}]_0$=15.56 mM, $[H_2O_2]_0$= 40.44 mM, $[Fe^{2+}]$= 1.44 mM, [NaCl]= 56.34 mM, 20 ºC, pH_0= 3, V_0= 1 L.

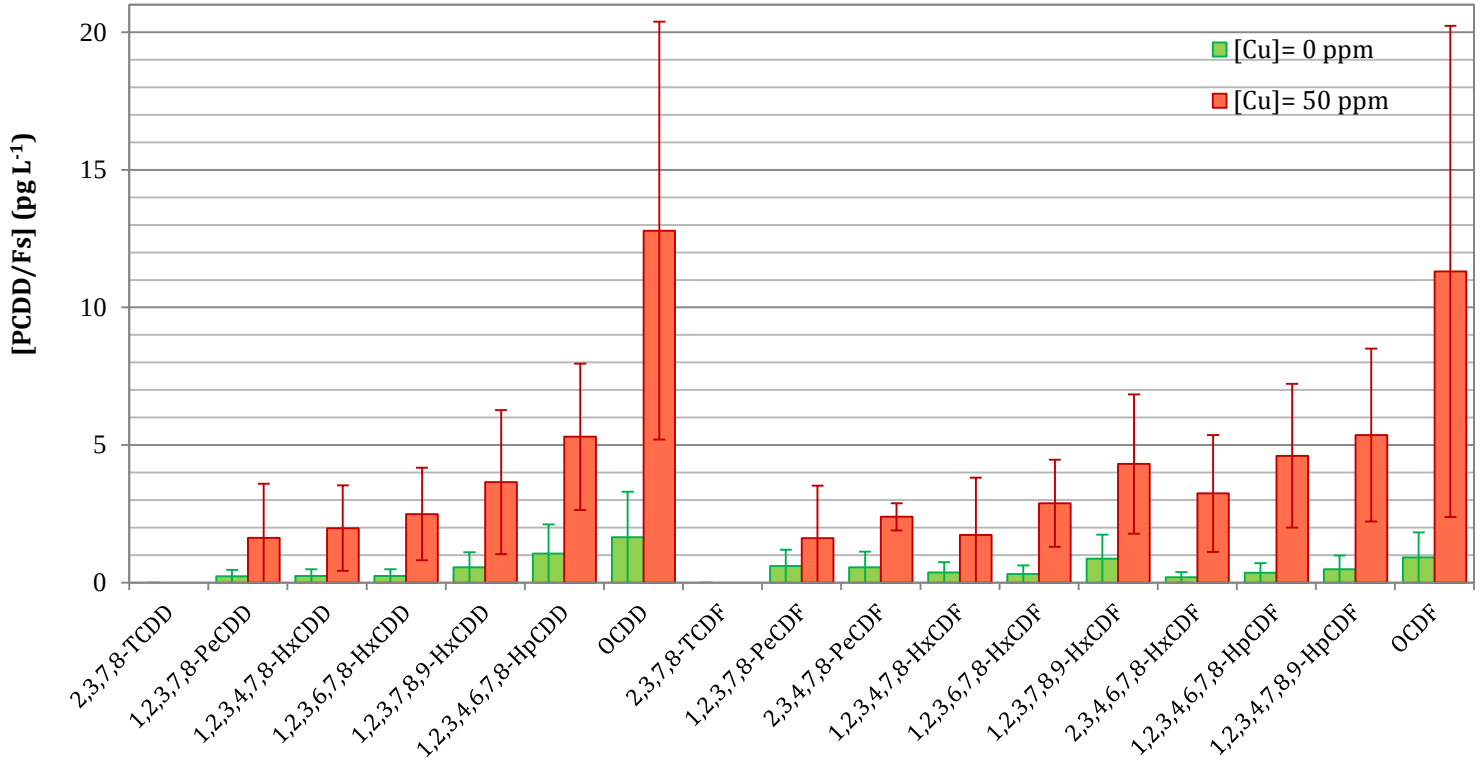

Figure 3.36. Effect of copper salt on the generation of 2,3,7,8-PCDD/Fs during the Fenton oxidation of 2-CP. $[2\text{-CP}]_0$= 15.56 mM, $[H_2O_2]_0$= 40.44 mM, $[Fe^{2+}]$= 1.44 mM, [NaCl]= 56.34 mM, 20 ºC, pH_0= 3, V_0= 1 L.

Starting from the point that there is scarce information about the generation of PCDD/Fs in aqueous phase, especially focused on the application of AOPs for the treatment of waste waters containing pollutants acting as precursors, less is known about the effect that copper has on the reaction pathway. Most of the information available in literature is related to gas phase, where copper acts as a heterogeneous catalyst, favoring the formation of PCDD/Fs via *de novo* synthesis and via precursor.[94] On the one hand, $CuCl_2$ serves as catalyst in the Deacon process (Reaction 3.29) leading to the formation of chlorine from hydrogen chloride that participates in chlorination reactions of the organic matter and direct precursors of PCDDD/Fs.[94,104,106] Furthermore, $CuCl_2$ participates as oxidation/chlorination agent during the *de novo* synthesis of PCDD/Fs (Reaction 3.30).[105] On the other hand, whereas alkali earth metals such as MgO and CaO suppress the generation of PCDD/Fs, CuO facilitates the chemisorption of the precursors on the catalyst surface and subsequent condensation (Scheme 3.6).[94]

$$4\ HCl + O_2 \xrightarrow{CuCl_2} 2\ H_2O + 2\ Cl_2 \tag{3.29}$$

$$2\ CuCl_2 + RH \rightarrow 2\ CuCl + RCl + HCl \tag{3.30}$$

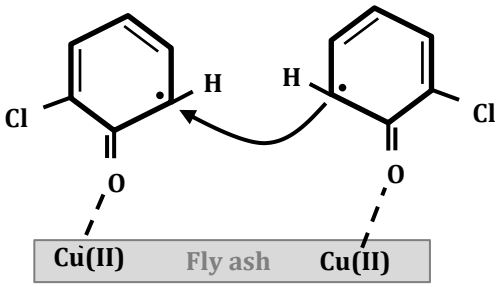

Scheme 3.6. Initial step in the formation of PCDFs on copper oxide surface from two adsorbed chlorophenoxy radicals.[94]

Therefore, while experimental and theoretical data are already available in literature with regard to the role of copper oxide and copper chloride as catalysts of the generation of PCDD/Fs in gas phase, further studies in water samples may lead to a deep comprehension of its role in the formation of PCDD/Fs in aqueous phase.[113]

3.3.2. Comparative analysis of the influence of operation variables

The influence of temperature, chloride dose, iron dose, copper dose and hydrogen peroxide in the Fenton treatment to 2-CP aqueous solutions has been assessed by the Advanced Separation Processes research group of the University of Cantabria, whose main results were partially studied in a previous thesis (Vallejo, 2013) and have continued in the present thesis.[114] A summary of the results, once the hydrogen peroxide was depleted or after 4 hours of Fenton oxidation, is gathered in Table 3.2 for each set of applied operational conditions.

Taking as reference the Fenton experiment at substoichiometric H_2O_2 dose and 20 ºC (E1, Table 3.2), the influence of temperature was assessed (70 ºC, E2, Table 3.2). It was observed that the increase of temperature had a positive effect on the reduction of COD (from 15 to 54%), TOC (form 3 to 27%) and tetra- to octa-CDD/Fs (from 312.9 to 46.3 pg L^{-1}). In this sense, Zazo et al. (2010) found in their studies that an increase in the temperature in the range 25–130 ºC resulted in a faster Fe-catalyzed conversion of H_2O_2 into ·OH enhancing mineralization rates.[17] The concentrations of aromatics at 70 ºC were lower than the quantified at 20 ºC while the concentrations of the aliphatic organic acids were higher increasing the temperature, showing, therefore, a better use of hydroxyl radicals that lead to the formation of short chain organics prior to the complete mineralization.[63]

With regard to the influence of NaCl, when chloride was initially added to the reaction medium (E3, Table 3.2), there were not significant variations in terms of 2-CP, COD and TOC reduction compared to the reference experiment (E1, Table 3.2), as it was previously explained in Sections 3.2.1 and 3.3.2, especially considering the error bars. However, the formation of PCDD/Fs (sum from tetra- to octa-PCDD/Fs) was favored with chloride in the aqueous solution (from 312.9 to 1094.5 pg L^{-1}). Chloride may scavenge ·OH leading to the formation of free chlorine that participates in the indirect oxidation of organics as well as addition and substitution reactions.

Table 3.2. Applied operational conditions during the Fenton oxidation of 2-CP and main results obtained once the reactions finished (Complete depletion of H_2O_2 or $t_{reaction}$= 4 h). n. m.: not measured.

	Experimental conditions							Results t= 4 h					
Effect	**E**	**T (ºC)**	**H_2O_2 (%)**	**[Fe^{2+}] (mM)**	**[H_2O_2]/[Fe^{2+}]**	**[NaCl] (mM)**	**[Cu^{2+}] (mM)**	**[2CP]/[2CP]$_0$**	**[COD]/[COD]$_0$**	**[TOC]/[TOC]$_0$**	**[H_2O_2]/[H_2O_2]$_0$**	**∑Te-OCDD/F (pg L^{-1})**	**Conclusions**
T	1	20	20	0.18	225	0	0	0	0.85	0.97	0	312.9	+ Effect on the reduction of COD, TOC and PCDD/Fs
	2	70	20	0.18	225	0	0	0	0.46	0.73	0	46.3	
NaCl	1	20	20	0.18	225	0	0	0	0.85	0.97	0	312.9	- Effect mainly on the reduction PCDD/Fs
	3	20	20	0.18	225	56.3	0	0.08	0.79	0.93	0	1094.5	
Fe	3	20	20	0.18	225	56.3	0	0.08	0.79	0.93	0	1094.5	Higher [PCDD/Fs] corresponded to 0.18 mM
	4	20	20	0.09	449	56.3	0	0.10	0.83	0.94	0	788.7	
	5	20	20	0.36	112	56.3	0	0.09	0.81	0.96	0	406.1	
	6	20	20	1.44	28	56.3	0	n. m.	0.80	0.95	0	184.7	
	7	20	20	2.88	14	56.3	0	n. m.	0.84	0.98	0	147.6	
Cu	6	20	20	1.44	28	56.3	0	n. m.	0.80	0.95	0	184.7	No effect of Cu
	8	20	20	0	-	56.3	0.79	1	n. m.	1	1	n. m.	
	9	20	20	1.44	28	56.3	0.02	0.06	n. m.	0.96	0	n. m.	
	10	20	20	1.44	28	56.3	0.79	0.07	n.m.	0.97	0	188.5	
H_2O_2	6	20	20	1.44	28	56.3	0	n. m.	0.80	0.95	0	184.7	+ Effect on the reduction of COD, TOC and PCDD/Fs
	11	20	100	7.22	28	56.3	0	0	0.30	0.55	0.1	85.1	

Regarding the iron dose, in the range of concentrations studied (0.09-2.88 mM Fe(II)), there was no influence on the reduction of 2-CP, COD or TOC (E3-E7, Table 3.2). In terms of PCDD/Fs (from tetra- to octa-), the major average concentration was obtained working with 0.18 mM Fe(II), decreasing the average value as the iron dose increased. Nonetheless, as it was depicted in Figure 3.33, the error bars do not permit to obtain a clear conclusion about the influence of this parameter over PCDD/Fs generation.

With respect to the effect of copper on the Fenton oxidation of 2-CP, as it was previously commented in the corresponding sections, there was not variation in the initial concentration of the oxidizing Fenton reagent (H_2O_2) working without the iron catalyst and, therefore, the concentrations of 2-CP and TOC remained constant because no reactions occur in the aqueous system (E6 and E8, Table 3.2). When both copper and iron salts were added to the solution (E9 and E10, Table 3.2), the results obtained were the same as when only iron was dissolved in the aqueous system (E6, Table 3.2).

Together with the temperature, hydrogen peroxide dose was the other operating variable that has the major influence on the reduction of COD (from 20 to 70%), TOC (from 5 to 45%) and PCDD/Fs (from 184.7 to 85.1 pg L^{-1}; E6 and E11, Table 3.2) as a consequence of the higher ·OH availability. When theoretical stoichiometric H_2O_2 amounts were used, the aromatic intermediates were not detected because larger availability of ·OH led to a faster aromatic ring cleavage producing aliphatic carboxylic acids and mineralization.[63]

3.4. Contribution to the scientific knowledge and open questions

Owing to the scarce information about (i) the mechanisms and behavior of the ROS involved in the oxidation reactions, and (ii) the possible generation of oxidation byproducts leading to higher toxicity after the treatment of wastewaters is still scarce, this thesis focuses on the analyses of the Fenton oxidation of a model aqueous solution of 2-CP, a well-known precursor of PCDD/Fs, in two ways, i.e., measurement of ROS and quantification of PCDD/Fs. In addition, the identification of organic radicals connects the formation of ROS with the generation of PCDD/Fs:

- The employment of DMPO as spin-trap and EPR spectroscopy is a feasible alternative in the identification and quantification of ·OH and ·OOH radicals. The EPR spectroscopy allowed identifying organic radicals even in the absence of the spin-trap DMPO. Semiquinone-type radicals were identified in this thesis; the presence of these radicals has a double noteworthy implication, i) the semiquinone radical participates in the reduction of Fe(III) to Fe(II), resulting in a higher effectiveness of the Fenton treatment; ii) the semiquinone radicals may lead to the formation of chlorophenoxy radicals whose condensation reactions yield PCDD/Fs.

- In terms of 2-CP degradation, substoichiometric H_2O_2 doses can achieve full 2-CP degradation. Nevertheless, higher hydrogen peroxide dose is needed to reduce COD and TOC. It has been observed in this chapter that when there is chloride in the aqueous medium, the generation of PCDD/Fs was favored. For the first time, a complete evaluation of the homologues group concentrations from unchlorinated DD/Fs to OCDD/Fs has been carried out, displaying the main formation of dichlorinated-DD/Fs. This is a relevant result since DCDD/Fs are sensitive to further chlorination reactions that could yield dioxins of higher chlorination degree groups, with 2,3,7,8-PCDD/Fs among them. Fortunately, the concentration of 2,3,7,8-WHO-TEQ was lower than the maximum toxicity equivalent level (30 pg L^{-1}). With regard to the iron and copper dose, no

influence was observed in terms of 2-CP, COD and TOC reduction, or PCDD/Fs formation.

In spite of all the results reached throughout the development of this chapter, there are still many open questions due to the novelty of this field that deserve further research:

- The design and development of new molecular probes selective towards the radical of interest as well as online measurements that will enable the quantification of radical species in real time.
- 2-CP is only an example of compounds that act as precursor of toxic byproducts such as PCDD/Fs. A deeper study of model solutions can give insights into the behavior of the real streams characterized by a mixture of different contaminants.
- In gas phase, surfaces have shown a fundamental role catalyzing the formation of PCDD/Fs, so it would be interesting to analyze how surfaces may interfere in the generation of dioxins in aqueous samples.

References

1. Fernández-Castro P, Vallejo M, San Román MF, Ortiz I. Insight on the fundamentals of advanced oxidation processes: Role and review of the determination methods of reactive oxygen species. J. Chem. Technol. Biotechnol. 90: 796-820 (2015).

2. Tai C, Peng J, Liu J, Jiang G, Zou H. Determination of hydroxyl radicals in advanced oxidation processes with dimethyl sulfoxide trapping and liquid chromatography. Anal. Chim. Acta 527: 73-80 (2004).

3. Erik P, Andersen VS. The formaldehyde-hydrogen sulphite system in alkaline aqueous solution. Kinetics, mechanisms, and equilibria. Acta Chem. Scand. 24: 1301-1306 (1970).

4. Murphy AP, Boegli WJ, Price MK, Moody CD. A Fenton-like reaction to neutralize formaldehyde waste solutions. Environ. Sci. Technol. 23: 166-169 (1989).

5. Viste A, Hogan RE. The formaldehyde-bisulfite clock reaction: Reexamination of a kinetics. Proc. S. Dak. Acad. Sci. 64: 70-76 (1985)

6. De Laat J, Le TG. Effects of chloride ions on the iron (III)-catalyzed decomposition of hydrogen peroxide and on the efficiency of the Fenton-like oxidation process. Appl. Catal. B-Environ. 66: 137-146 (2006).

7. Yoon J, Lee Y, Kim S. Investigation of the reaction pathway of OH radicals produced by Fenton oxidation in the conditions of wastewater treatment. Water Sci. Technol. 44: 15-21 (2001).

8. Matira EM, Chen T, Lu M, Dalida MLP. Degradation of dimethyl sulfoxide through fluidized-bed Fenton process. J. Hazard. Mater. 300: 218-226 (2015).

9. Bellotindos LM, Lu M, Methatham T, Lu M. Factors affecting degradation of dimethyl sulfoxide (DMSO) by fluidized-bed Fenton process. Environ. Sci. Pollut. Res. 21: 14158-14165 (2014).

10. Wen C, Wang C, Chou W, Chang W, Lee S. Degradation of DMSO in aqueous solutions by the Fenton reaction based advanced oxidation processes. Fresenius Environ. Bull. 21: 644-50 (2012).

11. de Luna, Mark Daniel G, Colades JI, Su C, Lu M. Comparison of dimethyl sulfoxide degradation by different Fenton processes. Chem. Eng. J. 232: 418-424 (2013).

12. Pliego G, Zazo JA, Garcia-Muñoz P, Munoz M, Casas JA, Rodriguez JJ. Trends in the intensification of the Fenton process for wastewater treatment: An overview. Crit. Rev. Environ. Sci. Technol. 45: 2611-2692 (2015).

13. Kang N, Lee DS, Yoon J. Kinetic modeling of Fenton oxidation of phenol and monochlorophenols. Chemosphere 47: 915-924 (2002).

14. Lee Y, Lee C, Yoon J. Kinetics and mechanisms of DMSO (dimethylsulfoxide) degradation by UV/H 2 O 2 process. Water Res. 38: 2579-2588 (2004).

15. Cotton F, Francis R. Sulfoxides as ligands. I. A preliminary survey of methyl sulfoxide complexes. J. Am. Chem. Soc. 82: 2986-2991 (1960).

16. Cotton F, Francis Rt, Horrocks Jr W. Sulfoxides as ligands. II. The infrared spectra of some dimethyl sulfoxide complexes. J. Phys. Chem. 64: 1534-1536 (1960).

17. Zazo JA, Pliego G, Blasco S, Casas JA, Rodriguez JJ. Intensification of the Fenton process by increasing the temperature. Ind. Eng. Chem. Res. 50: 866-870 (2010).

18. Riggs WM, Bricker CE. Thermal decomposition of iron (III) oxalates. J. Inorg. Nucl. Chem. 33: 1635-1647 (1971).

19. Han S, Nam S, Kang J. OH radical monitoring technologies for AOP advanced oxidation process. Water Sci. Technol. 46: 7-12 (2002).

20. Nam S, Han S, Kang J, Choi H. Kinetics and mechanisms of the sonolytic destruction of non-volatile organic compounds: Investigation of the sonochemical reaction zone using several OH monitoring techniques. Ultrason. Sonochem. 10: 139-147 (2003).

21. Kim J, Metcalfe I. Investigation of the generation of hydroxyl radicals and their oxidative role in the presence of heterogeneous copper catalysts. Chemosphere 69: 689-696 (2007).

22. Yang J, Dai J, Chen C, Zhao J. Effects of hydroxyl radicals and oxygen species on the 4-chlorophenol degradation by photoelectrocatalytic reactions with TiO_2-film electrodes. J. Photochem. Photobiol. A 208: 66-77 (2009).

23. Grela M, Coronel M, Colussi A. Quantitative spin-trapping studies of weakly illuminated titanium dioxide sols. implications for the mechanism of photocatalysis. J. Phys. Chem. 100: 16940-16946 (1996).

24. Yanagida H, Masubuchi Y, Minagawa K, Ogata T, Takimoto J, Koyama K. A reaction kinetics model of water sonolysis in the presence of a spin-trap. Ultrason. Sonochem. 5: 133-139 (1999).

25. Han SK, Hwang T, Yoon Y, Kang J. Evidence of singlet oxygen and hydroxyl radical formation in aqueous goethite suspension using spin-trapping electron paramagnetic resonance (EPR). Chemosphere 84: 1095-1101 (2011).

26. Cong Y, Wu Z. Electrocatalytic generation of radical intermediates over lead dioxide electrode doped with fluoride. J. Phys. Chem. C 111: 3442-3446 (2007).

27. Marselli B, Garcia-Gomez J, Michaud P, Rodrigo M, Comninellis C. Electrogeneration of hydroxyl radicals on boron-doped diamond electrodes. J. Electrochem. Soc. 150: D79-83 (2003).

28. Li L, Abe Y, Kanagawa K, Usui N, Imai K, Mashino T, Mochizuki M, Miyata N. Distinguishing the 5, 5-dimethyl-1-pyrroline N-oxide (DMPO)-OH radical quenching effect from the hydroxyl radical scavenging effect in the ESR spin-trapping method. Anal. Chim. Acta 512: 121-124 (2004).

29. Granados-Oliveros G, Gómez-Vidales V, Nieto-Camacho A, Morales-Serna JA, Cárdenas J, Salmón M. Photoproduction of H_2O_2 and hydroxyl radicals catalysed by natural and super acid-modified montmorillonite and its oxidative role in the peroxidation of lipids. RSC Advances 3: 937-944 (2013).

30. Kochany J, Bolton JR. Mechanism of photodegradation of aqueous organic pollutants. 2. measurement of the primary rate constants for reaction of hydroxyl radicals with benzene and some halobenzenes using an EPR spin-trapping method following the photolysis of hydrogen peroxide. Environ. Sci. Technol. 26: 262-265 (1992).

31. Goldstein S, Rosen GM, Russo A, Samuni A. Kinetics of spin trapping superoxide, hydroxyl, and aliphatic radicals by cyclic nitrones. J. Phys. Chem. A 108: 6679-6685 (2004).

32. Bruker Biospin. EPR spin trapping of free radicals with DMPO (5,5-dimethyl-1-pyrroline N-oxide) and BMPO (5-tert-butoxycarbonyl-5-methyl-1-pyrroline N-oxide). https://www.bruker.com/fileadmin/user_upload/8-PDF-Docs/MagneticResonance/EPR_brochures/superoxide.pdf (visited 15/12/2016).

33. Bosnjakovic A, Schlick S. Spin trapping by 5, 5-dimethylpyrroline-N-oxide in Fenton media in the presence of nafion perfluorinated membranes: Limitations and potential. J. Phys. Chem. B 110: 10720-10728 (2006).

34. Khachatryan L, Vejerano E, Lomnicki S, Dellinger B. Environmentally persistent free radicals (EPFRs). 1. Generation of reactive oxygen species in aqueous solutions. Environ. Sci. Technol. 45: 8559-8566 (2011).

35. Villamena FA, Hadad CM, Zweier JL. Kinetic study and theoretical analysis of hydroxyl radical trapping and spin adduct decay of alkoxycarbonyl and dialkoxyphosphoryl nitrones in aqueous media. J. Phys. Chem. A 107: 4407-4414 (2003).

36. Carmichael AJ, Makino K, Riesz P. Quantitative aspects of ESR and spin trapping of hydroxyl radicals and hydrogen atoms in gamma-irradiated aqueous solutions. Radiat. Res. 100: 222-234 (1984).

37. Andersen ML, Skibsted LH. Electron spin resonance spin trapping identification of radicals formed during aerobic forced aging of beer. J. Agric. Food Chem. 46: 1272-1275 (1998).

38. Fontmorin J, Castillo RB, Tang W, Sillanpää M. Stability of 5, 5-dimethyl-1-pyrroline-N-oxide as a spin-trap for quantification of hydroxyl radicals in processes based on Fenton reaction. Water Res. 99: 24-32 (2016).

39. Lipczynska-Kochany E, Kochany J, Bolton JR. Electron paramagnetic resonance spin trapping detection of short-lived radical intermediates in the direct photolysis of 4-chlorophenol in aerated aqueous solution. J. Photochem. Photobiol. A 62: 229-240 (1991).

40. Finkelstein E, Rosen GM, Rauckman EJ. Spin trapping of superoxide and hydroxyl radical: Practical aspects. Arch. Biochem. Biophys. 200: 1-16 (1980).

41. Fenton H. LXXIII.—Oxidation of tartaric acid in presence of iron. J. Chem. Soc., Trans. 65: 899-910 (1894).

42. Dröge, W. Oxidative stress and aging. In Hypoxia (pp. 191-200). Springer US (2003).

43. Yao Y, Jiang B, Mao Y, Chen J, Huang Z, Huang S, Zhang L. Extremely enhanced contaminant decomposition catalyzed by hemin via the coupling of persistent free radicals and ascorbic acid. Chem. Comm. 51: 16139-16142 (2015).

44. Shen Z, Xie S, Fan W, Zhang Q, Xie Z, Yang W, Wang Y, Lin J, Wu X, Wan H. Direct conversion of formaldehyde to ethylene glycol via photocatalytic carbon–carbon coupling over bismuth vanadate. Catal. Sci. Technol. 6: 6485-6489 (2016).

45. Ranguelova K, Mason RP. The fidelity of spin trapping with DMPO in biological systems. Magn. Reson. Chem. 49: 152-158 (2011).

46. Vallejo M, Fernández-Castro P, San Román MF, Ortiz I. Assessment of PCDD/Fs formation in the Fenton oxidation of 2-chlorophenol: Influence of the iron dose applied. Chemosphere 137: 135-141 (2015).

47. Buxton GV, Greenstock CL, Helman WP, Ross AB. Critical review of rate constants for reactions of hydrated electrons, hydrogen atoms and hydroxyl radicals (·OH/·O−) in aqueous solution. J. Phys. Chem. Ref. Data 17: 513-886 (1988).

48. Fernández-Castro P, San Román MF, Ortiz I. Theoretical and experimental formation of low chlorinated dibenzo-p-dioxins and dibenzofurans in the Fenton oxidation of chlorophenol solutions. Chemosphere 161: 136-144 (2016).

49. Sedoud A, Cox N, Sugiura M, Lubitz W, Boussac A, Rutherford AW. Semiquinone–Iron complex of photosystem II: EPR signals assigned to the low-field edge of the ground state doublet of QA•–Fe2 and QB•–Fe2. Biochem. 50: 6012-6021 (2011).

50. Guimarães E, Mangrich AS, Machado VG, Traghetta DG, Lobo MA. Criterious preparation and characterization of earthworm-composts in view of animal waste recycling: Part II. A synergistic utilization of EPR and ^{1}HNMR spectroscopies on the characterization of humic acids from vermicomposts. J. Brazil. Chem. Soc. 12: 734-741 (2001).

51. Pérez MG, Martin-Neto L, Saab SC, Novotny EH, Milori DM, Bagnato VS, Colnago LA, Melo WJ, Knicker H. Characterization of humic acids from a Brazilian oxisol under different tillage systems by EPR, 13C NMR, FTIR and fluorescence spectroscopy. Geoderma 118: 181-190 (2004).

52. Csay T, Homlok R, Illés E, Takács E, Wojnárovits L. The chemical background of advanced oxidation processes. Isr. J. Chem. 54: 233-241 (2014).

53. Pignatello JJ, Oliveros E, MacKay A. Advanced oxidation processes for organic contaminant destruction based on the Fenton reaction and related chemistry. Crit Rev Environ. Sci. Technol. 36: 1-84 (2006).

54. Pedersen JA. On the application of electron paramagnetic resonance in the study of naturally occurring quinones and quinols. Spectrochim. Acta A 58: 1257-1270 (2002).

55. Chen R, Pignatello JJ. Role of quinone intermediates as electron shuttles in Fenton and photoassisted Fenton oxidations of aromatic compounds. Environ. Sci. Technol. 31: 2399-2406 (1997).

56. Haines A. Methods for oxidation of organic compounds V2: Alcohols, alcohol derivatives, alky halides, nitroalkanes, alkyl azides, carbonyl compounds hydroxyarenes and aminoarenes. Elsevier, San Diego, CA(2012).

57. Parker DS, Kaiser RI, Troy TP, Kostko O, Ahmed M, Mebel AM. Toward the oxidation of the phenyl radical and prevention of PAH formation in combustion systems. J. Phys. Chem.y A 119: 7145-7154 (2014).

58. Tokmakov IV, Kim G, Kislov VV, Mebel AM, Lin MC. The reaction of phenyl radical with molecular oxygen: A G2M study of the potential energy surface. J. Phys. Chem. A 109: 6114-6127 (2005).

59. Altarawneh M, Dlugogorski BZ, Kennedy EM, Mackie JC. Quantum chemical investigation of formation of polychlorodibenzo-p-dioxins and dibenzofurans from oxidation and pyrolysis of 2-chlorophenol. J. Phys. Chem. A 111: 2563-2573 (2007).

60. Pan W, Zhang D, Han Z, Zhan J, Liu C. New insight into the formation mechanism of PCDD/Fs from 2-chlorophenol precursor. Environ. Sci. Technol. 47: 8489-8498 (2013).

61. Zhang Q, Li S, Qu X, Shi X, Wang W. A quantum mechanical study on the formation of PCDD/Fs from 2-chlorophenol as precursor. Environ. Sci. Technol. 42: 7301-7308 (2008).

62. Shongwe MS, Al-Rahbi SH, Al-Azani MA, Al-Muharbi AA, Al-Mjeni F, Matoga D, Gismelseed A, Al-Omari IA, Yousif A, Adams H. Coordination versatility of tridentate pyridyl aroylhydrazones towards iron: Tracking down the elusive aroylhydrazono-based ferric spin-crossover molecular materials. Dalton T. 41: 2500-2514 (2012).

63. Vallejo Montes M. Assessment of polychlorinated dibenzo-p-dioxins and dibenzofurans, PCDD/Fs, in the application of advanced oxidation processes. Doctoral Thesis, University of Cantabria, Santander (2014).

64. Terashima C, Rao TN, Sarada B, Tryk D, Fujishima A. Electrochemical oxidation of chlorophenols at a boron-doped diamond electrode and their determination by high-

performance liquid chromatography with amperometric detection. Anal. Chem. 74: 895-902 (2002).

65. Aissam H, Penninckx MJ, Benlemlih M. Reduction of phenolics content and COD in olive oil mill wastewaters by indigenous yeasts and fungi. World J. Microbiol. Biotechnol. 23: 1203-1208 (2007).

66. El-Ashtoukhy E, El-Taweel Y, Abdelwahab O, Nassef E. Treatment of petrochemical wastewater containing phenolic compounds by electrocoagulation using a fixed bed electrochemical reactor. Int. J. Electrochem. Sci. 8: 1534-1550 (2013).

67. Munoz M, de Pedro ZM, Casas JA, Rodriguez JJ. Assessment of the generation of chlorinated byproducts upon Fenton-like oxidation of chlorophenols at different conditions. J. Hazard. Mater. 190: 993-1000 (2011).

68. Poerschmann J, Trommler U, Górecki T, Kopinke F. Formation of chlorinated biphenyls, diphenyl ethers and benzofurans as a result of Fenton-driven oxidation of 2-chlorophenol. Chemosphere 75: 772-780 (2009).

69. Woolard CR, Irvine RL. Biological treatment of hypersaline wastewater by a biofilm of halophilic bacteria. Water Environ. Res. 66: 230-235 (1994).

70. Fuertes I, Gómez-Lavín S, Elizalde M, Urtiaga A. Perfluorinated alkyl substances (PFASs) in northern spain municipal solid waste landfill leachates. Chemosphere 168: 399-407 (2017).

71. Urtiaga A, Fernandez-Castro P, Gómez P, Ortiz I. Remediation of wastewaters containing tetrahydrofuran. Study of the electrochemical mineralization on BDD electrodes. Chem. Eng. J. 239: 341-350 (2014).

72. Anglada Á, Urtiaga A, Ortiz I. Contributions of electrochemical oxidation to waste-water treatment: Fundamentals and review of applications. J. Chem. Technol. Biotechnol. 84: 1747-1755 (2009).

73. Micó MM, Bacardit J, Malfeito J, Sans C. Enhancement of pesticide photo-Fenton oxidation at high salinities. Appl. Catal. B-Environ. 132: 162-169 (2013).

74. Pignatello JJ. Dark and photoassisted iron (3)-catalyzed degradation of chlorophenoxy herbicides by hydrogen peroxide. Environ. Sci. Technol. 26: 944-951 (1992).

75. Lu M, Chang Y, Chen I, Huang Y. Effect of chloride ions on the oxidation of aniline by Fenton's reagent. J. Environ. Manage. 75: 177-182 (2005).

76. Vallejo M, San Román MF, Ortiz I, Irabien A. The critical role of the operating conditions on the Fenton oxidation of 2-chlorophenol: Assessment of PCDD/Fs formation. J. Hazard. Mater. 279: 579-585 (2014).

77. Neyens E, Baeyens J. A review of classic Fenton's peroxidation as an advanced oxidation technique. J. Hazard. Mater. 98: 33-50 (2003).

78. Lopez A, Mascolo G, Detomaso A, Lovecchio G, Villani G. Temperature activated degradation (mineralization) of 4-chloro-3-methyl phenol by Fenton's reagent. Chemosphere 59: 397-403 (2005).

79. Duesterberg CK, Waite TD. Process optimization of Fenton oxidation using kinetic modeling. Environ. Sci. Technol. 40: 4189-4195 (2006).

80. Chamarro E, Marco A, Esplugas S. Use of Fenton reagent to improve organic chemical biodegradability. Water Res. 35: 1047-1051 (2001).

81. Babuponnusami A, Muthukumar K. A review on Fenton and improvements to the Fenton process for wastewater treatment. J. Environ. Chem. Eng. 2: 557-572 (2014).

82. Munoz M, Pliego G, de Pedro ZM, Casas JA, Rodriguez JJ. Application of intensified Fenton oxidation to the treatment of sawmill wastewater. Chemosphere 109: 34-41 (2014).

83. Nakagawa H, Yamaguchi E. Influence of oxalic acid formed on the degradation of phenol by Fenton reagent. Chemosphere 88: 183-187 (2012).

84. Zazo J, Casas J, Mohedano A, Gilarranz M, Rodriguez J. Chemical pathway and kinetics of phenol oxidation by Fenton's reagent. Environ. Sci. Technol. 39: 9295-9302 (2005).

85. Sedlak DL, Andren AW. Oxidation of chlorobenzene with Fenton's reagent. Environ. Sci. Technol. 25: 777-782 (1991).

86. Detomaso A, Lopez A, Lovecchio G, Mascolo G, Curci R. Practical applications of the Fenton reaction to the removal of chlorinated aromatic pollutants. Environ. Sci. Pollut. Res. 10: 379-384 (2003).

87. Munoz M, de Pedro ZM, Pliego G, Casas JA, Rodriguez JJ. Chlorinated byproducts from the Fenton-like oxidation of polychlorinated phenols. Ind. Eng. Chem. Res. 51: 13092-13099 (2012).

88. Çeçen F, Gürsoy G. Characterization of landfill leachates and studies on heavy metal removal. J. Environ. Monit. 2: 436-442 (2000).

89. Fan H, Shu H, Yang H, Chen W. Characteristics of landfill leachates in central Taiwan. Sci. Total Environ. 361: 25-37 (2006).

90. Rajor A, Xaxa M, Mehta R. An overview on characterization, utilization and leachate analysis of biomedical waste incinerator ash. J. Environ. Manage. 108: 36-41 (2012).

91. Renou S, Givaudan J, Poulain S, Dirassouyan F, Moulin P. Landfill leachate treatment: Review and opportunity. J. Hazard. Mater. 150: 468-493 (2008).

92. Scott J, Beydoun D, Amal R, Low G, Cattle J. Landfill management, leachate generation, and leach testing of solid wastes in Australia and overseas. Crit. Rev. Environ. Sci. Technol. 35: 239-332 (2005).

93. Garcia-Segura S, Brillas E, Cornejo-Ponce L, Salazar R. Effect of the Fe3/Cu2 ratio on the removal of the recalcitrant oxalic and oxamic acids by electro-Fenton and solar photoelectro-fenton. Solar Energy 124: 242-253 (2016).

94. Altarawneh M, Dlugogorski BZ, Kennedy EM, Mackie JC. Mechanisms for formation, chlorination, dechlorination and destruction of polychlorinated dibenzo-p-dioxins and dibenzofurans (PCDD/Fs). Prog. Energy Combust. Sci. 35: 245-274 (2009).

95. Gullett BK, Bruce KR, Beach LO. The effect of metal catalysts on the formation of polychlorinated dibenzo-p-dioxin and polychlorinated dibenzofuran precursors. Chemosphere 20: 1945-1952 (1990).

96. McKay G. Dioxin characterisation, formation and minimisation during municipal solid waste (MSW) incineration: Review. Chem. Eng. J. 86: 343-368 (2002).

97. Ryu J, Mulholland JA, Takeuchi M, Kim D, Hatanaka T. $CuCl_2$-catalyzed PCDD/F formation and congener patterns from phenols. Chemosphere 61: 1312-1326 (2005).

98. Takaoka M, Shiono A, Nishimura K, Yamamoto T, Uruga T, Takeda N, Tanaka T, Oshita K, Matsumoto T, Harada H. Dynamic change of copper in fly ash during de novo synthesis of dioxins. Environ. Sci. Technol. 39: 5878-5884 (2005).

99. Friedrich LC, Machulek Jr A, Silva VdO, Quina FH. Interference of inorganic ions on phenol degradation by the Fenton reaction. Sci. Agr. 69: 347-351 (2012).

100. Pagano M, Volpe A, Lopez A, Mascolo G, Ciannarella R. Degradation of chlorobenzene by Fenton-like processes using zero-valent iron in the presence of Fe_3 and Cu_2. Environ. Technol. 32: 155-165 (2011).

101. Choi K, Lee W. Enhanced degradation of trichloroethylene in nano-scale zero-valent iron Fenton system with Cu(II). J. Hazard. Mater. 211: 146-153 (2012).

102. Han Y, Liu W, Pan W, Wang P, Tian Z, Zhao Y, Wang M, Chen X, Liao X, Zheng M. Formation pathways of mono-to octa-chlorinated dibenzo-p-dioxins and dibenzofurans in main organochemical industries. Environ. Sci. Technol. 49: 10945-10950 (2015).

103. U.S. EPA. U.S. EPA 811-F-95-003C. National primary drinking water regulations: Contaminant specific fact sheets, synthetic organic chemicals. 1-62 (1995).

104. Bruce KR, Beach LO, Gullett BK. The role of gas-phase Cl2 in the formation of PCDD/PCDF during waste combustion. Waste Manage. 11: 97-102 (1991).

105. Wikström E, Ryan S, Touati A, Telfer M, Tabor D, Gullett BK. Importance of chlorine speciation on de novo formation of polychlorinated dibenzo-p-dioxins and polychlorinated dibenzofurans. Environ. Sci. Technol. 37: 1108-1113 (2003).

106. Gullett B, Sarofim A, Smith K, Procaccini C. The role of chlorine in dioxin formation. Process Saf. Environ. Prot. 78: 47-52 (2000).

107. Wang X, Zhang H, Ni Y, Du Q, Zhang X, Chen J. Kinetics of PCDD/Fs formation from non-wood pulp bleaching with chlorine. Environ. Sci. Technol. 48: 4361-4367 (2014).

108. Ryan SP, Altwicker ER. Understanding the role of iron chlorides in the de novo synthesis of polychlorinated dibenzo-p-dioxins/dibenzofurans. Environ. Sci. Technol. 38: 1708-1717 (2004).

109. Font R, Gálvez A, Moltó J, Fullana A, Aracil I. Formation of polychlorinated compounds in the combustion of PVC with iron nanoparticles. Chemosphere 78: 152-159 (2010).

110. Nganai S, Lomnicki S, Dellinger B. Formation of PCDD/Fs from oxidation of 2-monochlorophenol over an Fe_2O_3/silica surface. Chemosphere 88: 371-376 (2012).

111. Gu C, Liu C, Johnston CT, Teppen BJ, Li H, Boyd SA. Pentachlorophenol radical cations generated on Fe(III)-montmorillonite initiate octachlorodibenzo-p-dioxin formation in clays: Density functional theory and fourier transform infrared studies. Environ. Sci. Technol. 45: 1399-1406 (2011).

112. Fukushima M, Tatsumi K, Morimoto K. Influence of iron (III) and humic acid on the photodegradation of pentachlorophenol. Environ. Toxicol. Chem. 19: 1711-1716 (2000).

113. Pulido YF, Suárez E, López R, Menéndez MI. The role of CuCl on the mechanism of dibenzo-p-dioxin formation from poly-chlorophenol precursors: A computational study. Chemosphere 145: 77-82 (2016).

114. Vallejo M, San Román MF, Ortiz I. Quantitative assessment of the formation of polychlorinated derivatives, PCDD/Fs, in the electrochemical oxidation of 2-chlorophenol as function of the electrolyte type. Environ. Sci. Technol. 47: 12400-1248 (2013).

Chapter 4

Mechanistic study in the oxidation of the PCDD/Fs precursor 2-chlorophenol

Chapter 4

Mechanistic study in the oxidation of the PCDD/Fs precursor 2-chlorophenol

Abstract

The main objective of this chapter is to explain theoretically the experimental results obtained in the previous chapter. Firstly, quantum chemical calculations will be employed to describe the pathway followed in the electrophilic chlorination of phenol and 2-chlorophenol, not only in aqueous but also in gas phase, since it will allow following the behavior in both phases in which the generation of PCDD/Fs from chlorophenolic compounds has been observed. Then, these results will be compared with those previously obtained in the Advanced Separation Processes research group of the University of Cantabria (aqueous phase) and the Fire Safety and Combustion Kinetics Lab of Murdoch University (gas phase), as well as with experimental data from other studies already published in bibliography. Afterwards, these theoretical results will be employed in the justification of the main oxidation byproducts obtained during the Fenton oxidation of 2-CP. In a second part, the mechanistic pathway for the formation of PCDD/Fs after Fenton oxidation of 2-CP molecule will be proposed based on the computational calculations published in this respect for gas phase reactions. Finally, with the aim of knowing the effect of water in the generation of PCDD/Fs from 2-CP, some calculations taking into account the solvation effect (aqueous phase) and the reaction with H_2O molecule (gas phase) will be reported.

4.1 Application of computational chemistry to the study of phenolic chlorination and hydroxylation reactions via electrophilic substitution

As it was previously mentioned, phenol and chlorophenols have a critical importance as intermediates in prominent chemical industries; most notably manufacturing of insecticides, herbicides, etc.[1,2] Elevated concentrations of chlorophenols have been detected in aquatic media, including natural waters and wastewaters as well as in sediments and soils.[3] Gas phase chlorophenols can be formed as unwanted pollutants in combustion processes such as municipal solid waste incineration. Likewise, fission of the phenolic constituents in lignin during thermal treatment of biomass results in the formation of un-substituted phenolic entities.[4]

The concern about the release of this kind of compounds has increased owing to their toxicity and persistence.[5] For instance, pentachlorophenol has been listed as priority pollutant by the U.S. EPA's Clean Water Act, the European Decision 2455/2001/CE and the Stockholm Convention, whereas the rest of chlorophenols are only considered "priority pollutants" by U.S. EPA.[6-9] Although the use of pentachlorophenol has been restricted, it can be formed during the chlorination reactions of phenol or low chlorinated phenols under the presence of a chlorine source. In aqueous phase, the source can be the chlorine used during disinfection steps or even the chloride ions present in wastewaters.[10-13] However, the main environmental and health burdens of chlorinated phenols stems from their well-documented role as the most important building blocks for the formation of the notorious carcinogenic polychlorodibenzo-p-dioxins and dibenzofurans, PCDD/F, via complex homogenous and surface-mediated pathways.[5,14]

While the great deal of experimental and molecular modeling-based research over the last two decades has shed light on the major mechanistic steps involved in the various synthesis routes of PCDD/F, the most intriguing remaining questions are pertinent to the governing chlorination pathways. The most sweeping discussion is focused on whether the isomer distribution within each homologue group of

PCDD/F is thermodynamically or kinetically controlled.[14] Congener patterns among various emission sources were found to be highly consistent; indicating that, the chlorination mechanism does not depend on the combustion conditions, such as the exact value of temperatures or gas velocity. Addink et al. (1996 and 1998) established that the isomer distribution in each homologue group in the *de novo* synthesis is not kinetically controlled; i.e., isomer distributions remain independent of the reaction time.[15,16] Likewise, inconsistency between the final distribution of isomers and profiles of Gibbs free energies indicate lack of thermodynamic control as well.

Molecular-based descriptors have emerged as powerful tools in elucidating theoretical rational into experimentally observed homologue profiles. For example, Wehrmeier et al. (1998) correlated the relative abundance of PCDD isomers with the energy differences between their frontier molecular orbitals; that is, between the highest occupied molecular orbitals and the lowest unoccupied molecular orbitals (HOMO-LUMO).[17] In a recent paper, Altarawneh and Duglogorski (2015) established a conclusive consistency between trends in Fukui-based electrophilic indices and the measured profiles of chlorinated nitrogen-analogous of dibenzofuran; i.e., carbazole.[18] The source of chlorine in thermal systems includes metal chlorides, ash-bound inorganic chlorine transfer, and the so-called Deacon reaction.[14] Nonetheless, consensus in the literature highlights that electrophilic substitution represents the most plausible chlorination mechanism, especially in heterogeneous pathways. These routes nearly account for the majority of formed PCDD/F in thermal systems in reference to the gas phase precursor's corridor.

In surface-mediated coupling of precursors (Langmuir-Hinshelwood or L-H and Eley-Rideal or E-R mechanisms) phenolic species adsorbed very strongly on the surface.[19] This facilitates chlorination of adsorbed phenols and phenoxy radical (i.e., phenolate) by electrophilic substitution. In principle, chlorination patterns of formed PCDD/F may stem from the chlorination order and pattern of the chlorophenol precursors. It follows that it is of importance to investigate the pattern of phenol chlorination by electrophilic substitution as a crucial aspect in

comprehending the overall chlorination mechanisms of PCDD/F. To this end, this point covers trends dictating chlorination sequence of phenol and phenoxy radicals in the aqueous and the gas phases. Hirshfeld charge distributions and Fukui indices have been estimated herein for assessing the pathway of the electrophilic substitution of phenol, and compared with those obtained from water treatments and from the incineration of municipal solid wastes.[20,21]

Furthermore, based on the theoretical results for electrophilic Fukui indices, the product distribution of the Fenton oxidation of 2-CP presented through the Chapter 3 has been analyzed to check if hydroxylation reactions fulfil this pattern.

Computational details

As it was described in Chapter 2, density functional theory (DFT) calculations have been performed using DMol^3 implemented in Materials Studio 8.0.[22] Hirshfeld charge distributions (Figure 4.1) and Fukui indices of electrophilic attack, $f^{-1}(\vec{r})$, for unsubstituted phenol were conducted using generalized gradient approximation (GGA) level with the double numerical plus *d*-functions (DND) basis set.

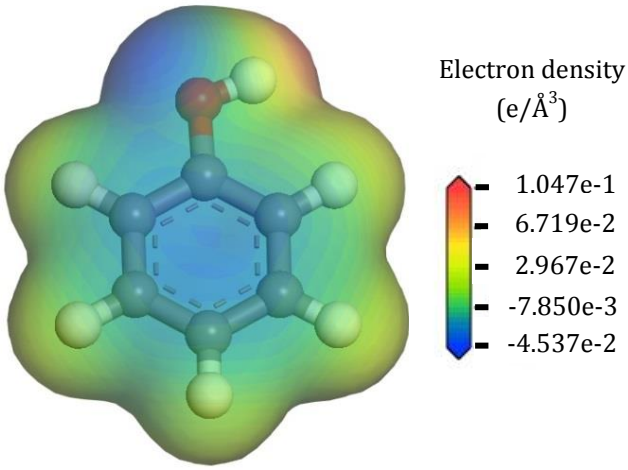

Figure. 4.1. Electronic charge density on phenol.

Fukui indices serve as a measure to assess the chemical reactivity of a compound; that is, the higher electrophilic Fukui value for one atom in a molecule implies higher probability of that atom to be halogenated.[18,23] Equation 4.1 expresses the dependency of the Fukui function on the electronic density ($\rho(\vec{r})$) (plotted in Figure 1 for phenol) and the number of electrons (N), maintaining constant the external potential exerted by the nuclei (v).[24]

$$f(\vec{r}) = \left(\frac{\partial \rho(\vec{r})}{\partial N}\right)_v \qquad \text{(Eq. 4.1)}$$

In the case of the Fukui function for an electrophilic attack and assuming the frozen core approximation, the diminishment in the number of electrons (N – dN) only affects the frontier orbital, and the Fukui function corresponds to the electronic density of the HOMO ($\rho_H(\vec{r})$, Equation 4.2).[24]

$$f^{-1}(\vec{r}) \cong \rho_H(\vec{r}) \qquad \text{(Eq 4.2)}$$

A convergence tolerance of $1 \cdot 10^{-5}$ Ha, which specifies the convergence threshold for the maximum energy change during the geometry optimization, has been applied in all optimizations. Finally, a conductor-like screening model (COSMO) simulated an aqueous-phase environment. This model reproduces in a good way the solute energies and properties obtained by means of the polarizable continuum model (PCM) and the experimental data when the characteristic dielectric constant is selected.[25]

4.1.1. Electrophilic chlorination of chlorophenolic family

Chlorination pathways in aqueous phase

The chlorophenolic family has been identified in natural water streams related in many cases to the reactions involving natural organic matter.[10] The chlorination disinfection applied in water treatment results in the successive chlorination of phenol to yield the fifteen isomers of chlorophenols. On the other hand, phenols and chlorophenols have been detected in industrial wastewaters, surface and

groundwater, and soils because of their wide and long-term use in industrial processes and daily life.[26] The application of advanced oxidation processes in the presence of chlorine has shown that additional chlorination reactions may yield chlorophenols of higher chlorination degree.[13] *Ortho*/*para* electrophilic substitutions are expected during the halogenation of phenol due to the fact that hydroxyl radical is a highly active *ortho*/*para* directing group.[13,27] Figure 4.2 depicts the chlorination sequence inferred for $f^{-1}(\vec{r})$ indices.

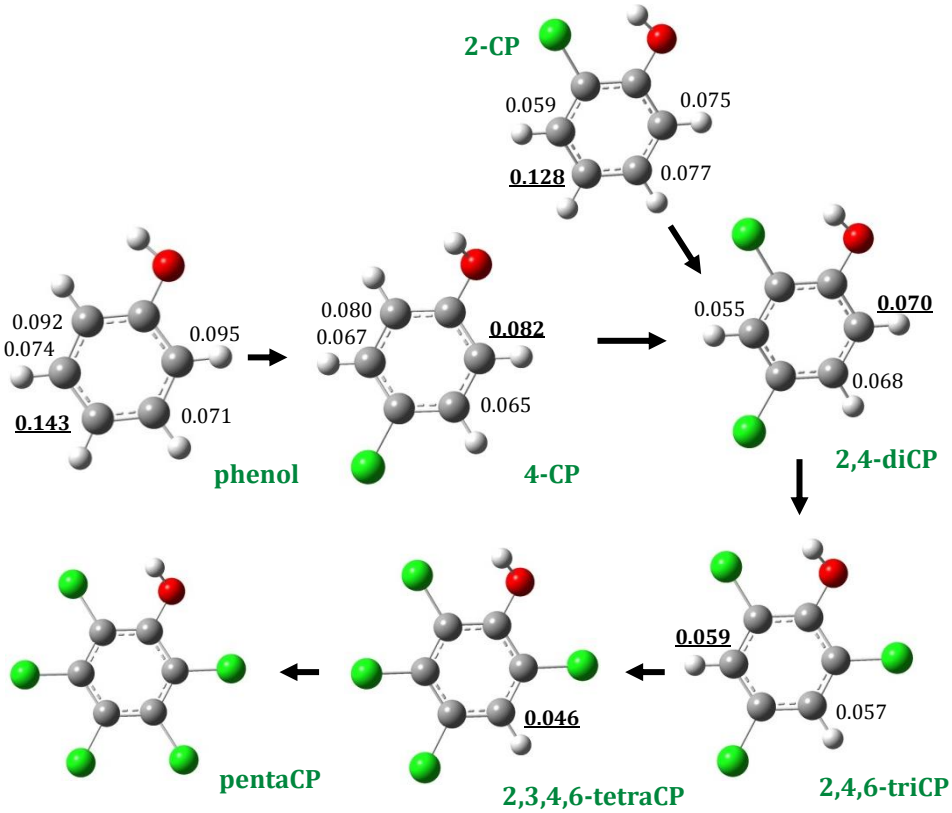

Figure 4.2. Chlorination sequence of phenol in aqueous phase. Prediction based on Fukui indices of electrophilic attack, $f^{-1}(\vec{r})$. Higher values of $f^{-1}(\vec{r})$ are underlined and in bold. The chemical structures are represented by carbon (grey), hydrogen (white), oxygen (red) and chlorine (green) atoms.

In Figure 4.2, the two *meta* positions in phenol attain the lowest $f^{-1}(\vec{r})$ value indicating a lower chlorination probability in reference to *para* and *ortho* sites. *Para*

carbon holds profoundly higher $f^{-1}(\vec{r})$ value, 0.143 against 0.095 obtained at *ortho* position (Figure 4.2). This is expected to translate into higher chlorination tendency of phenol leading to the formation of 4-chlorophenol (4-CP). Once 4-CP is formed, the position sensitive to further chlorination is the *ortho* position ($f^{-1}(\vec{r})$= 0.082, Figure 4.2) yielding 2,4-diCP. On the other hand, starting from 2-CP, the likely chlorination product according to the electrophilic Fukui indices is also 2,4-diCP by means of the chlorination of the *para* position ($f^{-1}(\vec{r})$= 0.128 against 0.075 at *ortho* position). The electrophilic substitution with another chlorine atom probably occurs at *ortho* position ($f^{-1}(\vec{r})$= 0.070) leading to the formation of 2,4,6-triCP, leaving unsubstituted *meta*-positions.

In spite of the fact that higher chlorinated phenols from 2-CP were not detected during the Fenton oxidation as it was explained in Chapter 3, the predicted chlorination sequence in Figure 4.2 coincides with the experimental profiles obtained from the chlorination of water streams containing phenol and the treatment of 2-CP solutions by electrochemical oxidation.[10,11,13,28,29] However, it must be noted that the chlorination product distribution depends on the reaction medium; the formation of 2-CP is favored in non-polar solvent medium such as dichloromethane or hexane among others.[2] Additional chlorination reactions lead to the formation of 2,4-diCP and 2,6-diCP obtaining higher concentrations of 2,4-diCP, thus preserving the trend of ortho/para substitution.[10,11,28,29] Further reaction with chlorine yielded 2,4,6-triCP, i.e the isomer predicted by the theoretical model for electrophilic attack herein.[10,11,28,29]

Chlorination pathway in gas phase

Gaseous streams emitted during the manufacture of phenolic species contain chlorophenols, as does the incineration of wastes. Trace quantities of chlorophenols also arise in the combustion of wood or coal.[3,30] In homogeneous systems, chlorophenoxy radicals (CPhxy) evolve either through unimolecular decomposition or through bimolecular reactions with the OH/H radical pool (Scheme 4.1) in the temperature window of 550 – 700 °C, whereas in heterogeneous systems CPhxy

form on surfaces at lower temperatures of 250 – 400 °C, as illustrated in Scheme 4.2.[31] Formation of PCDD/F from chlorophenoxy radicals through open-shell represents a more facile corridor than closed-shell pathways incorporating chlorophenols. Furthermore, chlorophenoxy radicals chemisorbed on surfaces of ash particles exhibit long life in the environment.[32] This persistency enhances their availability for electrophilic substitution

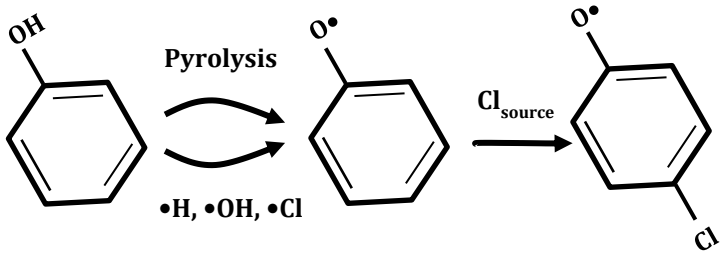

Scheme 4.1. Formation of (chloro)phenoxy radical from unimolecular decomposition and bimolecular reactions.

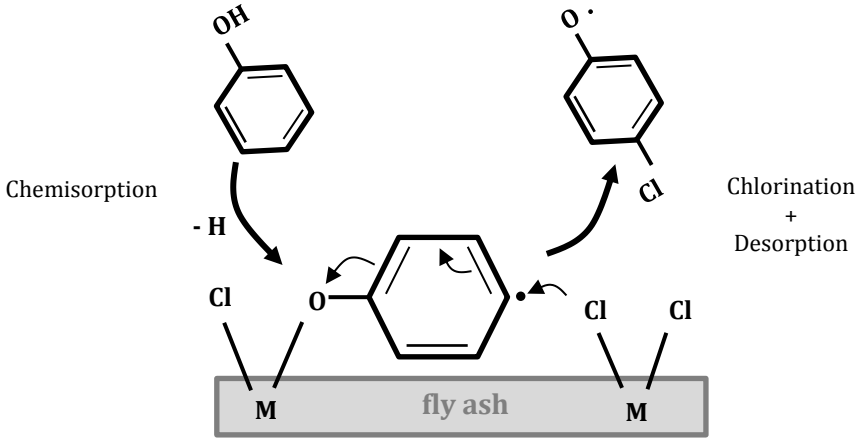

Scheme 4.2. Formation of (chloro)phenoxy radical over fly ash surface. M: metal.

Combustion reactions generate as side products bottom ashes and air pollution fly ashes residues.[33] Usually, fly ashes are characterized by high content of chlorides (5%), heavy metals and organic mater.[34,35] Therefore, together with the gas phase chlorine, fly ash may constitute an important source of chlorine and it is clear from previous works that its surface plays a fundamental role in catalyzing prominent chlorination reactions (Scheme 4.2).[14,36]

Figure 4.3 portrays the chlorination sequence for gas phase phenoxy/chlorophenoxy radicals.

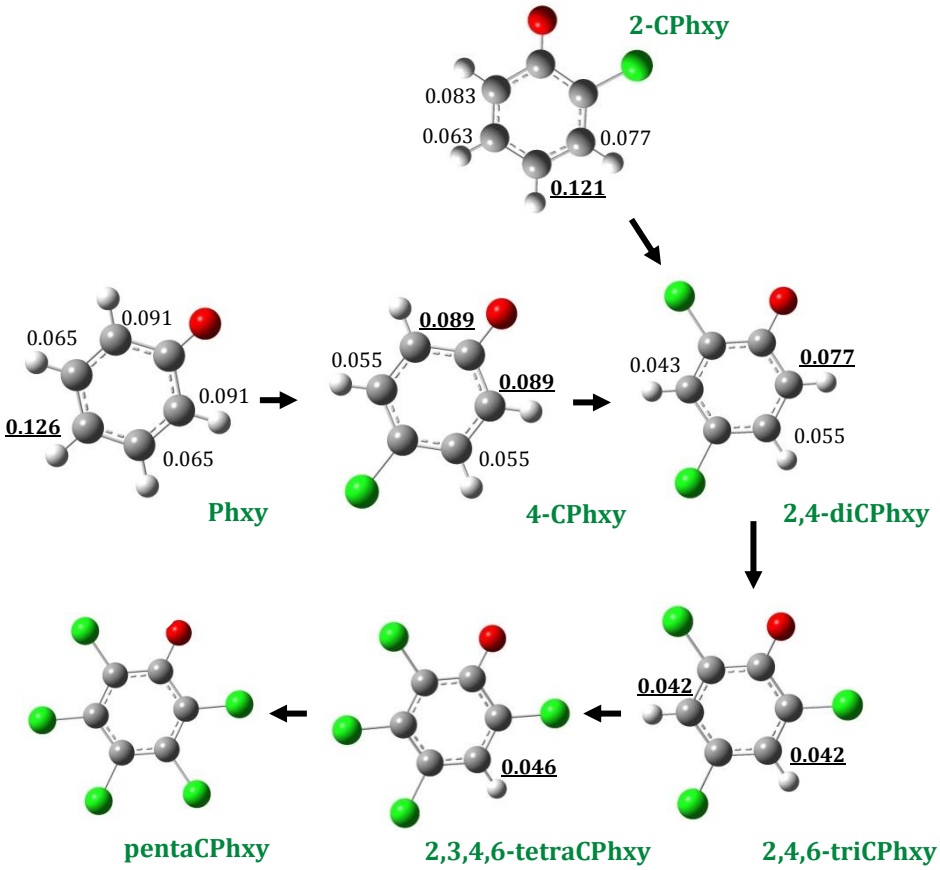

Figure 4.3. Chlorination sequence of phenoxy radicals in gas phase predicted based on Fukui indices of electrophilic attack, $f^{-1}(\vec{r})$.

The estimation of Hirshfeld charge distribution and Fukui indices for phenoxy electrophilic attack displayed the preference of *para* and *ortho* positions against *meta*-position. The likely position in phenoxy radical to be electrophilically substituted is the *para* position yielding 4-CPhxy ($f^{-1}(\vec{r})$= 0.126), as it could be expected from the symmetry of phenoxy radical, both *ortho* positions and both *meta* positions have identical Fukui indices, respectively. The same occurs with 4-CPhxy, where the electrophilic attack in *ortho* is preferred over *meta* positions, leading to the generation of 2,4-diCPhxy ($f^{-1}(\vec{r})$= 0.089). The electrophilic attack of 2-CPhxy

yields also 2,4-diCPhxy. Further chlorination of 2,4-diCPhxy forms 2,4,6-triChxy radical as a consequence of the chlorination of the *ortho* position ($f^{-1}(\vec{r})$= 0.077). Then, only *meta* positions are available for electrophilic substitution by chlorine.

Figure 4.4 presents the chlorination sequence for gas phase chlorophenols. The chlorophenolic product distribution observed during municipal waste incineration showed consistent results with those theoretically obtained considering the electrophilic attack (Figures 4.3 and 4.4).[36-39]

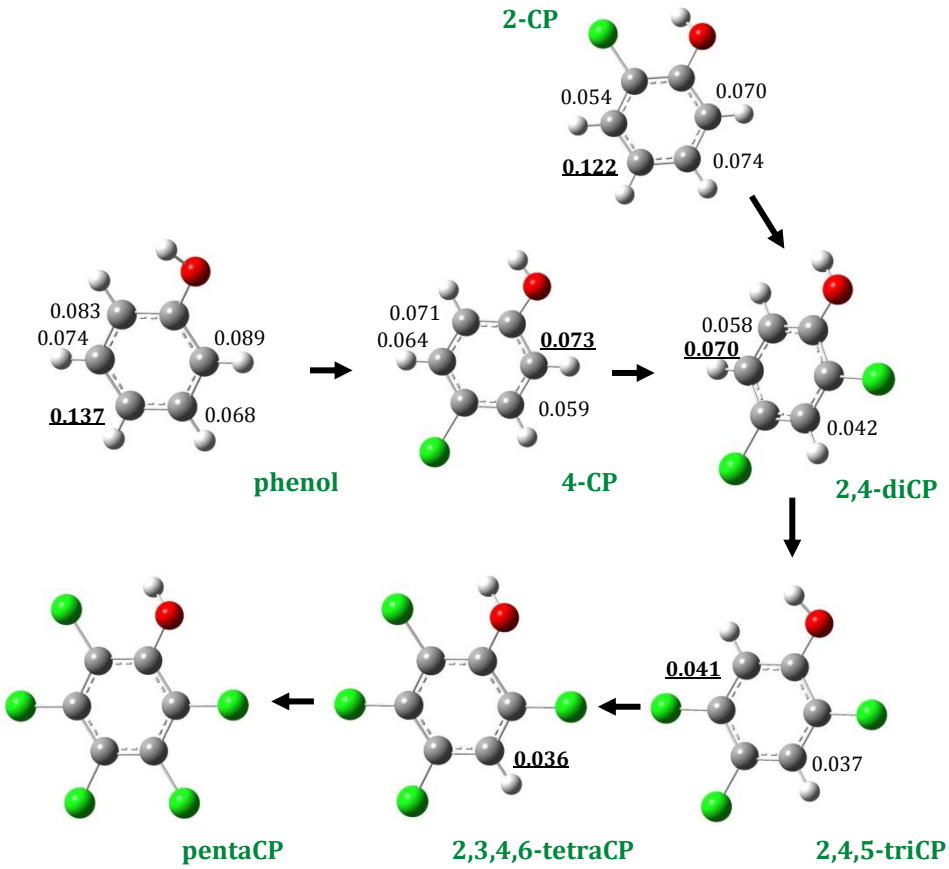

Figure 4.4. Chlorination sequence of phenol in gas phase predicted based on Fukui indices of electrophilic attack, $f^{-1}(\vec{r})$.

The experimental results presented in literature displayed that 4-CP is the main monochlorinated product resulting in 52.0% of the total monochlorophenol

generated, and followed by 2-CP (44.9%). The percentages given in this section correspond to the average product distribution calculated from the references presented above pertinent to municipal waste incineration. 2,4-diCP is the major dichlorinated phenol (68.0%) whereas 2,6-diCP was the secondary product (26.6%) entailing, thus, *ortho*/*para* substitution. Regarding trichlorophenols, 2,4,6-triCP was the principal isomer in terms of concentration (82.5% of the total trichlorophenols in the product distribution) as Figure 4.3 depicts, but it was present as a mixture of different isomers. For instance, the isomer 2,4,5-triCP had the highest concentration after 2,4,6-triCP (5.7%). In this sense, from the theoretical calculations of Hirshfeld charge distribution and Fukui indices for the electrophilic substitution on 2,4-diCP molecule in gas phase, 2,4,5-triCP was expected to be the main product in electrophilic chlorination reactions (Figure 4.4), different from the expected during the electrophilic chlorination of 2,4-diCPhxy (Figure 4.3). Therefore, the open-shell reaction through 2,4-diCPhxy is favored. Further chlorination of 2,4,6-triCPhenoxy and 2,4,5-triCP yields 2,3,4,6-tetraCP (88.2%) rather than 2,3,4,5-tetraCP (10.6%).

4.1.2. Electrophilic hydroxylation of 2-CP

The main purpose of this section is to relate the theoretical results obtained in the previous point by Fukui indices with the oxidation byproducts found when Fenton oxidation was applied to an aqueous solution containing 2-CP, taking into consideration the participation of hydroxyl radicals that are strong electrophilic radicals.[40]

Figure 4.5 displays the Fukui indices for the electrophilic attack of 2-CP and the schematic oxidation pathway including the main intermediate products during the Fenton oxidation of 2-CP. According to the Fukui indices, the *para* position is the position with a higher Fukui index value ($f^{-1}(\vec{r})$= 0.128) that indicates a higher probability of that position to suffer an electrophilic substitution. In this sense, 2-chlorohydroquinone (2-chloro-1,4-benzenediol, Scheme 3.5a) was identified by means of GC-MS but not during the HPLC analysis, which indicates a low concentration of this oxidation product.

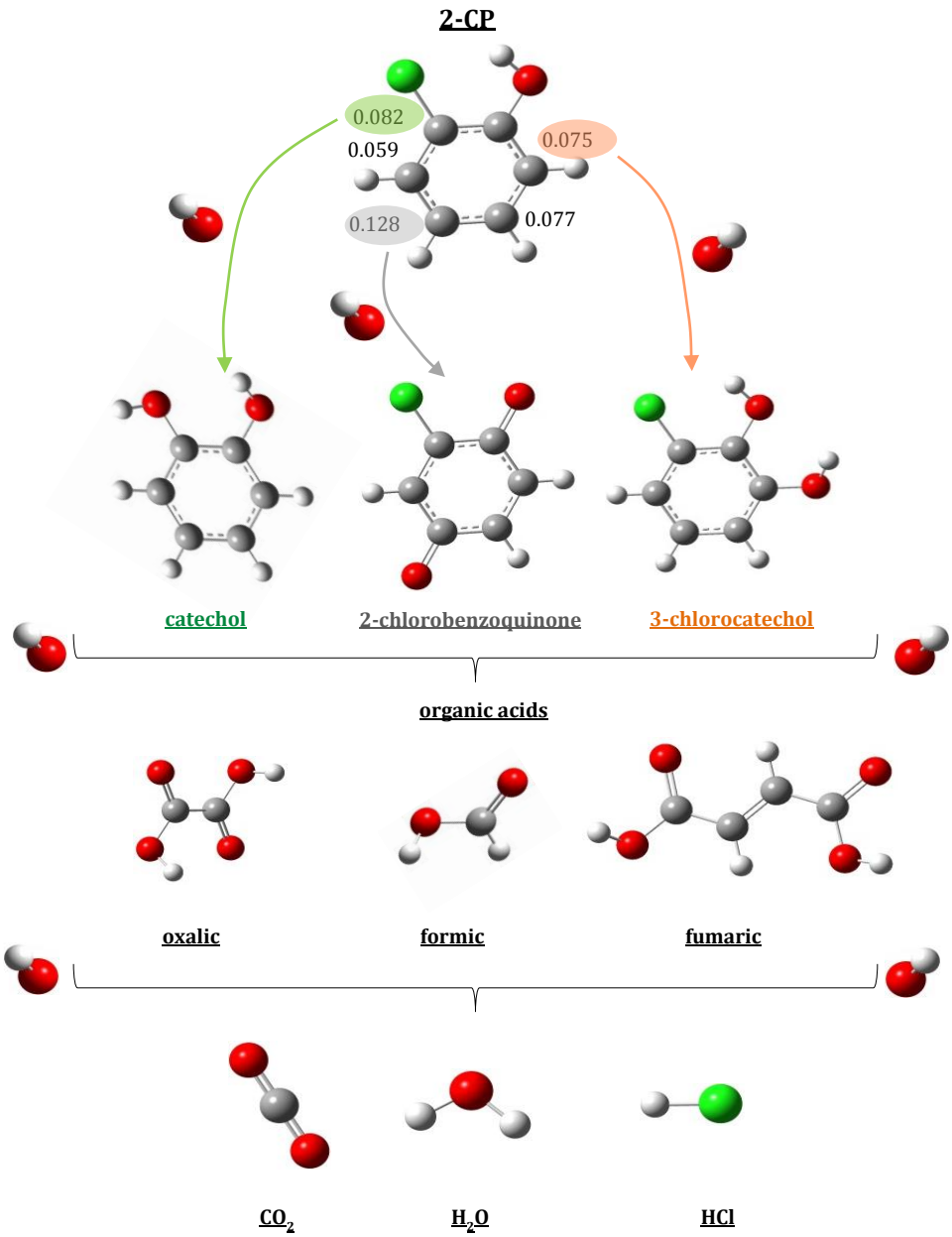

Figure 4.5. Scheme for the formation of the main intermediate products during the Fenton oxidation of 2-CP.

However, 2-chlorobenzoquinone (2-chloro-1,4-benzoquinone) was the major byproduct quantified (Figure 3.25) under substoichiometric conditions. Perhaps, 2-chlorohydroquinone is initially formed by hydroxylation in the *para* position (Figure 4.5), rapidly converted to a semiquinone-type radical, which was observed during the EPR analysis, (Reactions 4.1-4.3) and, then, oxidized to chlorobenzoquinone by means of Fe(III) (Reaction 4.4). Although Reactions 4.1-4.4, which are also included in Chapter 3 do not include compounds with chlorine in their structure, it has been assumed that the chlorinated forms undergo the same reactions described here.

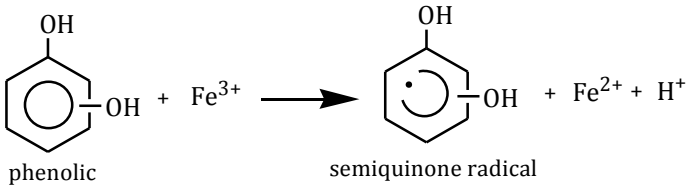

(4.1)

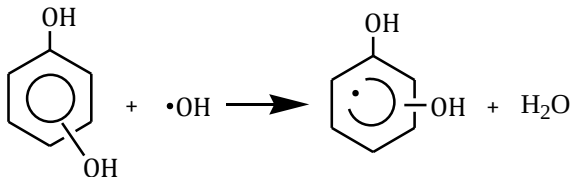

(4.2)

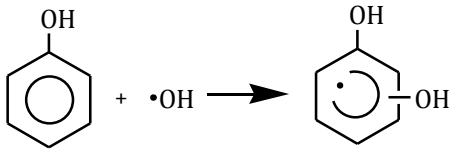

(4.3)

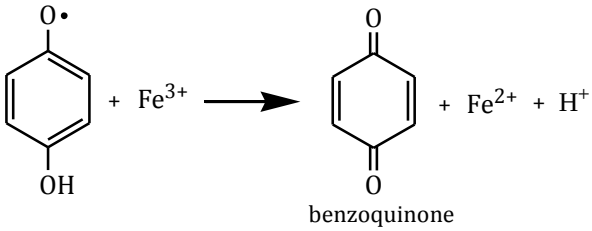

(4.4)

The next position with a higher Fukui index value is the corresponding to the *ortho* position containing the chlorine atom ($f^{-1}(\vec{r})$= 0.082). This chlorine atom can be electrophilically substituted by ·OH, leading to the formation of catechol (Figure

4.5) that was also identified as one of the main oxidation byproducts. These results showed the preference for the *ortho* and *para* positions since the hydroxyl group of the aromatic ring acts as *ortho/para* director.[41] Considering this information, the *ortho* position should be expected to be hydroxylated rather than the *meta* position in spite of having similar Fukui indices (Figure 4.5), leading to the generation of 3-chlorocatechol that is another significant intermediate during the Fenton oxidation of 2-CP.

Other intermediates such as 4-chlorocatechol (4-chloro-1,2-benzenediol, Scheme 3.5b) or 4-chlororesorcinol (4-chloro-1,3-benzenediol, Scheme 3.5c) were identified by GC-MS. The first one could found its origin in the chlorination reaction of catechol in the preferred *para* position (Figure 4.5), whereas 4-chlororesorcinol would correspond to the hydroxylation of *meta* position indicated with a Fukui index of 0.077 in Figure 4.6. Further oxidation of the aromatic byproducts resulted in the opening of the aromatic ring and the cleavage of the organic chain to produce acids with less number of carbon atoms, whose additional oxidation generates the final mineralization products CO_2, H_2O and HCl (Figures 3.25, 3.26 and 4.5).

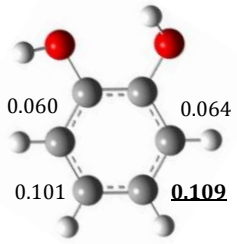

Figure 4.6. Fukui indices for the electrophilic attack of catechol.

4.2 Mechanistic proposal for the formation of PCDD/Fs from 2-CP based on previous theoretical studies

This section aims to predict the mechanisms involved in the generation of PCDD/Fs from 2-CP throughout the application of Fenton oxidation. The results presented in Chapter 3 in terms of PCDD/Fs concentration will allow proposing the mechanistic pathway for their formation from an aqueous 2-CP solution, supported by the theoretical data already published in literature for PCDD/Fs generation in gas phase.

Over the last decade, the application of quantum chemistry calculations in the framework of density functional theory (DFT) has allowed the optimization of the geometries and vibrational frequencies of all species and transition states involved in a chemical reaction as well as the evaluation of energetic parameters (such as activation and reaction energies).[42,43] In this sense, there are several works that make the most of the computational methods to ascertain and describe the mechanisms of PCDD/Fs formation from 2-CP solutions when thermal processes, combustion and pyrolysis, were applied.[31,42-50] Nevertheless, gas phase results appear to differ from the results obtained taking into consideration the solvation effect of water, which may affect the electronic properties, nuclear distribution, tautomerism and acidity by varying the activation energy and, therefore, the reaction rates.[51-53]

As a consequence of the scarce information about the mechanisms involved in the formation of PCDD/Fs from organochlorinated precursors in aqueous solutions, a detailed study of the likely routes associated to the generation of PCDD/Fs will be presented here, by analyzing and comparing the theoretically predicted mechanisms discussed in literature for gas phase reactions with experimental results obtained from the advanced oxidation treatment of aqueous solutions of 2-CP (Chapter 3). For this purpose, Fenton oxidation was selected as a model AOP and the operational parameters were selected in a way that higher concentrations of PCDD/Fs were obtained; thus, enabling the proper description of the mechanisms

implicated in the oxidation process yielding PCDD/Fs. Furthermore, whereas previous experimental studies related to the generation of PCDD/Fs in wastewaters were focused on homologue groups from tetra- to octa-PCDD/Fs, in this thesis a deepen study in the formation of non-chlorinated and low chlorinated DD/Fs (from mono- to tri-), both experimental and theoretically, to assist the identification of the reaction pathway that leads to PCDD/Fs in aqueous phase oxidation media has been developed.

According to the theoretical works reported in literature, chlorophenols can not only undergo electrophilic substitution reactions, or ring opening and chain closure reactions during the oxidation process (both described in Section 4.1), they lead also to the generation of PCDD/Fs. The formation of PCDD/Fs may succeed through molecule-molecule, molecule-radical and radical-radical coupling.[42] However, the considerable energy barriers make unlikely the generation of PCDD/Fs through the condensation of 2-CP molecules. Although radical-molecule pathways have significantly lower activation barriers than molecule-molecule route (even 30 kcal mol^{-1} less compared to molecule-molecule), the former is not competitive with radical-radical pathway, which is energetically favored (in the case of radical-molecule the energetic barrier is higher than 30 kcal mol^{-1} compared to radical-radical).[42,48] Furthermore, although chlorophenoxy radicals were not detected in the Fenton medium probably due to the low stability in aqueous phase or to a concentration below the limit of detection (Chapter 3), the presence of quinone and semiquinone-type radicals, which are related to the generation of chlorophenoxy radicals (Reactions 4.5 and 4.6) was observed throughout the Fenton oxidation of 2-CP. Therefore, the theoretical analysis of the formation of PCDD/Fs will consider the reaction between chlorophenoxy radicals formed from the oxidation of 2-CP.

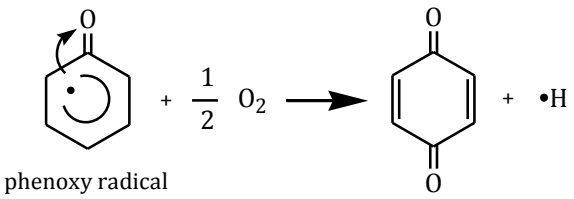

(4.5)

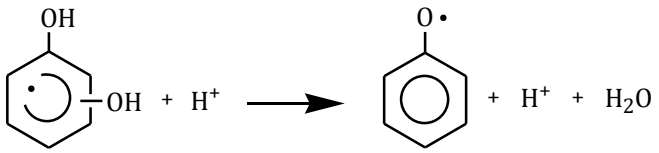

(4.6)

semiquinone radical phenoxy radical

Finally, although the computational studies described in the literature present results in which different radical species take part, i.e., hydrogen and chloride radicals in pyrolysis (·H and ·Cl, respectively) or hydroxyl radical (·OH) and ·Cl in combustion for the formation of aromatic active radicals, the proposed mechanisms were focused on those reactions that involve the participation of ·OH which are considered the main oxidizing agents generated during the application of AOPs and as the results during the Fenton oxidation in the presence of DMPO as spin-trap showed (Chapter 3).[5]

4.2.1. Study of the mechanisms of PCDD/Fs formation from the radical-radical pathway

Figure 4.7 displays the formation pathways of DD, MCDD and DCDD, and the average values of the activation energy (E_a) and the relative reaction energy (E_r) obtained from the existing computational calculations for gas phase, where the variance between these studies is due to the selection of different DFT methods and/or basis sets to optimize the molecular geometry and determine the energetic parameters.[31,42,43,48] The hydrogen abstraction from the alcoholic group of a 2-CP molecule with a hydroxyl radical leads to 2-chlorophenoxy radical (2-CPhxy, Figure 4.7).[31,39,42,48] 2-ChPxy is characterized by significant resonance stabilization owing to the delocalization of the unpaired electron (Scheme 4.3). Depending on its localization, the condensation of two 2-CPhxy may lead to the formation of dioxins (Figure 4.7) and furans (Figure 4.10). The reaction pathways from the literature considered in this thesis were those with lower energetic barriers (E_a).

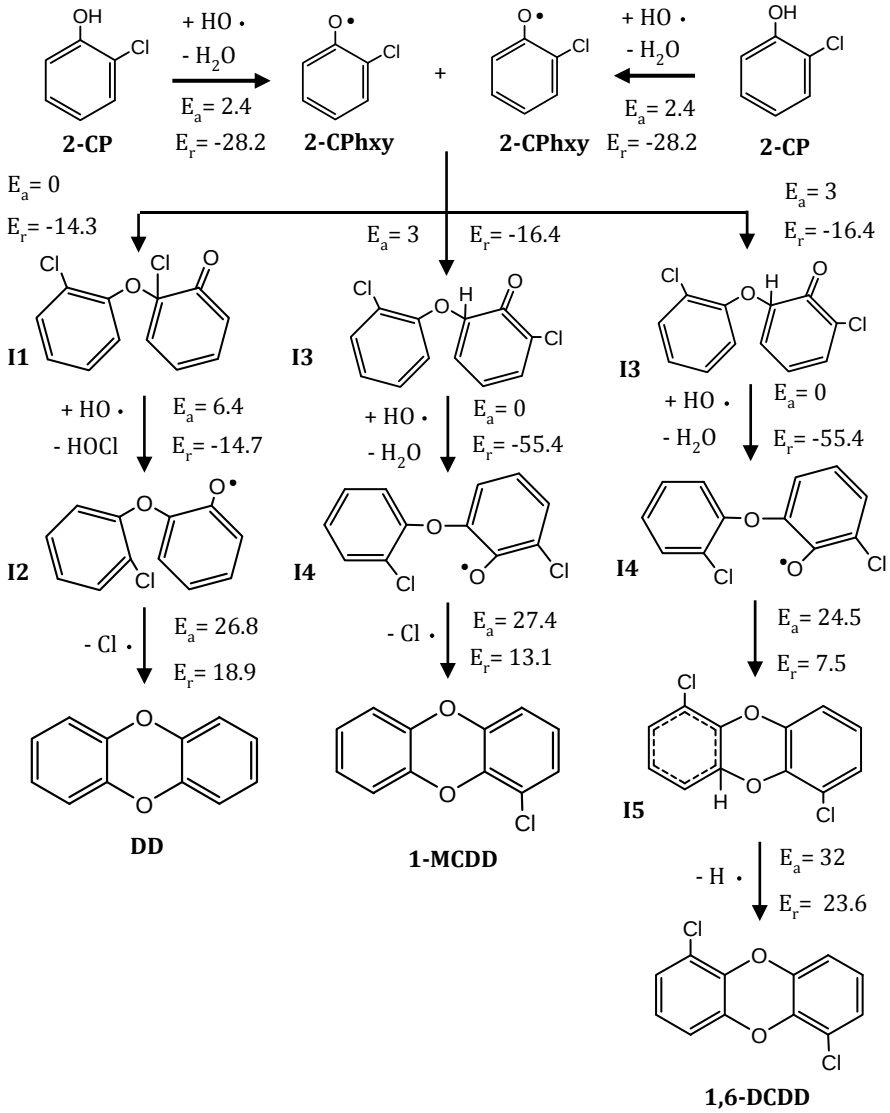

Figure 4.7. Formation pathways of DD, MCDD and DCDD from 2-CP by condensation of two 2-CPhxy. Energetic values (kcal mol^{-1}) were calculated at 0 K and correspond to the average results obtained by Altarawneh et al. (2007, 2008), B3LYP/6-311+G(3df,2p)//B3LYP/6-31G(d) level of theory; Zhang et al. (2008), MPWB1K/6-31+G(d,p)// MPWB1K/ 6-311+G(3df,2p) level; and Pan et al. (2013), BB1K/6-311G(d,p)// BB1K/6-311+G(3df,2p) level.[31,42,43,48] E_a represents the activation energy and E_r the relative reaction energy.

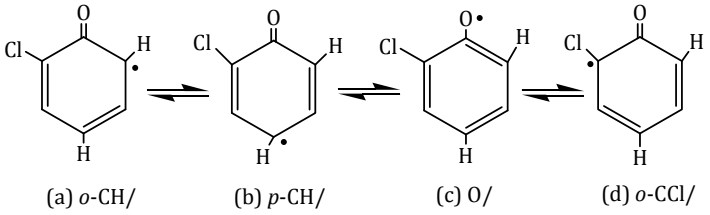

Scheme 4.3. Resonance form of 2-CPhxy radical.

The formation of dioxins requires two CPhxy with chlorine in *ortho*-position and the attack of an oxygen centered CPhxy (Scheme 4.3c) to an *ortho*-carbon centered CPhxy (Scheme 4.3a and d). The reaction of CPhxy yields the initial intermediates I1 (E_a= 0 kcal mol^{-1}) and I3 (E_a= 3 kcal mol^{-1}), whose further chlorine and hydrogen abstraction (I2 -E_a= 6.4 kcal mol^{-1}- and I4-E_a= 0 kcal mol^{-1}), dechlorination and ring closure yield DD and MCDD (E_a= 26.8 kcal mol^{-1} and 27.4 kcal mol^{-1}, respectively). However, in the case of DCDD instead of the dechlorination reaction of I4, the ring closure occurs (I5) followed by a dehydrogenation step (E_a= 24.5 kcal mol^{-1} and 32 kcal mol^{-1}, each stage). From the results, the similarities in the energetic barriers to form DD ($E_{a,total}$= 38 kcal mol^{-1}) and MCDD ($E_{a,total}$= 35.2 kcal mol^{-1}) can be inferred, where the most energetically demanding stage is the ring closure (I2→DD and I4→MCDD, respectively). However, whereas the chlorine elimination and ring closure occurs in one step for DD and MCDD, the ring closure and hydrogen abstraction to generate DCDD succeeds in two steps with an additional energetic barrier of 32 kcal mol^{-1} ($E_{a,total}$= 64.3 kcal mol^{-1}).

Otherwise, Pan et al. (2013) reported a deep analysis of the formation of PCDD/Fs considering also the generation of other active species, which have been proved to be active in the generation of polycyclic aromatic hydrocarbons (PAHs), polychlorinated biphenyls (PCBs) and PCDD/Fs. They incorporated to their computational studies not only 2-CPhxy but also chlorinated α-ketocarbene (Cα-k) and 2-chlorophenyl radical (2-CPh).[43] Figure 4.8 portrays the stages and energetic requirements involved in the formation of Cα-k and 2-CPh radicals considered by Pan et al. (2013). Cα-k is formed by hydrogen abstraction from the aromatic ring of

a 2-CPhxy, while 2-CPh is generated by means of hydrogen abstraction from the aromatic ring of a 2-CP molecule.

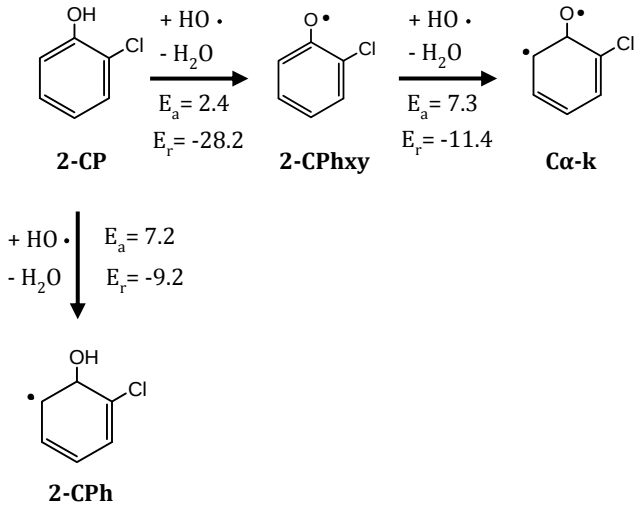

Figure 4.8. Formation pathways of Cα-k and 2-CPh radicals from 2-CP. Energetic values (kcal mol^{-1}) were calculated at 0 K and correspond to the results obtained by Pan et al. (2013), BB1K/6-311G(d,p)// BB1K/6-311+G(3df,2p) level.[43] E_a represents the activation energy and E_r the relative reaction energy.

Pan et al. (2013) identified different available pathways based on the combination of 2-CPhxy, 2-CPh and Cα-k that conduct to the formation of PCDD/Fs and, interestingly, they found alternative routes to yield DCDD and DCDF with lower energetic barriers and less number of reactions compared to previous studies.[43] Figure 4.9a depicts a five-stage DCDD formation based on the reaction of 2-CPhxy, but taking into account that Cα-k arises as a potential radical precursor. The profile of PCDDs generated during the Fenton oxidation of 2-CP under substoichiometric hydrogen peroxide dose in presence of 56.34 mM NaCl has been included in Figure 4.9b to facilitate the definition of the main pathways. The concentration of each homologue corresponds to the average value considering the results for the range of iron dose studied (0.09-2.88 mM). The formation of the high-chlorinated DDs will be discussed later.

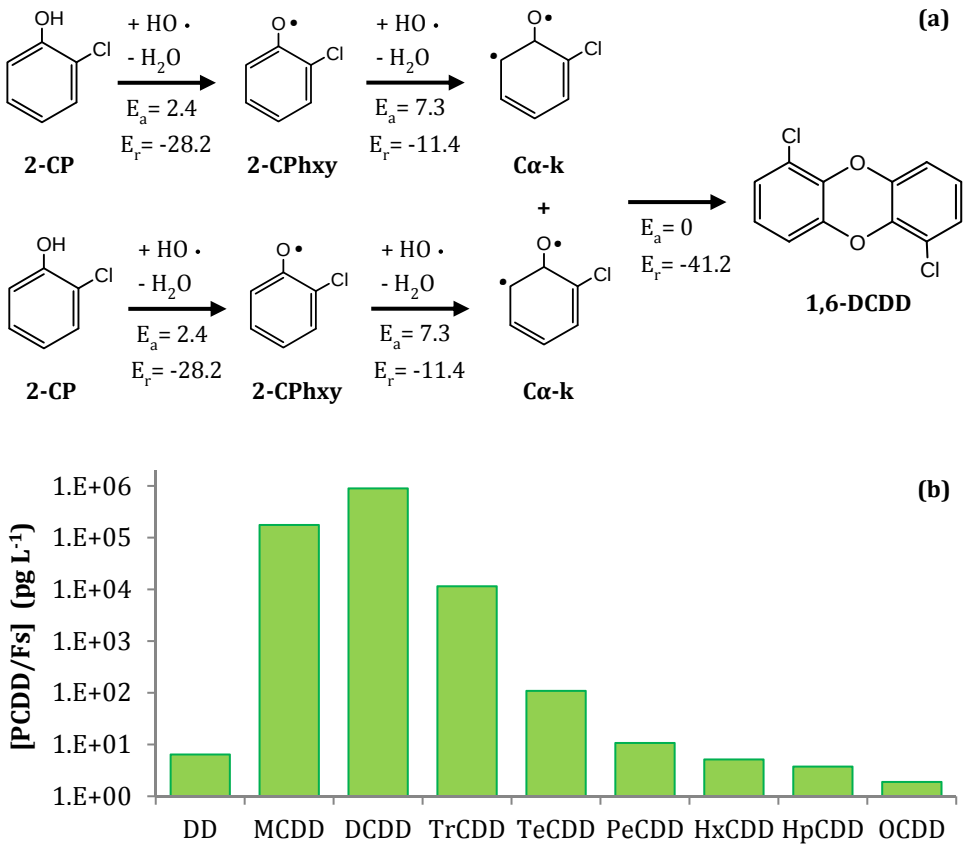

Figure 4.9. (a) Formation route of DCDD from 2-CP by condensation of two Cα-k. Energetic values (kcal mol^{-1}) were calculated at 0 K at BB1K/6-311G(d,p)// BB1K/6-311+G(3df,2p) level.[43] E_a represents the activation energy and E_r the relative reaction energy. (b) Distribution of dioxins during the Fenton oxidation of 15.56 mM 2-CP under substoichiometric H_2O_2 dose (40.44 mM). The concentration of each homologue corresponds to the average value for the different iron doses (0.09-2.88 mM).

Pan et al. (2013) concluded that the reaction of two Cα-k was barrierless and directly yields DCDD (Figure 4.9a). This is a relevant ascertainment because it implies a reduction of the energetic barrier from a total of 64.3 kcal mol^{-1} (Figure 4.7) to 19.4 kcal mol^{-1}(Figure 4.9a), being this pathway the most favorable to form DCDD in thermodynamic terms. Therefore, taking into account the energetic barriers described in Figures 4.7 (DD and MCDD) and 4.9a (DCDD) the formation of

DCDD is preferred due to the lower energetic requirements. In this sense, the results presented in Figure 4.9b shows a predominance of DCDD ($9.0 \cdot 10^5$ pg L^{-1}) over MCDD ($1.8 \cdot 10^5$ pg L^{-1}) and DD (6 pg L^{-1}). Regarding the DD/MCDD ratio, the abstraction of chlorine with ·OH (I1→ I2, 6.4 kcal mol^{-1}, Figure 4.7) is not expected to be competitive with the abstraction of hydrogen with ·OH (I3→ I4, 0 kcal mol^{-1}, Figure 4.7) owing to the higher energetic barrier that meets with the experimental results where the generation of DD was almost zero. Therefore, the product distribution observed for dioxins through the mechanistic studies and the experimental results from Fenton oxidation of 2-CP agrees with the product distribution identified during the gas-phase oxidative thermal degradation of 2-CP, DCDD>MCDD>DD.[54,55]

With regard to the formation of furans, Figure 4.10 portrays the formation pathways of MCDF and DCDF, and the corresponding average values of the activation energy (E_a) and relative reaction energy (E_r) obtained from the existing computational calculations, where the variance between these studies is due to the selection of different DFT methods and/or basis sets to optimize the molecular geometry and determine the energetic parameters.[31,39,42,48]

The generation of furans requires two CPhxy with at least one hydrogen bonded to an *ortho*-carbon (H-*o*-C) and the union of the CPhxy occurs between two *ortho*-carbon centered radicals (Scheme 4.3a and d).[39,42] The union of a H-*o*-C chlorophenoxy with Cl-*o*-C or H-*o*-C chlorophenoxy leads to the formation of different intermediates (I6 –E_a= 7 kcal mol^{-1}- and I10 -E_a= 5.8 kcal mol^{-1}) that are precursors of MCDF and DCDF (Figure 4.10), respectively. The next step is the chlorine and hydrogen abstraction to form I7 (E_a= 5.4 kcal mol^{-1}) and I11 (E_a= 3.5 kcal mol^{-1}), respectively. Further reactions are common for both pathways: H-shift (I8 and I12- E_a= 27.0 and 28.1 kcal mol^{-1}, respectively), ring closure (I9 and I13 -E_a= 30.2 and 30.3 kcal mol^{-1}, respectively), and ·OH elimination (MCDF and DCDF -E_a= 16.9 and 18.4 kcal mol^{-1}, respectively).

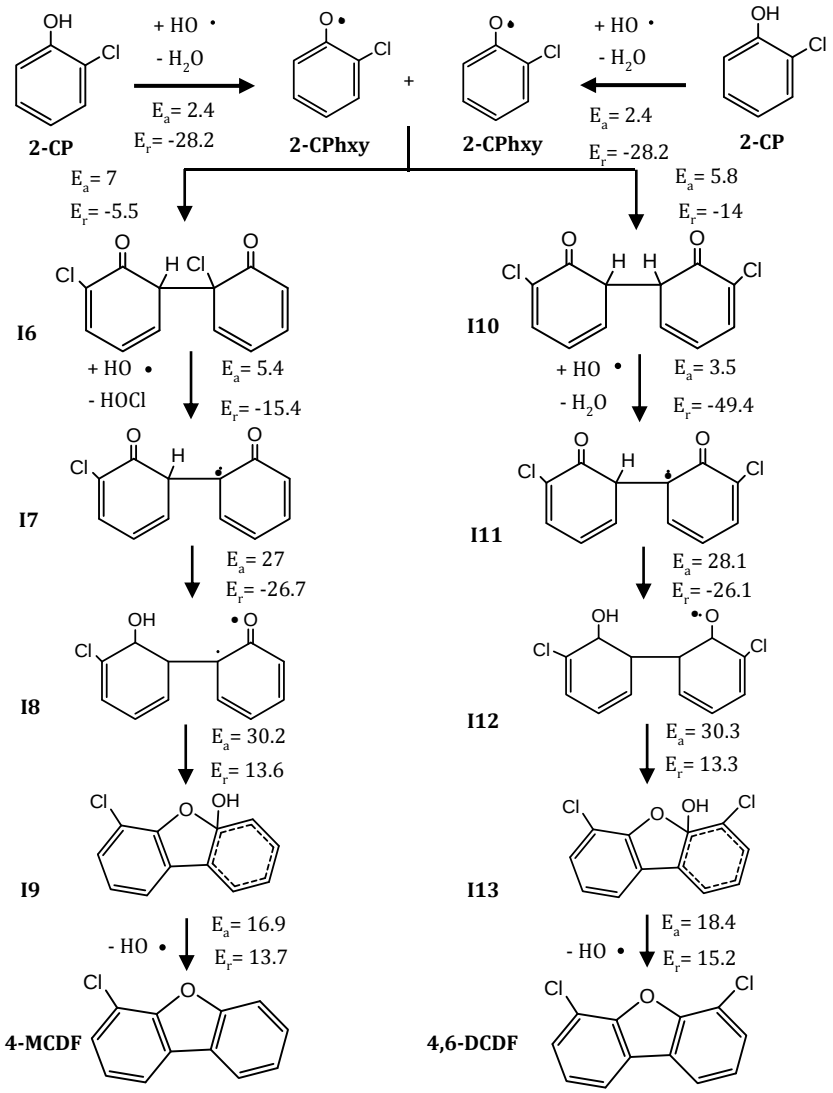

Figure 4.10. Formation pathways of MCDF and DCDF from 2-CP by condensation of two 2-CPhxy. Energetic values (kcal mol^{-1}) were calculated at 0 K and correspond to the average results obtained by Altarawneh et al. (2007, 2008), B3LYP/6-311+G(3df,2p)//B3LYP/6-31G(d) level of theory; Zhang et al. (2008), MPWB1K/6-31+G(d,p)// MPWB1K/ 6-311+G(3df,2p) level; and Pan et al. (2013), BB1K/6-311G(d,p)// BB1K/6-311+G(3df,2p) level.[31,42,43,48] E_a represents the activation energy and E_r the relative reaction energy.

Both MCDF and DCDF have similar energetic requirements (91.3 and 90.9 kcal mol^{-1}, respectively) and the highest barrier corresponds to the ring closure step (30.3 kcal mol^{-1} in both cases). However, Pan et al. (2013) proposed an alternative route based on the formation of Cα-k and 2-CPh radicals that has been represented in Figure 4.11a.[43] The PCDFs concentrations profile obtained when working under substoichiometric H_2O_2 doses has been included in Figure 4.11b. The formation of the high-chlorinated DFs will be discussed later.

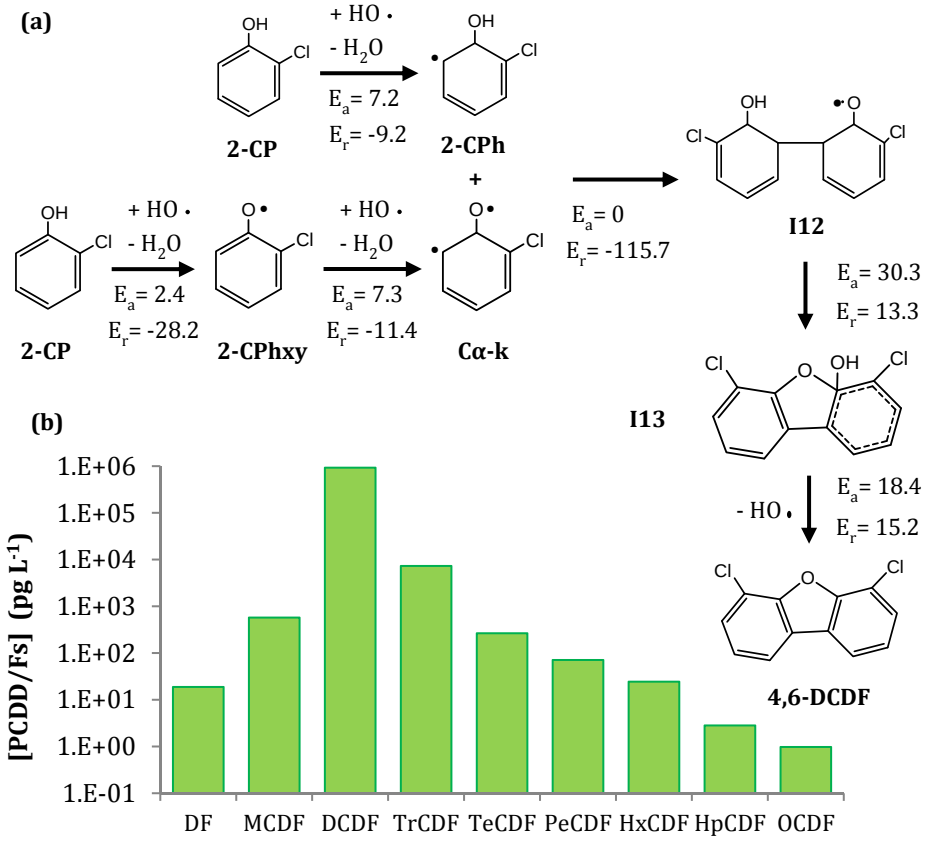

Figure 4.11. (a) Formation route of DCDF from 2-CP by condensation of 2-CPhR and Cα-k. Energetic values (kcal mol^{-1}) were calculated at 0 K at BB1K/6-311G(d,p)// BB1K/6-311+G(3df,2p) level.[43] E_a represents the activation energy and E_r the relative reaction energy. (b) Distribution of furans during the Fenton oxidation of 15.56 mM 2-CP under substoichiometric H_2O_2 dose (40.44 mM). The concentration of each homologue corresponds to the average value for the different iron doses (0.09-2.88 mM).

Pan et al. (2013) observed a reduction of the energetic barriers and the number of stages through the formation of DCDF from the reaction between 2-CPhR and Cα-k (Figure 4.11a). Though the generation of these radicals is energetically more demanding than 2-CPhxy ($E_{a,c\alpha\text{-}k}$= 9.7 kcal mol^{-1}, $E_{a,2\text{-}CPh}$= 7.2 kcal mol^{-1}, $E_{a,2\text{-}CPhxy}$= 2.4 kcal mol^{-1}), two steps with activation energy of 3.5 and 28.1 kcal mol^{-1} were suppressed (formation of I10 and I11, Figures 4.10a and 4.11a), reducing the energetic barrier of DCDF from 90.9 kcal mol^{-1} down to 65.6 kcal mol^{-1}, and keeping 91.3 kcal mol^{-1} for MCDF. Fenton oxidation of 2-CP led to the preferential formation of DCDF ($9.3\cdot10^5$ pg L^{-1}) over MCDF ($5.7\cdot10^5$ pg L^{-1}), as it would be expected from the energetic analysis, with a yield in DCDF around three orders of magnitude higher than MCDF. This product distribution, DCDF>MCDF, has been previously observed during the homogeneous gas-phase thermal oxidation of 2-CP.[54,55]

Concerning the DCDD/DCDF ratio (Figures 4.9b and 4.11b), similar concentrations of both groups were obtained ($9.0\cdot10^5$ pg L^{-1} versus $9.3\cdot10^5$ pg L^{-1}). Sidhu et al. (2002) described different product distribution depending on the initial 2-CP concentration, and they registered for high 2-CP concentrations (684 mg L^{-1}) the preferential formation of DCDF over DCDD.[55] This could be explained during the reaction of 2-CP with ·OH that leads to radical active species characterized by the resonance stabilization phenomena, *eno* and *keto* forms with the unpaired electron on the phenolic oxygen (Scheme 4.3c) or *ortho*-/*para*- carbons (Scheme 4.3a, b and c), respectively. High initial 2-CP concentration favors its reaction with the generated radicals, lowering the availability of radicals in the medium and, therefore, their recombination. Owing to the upper stability of the *keto* form, the decrease of the *eno* form was favored.[55] As a consequence, due to the fact that furans require only the more stable *keto* forms, higher DCDF yields would be expected.

Considering the computational studies based on the condensation of 2-CP related species, the product distribution of dioxins and furans involved only the generation of CDD/Fs with up to two chlorine atoms. However, the homologue distribution profile on Figures 4.9b and 4.11b shows the presence of higher chlorinated CDD/Fs, especially tri-CDD/Fs. The formation of high chlorinated-DD/Fs

may occur from the chlorination of 2-CP (as it was presented in Section 4.1) and subsequent condensation reactions of di-, tri-, tetra-, pentachlorinated phenols, or from the condensation of 2-CP (related radicals) and posterior chlorination reactions.[56] However, there is not a detailed study in which both phenomena take place simultaneously. During AOPs, the chloride present in the aqueous medium unselectively reacts with the generated ·OH (k, $4.3 \cdot 10^9$ L mol^{-1} s^{-1}) leading to the formation of free chlorine species: ·Cl, Cl_2 (pH ≤ 3.3), HClO (pH < 7.5) and ClO^- (Reactions 3.17-3.21).[5,12,57,58] However, the presence of active chlorine species could not be measured in these experiments because the solution had a brownish color that hindered their quantification by means of a colorimetric method.[12]

The proposed pathway in the first place is the chlorination reaction of 2-CP followed by condensation of higher chlorinated phenols. The experimental and mechanistic works in thermal oxidation processes in gas phase have demonstrated that the higher the chlorination degree of phenols that act as precursors, the higher the chlorination degree of PCDD/Fs.[59-62] However, high chlorinated phenols, i.e., di-, tri-, tetra- or pentaCPs have not been detected in the Fenton treatment of 2-CP. As a result, this reaction pathway has been discarded in the mechanistic explanation of the formation of PCDD/Fs from Fenton oxidation of 2-CP under the experimental conditions applied.

The proposed pathway in second instance is the condensation of 2-CP (related radical species) followed by chlorination reactions (Figure 4.12a). During the thermal oxidation of 2-CP no formation of PCDD/Fs with a chlorination degree higher than two had been observed.[36,39,54,55,63] Nevertheless, these works did not analyze the influence of the presence of chlorine sources in the reaction medium. Figure 4.12 displays a general description for the formation of high chlorinated CDD/Fs from low chlorination degree and the average concentration obtained during the Fenton treatment of 2-CP under substoichiometric H_2O_2 considering an average concentration among the different iron doses employed.

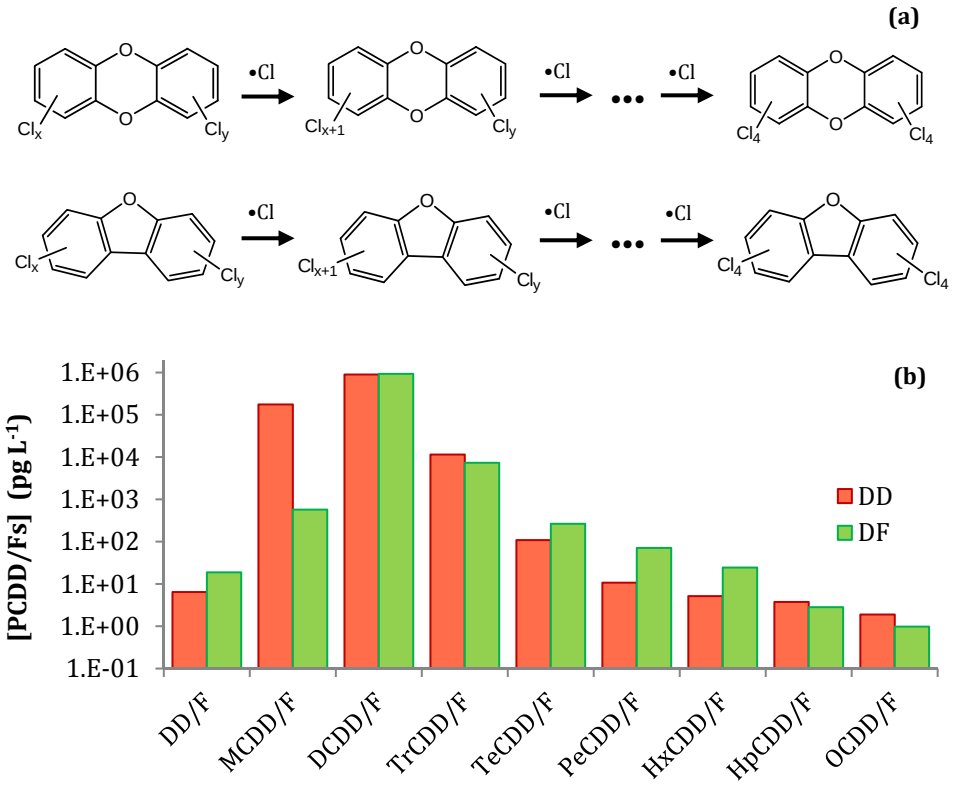

Figure 4.12. (a) General description for the chlorination reactions from the lower chlorinated DD/Fs up to OCDD/Fs. (b) Distribution of PCDDs and PCDFs during the Fenton oxidation of 15.56 mM 2-CP under substoichiometric H_2O_2 dose (40.44 mM). The concentration of each homologue corresponds to the average value for the different iron doses (0.09-2.88 mM).

Figure 4.12b shows the presence of highly chlorinated PCDD/Fs groups with a progressive decrease in their concentration from DCDD/F to OCDD/F; the formation of these groups could be explained by the gradual chlorination from DCDD/Fs to higher chlorinated species as shown in Figure 4.12a. This chlorination process has been also described not only in gas phase experiments with $CuCl_2$ as catalyst and chlorination agent, but also when a Cl_2 stream was in contact with dioxins/furans in gas and aqueous phase.[16,64-72]

4.2.2. Study of the solvation effect and reaction with H_2O during PCDD/Fs from 2-CP as precursor

This point will cover a brief analysis of the solvent effect in aqueous solution and the influence of water participating in gas phase reactions to form PCDD/Fs focusing on the original reactions of higher energetic requirements presented by Altarawneh et al. (2007).[42] This work was developed in the framework of a research internship of the PhD candidate in their laboratory (Fire Safety and Combustion Kinetics Lab). These computational studies constitute a preliminary evaluation and were motivated by the lack of theoretical results applied to aqueous phase; with the aim of broaden the knowledge about the influence of water in the energetic requirements for both phases, aqueous (through hydrogen bonds) and gas (through the participation of H_2O as reagent), and compare with the results for gas phase without considering the water molecule. This methodology has been preliminary employed with the aim of applying it to all the stages and alternative pathways involved in the formation of PCDD/Fs during the application of AOPs in the future. Until now, the results presented in this thesis were focused on the selection of the likely stages characterized by lower energetic barriers without considering the influence of H_2O. Consequently, those stages that were discarded because of their high activation barriers will be analyzed in this section, i.e., three different stages in the generation of DD and 4,6-DCDF.

Figure 4.13 presents the first of the three stages studied, centered on the transference of a hydrogen atom from a diketo dimer (D1), formed as a consequence of the coupling of two chlorophenoxy radicals, leading to an enol-keto structure as an intermediate byproduct prior to the formation of 4,6-DCDF (the stage of interest is highlighted in green). Besides, this figure presents the theoretical E_a obtained by Altarawneh et al. (2007) for gas phase calculated at 0 K with Gaussian 03 and the level of theory B2LYP/6-311+G(3df,2p)//B3LYP/6-31G(d), and the results obtained in this thesis by using DMol3 implemented in Materials Studio 8.0 (Accelrys Inc.), GGA level and DND basis set for gas phase, aqueous phase considering the solvation effect, and gas phase considering the reaction with a water molecule.[42] The pathway

presented in this figure is an alternative discarded in the proposal of the mechanisms described in Section 4.2.1 because of the higher energetic barrier than that displayed in Figure 4.10 (from I10 to 4,6-diCDF).

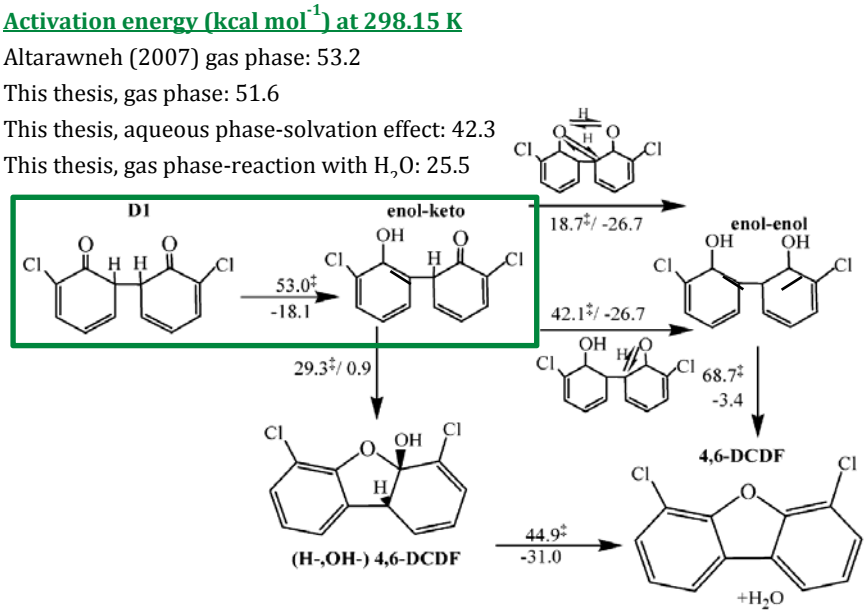

Figure 4.13. Formation of 4,6-DCDF from the coupling of two 2-CPhxy through the formation of 3,3'-dichloro-1,1'-bi(cyclohexa-3,5-diene)-2,2-dione (D1); E_a are denoted as ‡ and the other values are the reactions energies (kcal mol^{-1}) at 0 K from Altarawneh et al. (2007).[42] The stage of interest is highlighted and the E_a calculated (298.15 K) in this thesis for gas phase, aqueous phase (solvation effect) and gas phase considering the reaction with water are included above the highlighted section. The double arrows indicate migration of H atom.

The activation energy (E_a) obtained by Altarawneh et al. (2007) was 53.2 kcal mol^{-1}.[42] During the calculations carried out in this thesis the result obtained was E_a= 51.6 kcal mol^{-1}, similar to that previously obtained by Altarawneh et al. (2007). Once the validity of the results was checked, DMol^3 calculations were applied to study the solvation effect considering water as solvent, obtaining a decrease in the activation barrier of almost 10 kcal mol^{-1} (42.3 kcal mol^{-1}). Therefore, water has a relevant role reducing the activation energy by means of electrostatic forces. Scheme 4.4 displays

an overview of the phenomena happening in the aqueous phase where H_2O molecule facilitates the H-shift thanks to the H-bonds between D1 and H_2O.

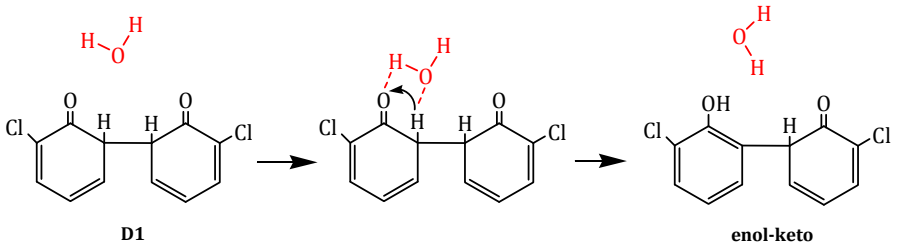

Scheme 4.4. Solvation effect of H_2O in the reaction from D1 to enol-keto displayed in Figure 4.13 in aqueous phase.

In a recent study, Shi et al. (2015) showed that water present in the gas phase reaction medium may participate in transference reactions of H owing to its ability to form hydrogen bonds, resulting in a bimolecular reaction in which H_2O is considered to act as a catalyst that reduces the energy requirements, as it is depicted in Scheme 4.5.[46] With this regard, additional computational calculations were done resulting in an important decrease of more than 26 kcal mol^{-1} in the activation energy (25.5 kcal mol^{-1}) compared to gas phase without considering the presence of H_2O.

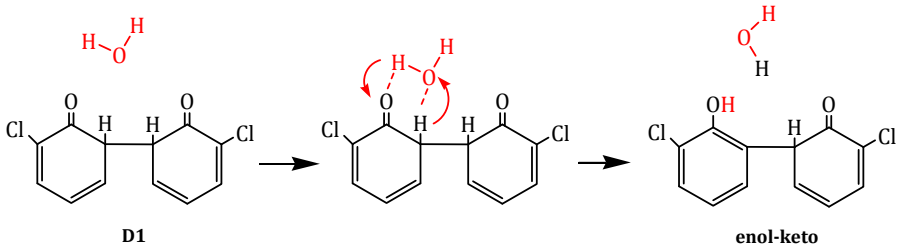

Scheme 4.5. Participation of water as catalyst in the reaction from D1 to enol-keto displayed in Figure 4.13.

Figure 4.14 depicts the second stage analyzed: tautomerization from keto-keto· radical to enol-keto· radical (highlighted in green). The pathway presented in this figure is an alternative rejected in the proposal of the mechanisms described in Section 4.2.1 because of the higher energetic barrier than that displayed in Figure 4.10 (from I11 to 4,6-diCDF). It has been included in Figure 4.14 the theoretical E_a

obtained by Altarawneh et al. (2007) for gas phase (complete mechanism from the condensation product D1), and the results obtained in this thesis for gas phase, aqueous phase considering the solvation effect, and gas phase considering the reaction with a water molecule.[42] In this case, owing to the difficulties arisen during the computational calculations with DMol[3] that did not allow the proper optimization of the geometry of reactants and products, Gaussian 09 was employed with a M062X function (based on GGA), and 6-311+G(d,p) level of theory.

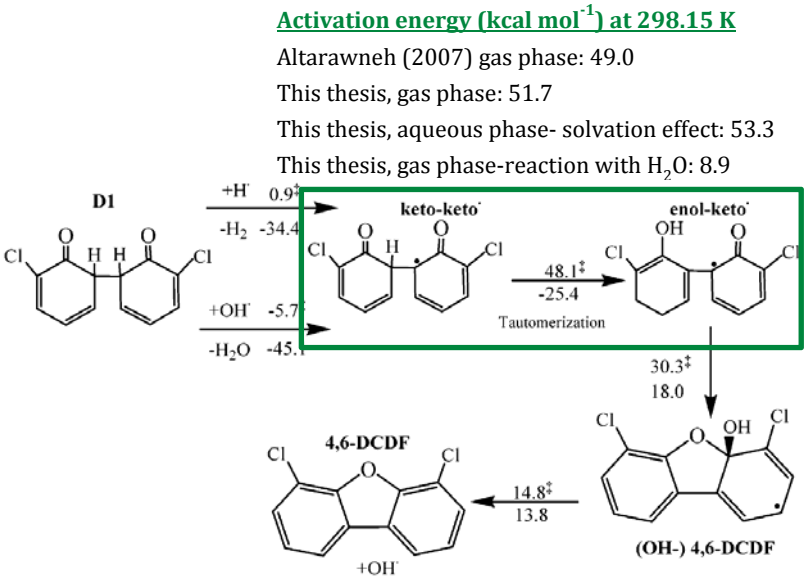

Figure 4.14. Formation of 4,6-DCDF from the coupling of two 2-CPhxy through the formation of 3,3'-dichloro-1,1'-bi(cyclohexa-3,5-diene)-2,2-dione (D1); E_a are denoted as ‡ and the other values are the reactions energies at 0 K from Altarawneh et al. (2007).[42] The stage of interest is highlighted and the E_a calculated (298.15 K) in this thesis for gas phase, aqueous phase (solvation effect) and gas phase considering the reaction with water are included above the highlighted section. The double arrows indicate migration of H atom.

By using Gaussian, the activation energy was E_a=51.7 kcal mol^{-1}, comparable to that obtained by Altarawneh et al (2007), E_a= 49.0 kcal mol^{-1}, where the slight differences may be caused by the selection of two alternative functions.[42] When solvation effect was taken into account, the energetic barrier kept almost invariable (E_a= 53.3 kcal mol^{-1}). Nevertheless, the calculations carried out in gas phase

considering the presence of water molecules displayed a positive effect by decreasing the activation barrier, E_a= 8.9 kcal mol^{-1}. The mechanisms of solvation effect in aqueous phase and reaction with H_2O are similar to those presented in Schemes 4.4 and 4.5)

Finally, a third example was chosen. Figure 4.15 depicts the stage corresponding to the formation of DD from 2-(2-chlorophenoxy)phenol (preD1) by the elimination of HCl from the reactant, and the closure of the ring (stage highlighted in green). Figure 4.15 displays the theoretical E_a obtained by Altarawneh et al. (2007) for gas phase, and the results obtained in this thesis for gas and aqueous phase considering the solvation effect.[42]

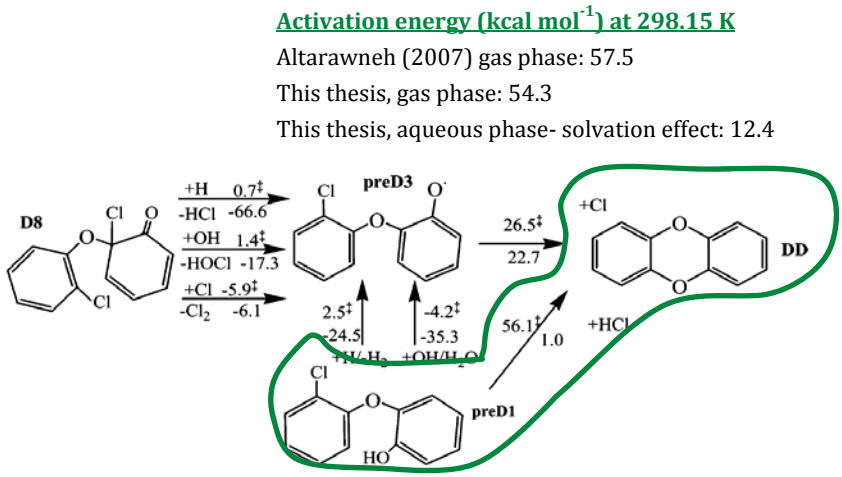

Figure 4.15. Formation of DD from the coupling of 2-CP and 2-CPhxy through the formation of 2-(2-chlorophenoxy)phenol (preD1); E_a are denoted as ‡ and the other values are the reactions energies at 0 K from Altarawneh et al. (2007).[42] The stage of interest is highlighted and the E_a calculated (298.15 K) in this thesis for gas phase and aqueous phase (solvation effect).

According to the results published by Altarawneh et al. (2007), the energetic barrier was E_a= 57.1 kcal mol^{-1}.[42] The verification of these values by DMol^3 resulted in 54.3 kcal mol^{-1}, which was quite similar to that found in bibliography. The employment of DMol^3 for the assessment of the solvent effect displayed a significant diminishment of the activation energy: E_a= 12.4 kcal mol^{-1}, highlighting the

importance of the electrostatic forces provided by water over the energetic requirements.

In line with the results obtained during the development of this thesis with regard to the influence of water in the estimation of the energy requirements, Shi et al. (2015) showed in a previous study the influence of water in gas phase oxidation of 2-CP, finding also a positive influence of the H_2O molecule in all the steps analyzed by decreasing by an average of 5 kcal mol^{-1} the activation barrier compared to the gas phase reaction without considering water.[46,48] In the case of the H-shift step (I7 → I8, Figure 4.10), a diminishment of 4.5 kcal mol^{-1} was found taking into consideration H_2O and comparing it with the value reported by Zhang et al. (2008).[48] Furthermore, these authors showed that the presence of water on the homogeneous gas-phase medium promotes the formation of hydrogen-bonded complexes OH-H_2O. The reaction of 2-CP with OH-H_2O led to a six-center cyclic structure, formed by two hydrogen bonds (Scheme 4.6), corresponding to a transition state with higher stability than the non-hydrated transition state, lowering the energetic barrier of the hydrogen abstraction from 2-CP.

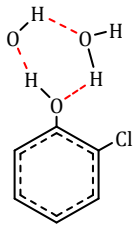

Scheme 4.6. Water-assisted H abstraction reaction from 2-CP by ·OH.

Thus, it has been proved that the consideration of the solvation effect in aqueous phase and the participation of water in gas phase reactions led to minor theoretical energetic barriers and, therefore, promoting the formation of PCDD/Fs. Nevertheless, this is a preliminary assessment that should be broaden in order to understand and evidence the mechanisms involved in the formation of PCDD/Fs in aqueous phase from precursors such as 2-CP. The application of the solvation effect to all the possible pathways would be an essential tool to properly define the mechanisms for the formation of PCDD/Fs from precursors in aqueous streams.

4.3. Contribution to the scientific knowledge and open questions

In line with the comments given in Chapter 4, the mechanisms for the formation of PCDD/Fs are well described for gas phase, but studies for aqueous environments are lacking. In this sense, this chapter goes one step forward towards the study of the mechanisms involved in the reactions of chlorophenols.

- The theoretical results on the distribution of chlorinated phenols, based on DFT calculations and on the employment of Fukui indices and Hirshfeld electron distribution for electrophilic attack, concur with experimental measurements available in literature for water treatment and incineration of municipal waste.

- In the same way as in the previous point, the theoretical results based on Fukui indices for the electrophilic attack have been used for the first time for the proper description of the experimental products distribution obtained during the Fenton oxidation reactions of 2-CP by ·OH radical.

- The mechanistic pathways for the formation of PCDD/Fs in aqueous phase from 2-CP have been proposed based on the gas phase DFT theoretical results already published to optimize the molecular geometry and estimate the energetic barrier (E_a). In addition, this chapter includes a preliminary study of the influence that water has in the energy requirements during the generation of PCDD/Fs in both aqueous (solvation effect) and gas phase (reaction with H_2O).

Nevertheless, a deep theoretical assessment with regard to the formation of PCDD/Fs in aqueous phase should be done. An initial assessment may be carried out considering the reaction in gas phase but applying the solvent effect to all the stages to determine what reactions would be feasible in aqueous solution.

Finally, the use of computational chemistry tools will allow describing the reactions taking place in the reaction media, decreasing the number of experiments and, thus, reducing the risks associated to direct contact with the samples, the management of the toxic residues and the experimental economic costs.

References

1. Desmurs J, Ratton S. Chlorophenols. kirk-othmer encyclopedia of chemical technology. 4th Edition (1993).

2. Muller F, Caillard L. Chlorophenols. Ullmann's encyclopedia of industrial chemistry. Willey Online Library (1986).

3. Czaplicka M. Sources and transformations of chlorophenols in the natural environment. Sci. Total Environ. 322: 21-39 (2004).

4. Tame NW, Dlugogorski BZ, Kennedy EM. Formation of dioxins and furans during combustion of treated wood. Prog. Energy Combust. Sci. 33: 384-408 (2007).

5. Fernández-Castro P, San Román MF, Ortiz I. Theoretical and experimental formation of low chlorinated dibenzo-p-dioxins and dibenzofurans in the Fenton oxidation of chlorophenol solutions. Chemosphere 161: 136-144 (2016).

6. U.S. EPA. U.S. EPA 811-F-95-003C. National primary drinking water regulations: Contaminant specific fact sheets, synthetic organic chemicals. 1-62 (1995).

7. European Commission. Directive 2455/2001/EC of the european parliament and of the council of 20 november 2001 establishing the list of priority substances in the field of water policy and amending Directive 2000/60/EC. Official Journal 15: 1-5 (2001).

8. Stockholm convention clearing house: Http://chm.pops.int/Implementation/PublicAwareness/10thAnniversary/tabid/2231/Default.aspx (consulted 18/11/2016).

9. U.S. EPA. Appendix A to part 423 - 126 priority pollutants. Title 40 - protection of environment. chapter I - environmental protection agency (continued). subchapter N - effluent guidelines and standards. part 423 - steam electric power generating point source category. https://www.gpo.gov/fdsys/pkg/CFR-2014-title40-vol29/xml/CFR-2014-title40-vol29-part423-appA.xml (consulted 29/11/2016).

10. Ge F, Zhu L, Chen H. Effects of pH on the chlorination process of phenols in drinking water. J. Hazard. Mater. 133: 99-105 (2006).

11. Lee GF, Morris JC. Kinetics of chlorination of phenolchlorophenolic tastes and odors. Air Water Pollut. 6: 419-431 (1962).

12. Urtiaga A, Fernandez-Castro P, Gómez P, Ortiz I. Remediation of wastewaters containing tetrahydrofuran. study of the electrochemical mineralization on BDD electrodes. Chem. Eng. J. 239: 341-350 (2014).

13. Vallejo M, San Román MF, Ortiz I. Quantitative assessment of the formation of polychlorinated derivatives, PCDD/Fs, in the electrochemical oxidation of 2-chlorophenol as function of the electrolyte type. Environ. Sci. Technol. 47: 12400-12408 (2013).

14. Altarawneh M, Dlugogorski BZ, Kennedy EM, Mackie JC. Mechanisms for formation, chlorination, dechlorination and destruction of polychlorinated dibenzo-p-dioxins and dibenzofurans (PCDD/Fs). Prog. Energy Combust. Sci. 35: 245-274 (2009).

15. Addink R, Govers HA, Olie K. Isomer distributions of polychlorinated dibenzo-p-dioxins/dibenzofurans formed during de novo synthesis on incinerator fly ash. Environ. Sci. Technol. 32: 1888-1893 (1998).

16. Addink R, Antonioli M, Olie K, Govers HA. Reactions of dibenzofuran and 1, 2, 3, 4, 7, 8-hexachlorodibenzo-p-dioxin on municipal waste incinerator fly ash. Environ. Sci. Technol. 30: 833-836 (1996).

17. Wehrmeier A, Lenoir D, Schramm K, Zimmermann R, Hahn K, Henkelmann B, Kettrup A. Patterns of isomers of chlorinated dibenzo-p-dioxins as tool for elucidation of thermal formation mechanisms. Chemosphere 36: 2775-2801 (1998).

18. Altarawneh M, Dlugogorski BZ. Formation and chlorination of carbazole, phenoxazine, and phenazine. Environ. Sci. Technol. 49: 2215-2221 (2015).

19. Assaf NW, Altarawneh M, Oluwoye I, Radny M, Lomnicki SM, Dlugogorski BZ. Formation of environmentally persistent free radicals on α-Al_2O_3. Environ. Sci. Technol. 50: 11094-11102 (2016).

20. Hirshfeld FL. Bonded-atom fragments for describing molecular charge densities. Theoretical Chemistry Accounts: Theory, Computation, and Modeling. Theor. Chim. Acta 44: 129-138 (1977).

21. Fukui K. Role of frontier orbitals in chemical reactions. Science 218: 747-754 (1982).

22. Delley B. From molecules to solids with the DMol 3 approach. J. Chem. Phys. 113: 7756-7764 (2000).

23. Thanikaivelan P, Padmanabhan J, Subramanian V, Ramasami T. Chemical reactivity and selectivity using fukui functions: Basis set and population scheme dependence in the framework of B3LYP theory. Theor. Chem. Acc. 107: 326-335 (2002).

24. Mendoza Huizar LH, Rios-Reyes CH, Olvera-Maturano NJ, Robles J, Rodriguez JA. Chemical reactivity of quinclorac employing the HSAB local principle-fukui function. Open Chem. 13 (2015).

25. Barone V, Cossi M. Quantum calculation of molecular energies and energy gradients in solution by a conductor solvent model. J. Phys. Chem. A 102: 1995-2001 (1998).

26. Vallejo M, San Román MF, Ortiz I, Irabien A. Overview of the PCDD/Fs degradation potential and formation risk in the application of advanced oxidation processes (AOPs) to wastewater treatment. Chemosphere 118: 44-56 (2015).

27. Deborde M, von Gunten U. Reactions of chlorine with inorganic and organic compounds during water treatment-kinetics and mechanisms: A critical review. Water Res. 42: 13-51 (2008).

28. Horth H, Haley J, Sayth K, Williams DK. The production of chlorophenols during the chlorination of natural waters. http://www.dwi.gov.uk/research/completed-research/reports/dwi0030.pdf (consulted 19/11/2016).

29. Chen L, Campo P, Kupferle MJ. Identification of chlorinated oligomers formed during anodic oxidation of phenol in the presence of chloride. J. Hazard. Mater. 283: 574-581 (2015).

30. Peng Y, Chen J, Lu S, Huang J, Zhang M, Buekens A, Li X, Yan J. Chlorophenols in municipal solid waste incineration: A review. Chem. Eng. J. 292: 398-414 (2016).

31. Altarawneh M, Dlugogorski BZ, Kennedy EM, Mackie JC. Quantum chemical and kinetic study of formation of 2-chlorophenoxy radical from 2-chlorophenol: Unimolecular decomposition and bimolecular reactions with H, OH, cl, and O2. J. Phys. Chem. A 112: 3680-3692 (2008).

32. Lomnicki S, Truong H, Vejerano E, Dellinger B. Copper oxide-based model of persistent free radical formation on combustion-derived particulate matter. Environ. Sci. Technol. 42: 4982-4988 (2008).

33. Margallo M, Taddei MBM, Hernández-Pellón A, Aldaco R, Irabien Á. Environmental sustainability assessment of the management of municipal solid waste incineration residues: A review of the current situation. Clean Technol. Environ. Policy 17: 1333-1353 (2015).

34. Stanmore BR. The formation of dioxins in combustion systems. Combust. Flame 136: 398-427 (2004).

35. Zhou H, Meng A, Long Y, Li Q, Zhang Y. A review of dioxin-related substances during municipal solid waste incineration. Waste Manage. 36: 106-118 (2015).

36. Born JGP, Louw R, Mulder P. Fly ash mediated (oxy)chlorination of phenol and its role in PCDD/F formation. Chemosphere 26: 2087-2095 (1993).

37. Mosallanejad S, Dlugogorski BZ, Kennedy EM, Stockenhuber M, Lomnicki SM, Assaf NW, Altarawneh M. Formation of PCDD/Fs in oxidation of 2-chlorophenol on neat silica surface. Environ. Sci. Technol. 50: 1412-1418 (2016).

38. Tuppurainen K, Aatamila M, Ruokojärvi P, Halonen I, Ruuskanen J. Effect of liquid inhibitors on PCDD/F formation. Prediction of particle-phase PCDD/F concentrations using PLS modelling with gas-phase chlorophenol concentrations as independent variables. Chemosphere 38: 2205-2217 (1999).

39. Weber R, Hagenmaier H. PCDD/PCDF formation in fluidized bed incineration. Chemosphere 38: 2643-2654 (1999).

40. Huang C, Chu C. Indirect electrochemical oxidation of chlorophenols in dilute aqueous solutions. J. Environ. Eng. 138: 375-385 (2011).

41. Morrison RT, Boyd RN. Química orgânica. Pearson Educación, 5ª Edición, NY (1998).

42. Altarawneh M, Dlugogorski BZ, Kennedy EM, Mackie JC. Quantum chemical investigation of formation of polychlorodibenzo-p-dioxins and dibenzofurans from oxidation and pyrolysis of 2-chlorophenol. J. Phys. Chem. A 111: 2563-2573 (2007).

43. Pan W, Zhang D, Han Z, Zhan J, Liu C. New insight into the formation mechanism of PCDD/Fs from 2-chlorophenol precursor. Environ. Sci. Technol. 47: 8489-8498 (2013).

44. Altarawneh M, Dlugogorski BZ, Kennedy EM, Mackie JC. Theoretical study of reaction pathways of dibenzofuran and dibenzo-p-dioxin under reducing conditions. J. Phys. Chem. A 111: 7133-7140 (2007).

45. Altarawneh M, Dlugogorski BZ. Formation of dibenzofuran, dibenzo-p-dioxin and their hydroxylated derivatives from catechol. Phys. Chem. Chem. Phys. 17: 1822-1830 (2015).

46. Shi X, Zhang R, Zhang H, Xu F, Zhang Q, Wang W. Influence of water on the homogeneous gas-phase formation mechanism of polyhalogenated dioxins/furans from chlorinated/brominated phenols as precursors. Chemosphere 137: 142-148 (2015).

47. Shi X, Yu W, Xu F, Zhang Q, Hu J, Wang W. PBCDD/F formation from radical/radical cross-condensation of 2-chlorophenoxy with 2-bromophenoxy, 2, 4-dichlorophenoxy with 2, 4-dibromophenoxy, and 2, 4, 6-trichlorophenoxy with 2, 4, 6-tribromophenoxy. J. Hazard. Mater. 295: 104-111 (2015).

48. Zhang Q, Li S, Qu X, Shi X, Wang W. A quantum mechanical study on the formation of PCDD/Fs from 2-chlorophenol as precursor. Environ. Sci. Technol. 42: 7301-7308 (2008).

49. Zhang Q, Yu W, Zhang R, Zhou Q, Gao R, Wang W. Quantum chemical and kinetic study on dioxin formation from the 2, 4, 6-TCP and 2, 4-DCP precursors. Environ. Sci. Technol. 44: 3395-3403 (2010).

50. Zhang Y, Zhang D, Gao J, Zhan J, Liu C. New understanding of the formation of PCDD/Fs from chlorophenol precursors: A mechanistic and kinetic study. J. Phys. Chem. A 118: 449-456 (2014).

51. Mayo FR. Comparison of liquid-phase and gas-phase reactions of free radicals. J. Am. Chem. Soc. 89: 2654-2661 (1967).

52. Orozco M, Luque FJ. Theoretical methods for the description of the solvent effect in biomolecular systems. Chem. Rev. 100: 4187-4226 (2000).

53. Tachikawa H, Lunell S, Törnkvist C, Lund A. Theoretical study on solvation effects in chemical reactions: A vibrational coupling model. Int. J. Quant. Chem. 43: 449-461 (1992).

54. Evans CS, Dellinger B. Mechanisms of dioxin formation from the high-temperature oxidation of 2-chlorophenol. Environ. Sci. Technol. 39: 122-127 (2005).

55. Sidhu S, Edwards P. Role of phenoxy radicals in PCDD/F formation. Int. J. Chem. Kinet. 34: 531-541 (2002).

56. Briois C, Ryan S, Tabor D, Touati A, Gullett BK. Formation of polychlorinated dibenzo-p-dioxins and dibenzofurans from a mixture of chlorophenols over fly ash: Influence of water vapor. Environ. Sci. Technol. 41: 850-856 (2007).

57. Anglada A, Urtiaga A, Ortiz I. Contributions of electrochemical oxidation to waste-water treatment: Fundamentals and review of applications. J. Chem. Technolo. Biotechnol. 84: 1747-1755 (2009).

58. Buxton GV, Greenstock CL, Helman WP, Ross AB. Critical review of rate constants for reactions of hydrated electrons, hydrogen atoms and hydroxyl radicals (·OH/·O^-) in aqueous solution. J. Phys. Chem. Ref. Data 17: 513-886 (1988).

59. Briois C, Ryan S, Tabor D, Touati A, Gullett BK. Formation of polychlorinated dibenzo-p-dioxins and dibenzofurans from a mixture of chlorophenols over fly ash: Influence of water vapor. Environ. Sci. Technol. 41: 850-856 (2007).

60. Xu F, Yu W, Zhou Q, Gao R, Sun X, Zhang Q, Wang W. Mechanism and direct kinetic study of the polychlorinated dibenzo-p-dioxin and dibenzofuran formations from the radical/radical cross-condensation of 2,4-dichlorophenoxy with 2-chlorophenoxy and 2,4,6-trichlorophenoxy. Environ. Sci. Technol. 45: 643-650 (2011).

61. Ryu J, Mulholland JA. Dioxin and furan formation on $CuCl_2$ from chlorinated phenols with one ortho chlorine. Proc. Combust. Inst. 29: 2455-2461 (2002).

62. Ryu J, Mulholland JA, Takeuchi M, Kim D, Hatanaka T. $CuCl_2$-catalyzed PCDD/F formation and congener patterns from phenols. Chemosphere 61: 1312-1326 (2005).

63. Evans CS, Dellinger B. Mechanisms of dioxin formation from the high-temperature pyrolysis of 2-bromophenol. Environ. Sci. Technol. 37: 5574-5580 (2003).

64. Bruce KR, Beach LO, Gullett BK. The role of gas-phase Cl_2 in the formation of PCDD/PCDF during waste combustion. Waste Manage. 11: 97-102 (1991).

65. Dimmel DR, Riggs KB, Pitts G, White J, Lucas S. Formation mechanisms of polychlorinated dibenzo-p-dioxins and dibenzofurans during pulp chlorination. Environ. Sci. Technol. 27: 2553-2558 (1993).

66. Eiceman G, Rghei H. Chlorination reactions of 1, 2, 3, 4-tetrachlorodibenzo-p-dioxin on fly ash with HC1 in air. Chemosphere 11: 833-839 (1982).

67. Rghei H, Eiceman G. Adsorption and chlorination of dibenzo-p-dioxin and 1-chlorodibenzo-p-dioxin on fly ash from municipal incinerators. Chemosphere 13: 421-426 (1984).

68. Rghei H, Eiceman G. Reactions of 1, 2, 3, 4-TCDD on fly ash in mixed gases of H_2O, NO_2, HCl, and SO_X in air. Chemosphere 14: 259-265 (1985).

69. Ryu J, Mulholland JA, Chu B. Chlorination of dibenzofuran and dibenzo-p-dioxin vapor by copper (II) chloride. Chemosphere 51: 1031-1039 (2003).

70. Visez N, Sawerysyn J. Chlorination and thermal degradation of 2-chlorodibenzodioxin and dibenzofuran by CuCl 2 or CuCl at 350° C. Chemosphere 73: S90-93 (2008).

71. Wang X, Zhang H, Ni Y, Du Q, Zhang X, Chen J. Kinetics of PCDD/Fs formation from non-wood pulp bleaching with chlorine. Environ. Sci. Technol. 48: 4361-4367 (2014).

72. Wikström E, Marklund S. Secondary formation of chlorinated dibenzo-p-dioxins, dibenzofurans, biphenyls, benzenes, and phenols during MSW combustion. Environ. Sci. Technol. 34: 604-609 (2000).

Chapter 5

Conclusions and Challenges for future research

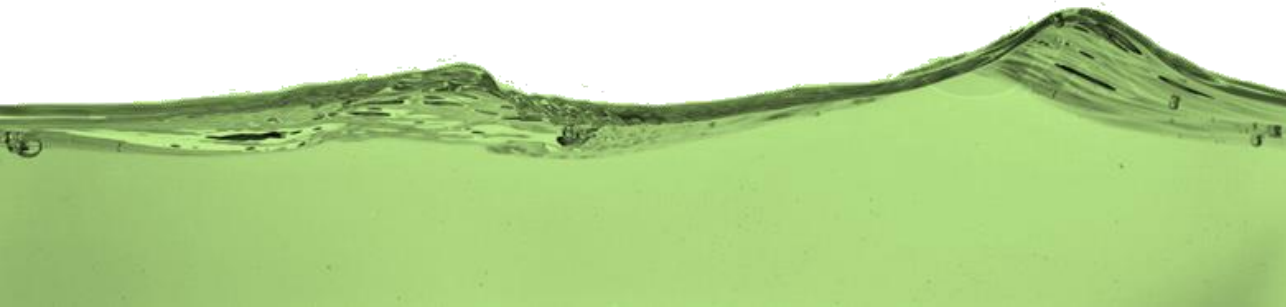

Chapter 5

Conclusions and Challenges for future research

Abstract

This thesis aims to make progress on the study of the reactivity of advanced oxidation media by monitoring the generation of reactive oxygen species, paying special attention to the generation of unwanted toxic products such as PCDD/Fs during the Fenton treatment of 2-chlorophenol and deepening in the mechanisms by means of computational chemistry. This chapter summarizes the main results that have been achieved, draws the conclusions derived from the analysis of the results and highlights future challenges not only related to the highly reactive oxygen species, but also those that should be faced in order to deepen on the mechanisms involved in the generation of PCDD/Fs and the ways to to prevent their formation.

5.1 Conclusions

This thesis is focused on the assessment of PCDD/Fs formation during the application of advanced oxidation processes (AOPs, Fenton) to pollutants that act as precursors of these toxic and persistent byproducts, taking 2-chlorophenol as model contaminant. Because these processes are based on the generation of ROS of short life time, a thorough study about the methods described in literature to measure their concentration has been carried out, revealing in many cases the difficulty to properly quantify the concentration. Variables such as probe choice, probe content and analytical technique are related to the expected ROS concentration and, as a result, depend on the AOP selected.

Two different molecular probes (DMSO and DMPO) were selected to evaluate the generation of hydroxyl radical as well as other radicals of both inorganic and organic nature. With regard to the employment of DMSO to quantify ·OH, it was observed that its use is not feasible during the application of Fenton oxidation as it probably inhibits the reaction between iron and hydrogen peroxide as the yield of the maximum potential concentration displayed (0.26-0.79%). When DMSO was used during the electrochemical oxidation with BDD electrodes (Annex VI), competitive reactions occurred between DMSO and formaldehyde in their reaction with ·OH, resulting in a misinterpretation of the hydroxyl radical concentration. Therefore, DMSO is not an advisable probe in during the Fenton oxidation although it could be an attractive probe limited to the qualitative study of the generation of hydroxyl radicals during the application of electrochemical treatments.

The use of DMPO as molecular probe is well known especially in biological samples. Besides, it is an interesting reagent for its use during the application of advanced oxidation processes as it is capable of reacting with different radical species leading to different radicals that, afterwards, can be differentiated by EPR spectroscopy. DMPO was useful to identify hydroxyl (·OH) and hydroperoxyl (HO_2·) radicals, allowing their quantification. Nevertheless, high generation of radical species may cause the degradation of the adduct DMPO-·OH resulting in the

generation of other species such as DMPO-·DMPO or DMPO-·CH_2OH/·CH_2CH_2OH and, consequently, in an underestimation of the total concentration of ·OH. The selection of adequate initial concentration of DMPO, depending on the oxidation conditions ([DMPO]/[H_2O_2]= 25, in this work), enable this method to be a good tool to assess the formation of radical species, taking advantage of the high sensitivity of the EPR methodology. EPR spectroscopy has demonstrated to be a suitable and sensitive technique in the identification of radical species even in the absence of molecular probe, as semiquinone-type radicals were detected.

One of the handicaps of the employment of DMPO as molecular probe is that after its reaction with ROS (e.g. ·OH), it leads to the formation of other radical species that are not stable (e.g. DMPO-·OH) in spite of having half-life time longer than the corresponding to ·OH. With this regard, the coupling of the EPR resonator with the reaction system may facilitate instantaneous analysis in real time. Stopped-flow reactor has shown that it is a good option to analyze the radical species generated at initial times. In this sense, proper cell size should be selected to ensure enough concentration of the radical species above the limit of detection.

With regard to the application of Fenton oxidation to a known PCDD/Fs precursor, 2-chlorophenol, it has been observed that it is capable of completely degrading 15.56 mM 2-CP even with substoichiometric H_2O_2 doses needed for the complete mineralization (95% of 2-CP removal using only 20% of the stoichiometric dose, 40.44 mM). In general terms, no influence was detected when chloride ions (0-56.35 mM), iron dose (0.09-2.88 mM) and copper dose (0-0.787 mM) were added to the aqueous media regarding the concentration profiles of 2-CP (95% reduction), COD (20% reduction) or TOC (5% mineralization) more than higher rates increasing the concentration of Fe(II). On the other hand, higher reaction rates for H_2O_2 were observed when 2-CP was present in the solution compared to a control medium (only adding Fe(II) and H_2O_2). This has been commonly related to the formation of semiquinone radicals that react with Fe(III). Precisely, the reduction from Fe(III) to Fe(II) is the slowest step, so semiquinone-type radicals enhance the efficacy of the Fenton reaction.

It was found that the use of substoichiometric hydrogen peroxide dose resulted in low mineralization degree and, consequently, the formation of a wide variety of oxidation products that make difficult their complete identification. Compounds such as 2-chlorobenzoquinone (2-CBQ), 3-chlorocatechol (3-CC), catechol, oxalic and formic acids were detected but there was still a 55% of TOC unidentified. Commonly, the reactions taking place in the aqueous medium lead to oxidized byproducts that tend to be smaller in size as a consequence of the ring opening and chain cleavage. Nevertheless, products from the condensation of aromatics have been identified. Some of them are of special relevance as it is the case of PCDD/Fs.

PCDD/Fs are mainly formed at the initial stages of the oxidation reaction (65.4 pg Te-OCDD/Fs L^{-1} at 1 h of Fenton oxidation and 19.1 pg Te-OCDD/Fs L^{-1} at 4 h, using 100% H_2O_2 dose) and their concentration can be diminished with additional hydrogen peroxide doses (down to 95% when the H_2O_2 dose was increased from 20% to 100%). Under substoichiometric H_2O_2 concentration, the presence of chloride in the medium is really important as higher concentrations of tetra- to octa-CDD/Fs were quantified at high chloride concentrations, 3795.1 pg L^{-1} *vs* 1013.4 pg L^{-1} when no chloride was added. This fact supports also the pathway leading to free chlorine species based on the Cl^- potential to act as scavenger of ·OH.

For the first time, the concentration distribution of non-chlorinated and low chlorinated CDD/Fs has been reported during the application of AOPs. The assessment of the influence of iron concentration in the final concentration of PCDD/Fs when working with substoichiometric Fenton, did not allow extracting a clear conclusion about the influence of this operational variable due to the significant errors between different replicates, $2.2 \cdot 10^6 \pm 0.6 \cdot 10^6$ pg L^{-1}. However, it is clear that maximum concentrations were reached for DCDD (an average of $9.0 \cdot 10^5$ pg L^{-1} *vs* ∑PCDD= $1.1 \cdot 10^6$ pg L^{-1}) and DCDF (an average of $9.3 \cdot 10^5$ pg L^{-1} *vs* ∑PCDF= $9.4 \cdot 10^5$ pg L^{-1}), which act as precursors of PCDD/Fs of higher chlorination degree, as there is a decreasing trend in the concentration profile of PCDD/Fs as the chlorination degree augments, from DCDD/Fs to OCDD/Fs. On the other hand, the addition of copper salt did not seem to have special relevance under the

experimental conditions employed during the development of this thesis (at least considering the error bars) although copper is usually related to a higher formation of PCDD/Fs during high temperature gas phase reactions. Anyway, the total concentration of the most toxic congeners (2,3,7,8-PCDD/Fs) during the Fenton oxidation of 2-CP resulted in TEQ< 2 pg L^{-1}, lower than 30 pg L^{-1} t is the maximum contaminant level stablished by the US-EPA.

Regarding the mechanistic studies developed in this thesis, the employment of the $DMol^3$ calculations (software Materials Studio) have enabled to predict the chlorination pattern of phenol in aqueous (2-CP→ 4-CP→ 2,4-diCP→ 2,4,6-triCP→ 2,3,4,6-tetraCP→ pentaCP) and gas phase (2-CP→ 4-CP→ 2,4-diCP→ 2,4,6- and 2,4,5-triCP→ 2,3,4,6-tetraCP→ pentaCP) based on Fukui indices and Hirshfeld charge for the electrophilic substitution. These results successfully fitted with those already published in literature for both phases. On the other hand, taking advantage of this tool, the theoretical calculations for the electrophilic substitution of 2-CP by ·OH were in agreement with the oxidation byproducts identified during the Fenton oxidation reactions of 2-chlorophenol: 2-CBQ, 3-CC and catechol.

Finally, for the first time a mechanistic proposal for the formation of PCDD/Fs from 2-CP in aqueous phase has been proposed taking into account the available information in bibliography for gas phase. The theoretical results already published in bibliography support the distribution in the concentrations of the different homologues groups experimentally obtained in this thesis. Furthermore, additional calculations in certain stages that were found to be highly energetic according to bibliography, were carried out by means of the software Materials Studio ($DMol^3$) and Gaussian taking into account the solvation effect or the interaction of the water molecule during gas phase reactions, revealing the importance of water in the medium, which is capable of decreasing the activation energy of the reactions that lead to the formation of PCDD/Fs down to 77.2% and 81.8%, respectively.

5.2 Challenges for future research

This thesis intended to gain knowledge on the role of oxidizing species during the application of AOPs for the treatment of recalcitrant pollutants as well as on the assessment of PCDD/Fs during this type of treatments. In this sense, although there is a large number of references related to the evaluation of the suitability of AOPs and the optimization of their efficacy, little is known about the generation of unwanted byproducts characterized by high toxicity or even carcinogenic character, as it occurs during the advanced oxidation treatment of chlorophenolic compounds.

One of the main challenges with regard to the analysis of reactive oxygen species is associated to the molecular probes. The design, development and/or use of new probes will overcome the limitations of the current ones in terms of selectivity, stability, etc.; namely, gather the appropriate features to approach the ideal probe. Another fundamental aspect is the relevance of the operational conditions, in which there must be a minimum in the concentration to ensure the total capture of the generated radicals. On the other hand, all these issues could be resolve by means of an appropriate method that allows direct analysis of the solutions under study, but it is not easy from the point of view of the short life time of the radical species. Additionally, screening under real conditions could be obtained by improving the connection between the reaction system and the analytical equipment; working with enough volume of the sample will enable to overcome the restrictions associated to the limit of detection.

One issue of increasing concern is the growth in the number of contaminants as a consequence of the development of new materials and new compounds with wide use in chemical and pharmaceutical industry, many of which are considered toxic, non-biodegradable and persistent. Conventional physico-chemical and biological treatments are not powerful enough to degrade this type of compounds, so alternative technologies such as AOPs have been developed to deal with their difficult treatment. However, although in many cases AOPs find a commercial application, further improvements in their performance and cost must be done. In

this sense, it has been observed throughout this thesis document that incomplete treatment of contaminated streams may lead to the formation of pollutants even more dangerous than the original ones. Therefore, advanced technologies will have to assure a proper treatment so that they do not pose a serious issue for the environment and health.

Taking into account the aforementioned paragraphs, the analysis of radicals, both inorganic radical species (ROS) and organic radicals, may help to clarify the mechanisms involved in the generation of other pollutants during the treatment of aqueous solutions as well as to prevent their generation. That is why more studies in aqueous phase with this regard should be done. Besides, the development of chemical computation software has provided a really useful tool to foresee what can happen in a reaction system. Up to date most of the computational studies have been focused on gas phase reactions whereas liquid systems have been ignored. Hence, the application of computational tools may be a powerful methodology to predict what can happen in the reaction system.

Finally, in the particular case of PCDD/Fs, most of the studies (especially in aqueous phase) have been focused on the formation of dioxins and furans of high chlorination degree and, specifically, those with chlorine atoms at least in the positions 2,3,7,8. However, more attention should be paid to DDs and DFs that in a medium containing chlorine/chloride may act as precursors of the most toxic PCDD/Fs congeners. In addition, the results presented in aqueous phase up to date should be complemented with additional studies such as i) the assessment of the effect that solid surfaces may have during the oxidation treatment (for instance if the reactor wall contributes and catalyzes PCDD/Fs formation over its surface), ii) study of the effect of having several CPs of different chlorination degree on the final PCDD/Fs distribution.

5.3 Conclusiones

Esta tesis se centra en la evaluación de la formación de PCDD/Fs durante la aplicación de procesos de oxidación avanzada (POAs, Fenton) a contaminantes que actúan como precursores de estos subproductos tóxicos y persistentes, tomando como contaminante modelo el 2-clorofenol. Debido a que estos procesos están basados en la generación de especies reactivas de oxígeno caracterizadas por cortos tiempos de vida, se realizó un profundo estudio acerca de las metodologías descritas en la bibliografía para medir su concentración. La selección del sensor molecular, su concentración y la técnica analítica a emplear dependerán de la concentración esperada de ROS y, por tanto, del POA seleccionado.

Se escogieron dos sensores moleculares diferentes (DMSO y DMPO) con el objetivo de evaluar la generación de radicales tanto de naturaleza inorgánica (como son los radicales hidroxilo) como orgánica. Con respecto al empleo de DMSO en la cuantificación de ·OH, se observó que su uso no es factible durante la aplicación de oxidación Fenton ya que probablemente el DMSO o sus productos de oxidación inhiben la reacción entre el hierro y el peróxido de hidrógeno tal y como mostró el bajo rendimiento en la concentración potencial máxima (0.26-0.79%). Cuando se utilizó DMSO durante el proceso de oxidación electroquímica con electrodos de BDD (Anexo VI), hay competencia entre las reacciones de DMSO y formaldehído con los radicales ·OH, dando lugar a malinterpretaciones en la concentración de ·OH generado. Por lo tanto, el uso de DMSO como sensor molecular no es aconsejable durante la oxidación Fenton y se debe limitar a estudios cualitativos en el caso de la generación de radicales hidroxilo durante el tratamiento electroquímico.

Por otro lado, es conocido el empleo de DMPO como sensor molecular durante el análisis de especies radicalarias en medios biológicos. Además, es un reactivo que resulta interesante durante la aplicación de procesos de oxidación avanzada ya que es capaz de reaccionar con diferentes especies radicalarias dando lugar a la generación de radicales más estables que conllevan un mayor tiempo de vida y que pueden ser diferenciados por medio de espectroscopia EPR. El uso de DMPO

permitió la identificación de radicales hidróxido (·OH) e hidroperóxido (HO_2·), e incluso su cuantificación. Sin embargo, tal y como ocurre con el DMSO, la alta generación de especies radicalarias puede causar la degradación del aducto DMPO-·OH en otras especies como son las especies radicalarias DMPO-·DMPO o DMPO-·CH_2OH/·CH_2CH_2OH y, en consecuencia, resultar en la infraestimación de la concentración total de ·OH. La selección de concentraciones iniciales de DMPO apropiadas en función de las condiciones de oxidación ([DMPO]/[H_2O_2]= 25, en este trabajo) permite el uso de este método como una buena herramienta en la evaluación de la formación de radicales, aprovechándose de la alta sensibilidad de la espectroscopia EPR. Esta técnica, ha demostrado ser adecuada y sensible a la identificación de especies radicalarias incluso en ausencia de sensor molecular, tal y como mostró la detección de radicales de tipo semiquinona.

Uno de los puntos débiles del uso de DMPO como sensor molecular es que tras reaccionar con los radicales (p. ej. ·OH), da lugar a la formación de otras especies radicalarias (p. ej. DMPO-·OH) que no son estables a pesar de tener mayor tiempo de vida con respecto a ·OH. Por ello, el acoplamiento del sistema de reacción con el resonador del espectrómetro EPR puede facilitar el análisis instantáneo a tiempo real. El uso del "stopped-flow reactor" es una buena opción para analizar las especies radicalarias generadas a tiempos iniciales. En este sentido, es por ello que la selección un tamaño de celda apropiado para asegurar concentraciones de las especies radicalarias por encima del límite de detección es determinante.

Respecto a los resultados correspondientes a la oxidación Fenton de 2-clorofenol, conocido por ser precursor de PCDD/Fs, se observó la capacidad de este proceso para degradar completamente 15.56 mM 2-CP incluso en dosis inferiores a la necesaria para mineralizarlo completamente (95% de eliminación de 2-CP utilizando tan solo un 20% de la dosis estequiométrica, 40.44 mM). En términos generales, no se vio influencia en los perfiles de concentración de 2-CP (reducción del 95%), DQO (disminución del 20%) y COT (mineralización del 5%) cuando se añadió al medio acuoso cloruro (0-56.35 mM), diferentes dosis de hierro (0.09-2.88 mM) y de cobre (0-0.787 mM); únicamente se observaron mayores velocidades de

degradación incrementando la concentración de Fe(II). Por otro lado, se observaron mayores velocidades de reacción de H_2O_2 en presencia de 2-CP en disolución comparado con el medio de control (añadiendo solamente Fe(II) y H_2O_2), lo cual se relaciona con la formación de radicales semiquinona que reaccionan con el Fe(III). Precisamente, la etapa de reducción de Fe(III) a Fe(II) es la más lenta, de tal manera que estos radicales mejoran la eficacia de las reacciones Fenton.

El empleo de dosis subestequiométricas de peróxido de hidrógeno resultó en menor grado de mineralización y, consecuentemente, en la formación de una gran variedad de productos de oxidación que dificultan su completa identificación. Se detectaron compuestos como son la 2-clorobenzoquinona (2-CBQ), el 3-clorocatecol (3-CC), el catecol y los ácidos oxálico y fórmico aunque tras el agotamiento del H_2O_2 quedaba un 55% del COT sin identificar. Normalmente, las reacciones que tienen lugar en el medio acuoso conducen a subproductos de oxidación que tienden a ser de menor tamaño como consecuencia de la apertura del anillo y la ruptura de la cadena. Sin embargo, se han identificado productos de la condensación de los compuestos aromáticos, algunos de los cuales son de especial relevancia como es el caso de las PCDD/Fs.

Las PCDD/Fs se forman principalmente en las etapas iniciales de oxidación (65.4 pg Te-OCDD/Fs L^{-1} tras 1 h de oxidación Fenton y 19.1 pg Te-OCDD/Fs L^{-1} tras 4 h, utilizando el 100% de la dosis de H_2O_2) y su concentración se puede disminuir añadiendo dosis adicionales de H_2O_2 (hasta un 95% de reducción incrementando la dosis de H_2O_2 desde el 20 al 100%). En condiciones subestequiométricas de H_2O_2, la presencia de cloro en el medio es verdaderamente importante ya que se cuantificaron mayores concentraciones de tetra- a octa-DD/Fs, pasando de 1013.4 pg L^{-1} a 3795.1 pg L^{-1} al añadir cloruro en el medio acuoso. Este hecho apoya la premisa de que se están generando especies de cloro activo a partir de la reacción del ion Cl^- con el radical hidroxilo.

Por primera vez, se ha reportado la distribución de concentraciones de CDD/Fs no clorados y de bajo grado de cloración durante la aplicación de POAs. La

evaluación de la influencia de la concentración de hierro en la concentración final de PCDD/Fs trabajando en condiciones subestequiométricas no ha permitido extraer conclusiones claras en relación a su efecto ya que todas las concentraciones se encuentran dentro de los márgenes de error entre diferentes réplicas, $2.2\cdot10^6\pm0.6\cdot10^6$ pg L^{-1}. Sin embargo, se puede observar claramente que las concentraciones máximas se obtuvieron para DCDD (una concentración media de $9.0\cdot10^5$ pg L^{-1} frente a ∑PCDD= $1.1\cdot10^6$ pg L^{-1}) y DCDF (una media de $9.3\cdot10^5$ pg L^{-1} frente a ∑PCDF= $9.4\cdot10^5$ pg L^{-1}), que actúan como precursores de PCDD/Fs de mayor grado de cloración, tal y como muestra la tendencia a la baja en las concentraciones de PCDD/Fs conforme el grado de cloración aumenta desde DCDD/Fs hasta OCDD/Fs. Por otro lado, bajo las condiciones experimentales utilizadas en esta tesis, la adición de sal de cobre no tuvo especial importancia en la distribución de PCDD/Fs a pesar de estar íntimamente relacionada con la formación de PCDD/Fs durante los procesos en fase gas que involucran altas temperaturas. En cualquier caso, las concentraciones de los congéneres más tóxicos (2,3,7,8-PCDD/Fs) durante la oxidación Fenton de 2-CP se mantuvieron en valores de toxicidad equivalente TEQ< 2 pg L^{-1}, que está por debajo de los 30 pg L^{-1} marcados como valor máximo de contaminante por la US-EPA.

En relación a los estudios mecanísticos desarrollados en esta tesis, el uso de cálculos computacionales en el entorno de DMol^3 (*software "Materials Studio"*) basados en el índice de Fukui y la carga Hirshfled de sustitución electrofílica han permitido predecir el patrón de cloración de la molécula de fenol en fase acuosa (2-CP→ 4-CP→ 2,4-diCP→ 2,4,6-triCP→ 2,3,4,6-tetraCP→ pentaCP) y en fase gas (2-CP→ 4-CP→ 2,4-diCP→ 2,4,6- and 2,4,5-triCP→ 2,3,4,6-tetraCP→ pentaCP). Estos resultados se ajustan satisfactoriamente a aquellos resultados experimentales publicados en la literatura para ambas fases. Por otro lado, aprovechando el empleo de esta herramienta, se realizaron cálculos teóricos para la sustitución electrofílica de 2-CP mediante ·OH, mostrando concordancia con los subproductos identificados durante la oxidación Fenton de 2-clorofenol: 2-CBQ, 3-CC y catecol.

Finalmente, por primera vez se ha propuesto mecanísticamente la formación de PCDD/Fs partiendo de 2-CP, teniendo en cuenta la información disponible en la bibliografía para fase gas. Dichos resultados teóricos apoyan la distribución en las concentraciones de los diferentes grupos de homólogos obtenidos experimentalmente. Además, en el desarrollo de esta tesis se realizaron cálculos adicionales en ciertas etapas de la formación de PCDD/Fs, caracterizadas por elevados requerimientos energéticos de acuerdo a la biliografía, utilizando "*Gaussian*" y considerando el efecto de solvatación y la interacción de la molécula de agua durante las reacciones en fase gas, los cuales revelaron la capacidad del agua para disminuir las energías de activación de las reacciones que participan en la formación de PCDD/Fs, reduciendo un 77.2% y un 81.8% las energías de activación, respectivamente.

5.4 Desafíos futuros

Esta tesis ha tenido como principales objetivos aumentar el conocimiento en relación i) al papel que tienen las especies oxidantes durante la aplicación de POAs para el tratamiento de contaminantes recalcitrantes, e ii) a la evaluación de la generación de PCDD/Fs durante este tipo de tratamientos así como los mecanismos de formación. En este sentido, aunque hay un gran número de referencias relacionadas con la evaluación de la idoneidad de los POAs y la optimización de su eficacia, apenas hay conocimiento acerca de la generación de subproductos no deseados caracterizados por alta toxicidad o incluso carácter carcinogénico, tal y como ocurre durante la aplicación de POAs a compuestos clorofenólicos.

Uno de los principales desafíos en relación al análisis de especies reactivas de oxígeno está asociado a los sensores moleculares. El diseño, desarrollo y/o uso de nuevos sensores permitirá superar las limitaciones de los actualmente existentes en términos de selectividad, estabilidad, etc.; esto es, reunir las características apropiadas para aproximarse a la definición de sensor molecular ideal. Otro aspecto fundamental es la importancia de las condiciones de operación, en las que se debe suministrar una concentración suficiente del sensor para asegurar la total captura

de los radicales generados. Es importante tener en cuenta que todas estas cuestiones podrían ser resueltas a través de una metodología de análisis que permita analizar de forma directa las disoluciones bajo estudio, lo cual no es sencillo desde el punto de vista del corto tiempo de vida de los radicales. Por otra parte, el análisis en condiciones reales podría realizarse mejorando la conexión entre el sistema de reacción y el equipo analítico, garantizando una cantidad de muestra suficiente que permita superar las restricciones en términos de límites de detección.

Una cuestión que preocupa de manera creciente es el aumento del número de contaminantes como consecuencia del desarrollo de nuevos materiales y nuevos compuestos de amplio uso en la industria química y farmacéutica, muchos de los cuales se consideran tóxicos, no biodegradables y persistentes. Los tratamientos físico-químicos y biológicos convencionales no son suficientemente poderosos para degradar este tipo de compuestos, por lo que se han desarrollado tratamientos alternativos como son los POAs para afrontar su tedioso tratamiento. Sin embargo, a pesar de que los POAs encuentran aplicación comercial, se debe mejorar la eficacia en los resultados y el coste de los mismos. Durante el desarrollo de esta tesis doctoral se observó que el tratamiento incompleto de las corrientes contaminadas puede dar lugar a la generación de contaminantes incluso más peligrosos que los originales. Por lo tanto, los POAs tendrán que garantizar el tratamiento apropiado de manera que no comprometan la salud y el medioambiente.

Teniendo en cuenta toda la información previamente mencionada, el análisis de radicales (tanto inorgánicos como orgánicos) puede ayudar a vislumbrar los mecanismos involucrados en la generación de otras especies contaminantes durante el tratamiento de disoluciones acuosas, así como prevenir su formación. Esta es la razón por la que se deberían llevar a cabo más estudios en fase acuosa. Además, el desarrollo de *software* de química computacional ha supuesto una herramienta verdaderamente útil para prever qué puede ocurrir en los sistemas de reacción. Hasta la fecha, la mayoría de los estudios computacionales se han centrado en reacciones en fase gas mientras que los sistemas líquidos han sido ignorados. De

esta manera, la aplicación de herramientas computacionales puede ser una herramienta poderosa para predecir qué sucede en estos sistemas reactivos.

Finalmente, en el caso particular de PCDD/Fs, la mayoría de los estudios (especialmente en fase acuosa) se han focalizado en la formación de dioxinas y furanos de alto grado de cloración y, específicamente, aquellos con cloro en las posiciones 2,3,7,8. Sin embargo, se debería prestar mayor atención a las dioxinas y furanos que en un medio conteniendo cloro/cloruro pueden actuar como precursores de los PCDD/Fs más tóxicos. Además, los resultados presentados en fase acuosa hasta la fecha se deberían complementar con estudios adicionales como son i) la evaluación del efecto que tienen las superficies sólidas durante el tratamiento de oxidación (por ejemplo si la pared del reactor contribuye y cataliza la formación de PCDD/Fs), ii) el estudio del efecto de tener una mezcla de clorofenoles con diferente grado de cloración en la distribución final de PCDD/Fs.

Annexes

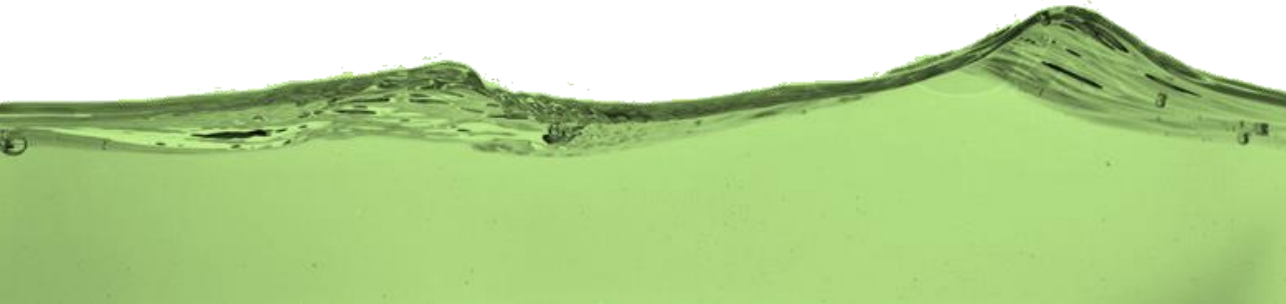

Annexes

Annex I- Nomenclature

AOPs	advanced oxidation processes
ATR	attenuated total reflection
BDD	boron doped diamond
BDPA	bis Diphenyl Allyl-Benzene Complex
BLYP	Becke-Lee-Yang-Parr correlation functional
Cα-k	chlorinated α-ketocarbene
COD	chemical oxygen demand
DLaTGS	deuterated L-alanine doped triglycine sulfate
DFT	density functional theory
DMPO	5,5-Dimethyl-1-pyrroline N-oxide
DMSO	dimethyl sulfoxide
DND	double numerical plus *d*-functions
DNPH	2,4-dinitrophenylhidrazine
EC	European Commission
EEC	European Economic Community
EPA	Environmental Protection Agency
EPR	electroparamagnetic resonance spectroscopy
EQS	environmental quality standards
FTIR	Fourier transform infrared spectroscopy
GC-MS	gas chromatography with mass spectrometry
GGA	generalized gradient approximation
$HO_2^{\bullet}$	hydroperoxyl radical
HPLC	high performance liquid chromatography
HRGC-HRMS	high resolution gas chromatography with high resolution mass spectrometry
IC	inorganic carbon

Annex I- Nomenclature (Continuation)

j	current density
LCS	labelled compound stock solution
MAC	maximum admissible concentration
MCT	mercury cadmium telluride
$^1O_2$	singlet oxygen
$O_2^{-\bullet}$	superoxide radical
·OH	hydroxyl radical
PAH	polycyclic aromatic hydrocarbons
PCB	polychlorinated biphenyl
PCDD	polychlorinated dibenzo-*p*- dioxin
PCDF	polychlorinated dibenzofuran
PDA	photodiode array
Ph	Phenyl radical
Phxy	Phenoxy radical
POP	persistent organic pollutant
PW91	Perdew and Wang's 1991 gradient-corrected correlation functional
TC	total carbon
TEF	toxic equivalency factor
TEQ	toxic equivalent
TOC	total organic carbon
ROS	reactive oxygen species
RSD	relative standard deviation
UP	ultrapure
WHO	World Health Organization

Annex II- Specific Nomenclature for PCDD/Fs

DD	dibenzo-*p*-dioxin
MCDD	monochlorodibenzo-*p*- dioxin
DCDD	dichlorodibenzo-*p*- dioxin
triCDD	trichlorodibenzo-*p*- dioxin
TCDD	tetrachlorodibenzo-*p*- dioxin
PeCDD	pentachlorodibenzo-*p*- dioxin
HxCDD	hexachlorodibenzo-*p*- dioxin
HpCDD	heptachlorodibenzo-*p*- dioxin
OCDD	octachlorodibenzo-*p*- dioxin

DF	dibenzofuran
MCDF	monochlorodibenzofuran
DCDF	dichlorodibenzofuran
triCDF	trichlorodibenzofuran
TCDF	tetrachlorodibenzofuran
PeCDF	pentachlorodibenzofuran
HxCDF	hexachlorodibenzofuran
HpCDF	heptachlorodibenzofuran
OCDF	octachlorodibenzofuran

Annex III- General features of the probes employed in the determination of radical ·OH, $O_2^{-\bullet}/HO_2^{\bullet}$ and $^1O_2$

Table III.1. Main features of the probes used in the determination of ·OH.

Probe	AOPs	Analytical features	Strengths	Limitations	Ref.
BA: 0.1-10 mM	Fenton Electro-Fenton Photolysis	Analysis of o-, m- and p-HBA. HPLC with PDA or UV detector, fluoresecence detection or UV/vis spectrophotometry. Fluorescence detection: o-HBA, pH: 4.9; m- and p-HBA pH>11 [·OH]: 0.012- 0.9 mM	Selectivity towards ·OH Repeatability and accuracy in the analysis The reaction products are stable BA is stable in presence of H_2O_2 and photochemically inert The presence of cations (Na^+,K^+,Ca^{2+},Cu^{2+},Ni^{2+}) in Fenton systems did not influence in the product concentration Results consistent with those obtained using n-propanol and methanol as probes	When Cl^- is present in the reaction media it acts as ·OH scavenger In general, the references studied consider this method as qualitative of ·OH generation pHBA can also be oxidized by ·OH with a similar rate constant than BA ($k_{\bullet OH,pHBA}$= $6\cdot10^9$ l/mol/s > $k_{\bullet OH,BA}$= $4.3\cdot10^9$ l/mol/s) Generation of several products such as di and tri-hydroxylated BA	1-8
Benzene: 1.2-7 mM	Photocatalysis Electrochemical oxidation	Analysis of phenol HPLC with UV/vis detector [·OH]: 50nM, 0.1-0.23 mM	Selectivity towards ·OH Easy determination of phenol Phenol formation rate > phenol oxidation rate Repeatability, especially when the withdrawal of the sample is automatized There is no direct formation of phenol under UV irradiation Negligible effect of [NO_3^-] in the reaction between benzene-·OH	The presence of Cl^-, Br^- and citrate ions may result in the scavenging of ·OH Benzene is highly toxic and its use is restricted in many countries The phenol stability in natural waters is just 1 h The formation of other products than phenol, such as hydroquinone, catechol, resorcinol and benzoquinone was observed in electro-oxidation	9-13

Table III.1. Main features of the probes used in the determination of ·OH (continuation).

Probe	AOPs	Analytical features	Strengths	Limitations	Ref.
3-carboxy-proxyl: 0.8 mM	Photocatalysis	Analysis of proxyl-NH EPR spectroscopy [·OH]: up to 0.25 mM	Selectivity towards ·OH Simplicity Under dark conditions, TiO_2 does not affect the concentration of 3-carboxyproxyl	A fraction of 3-carboxyproxyl may react with the electrons of the conduction band leading to the formation of proxyl-OH, which implies the loss of the probe 3-carboxyproxyl may react with itself when it is irradiated Formation of several reaction products When sodium salts are present, they compete for ·OH	14
3-CCA: 0.1-30 mM	γ-radiolysis and heavy ions	Analysis of 7OH-3CCA HPLC with fluorescence detection (pH 6.8) or fluorescence spectrophotometry [·OH]: Qualitative	Simple, sensitive, accurate and reproducible method Commercial availability of the probe and the product	The fluorescence is pH dependent. The analysis of the samples must be done at pH optimum that guarantees the maximum intensity In fluorescence analyses samples must be diluted to avoid filter effects on the fluorescence Formation of other hydroxylated products	15, 16

Table III.1. Main features of the probes used in the determination of ·OH (continuation).

Probe	AOPs	Analytical features	Strengths	Limitations	Ref.
Coumarin: 0.1-0.2 mM	Photocatalysis Fenton Electrochemical oxidation γ-radiolysis	Analysis of 7HC HPLC with fluorescence detection or fluorescence spectrophotometry [·OH]: 1.6 nM- 0.02 mM	Good selectivity towards ·OH, though it may react with O_3 Sensitive and fast method Good reproducibility Good scavenger in the concentration range 10^{-3}-10^{-5} M Fluorescence only due to 7HC 7HC is a stable product and it is commercially available The direct photoelectrolysis of coumarin did not occur Coumarin is not oxidized in active anodes, it requires the presence of ·OH	Disappearance of 7HC in the presence of O_2 y $O_2^{\bullet-}$ The production of HC isomers with the hydroxyl group in the positions 3 ,4, 5, 6, 7 and 8 is likely Different values in the yield of coumarin-·OH to give 7HC are reported Photocatalysis: Slow disappearance of coumarin under UV. Besides, only dissolved ·OH reacts with coumarin. At low coumarin concentration, the photocatalysis of 7HC occurs. Coumarin may cause a filter effect absorbing a fraction of the incident light Photo-Fenton and electro-oxidation: reaction between 7HC and ·OH	17-27
4-CP: 1-1.72 mM	Photocatalysis Fenton	Analysis of 4CC HPLC with PDA detector [·OH]: Qualitative	Selectivity towards ·OH	4CC may react also with ·OH 4CP may be degraded by direct photolysis Formation of several products: 4CC, hydroquinone, benzoquinone and products derived from the ring opening	28-30
DMPO: 1-300 mM	Fenton Photocatalysis Electrochemical oxidation Sonolysis	Analysis of DMPO-·OH ESR/EPR spectroscopy; LC with positive ion electrospray ionization using a tandem mass spectrometer (LC/ESI-MS/MS) [·OH]: 0.2 μM- 0.15 mM	High sensitivity and reproducibility Good solubility of DMPO Short analysis time EPR analysis is not affected by the photocatalytic suspension Direct photolysis of DMPO was not observed	DMSO, mannitol, Fe(II) and PO_4^{3-} present in solution act as ·OH scavengers DMPO may also react with the photogenerated holes in the catalyst Low DMPO-OH stability: half-life of DMPO-·OH is about 20 min. This compound disappears in the presence of Fe(II), PO_4^{3-} and high ·OH concentration Non-selective towards ·OH. Reactions with con $O_2^{\bullet-}$, $^1O_2$ and ROO· may occur	28, 30-41

Table III.1. Main features of the probes used in the determination of ·OH (continuation).

Probe	AOPs	Analytical features	Strengths	Limitations	Ref.
DMSO: 5-500 mM	Fenton Photolysis Electrochem. oxidation	Analysis of HCHO-DNPH HPLC with UV detector (pH 4) [·OH]: 0.08 mM- 0.2 mM	Selectivity DMSO-·OH Good reproducibility, simple and sensitive method, easy to operate One quantitative product High solubility of DMSO and low volatility Commercial availability of DMSO and DNPH Comparison of the ·OH formation rates was identical using NaTA as scavenger	Inorganic salts and other compounds present in the solution may act as scavengers The derivatization time of HCHO with DNPH requires 30 min Degradation of DMSO (C_0=1mM) and HCHO applying UV/H_2O_2 that implies an underestimation in the quantification of ·OH	18, 42-46
	Fenton	Analysis of $C_{13}H_{15}O_2N$ Fluorescence spectrometry (pH 4.5) [·OH]: Qualitative	Selectivity DMSO-·OH Sensitive, simple and inexpensive method One quantitative product Fluorescence only due to ·OH reaction	Scavenging of ·OH in the presence of ascorbic acid A heating step is required (95ºC for 20 min) once all the reagents are added to the sample prior to the analysis	47
	Fenton	Analysis of o-MHA: o-methyl hydroxylamine Fluorescence spectrophotometry [·OH]: Qualitative	Fluorescence caused only by the reaction with ·OH Sensitive, simple and inexpensive method One quantitative product	NN was synthesized in the laboratory In the presence of reducing agents or carbon centered radicals, o-alkoxylamine derivatives may be produced, increasing the fluorescence signal	48
	Photolysis	Analysis of the fluorescent compound generated by HPLC with fluorescence detection (pH 8) [·OH]: Qualitative	Fluorescence caused only by the reaction with ·OH Method applied to fresh and sea waters under aerobic and anaerobic conditions and in the presence/absence of organic matter	The purification of aminonitroxide is needed The fluorescent product has been prepared in the laboratory In the absence of nitrate or nitrite (or in presence of organic matter) the irradiation of DMSO and nitroxide solutions may generate ·CH_3 Competition between the reaction of ·OH with DMSO and nitrite in anaerobe media Competition between the reaction of ·CH_3 with O_2 and nitroxide in aerobe media	49

Table III.1. Main features of the probes used in the determination of ·OH (continuation).

Probe	AOPs	Analytical features	Strengths	Limitations	Ref.
DPCI: 1 mM	Sonocatalysis Photocatalysis	Analysis of DPCO UV/vis spectrophotometry [·OH]: Qualitative	The fluorescence is only caused by the oxidation of DPCI Rapid and accurate detection The required equipment is simple and the reagents are non-expensive Wide range of detection	The oxidation of DPCI to DPCO takes place through the reaction with different ROS. Different scavengers have to be added depending on the ROS studied when ·OH is evaluated, 2,6-di-tert-butyl-methylphenol (BHT) was used as scavenger Oxidation-Extraction photometry method: extraction of DPCO with a mixture of benzene-CCl_4 The concentration of ROS was not quantified in these works	50, 51
FDMPO: 50 mM	Fenton	Analysis of FDMPO-OH ESR/EPR spectroscopy or nuclear magnetic resonance (NMR) [·OH]: Qualitative	Higher stability than DMPO Signal/background noise ratio higher than when DMPO is used as a probe	FDMPO was synthesized in the laboratory FDMPO reacts also with carbon centered radicals (·CH_3, ·CH_2OH) The EPR spectra in the presence of $O_2^{\bullet-}$ is identical to the corresponding FDMPO-·OH	52
4-HBA 2-10 mM	Photocatalysis Electrocatalysis Fenton	Analysis of 3,4-dHBA Voltammetry and HPLC with UV/vis detector [·OH]: up to 7 mM	Selective method High sensitivity and trapping efficiency One quantitative product of importance Effective discrimination between 4HBA and 3,4-dHBA peaks during the HPLC analysis Short analysis time	CO_3^{2-} acts as scavenger of ·OH Generation of oxidation intermediates during the treatment of an aqueous solution of 4HBA High ratio signal/background	53-56
IBG: 1.1 μM	Fenton	Analysis of the chemiluminescence generated BJL analyzer with high sensitivity detector [·OH]: Qualitative	Selectivity towards ·OH. The chemiluminescent product do not react with $O_2^{\bullet-}$ or H_2O_2 Rapid and specific method	It would be necessary to know the commercial availability of the chemiluminescent product generated in order to quantify the ·OH concentration	57

Table III.1. Main features of the probes used in the determination of ·OH (continuation).

Probe	AOPs	Analytical features	Strengths	Limitations	Ref.
Methanol: 2-400 mM	Photolysis	Analysis of HCOOH-DNPH HPLC with UV detector [·OH]: 0.6 µM- 0.5 mM	Higher sensitivity compared with BA as probe. The results obtained with both probes were the same Methanol is stable in presence of H_2O_2 and photochemically inert	Less efficiency in trapping ·OH regarding BA	1, 3, 58
Ninhydrin: 22.5 mM	Fenton-like	Analysis of HO-ninhydrin Fluorescence spectrophotometry with FIA (pH 7.27) [·OH]: up to 0.02 mM	Selectivity ninhydrin-·OH Simple and fast technique (22 samples/h) Sensitive and accurate technique The presence of Na^+, K^+, NH_4^+, F^-, Cl^-, Br^-, $O_2^{\bullet-}$ did not interfere in the fluorescence intensity	An excess of ninhydrin concentration may result in fluorescence quenching and, therefore, the concentration of ·OH could be underestimated	59
Nitrone: 3 mM	Fenton	Analysis of the nitroxide 2-hydroxy-2-(2-pyridyl)-3H-indol-3-on-1-oxy ESR spectroscopy (pH 7.4) [·OH]: Study of the probe viability	Commercial availability of the catalyst and reagents for the probe preparation Nitrone does not react with $O_2^{\bullet-}$	The probe was synthesized in the laboratory The efficiency of the method is limited: the utility of nitrone in the characterization of ·OH is oriented to specific experimental designs Direct oxidation reaction with H_2O_2	60
NPG: 0.5 mM	Photocatalysis	Analysis of o- and p-HNPG HPLC with PDA detector (pH 9) [·OH]: Qualitative	-	The hydroxylation reaction is pH dependent (adjusted at pH 9) Synthesis of NPG in the laboratory	61
n-propanol: 5 mM	Fenton	Analysis of propionaldehyde-DNPH HPLC with PDA detector [·OH]: up to 0.3 mM	Results consistent with those obtained using BA	The estimated yield for the reaction n-propanol-·OH to give propionaldehyde is 46% Derivatization with DNPH: 12 h	5

Table III.1. Main features of the probes used in the determination of ·OH (continuation).

Probe	AOPs	Analytical features	Strengths	Limitations	Ref.
OPDA: 3 mM	Photo-Fenton	Analysis of DAPN UV/vis spectrophotometry [·OH]: 0.012-0.039 mM	Good selectivity towards ·OH Simple and accurate measurement	H_2O_2 may react with OPDA giving DAPN, but it was insignificant	62
p-CBA: 2-60 μM	Photocatalysis Sonocatalysis	Disappearance of p-CBA, formation of 4-CP HPLC with UV/vis detector [·OH]: Qualitative	Selectivity towards ·OH Low reactivity with O_3 Non-volatile	A different product distribution is obtained depending on the AOP applied: 4-CP, hydroquinone, catechol, benzoquinone and products derived from the ring opening The concentration of 4-CP decreased with treatment time leading to an underestimation of ·OH concentration[63] In presence of O_3, the degradation of p-CBA may occurs	32, 58, 63-65
Phenol: 2.5-10 mM	Fenton Electrochemical oxidation	Analysis of pyrocatechol HPLC with EC detector [·OH]: Qualitative	Selectivity towards ·OH The presence of SO_4^{2-} does not influence the degradation of phenol	Generation of several products after the reaction with ·OH Formation of a polymer in dimensionally stable electrodes Br^- acts as scavenger of ·OH and the presence of Cl^- implies the formation of active chlorine and chloride species that participate in the oxidation process	66, 67
Phenylala-nine: 20 mM	Fenton	Analysis of o-, m- and p-tyrosine HPLC with UV detector and LC-MS [·OH]: Qualitative	Time analysis lower than 6 min Additional LC-MS allows the discrimination and identification of the signal generated by each product	Generation of several products	68

Table III.1. Main features of the probes used in the determination of ·OH (continuation).

Probe	AOPs	Analytical features	Strengths	Limitations	Ref.
Phth: 0.1-4 mM	Fenton Electrochem. methods	Analysis of 5OH-Phth and 6OH-Phth Chemiluminescence analysis in a PMT, luminometer or HPLC-UV followed by a luminometer (pH 4.5-9.5) [·OH]: 1.5 μM-1 mM	Selectivity towards ·OH Phth is not oxidized by $HO_2^{\bullet}$, HO^-, SO_4^{2-}, Co(III) or Ce(IV). There is no influence of transition metals in the pH region 4.5-9.5 Sensitive and reproducible method Stability of the oxidation products Good solubility at neutral and alkaline pH Phth does not produce background chemiluminescence A separation stage was not required prior to the analysis in a Fenton-like system (Cu(II)) The product distribution is not dependent of Fe(III) or Cu(II) when lower than 1mM	Br^-, Na_2CO_3 and organics act as scavengers of ·OH H_2O_2 concentration higher than 0.15 mM and DTPA/EDTA ratio greater than 0.10 mM may interfere in the analysis Generation of several products, other than 5OH-Phth and 6OH-Phth Luminescence emission of 5OH-Phth is 40 times higher than 6OH-Phth, which could result in an underestimation of ·OH concentration The chemiluminescence is pH dependent A prior HPLC stage to separate the oxidation products is very useful	69-72
Pyrocate-chol: 2.5 mM	Fenton	Analysis of pryogallic acid HPLC with EC detector [·OH]: Qualitative	Selectivity towards ·OH	-	66
Quinoline: 0.15-0.95 mM	Fenton Photocatalysis	Quantification of all the identified products HPLC with PDA detector and GC-MS [·OH]: Qualitative	Easiness in the identification of the reaction of quinoline with ·OH or other ROS Good stability of quinoline The product distribution is not affected by steric impediments The solubility of quinoline is high enough to let an appropriate initial quinoline concentration for trapping all the generated ·OH Quinoline is moderately polar and basic which prevents the degradation by ionic associations	Quinoline reacts with $O_2^{\bullet-}$, which is favored at high pH In photocatalysis, the use of both analytical techniques, HPLC and GC-MS, is required because one of the products (8-hydroxyquinoline) does not elute correctly by HPLC Generation of several products Synthesis in the laboratory of all the identified products	73, 74

Table III.1. Main features of the probes used in the determination of ·OH (continuation).

Probe	AOPs	Analytical features	Strengths	Limitations	Ref.
RhB: 0.2 mM	Fenton	Analysis of the absorbance of RhB UV/vis spectrophotometry [·OH]: Qualitative	Simple and cost-effective method Reproducibility RhB is not oxidized by H_2O_2	In Fenton system, the concentration of RhB diminishes slightly due to the absorption on Fe(II)	75
RNO: 1.5-67 μM	Photocataly-sis Electrochem. oxidation	Analysis of RNO decrease UV/vis spectrophotometry (pH 6-12) [·OH]: $4.17 \cdot 10^{-13}$ M	RNO does not react with $^1O_2$, $O_2^{\bullet-}$ or other peroxy compounds	RNO is oxidized by O_3, Cl_2, HClO and ClO^- In photocatalysis, and in the absence of O_2, RNO is reduced by the generated electrons In active anodes (Ti/Pt and Ti/RuO_2), RNO may be oxidized by the O_2 adsorbed on the anode Analysis at pH 6-12 to avoid the protonated specie that results in an absorbance diminishment	76-79
$Ru(bpy)_3^{2+}$: 0.5 mM	Fenton	Analysis of the chemiluminescence of the excited $Ru(bpy)_3^{2+}$ FIA with EC detector [·OH]: Qualitative	Selectivity towards ·OH Accurate method Processing of 80 samples/h	$Ru(bpy)_3^{3+}$ is unstable in aqueous solution. Its preparation is carried out in an electrochemical reactor from $Ru(bpy)_3^{2+}$ prior the detector Antioxidant compounds such as ascorbic and gallic acid act as scavengers of ·OH	80
$Ru(NH_3)_6^{3+}$: 5 mM	Fenton Photolysis	$Ru(NH_3)_6^{3+}/Ru(NH_3)_6^{2+}$ CV and CA [·OH]: $9.1 \cdot 10^{-12}$-$9.5 \cdot 10^{-11}$ M	Results consistent with those obtained with SA as a probe by HPLC analysis ROO· and $O_2^{\bullet-}$ do not interfere in the analysis	CV analysis: recommended when the uncovered electrode surface ranges between 2-70% CA analysis: Recommended when the uncovered electrode surface is lower than 2% In the presence of $KMnO_4$ the analytical signal increases	81

Table III.1. Main features of the probes used in the determination of ·OH (continuation).

Probe	AOPs	Analytical features	Strengths	Limitations	Ref.
SA: 0.2-10.9 mM	Fenton Photocatalysis Sonocatalysis Hydrodynamic cavitation Electrochem. technologies	2,3-dHBA and 2,5-dHBA HPLC-ECD (pH 7.4), HPLC-UV (pH 2), HPLC-PDA or HPLC-fluorescence (pH 5.9), capillary electrophoresis (pH 2.8 or 7.4), UV spectrophotometry [·OH]: 0.25 μM- 6.5 mM	Selectivity SA-·OH Sensitivity, reproducibility and repeatability Stability of the products Solubility of SA in water Good chromatographic separation There is no SA concentration change, when irradiated in the presence of TiO_2/SiO_2 Electrophoresis requires lower sample volume and cheaper instrumentation, shows higher efficiency and higher reproducibility, and is faster than HPLC Results consistent with those obtained with an electrochemical sensor	The presence of DMSO, mannitol or other organics result in the scavenging of ·OH The optimum concentration of SA to obtain a high efficiency in the capture of ·OH is different based on the AOP An excess of SA is recommended, avoiding solubility limitations Importance of the SA/2,5-dHBA ratio because of their similar hydroxylation kinetic constant Production of several products, including catechol and hydroquinone Capillary electrophoresis requires specific pH for the proper separation of reagents and products The mineralization process results in low reliability when electrochemical oxidation or electro-Fenton are applied	81-96
SCN^-: 100 μM	Radiolysis	Analysis of $(SCN)_2^{\bullet-}$ [·OH]: Qualitative	The results obtained for the kinetic constant are consistent with those observed by monitoring the evolution of dissolved organic carbon (DOC)	-	97

Table III.1. Main features of the probes used in the determination of ·OH (continuation).

Probe	AOPs	Analytical features	Strengths	Limitations	Ref.
TA and NaTA: 0.01-75 mM	Fenton Photocatalysis Sonolysis Electrochemical methods	Analysis of OHTA HPLC-UV/vis (pH 3), HPLC-fluorescence (pH 2.8 or 4.37) , fluorescence spectrophotometry (pH 6-11) [·OH]: 0.31-30 μM	High sensitivity Rapid and simple technique One quantitative product Fluorescence stability of OHTA lasts 24 h The UV analysis is possible at OHTA concentration higher than 1 mM NaTA presents lower solubility limitations than TA Good correlation between the results obtained by HPLC (TA), ESR (DMPO) and HPLC (DMSO) FIA allows the simple, fast ,accurate and automatic determination of the fluorescence	The reaction TA-·OH is affected by the solution pH Reaction of TA with $O_2^{\bullet-}$ and H_2O_2 The presence of inorganic salts and organics result in ·OH scavenging An excess of NaTA may quench the fluorescence Later oxidation, deprotonation or photolytic reactions are possible The chemical yield of TA-·OH is estimated around 80% Solubility limitations of TA Photocatalysis: TA reacts only with dissolved ·OH Photolytic degradation of OHTA OHTA has a higher hydroxylation kinetic rate constant value than TACarboxylic acids produced along the photocatalysis of TA (0.12-0.60 mM)	44, 56, 98-108

Table III.2. Main features of the probes used in the determination of $O_2^{\bullet-}/HO_2^{\bullet}$.

Probe	AOPs	Analytical features	Strengths	Limitations	Ref.
BA: 1 mM	Fenton system	Analysis of OHBA Fluorimetry (pH 11) $[O_2^{\bullet-}]$: 1 nM-3.1 μM	High sensitivity and easy calibration	Formation of numerous products: hydroxybenzene isomers and decarboxylated products The fluorescence signal could be increased by the impurities present in solution or diminished by competitive reactions Less sensitivity than NaTA Specific experimental setup	109-111
FC: 40 μM	Thermal decomposition	Analysis of the absorbance at a wavelength of 550 nm UV spectrophotometry $[O_2^{\bullet-}]$: 9 μM	Selectivity Insignificant extent of the reaction with H_2O_2 when its concentration is lower than < 0.1mM	FC reduction and oxidation by Cu and Mn species that implies an underestimation of $O_2^{-\bullet}$	112
Luminol: 40 μM- 7 mM	Fenton Photocatalysis Cyclic voltammetry	Analysis of the chemiluminescence generated Photon counting system with photomultiplier tube (pH 9-11) $[O_2^{\bullet-}]$: $3.9\cdot10^{-15}$-$1.8\cdot10^{-4}$ M	When photocatalysis is applied, the subsequent addition of luminol prevents its reaction with the photocatalyst	Luminol is not selective. It also reacts with H_2O_2 and other species including trace metals such as Co, Cu, Mn, Cr, Mg, Fe and certain complex of these metals, $N_3^{\bullet}$, $CO_3^{-\bullet}$, SCN^-, I^-, Br^-, $Br_2^{-\bullet}$ and ClO_2 Luminol produces background noise during their luminescence analysis and its detection is restricted to alkaline pH	72, 104, 105, 113-119
MCLA: 1-350 μM	Photocatalysis Cyclic voltammetry Thermal decomposition	Analysis of the chemiluminescence generated Photon counting system with photomultiplier tube $[O_2^{\bullet-}]$: 25-60 nM	Selective towards $O_2^{-\bullet}/HO_2^{\bullet}$ and $^1O_2$. $\cdot OH$ and H_2O_2 do not interfere in the analysis High sensitivity The method allows the quantification of $O_2^{-\bullet}/HO_2^{\bullet}$ at any pH	$O_2^{-\bullet}$ may react with buffer solutions containing amines Background chemiluminescence owing to the auto-oxidation of MCLA When pH<pKa=7.75, the chemiluminescence decreases	23, 72, 112, 114

Table III.2. Main features of the probes used in the determination of $O_2^{\bullet-}/HO_2^{\bullet}$ (continuation).

Probe	AOPs	Analytical features	Strengths	Limitations	Ref.
NaTA: 1 mM	Fenton system	Analysis of OHTA Fluorimetry (pH 11) [$O_2^{\bullet-}$]: Up to 5 μM	TA is more sensitive than BA	The half-life of $O_2^{-\bullet}/HO_2^{\bullet}$ depends on pH Specific experimental setup	109
NBD-Cl: 100 μM	Thermal decomposition	Analysis of the absorbance of the generated product UV spectrophotometry [$O_2^{\bullet-}$]: 20 μM	-	NBD-Cl may react with amino acids, amines, thiols, ketyl and alkoxyl radicals	112
NBT: 0.2-1 mM	Photocatalysis	Analysis of the absorbance of NBT or NBT-formazan UV-vis spectrophotometry [$O_2^{\bullet-}$]: Up to 0.17 mM	NBT does not react with ·OH or H_2O_2 NBT does not react with TiO_2	Negligible formation of $O_2^{-\bullet}/HO_2^{\bullet}$ under a N_2 atmosphere 2-propanol scavenges $O_2^{-\bullet}$ Low water solubility of NBT	64, 120, 121
XTT: 0.1 mM	Photocatalysis	Analysis of the absorbance of XTT-formazan UV-vis spectrophotometry [$O_2^{\bullet-}$]: 2.5 nM	Good selectivity High solubility of XTT in water, especially compared with NBT	-	64, 78

Table III.3. Main features of the probes used in the determination of $^1O_2$.

Probe	AOPs	Analytical features	Strengths	Limitations	Ref.
AAPD: 0.5-5 µM	Fenton-like	Analysis of the generated fluorescence Fluorescence spectrophotometry [$^1O_2$]: Qualitative	Selectivity towards $^1O_2$ High sensitivity	The probe is synthesized in the laboratory	122
Direct analysis	Photocatalysis	Monitoring of $^1O_2$ phosphorescence Photon-counting system with photomultiplier [$^1O_2$]: Up to 4.7 µM	Direct measurement	Under N_2 environment, the concentration of $^1O_2$ decreases, highlighting the importance of O_2 in its generation Methionine and folic acid act as $^1O_2$ scavengers The reaction with $O_2^{\bullet-}$ may deactivate $^1O_2$	123-125
DMAX: 10 µM	Thermal decomposition	Analysis of the fluorescent product Fluorescence spectrophotometry (pH 7.4) [$^1O_2$]: Qualitative	The reaction rate between $^1O_2$ and DMAX is higher than with DPAX Sensitivity of DMAX is 53-fold higher than that of DPAX Hydrophobicity of DMAX is less than that of DPAX Initial DMAX complex hardly emits fluorescence	DMAX is synthesized in the laboratory and. numerous steps are required	126
DPAX: 1 µM	Fenton-like	Analysis of the fluorescent product Fluorescence spectrophotometry [$^1O_2$]: Qualitative	Good selectivity towards $^1O_2$ Useful probe in basic and neutral aqueous solutions	DPAX is synthesized in the laboratory Fluorescence sharply decreases at acidic pH	127
FFA: 0.1-0.2 mM	Photocatalysis	Analysis of FFA decrease HPLC (pH 7) [$^1O_2$]: $6.7\cdot10^{-14}$-$1.8\cdot10^{-4}$ M	Good selectivity towards $^1O_2$ The reaction with $O_2^{\bullet-}$ becomes important at FFA concentrations higher than 10mM	O_2 and a sensitizer are essential in the production of $^1O_2$ N_3^- quenches $^1O_2$	64, 128

Table III.3. Main features of the probes used in the determination of $^1O_2$ (continuation).

Probe	AOPs	Analytical features	Strengths	Limitations	Ref.
MTTA-Eu^{3+}: 10 µM	Fenton-like	Analysis of the fluorescence: formation of a fluorescent product Fluorescence spectrophotometry [$^1O_2$]: Qualitative	Good selectivity and sensitivity towards $^1O_2$ High solubility of the probe in water The probe allows the work in a wide pH range Formation of a product with large fluorescence time Initial Eu (III) complex hardly emits fluorescence	Europium (III) complex is synthesized in the laboratory	129
Naphtho xazole-based:	Photo-sensitization	Analysis of the fluorescence: formation of a fluorescent product Fluorescence spectrophotometry [$^1O_2$]: Study of the probe viability	Good selectivity towards $^1O_2$ Negligible effects of self-sensitization Fluorescence enhancement factors up to 300-fold	The probe is synthesized in the laboratory	130
PATA-Tb^{3+}: 0.02-10 µM	Fenton-like	Analysis of the luminescence: formation of a luminescent product Luminescence spectrophotometry (pH 10.5) [$^1O_2$]: 6.8 µM	Good selectivity and sensitivity towards $^1O_2$ High solubility of the probe in water The probe allows the work in a wide pH range Formation of a product with large fluorescence time The possibility of working under time-resolved fluorescence mode lets the removal of fluorescence background Initial Tb(III) complex hardly emit fluorescence	Terbium chelate is synthesized in the laboratory	131
Re(I) complex : 2.8 mM	Fenton-like	Analysis of the luminescence: formation of a luminescent product Luminescence and UV/vis spectrophotometry [$^1O_2$]: Up to 40 mM	High selectivity and sensitivity towards $^1O_2$ Detection limit lower than other chemiluminescent methodologies and comparable with the probes based on Eu(III) y Tb(III) Re(I) may be excited under visible light Re(I) complex hardly emits fluorescence	Synthesis of the Re complex in the laboratory	132

Table III.3. Main features of the probes used in the determination of $^1O_2$ (continuation).

Probe	AOPs	Analytical features	Strengths	Limitations	Ref.
SOSG: >6 μM	Photo-sensitization	Analysis of the generated fluorescence Fluorescence spectrophotometry [$^1O_2$]: Qualitative	High selectivity towards $^1O_2$ Commercial availability of SOSG	Background fluorescence	133
SVE: 10 μM	Thermal decomposition	Analysis of the luminescence: formation of a luminescent product Luminometer [$^1O_2$]: 36 nM	Good selectivity towards $^1O_2$ Stable reaction product under neutral pH	The probe was synthesized in the laboratory	134
TTF: 20 μM	H_2O_2/NaOCl	Analysis of chemiluminescence and fluorescence Spectrophotometry [$^1O_2$]: 1.1-1.4 mM	High Selectivity towards $^1O_2$	TTF is synthesized in the laboratory Addition of tetrahydrofuran owing to the low solubility	135
TTFA dyad: 20 μM	H_2O_2/NaOCl	Analysis of chemiluminescence and fluorescence Spectrophotometry [$^1O_2$]: 1.21 mM	Selectivity towards $^1O_2$ Negligible effect of K(I), Ca(II), Mg(II),Mn(II), Ni(II), Zn(II), Al(III), Cl^-, HCO_3^-, NO_3^- and SO_4^{2-} Acceptable precision level (standard deviation around 4%)	TTFA is synthesized in the laboratory Low solubility in water Fe(III) and Cu(II) may oxidize tetrathiafulvalene unity causing interferences	136

Annex IV- PCDD/Fs concentration in labelled and native standards

Table IV.1. Concentration of PCDD/Fs in labelled, native and internal EPA 1613 standard solutions from Wellington Laboratories Inc. The LCS and ISS standards contain the PCDD/Fs isotopically labelled with $^{13}C_{12}$.

	Concentration (pg L^{-1})		
	LCS	PAR	ISS
1,2,3,4-TeCDD	-	-	200
2,3,7,8-TeCDD	100	40	-
1,2,3,7,8-PeCDD	100	200	-
1,2,3,4,7,8-HxCDD	100	200	-
1,2,3,6,7,8-HxCDD	100	200	-
1,2,3,7,8,9-HxCDD	-	200	200
1,2,3,4,6,7,8-HpCDD	100	200	-
OCDD	200	400	-
2,3,7,8-TCDF	100	40	-
1,2,3,7,8-PeCDF	100	200	-
2,3,4,7,8-PeCDF	100	200	-
1,2,3,4,7,8-HxCDF	100	200	-
1,2,3,6,7,8-HxCDF	100	200	-
1,2,3,7,8,9-HxCDF	100	200	-
2,3,4,6,7,8-HxCDF	100	200	-
1,2,3,4,6,7,8-HpCDF	100	200	-
1,2,3,4,7,8,9-HpCDF	100	200	-
OCDF	-	400	-

Table IV.2. Concentration of non-chlorinated and low chlorinated PCDD/Fs (mono- to tri-) in labelled and native standard solutions from Wellington Laboratories Inc. The MDDF contains the PCDD/Fs isotopically labelled with $^{13}C_{12}$.

	Concentration (µg mL^{-1})	
	DDF-MDT	MDDF-MDT
DD	1.0	1.0
2-MCDD	1.0	1.0
2,3-DCDD	1.0	1.0
2,3,7-triCDD	1.0	1.0
DF	1.0	1.0
2-MCDF	1.0	1.0
2,3-DCDF	1.0	1.0
2,3,8-triCDF	1.0	1.0

Table IV.3. EPA Method 1613 calibration and verification solutions CSL and CS1-CS4.

	Concentration (pg L^{-1})				
	1613CSL	1613CS1	1613CS2	1613CS3	1613CS4
2,3,7,8-TCDD	0.1	0.5	2	10	40
1,2,3,7,8-PeCDD	0.5	2.5	10	50	200
1,2,3,4,7,8-HxCDD	0.5	2.5	10	50	200
1,2,3,6,7,8-HxCDD	0.5	2.5	10	50	200
1,2,3,7,8,9-HxCDD	0.5	2.5	10	50	200
1,2,3,4,6,7,8-HpCDD	0.5	2.5	10	50	200
OCDD	1.0	5.0	20	100	400
2,3,7,8-TCDF	0.1	0.5	2	10	40
1,2,3,7,8-PeCDF	0.5	2.5	10	50	200
2,3,4,7,8-PeCDF	0.5	2.5	10	50	200
1,2,3,4,7,8-HxCDF	0.5	2.5	10	50	200
1,2,3,6,7,8-HxCDF	0.5	2.5	10	50	200
1,2,3,7,8,9-HxCDF	0.5	2.5	10	50	200
2,3,4,6,7,8-HxCDF	0.5	2.5	10	50	200
1,2,3,4,6,7,8-HpCDF	0.5	2.5	10	50	200
1,2,3,4,7,8,9-HpCDF	0.5	2.5	10	50	200
OCDF	1.0	5.0	20	100	400
$^{13}C_{12}$-2,3,7,8-TCDD	100	100	100	100	100
$^{13}C_{12}$-1,2,3,7,8-PeCDD	100	100	100	100	100
$^{13}C_{12}$-1,2,3,4,7,8-HxCDD	100	100	100	100	100
$^{13}C_{12}$-1,2,3,6,7,8-HxCDD	100	100	100	100	100
$^{13}C_{12}$-1,2,3,4,6,7,8-HpCDD	100	100	100	100	100
$^{13}C_{12}$- OCDD	200	200	200	200	200
$^{13}C_{12}$-2,3,7,8-TCDF	100	100	100	100	100
$^{13}C_{12}$-1,2,3,7,8-PeCDF	100	100	100	100	100
$^{13}C_{12}$-2,3,4,7,8-PeCDF	100	100	100	100	100
$^{13}C_{12}$-1,2,3,4,7,8-HxCDF	100	100	100	100	100
$^{13}C_{12}$-1,2,3,6,7,8-HxCDF	100	100	100	100	100
$^{13}C_{12}$-1,2,3,7,8,9-HxCDF	100	100	100	100	100
$^{13}C_{12}$-2,3,4,6,7,8-HxCDF	100	100	100	100	100
$^{13}C_{12}$-1,2,3,4,6,7,8-HpCDF	100	100	100	100	100
$^{13}C_{12}$-1,2,3,4,7,8,9-HpCDF	100	100	100	100	100
$^{37}Cl_4$-2,3,7,8-TCDD	0.1	0.5	2	10	40
$^{13}C_{12}$-1,2,3,4-TCDD	100	100	100	100	100
$^{13}C_{12}$-1,2,3,7,8,9-HxCDD	100	100	100	100	100

Annex V- Quality control and quality assurance (QC/QA) in the analysis of PCDD/Fs

Table V.1. Concentration of native PCDD/Fs in precision and recovery experiments and in methods blanks

	Precision and recovery experiments		Blank experiments	
	Average concentration (pg L^{-1})	RSD (%)	Average concentration (pg L^{-1})	DL (pg L^{-1})
2,3,7,8-TCDD	42.9	15.4	<DL	0.2
1,2,3,7,8-PeCDD	207.3	15.1	<DL	0.2
1,2,3,4,7,8-HxCDD	206.2	13.9	<DL	0.2
1,2,3,6,7,8-HxCDD	204.3	14.7	<DL	0.2
1,2,3,7,8,9-HxCDD	217.5	17.5	<DL	0.2
1,2,3,4,6,7,8-HpCDD	199.2	12.7	0.8	0.2
OCDD	403.2	10.8	<DL	0.5
2,3,7,8-TCDF	49.1	14.2	<DL	0.2
1,2,3,7,8-PeCDF	215.9	15.1	<DL	0.2
2,3,4,7,8-PeCDF	218.0	13.5	0.6	0.2
1,2,3,4,7,8-HxCDF	204.3	13.8	<DL	0.1
1,2,3,6,7,8-HxCDF	207.4	16.4	<DL	0.1
1,2,3,7,8,9-HxCDF	213.4	15.3	<DL	0.1
2,3,4,6,7,8-HxCDF	207.3	12.9	<DL	0.1
1,2,3,4,6,7,8-HpCDF	203.2	11.8	0.5	0.1
1,2,3,4,7,8,9-HpCDF	196.1	14.6	<DL	0.1
OCDF	392.7	10.7	1.4	0.2

Table V.2. Recoveries of labelled PCDD/Fs in precision and recovery experiments and in method blanks

	Precision and recovery experiments		Blank experiments	
	Average recovery (%)	RSD (%)	Average recovery (%)	RSD (%)
2,3,7,8-TCDD^{13}C	91.6	9.6	86.6	16.9
1,2,3,7,8-PeCDD^{13}C	93.0	7.4	81.6	17.8
1,2,3,4,7,8-HxCDD^{13}C	90.6	11.8	86.2	16.2
1,2,3,6,7,8-HxCDD^{13}C	87.8	18.1	85.0	16.3
1,2,3,7,8,9-HxCDD^{13}C	100.0	0.0	100.0	0.0
1,2,3,4,6,7,8-HpCDD^{13}C	90.6	11.0	88.0	16.9
OCDD^{13}C	81.6	15.8	85.5	14.4
2,3,7,8-TCDF	75.6	10.9	76.8	14.8
1,2,3,7,8-PeCDF^{13}C	89.4	8.7	85.2	20.2
2,3,4,7,8-PeCDF^{13}C	91.0	4.0	88.0	18.5
1,2,3,4,7,8-HxCDF^{13}C	87.4	17.4	84.6	13.6
1,2,3,6,7,8-HxCDF^{13}C	85.0	20.7	82.4	15.6
1,2,3,7,8,9-HxCDF^{13}C	89.0	6.7	86.4	12.1
2,3,4,6,7,8-HxCDF^{13}C	86.6	12.6	85.2	10.9
1,2,3,4,6,7,8-HpCDF^{13}C	79.6	19.6	81.2	14.2
1,2,3,4,7,8,9-HpCDF^{13}C	91.4	13.1	91.2	16.4

Table V.3. Labeled compound recovery stablished by EPA 1613 Method in samples when all CDD/Fs are tested.

	Test concentration (pg L^{-1})	Labelled compound recovery	
		(pg L^{-1})	(%)
$^{13}C_{12}$-2,3,7,8-TCDD	100	25-164	25-164
$^{13}C_{12}$-1,2,3,7,8-PeCDD	100	25-181	25-181
$^{13}C_{12}$-1,2,3,4,7,8-HxCDD	100	32-141	32-141
$^{13}C_{12}$-1,2,3,6,7,8-HxCDD	100	28-130	28-130
$^{13}C_{12}$-1,2,3,4,6,7,8-HpCDD	100	23-140	23-140
$^{13}C_{12}$- OCDD	200	34-313	17-157
$^{13}C_{12}$-2,3,7,8-TCDF	100	24-169	24-169
$^{13}C_{12}$-1,2,3,7,8-PeCDF	100	24-185	24-185
$^{13}C_{12}$-2,3,4,7,8-PeCDF	100	21-178	21-178
$^{13}C_{12}$-1,2,3,4,7,8-HxCDF	100	26-152	26-152
$^{13}C_{12}$-1,2,3,6,7,8-HxCDF	100	26-123	26-123
$^{13}C_{12}$-1,2,3,7,8,9-HxCDF	100	29-147	29-147
$^{13}C_{12}$-2,3,4,6,7,8-HxCDF	100	28-136	28-136
$^{13}C_{12}$-1,2,3,4,6,7,8-HpCDF	100	28-143	28-143
$^{13}C_{12}$-1,2,3,4,7,8,9-HpCDF	100	26-138	26-138
$^{37}Cl_4$-2,3,7,8-TeCDD	10	3.5-19.7	35-197

Annex VI- Characterization of the oxidation medium: Assessment of DMSO as molecular probe for the identification of ·OH in the electrochemical oxidation

Additional experiments to assess the viability of DMSO as molecular probe were conducted by applying an electrochemical oxidation process following the experimental procedure previously carried out by the Advanced Separation Processes research group. The electrochemical experiments were performed at a laboratory scale DiaCell 201 PP (Adamant Technologies, Switzerland) system comprised of two rectangular flow channels, separated by a bipolar electrode (Figure VI.1).[137] All anode, cathode and bipolar electrode consist of a boron-doped diamond (BDD) coating on a silicon plate, with circular shape. The total anodic area was 140 cm^2 (70 cm^2 each anode x 2 anodes) with an interelectrode gap between anode and cathode of 1 mm. A GW Instek GPR-6015D power supply (with a maximum output of 15 A and 60 V) was used. The system was also formed by a feed vessel, a recirculation pump (Iwaki Magnet MD-20R-220N) and a cooling system. The feed temperature was maintained at 20 ºC. A volume of 1 L of feed water was loaded in the jacketed feed tank and recirculated at a flow rate of 600 L h^{-1} (300 L h^{-1} through each cell compartment). The initial solution consisted of 267 mM DMSO and 9.15 mM Na_2SO_4 to provide a supporting electrolyte that increases the conductivity of the aqueous medium allowing the electrochemical process.

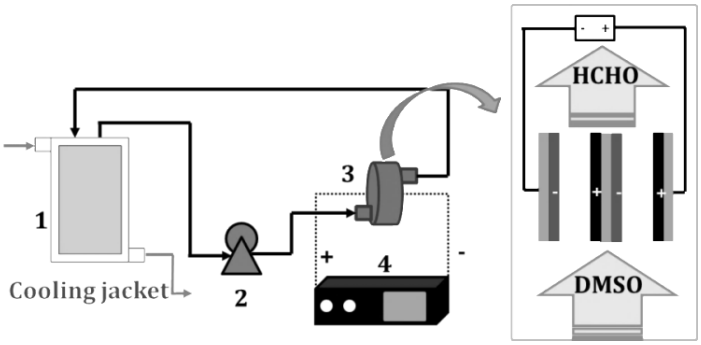

Figure VI.1. Electrochemical set-up formed by the thermostatized feed tank (1), pump (2), BDD electrochemical cell (3) and power supply (4).

The differences between the application of two current densities (j, 600 and 1200 A m^2) has been depicted in Figure VI.2 in terms of HCHO (Figure VI.2a) and ·OH concentrations (Figure VI.2b).

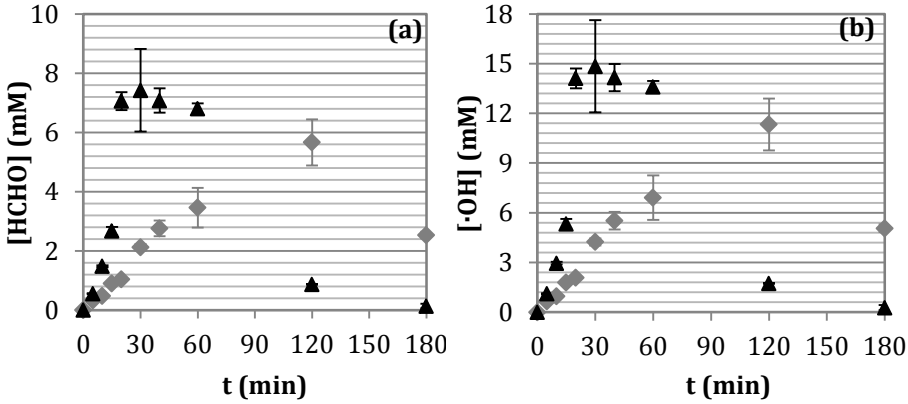

Figure VI.2. Cumulated concentration of (a) HCHO and (b) ·OH generated during the electrochemical oxidation of 267 mM DMSO applying ♦ 600 and ▲1200 A m^{-2}. $[Na_2SO_4]_0$: 9.15 mM.

A maximum concentration of 7.4 mM HCHO was obtained working with a current density of 1200 A m^{-2} (Figure VI.2a) and, therefore, a corresponding ·OH concentration of 14.8 mM (Figure VI.2b) according to the Reaction VI.1. An increase in HCHO concentration with the treatment time was observed for both current densities, but after reaching a maximum value there is a HCHO diminishment as a consequence of the further oxidation of formaldehyde. It is clear that the cumulated concentration of ·OH cannot diminish because they are continuously being formed, so after certain treatment time this method is not advisable for their quantification because it results in an underestimation, around 120 and 30 min for the current densities 600 and 1200 A m^{-2}, respectively.

$$2\ \mathrm{DMSO} + 2\ \mathrm{HO}\cdot \rightarrow \mathrm{HCHO} \qquad \text{(VI. 1)}$$

Keeping the lowest current density, 600 A m^{-2}, two additional experiments were conducted by preparing aqueous solution of 1.66 mM HCHO, which is an intermediate value of the HCHO observed during the application of Fenton and electrochemical oxidation, and 1.66 mM HCHO + 267 mM DMSO. Then, the results

were compared with the experiment containing only 267 mM DMSO. The results in terms of concentration of HCHO and concentration of generated HCHO are shown in Figure VI.3.

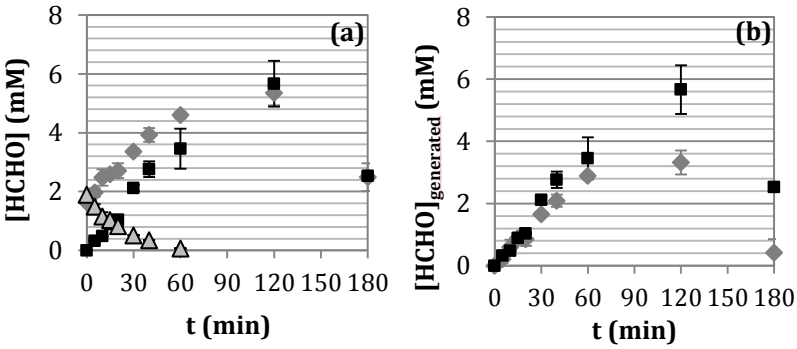

Figure VI.3. (a) Cumulated concentration of HCHO and (b) HCHO generated during the electrochemical oxidation of ■ 267 mM DMSO; ♦ 267 mM DMSO + 1.66 mM HCHO; and Δ 1.66 mM HCHO. j: 600 A m^{-2} $[Na_2SO_4]_0$: 9.15 mM.

Figure VI.3a displays the diminishment of HCHO when it is the only organic compound in solution, which resulted in its complete removal after 60 min of electrochemical oxidation. On the other hand, when both HCHO and DMSO were added to the aqueous medium, an increase in the concentration of HCHO was observed (Figure VI.3a) reaching the same maximum value obtained when the system was composed only by DMSO. However, subtracting the initial composition in HCHO it can be observed that the amount of HCHO generated is lower when the initial solution also contains HCHO with regard to the solution containing only DMSO (Figure VI.3b), especially at t= 120 min. According to Figure VI.3 there is a turning point in which the rate of HCHO oxidation equals the rate of generation. Owing to the high reactivity and the unselectivity of ·OH, competition oxidation reactions are taking place for DMSO and HCHO, characterized by second order kinetic constants of the same order of magnitude ($6.6 \cdot 10^9$ and $1 \cdot 10^9$ L mol^{-1} s^{-1}, respectively).[138] It is essential to take into account that electrochemical oxidation, especially the electrochemical cells with BDD anode, is a powerful technology in the oxidation and mineralization of the organic contents in synthetic and real waste waters that makes difficult the quantitative measurements, although it could serve as qualitative indicator to identify the optimal experimental conditions.[137,139-141]

Annex VII- List of scientific contributions

<u>List of papers published in indexed journals</u>

1. Insight on the fundamentals of advanced oxidation processes. Role and review of the determination methods of reactive oxygen species. P. Fernández-Castro, M. Vallejo, M.F. San Román, I. Ortiz. J. Chem. Technol. and Biotechnol. 90 (2015) 796–820. (JCR Impact Factor (2014): 2.738, Q1).

2. Assessment of PCDD/Fs formation in the Fenton oxidation of 2-chlorophenol: Influence of the iron dose applied. M. Vallejo, P. Fernández-Castro, M.F. San Román, I. Ortiz. Chemosphere 137 (2015) 135–141. (JCR Impact Factor (2014): 3.698, Q1).

3. Theoretical and experimental formation of low chlorinated dibenzo-p-dioxins and dibenzofurans in the Fenton oxidation of chlorophenol solutions. P. Fernández-Castro, M.F. San Román, I. Ortiz. Chemosphere 161 (2016) 136-144. (JCR Impact Factor (2014): 3.698, Q1).

4. Chlorophenol Signatures in Environmental Systems from Electrophilic Substitution. P. Fernández-Castro, M. Altarawneh, M.F. San Román, I. Ortiz, B.Z. Dlugogorski. Environ. Sci. Technol. *In preparation*.

Related papers published prior to this thesis

5. Remediation of wastewaters containing tetrahydrofuran. Study of the electrochemical mineralization on BDD electrodes. A. Urtiaga, P. Fernandez-Castro, P. Gómez, I. Ortiz. Chem. Eng. J. 239 (2014) 341–350. (JCR Impact Factor (2014): 4.321, Q1).

Contributions to scientific meetings

1. Influence of electrolyte type on the formation of PCDD/Fs during the electrochemical oxidation of 2-chlorophenol. M. Vallejo, M.F. San Román, P. Fernández Castro, I. Ortiz. 34th International Symposium on Halogenated Persistent Organic Pollutants. Madrid (Spain). September 2014. *Oral presentation*.

2. Assessment of PCDD/Fs formation in the Fenton oxidation of 2-chlorophenol: role of the operating conditions. P. Fernández Castro, M.F. San Román, I. Ortiz. 10th European Congress of Chemical Engineering. Nice (France). September 2015. *Oral presentation*.

3. Assessment of PCDD/Fs formation in the advanced oxidation treatment of model solutions of 2-chlorophenol. P. Fernández Castro, M. Vallejo M.F. San Román, I. Ortiz. 13th HCH & Pesticides Forum. Zaragoza (Spain). November 2015. *Oral presentation*.

4. Assessment of PCDD/Fs formation in the advanced oxidation treatment of landfill leachate. P. Fernández Castro, M. Vallejo M.F. San Román, I. Ortiz. 13th HCH & Pesticides Forum. Zaragoza (Spain). November 2015. *Poster*.

5. Formation of low and high chlorinated dibenzo-p-dioxins and dibenzofurans during the fenton oxidation of 2-chlorophenol. P. Fernández-Castro, C. Solá, M.F. San Román, I. Ortiz. V Reunión Nacional de Dioxinas, Furanos y compuestos orgánicos persistentes relacionados. Barcelona (Spain). June 2017. *Submitted*.

6. Formation of low and high chlorinated dibenzo-p-dioxins and dibenzofurans in the Fenton oxidation of 2-chlorophenol: an experimental and theoretical study. P. Fernandez Castro, C. Solá, M.F. San Román, I. Ortiz. 10th World Congress of Chemical Engineers. Barcelona (Spain). October 2017. *Submitted*.

Related meetings prior to this thesis

7. Eliminación de tetrahidrofurano en aguas residuales mediante oxidación electroquímica. P. Fernández, I. Ortiz, A. Urtiaga. XXXIV Reunión de la Real Sociedad Española de Química. Santander (Spain). September 2013. *Flash presentation*.

Other contributions

1. Insights into the formation of PCDD/Fs during the treatment of organo-chlorinated compounds by means of Fenton oxidation. P. Fernández-Castro, M.F. San Román, I. Ortiz. Atlas of Science. https://atlasofscience.org/insights-into-the-formation-of-pcddfs-during-the-treatment-of-organo-chlorinated-compounds-by-means-of-fenton-oxidation/

References

1. Kwon BG, Kwon J. Measurement of the hydroxyl radical formation from H_2O_2, NO_3^-, and Fe(III) using a continuous flow injection analysis. J. Ind. Eng. Chem. 16: 193-199 (2010).

2. Yang X, Xu X, Xu J, Han Y. Iron oxychloride (FeOCl): An efficient Fenton-like catalyst for producing hydroxyl radicals in degradation of organic contaminants. J. Am. Chem. Soc. 135: 16058-16061 (2013).

3. Zhou X, Mopper K. Determination of photochemically produced hydroxyl radicals in seawater and freshwater. Mar. Chem. 30: 71-88 (1990).

4. Oturan MA, Pinson J. Hydroxylation by electrochemically generated OH· radicals. mono- and polyhydroxylation of benzoic acid: Products and isomers' distribution. J. Phys. Chem. 99: 13948-13954 (1995).

5. Lindsey ME, Tarr MA. Quantitation of hydroxyl radical during Fenton oxidation following a single addition of iron and peroxide. Chemosphere 41: 409-417 (2000).

6. Ciotti C, Baciocchi R, Tuhkanen T. Influence of the operating conditions on highly oxidative radicals generation in Fenton's systems. J. Hazard. Mater. 161: 402-408 (2009).

7. Gazi S, Ananthakrishnan R. Semi-quantitative determination of hydroxyl radicals by benzoic acid hydroxylation: An analytical methodology for photo-Fenton systems. Curr. Anal. Chem. 8: 143-149 (2012).

8. Zhao J, Yang J, Ma J. Mn(II)-enhanced oxidation of benzoic acid by Fe(III)/H_2O_2 system. Chem. Eng. J. 239: 171-177 (2014).

9. Zhang C, Wang L, Wu F, Deng N. Quantitation of hydroxyl radicals from photolysis of Fe(III)-citrate complexes in aerobic water. Environ. Sci. Pollut. R. 13: 156-160 (2006).

10. Wang L, Zhang C, Wu F, Deng N, Glebov EM, Bazhin NM. Determination of hydroxyl radicals from photolysis of Fe(III)-pyruvate complexes in homogeneous aqueous solution. React. Kinet. Catal. L 89: 183-192 (2006).

11. Nakatani N, Hashimoto N, Shindo H, Yamamoto M, Kikkawa M, Sakugawa H. Determination of photoformation rates and scavenging rate constants of hydroxyl radicals in natural waters using an automatic light irradiation and injection system. Anal. Chim. Acta 581: 260-267 (2007).

12. Wu F, Li J, Peng Z, Deng N. Photochemical formation of hydroxyl radicals catalyzed by montmorillonite. Chemosphere 72: 407-413 (2008).

13. Oliveira RTS, Salazar-Banda GR, Santos MC, Calegaro ML, Miwa DW, Machado SAS, Avaca LA. Electrochemical oxidation of benzene on boron-doped diamond electrodes. Chemosphere 66: 2152-2158 (2007).

14. Schwarz PF, Turro NJ, Bossmann SH, Braun AM, Abdel Wahab A-A, Dürr H. A new method to determine the generation of hydroxyl radicals in illuminated TiO_2 suspensions. J. Phys. Chem. B 101: 7127-7134 (1997).

15. Baldacchino G, Maeyama T, Yamashita S, Taguchi M, Kimura A, Katsumura Y, Murakami T. Determination of the time-dependent OH-yield by using a fluorescent probe. application to heavy ion irradiation. Chem. Phys. Lett. 468: 275-279 (2009).

16. Manevich Y, Held KD, Biaglow JE. Coumarin-3-carboxylic acid as a detector for hydroxyl radicals generated chemically and by gamma radiation. Radiat. Res. 148: 580-591 (1997).

17. Czili H, Horváth A. Applicability of coumarin for detecting and measuring hydroxyl radicals generated by photoexcitation of TiO_2 nanoparticles. Appl. Catal. B-Environ. 81: 295-302 (2008).

18. Tang Q, Jiang W, Cheng Y, Lin S, Lim TM, Xiong J. Generation of reactive species by gas-phase dielectric barrier discharges. Ind. Eng. Chem. Res. 50: 9839-9846 (2011).

19. Nakabayashi Y, Nosaka Y. OH radical formation at distinct faces of rutile TiO_2 crystal in the procedure of photoelectrochemical water oxidation. J. Phys. Chem. C 117: 23832-23839 (2013).

20. Ikhlaq A, Brown DR, Kasprzyk-Hordern B. Mechanisms of catalytic ozonation on alumina and zeolites in water: Formation of hydroxyl radicals. Appl. Catal. B-Environ. 123-124: 94-106 (2012).

21. Zhang J, Nosaka Y. Quantitative detection of OH radicals for investigating the reaction mechanism of various visible-light TiO_2 photocatalysts in aqueous suspension. J. Phys. Chem. C 117: 1383-1391 (2013).

22. Cernigoj U, Štangar UL, Trebše P, Sarakha M. Determination of catalytic properties of TiO_2 coatings using aqueous solution of coumarin: Standardization efforts. J. Photochem. Photobiol. A 201: 142-150 (2009).

23. Oguma J, Kakuma Y, Murayama S, Nosaka Y. Effects of silica coating on photocatalytic reactions of anatase titanium dioxide studied by quantitative detection of reactive oxygen species. Appl. Catal. B-Environ. 129: 282-286 (2013).

24. Bejan D, Guinea E, Bunce NJ. On the nature of the hydroxyl radicals produced at boron-doped diamond and ebonex® anodes. Electrochim. Acta 69: 275-281 (2012).

25. Maezono T, Tokumura M, Sekine M, Kawase Y. Hydroxyl radical concentration profile in photo-Fenton oxidation process: Generation and consumption of hydroxyl radicals during the discoloration of azo-dye orange II. Chemosphere 82: 1422-1430 (2011).

26. Guan H, Zhu L, Zhou H, Tang H. Rapid probing of photocatalytic activity on titania-based self-cleaning materials using 7-hydroxycoumarin fluorescent probe. Anal. Chim. Acta 608: 73-78 (2008).

27. Louit G, Foley S, Cabillic J, Coffigny H, Taran F, Valleix A, Renault JP, Pin S. The reaction of coumarin with the OH radical revisited: Hydroxylation product analysis determined by fluorescence and chromatography. Radiat. Phys. Chem. 72: 119-124 (2005).

28. Kim JK, Metcalfe IS. Investigation of the generation of hydroxyl radicals and their oxidative role in the presence of heterogeneous copper catalysts. Chemosphere 69: 689-696 (2007).

29. Du Y, Fu QS, Li Y, Su Y. Photodecomposition of 4-chlorophenol by reactive oxygen species in UV/air system. J. Hazard. Mater. 186: 491-496 (2011).

30. Yang J, Dai J, Chen C, Zhao J. Effects of hydroxyl radicals and oxygen species on the 4-chlorophenol degradation by photoelectrocatalytic reactions with TiO_2-film electrodes. J. Photochem. Photobiol. A 208: 66-77 (2010).

31. Han S, Nam S, Kang J. OH radical monitoring technologies for AOP advanced oxidation process. Water Sci. Technol. 46: 7-12 (2002).

32. Nam S, Han S, Kang J, Choi H. Kinetics and mechanisms of the sonolytic destruction of non-volatile organic compounds: Investigation of the sonochemical reaction zone using several OH monitoring techniques. Ultrason. Sonochem. 10: 139-147 (2003).

33. Grela MA, Coronel MEJ, Colussi AJ. Quantitative spin-trapping studies of weakly illuminated titanium dioxide sols. implications for the mechanism of photocatalysis. J. Phys. Chem. 100: 16940-16946 (1996).

34. Yanagida H, Masubuchi Y, Minagawa K, Ogata T, Takimoto J, Koyama K. A reaction kinetics model of water sonolysis in the presence of a spin-trap. Ultrason. Sonochem. 5 :133-139 (1999).

35. Han SK, Hwang T, Yoon Y, Kang J. Evidence of singlet oxygen and hydroxyl radical formation in aqueous goethite suspension using spin-trapping electron paramagnetic resonance (EPR). Chemosphere 84: 1095-1101 (2011).

36. Cong Y, Wu Z. Electrocatalytic generation of radical intermediates over lead dioxide electrode doped with fluoride. J. Phys. Chem. C 111: 3442-3446 (2007).

37. Marselli B, Garcia-Gomez J, Michaud P-, Rodrigo MA, Comninellis C. Electrogeneration of hydroxyl radicals on boron-doped diamond electrodes. J. Electrochem. Soc. 150: D79-83 (2003).

38. Li L, Abe Y, Kanagawa K, Usui N, Imai K, Mashino T, Mochizuki M, Miyata N. Distinguishing the 5,5-dimethyl-1-pyrroline N-oxide (DMPO)-OH radical quenching effect from the hydroxyl radical scavenging effect in the ESR spin-trapping method. Anal. Chim. Acta 512: 121-124 (2004).

39. Granados-Oliveros G, Gómez-Vidales V, Nieto-Camacho A, Morales-Serna JA, Cárdenas J, Salmón M. Photoproduction of H_2O_2 and hydroxyl radicals catalysed by natural and super acid-modified montmorillonite and its oxidative role in the peroxidation of lipids. RSC Advances 3: 937-944 (2013).

40. Kochany J, Bolton JR. Mechanism of photodegradation of aqueous organic pollutants. 2. measurement of the primary rate constants for reaction of OH radicals with benzene and some halobenzenes using an EPR spin-trapping method following the photolysis of H_2O_2. Environ. Sci. Technol. 26: 262-265 (1992).

41. Yang F, Zhang R, He J, Abliz Z. Development of a liquid chromatography/electrospray ionization tandem mass spectrometric method for the determination of hydroxyl radical. Rapid Commun. Mass Spectrom. 21: 107-111 (2007).

42. Yuan S, Chen M, Mao X, Alshawabkeh AN. A three-electrode column for Pd-catalytic oxidation of TCE in groundwater with automatic pH-regulation and resistance to reduced sulfur compound foiling. Water Res. 47: 269-278 (2013).

43. de Luna MDG, Colades JI, Su C, Lu M. Comparison of dimethyl sulfoxide degradation by different Fenton processes. Chem. Eng. J. 232: 418-424 (2013).

44. Sahni M, Locke BR. Quantification of hydroxyl radicals produced in aqueous phase pulsed electrical discharge reactors. Ind. Eng. Chem. Res. 45: 5819-5825 (2006).

45. Tai C, Peng J, Liu J, Jiang G, Zou H. Determination of hydroxyl radicals in advanced oxidation processes with dimethyl sulfoxide trapping and liquid chromatography. Anal. Chim. Acta 527: 73-80 (2004).

46. Lee Y, Lee C, Yoon J. Kinetics and mechanisms of DMSO (dimethylsulfoxide) degradation by UV/H_2O_2 process. Water Res. 38: 2579-2588 (2004).

47. Tai C, Gu X, Zou H, Guo Q. A new simple and sensitive fluorometric method for the determination of hydroxyl radical and its application. Talanta 58: 661-667 (2002).

48. Yang X-, Guo X-. Study of nitroxide-linked naphthalene as a fluorescence probe for hydroxyl radicals. Anal. Chim. Acta 434: 169-177 (2001).

49. Vaughan PP, Blough NV. Photochemical formation of hydroxyl radical by constituents of natural waters. Environ. Sci. Technol. 32: 2947-2953 (1998).

50. Wang J, Guo Y, Liu B, Jin X, Liu L, Xu R, Kong Y, Wang B. Detection and analysis of reactive oxygen species (ROS) generated by nano-sized TiO_2 powder under ultrasonic irradiation and application in sonocatalytic degradation of organic dyes. Ultrason. Sonochem. 18: 177-183 (2011).

51. Guo Y, Cheng C, Wang J, Wang Z, Jin X, Li K, Kang P, Gao J. Detection of reactive oxygen species (ROS) generated by TiO_2(R), TiO_2(R/A) and TiO_2(A) under ultrasonic and solar light irradiation and application in degradation of organic dyes. J. Hazard. Mater. 192: 786-793 (2011).

52. Khramtsov VV, Reznikov VA, Berliner LJ, Litkin AK, Grigor'ev IA, Clanton TL. NMR spin trapping: Detection of free radical reactions with a new fluorinated DMPO analog. Free Radical Biol. Med. 30: 1099-1107 (2001).

53. Tung C, Chang J, Hsieh Y, Hsu J, Ellis AV, Liu W, Yan R. Comparison of hydroxyl radical yields between photo- and electro-catalyzed water treatments. J. Taiwan Inst. Chem. E 45: 1649-1654 (2014).

54. Hu Y, Lu Y, Zhou G, Xia X. A simple electrochemical method for the determination of hydroxyl free radicals without separation process. Talanta 74: 760-765 (2008).

55. Rivas FJ, Beltran FJ, Frades J, Buxeda P. Oxidation of p-hydroxybenzoic acid by Fenton's reagent. Water Res. 35: 387-396 (2001).

56. Wang Y, Calas-Blanchard C, Cortina-Puig M, Baohong L, Marty J. An electrochemical method for sensitive determination of antioxidant capacity. Electroanal. 21: 1395-1400 (2009).

57. Tsai C, Stern A, Chiou J, Chern C, Liu T. Rapid and specific detection of hydroxyl radical using an ultraweak chemiluminescence analyzer and a low-level chemiluminescence emitter: Application to hydroxyl radical-scavenging ability of aqueous extracts of food constituents. J. Agric. Food Chem. 49: 2137-2141 (2001).

58. Lester Y, Sharpless CM, Mamane H, Linden KG. Production of photo-oxidants by dissolved organic matter during UV water treatment. Environ. Sci. Technol. 47: 11726-11733 (2013).

59. Jing JG, Ke HX, Ji XH, Huang H, Tang B. Determination of trace hydroxyl radicals by flow injection spectrofluorometry and its analytical application. J. Agric. Food Chem. 54: 7968-7972 (2006).

60. Rosen GM, Tsai P, Barth ED, Dorey G, Casara P, Spedding M, Halpern HJ. A one-step synthesis of 2-(2-pyridyl)-3H-indol-3-one N-oxide: Is it an efficient spin trap for hydroxyl radical? J. Org. Chem. 65: 4460-4463 (2000).

61. Mencigar DP, Strlic M, Štangar UL, Korošec RC. Hydroxyl radical scavenging-based method for evaluation of TiO_2 photocatalytic activity. Acta Chim. Slov. 60: 908-912 (2013).

62. Fang YF, Deng AP, Huang YP. Determination of hydroxyl radical in Fenton system. Chin. Chem. Let. 20: 1235-1240 (2009).

63. He Y, Grieser F, Ashokkumar M. Kinetics and mechanism for the sonophotocatalytic degradation of p-chlorobenzoic acid. J. Phys. Chem. A 115: 6582-6588 (2011).

64. Chen C, Jafvert CT. Photoreactivity of carboxylated single-walled carbon nanotubes in sunlight: Reactive oxygen species production in water. Environ. Sci. Technol. 44: 6674-6679 (2010).

65. Lan B, Huang R, Li L, Yan H, Liao G, Wang X, Zhang Q. Catalytic ozonation of p-chlorobenzoic acid in aqueous solution using Fe-MCM-41 as catalyst. Chem. Eng. J. 219: 346-354 (2013).

66. Kilinc E. Determination of the hydroxyl radical by its adduct formation with phenol and liquid chromatography/electrochemical detection. Talanta 65: 876-881 (2005).

67. Chatzisymeon E, Fierro S, Karafyllis I, Mantzavinos D, Kalogerakis N, Katsaounis A. Anodic oxidation of phenol on Ti/IrO_2 electrode: Experimental studies. Catal. Today 151: 185-189 (2010).

68. Li M, Carlson S, Kinzer JA, Perpall HJ. HPLC and LC-MS studies of hydroxylation of phenylalanine as an assay for hydroxyl radicals generated from Udenfriend's reagent. Biochem. Biophys. Res. Commun. 312: 316-322 (2003).

69. Backa S, Jansbo K, Reitberger T. Detection of hydroxyl radicals by a chemiluminescence method- A critical review. Holzforschung 51: 557-564 (1997).

70. Miller CJ, Rose AL, Waite TD. Hydroxyl radical production by H_2O_2-mediated oxidation of Fe(II) complexed by suwannee river fulvic acid under circumneutral freshwater conditions. Environ. Sci. Technol. 47: 829-835 (2013).

71. Miller CJ, Rose AL, Waite TD. Phthalhydrazide chemiluminescence method for determination of hydroxyl radical production: Modifications and adaptations for use in natural systems. Anal. Chem. 83: 261-268 (2011).

72. Mahé E, Bornoz P, Briot E, Chevalet J, Comninellis C, Devilliers D. A selective chemiluminescence detection method for reactive oxygen species involved in oxygen reduction reaction on electrocatalytic materials. Electrochim. Acta 102: 259-273 (2013).

73. Cermenati L, Pichat P, Guillard C, Albini A. Probing the TiO_2 photocatalytic mechanisms in water purification by use of quinoline, photo-Fenton generated OH. radicals and superoxide dismutase. J. Phys. Chem. B 101: 2650-2658 (1997).

74. Jing J, Li W, Boyd A, Zhang Y, Colvin VL, Yu WW. Photocatalytic degradation of quinoline in aqueous TiO_2 suspension. J. Hazard. Mater. 237-238: 247-255 (2012).

75. Yu F, Xu D, Lei R, Li N, Li K. Free-radical scavenging capacity using the fenton reaction with rhodamine B as the spectrophotometric indicator. J. Agric. Food Chem. 56: 730-735 (2008).

76. Zhang B, Li-Xia Z, Jin-Ming L. Study on superoxide and hydroxyl radicals generated in indirect electrochemical oxidation by chemiluminescence and UV-visible spectra. J. Environ. Sci. 20: 1006-1011 (2008).

77. Muff J, Bennedsen LR, Søgaard EG. Study of electrochemical bleaching of p-nitrosodimethylaniline and its role as hydroxyl radical probe compound. J. Appl. Electrochem. 41: 599-607 (2011).

78. Kim C, Park H-, Cha S, Yoon J. Facile detection of photogenerated reactive oxygen species in TiO_2 nanoparticles suspension using colorimetric probe-assisted spectrometric method. Chemosphere 93: 2011-2015 (2013).

79. Simonsen ME, Muff J, Bennedsen LR, Kowalski KP, Søgaard EG. Photocatalytic bleaching of p-nitrosodimethylaniline and a comparison to the performance of other AOP technologies. J. Photochem. Photobiol. A 216: 244-249 (2010).

80. Nobushi Y, Uchikura K. Selective detection of hydroxyl radical scavenging capacity based on electrogenerated chemiluminescence detection using tris(2,2'-bipyridine) ruthenium(III) by flow injection analysis. Chem. Pharm. Bull. 58: 117-120 (2010).

81. Gualandi I, Tonelli D. A new electrochemical sensor for OH radicals detection. Talanta 115: 779-786 (2013).

82. Guinea E, Arias C, Cabot PL, Garrido JA, Rodríguez RM, Centellas F, Brillas E. Mineralization of salicylic acid in acidic aqueous medium by electrochemical advanced oxidation processes using platinum and boron-doped diamond as anode and cathodically generated hydrogen peroxide. Water Res. 42: 499-511 (2008).

83. Diez L, Livertoux M, Stark A, Wellman-Rousseau M, Leroy P. High-performance liquid chromatographic assay of hydroxyl free radical using salicylic acid hydroxylation during in vitro experiments involving thiols. J. Chromatogr. B 763: 185-193 (2001).

84. Jen J, Leu M, Yang TC. Determination of hydroxyl radicals in an advanced oxidation process with salicylic acid trapping and liquid chromatography. J. Chromatogr. A 796: 283-288 (1998).

85. Li S, Hu S, Zhang H. Formation of hydroxyl radicals and hydrogen peroxide by a novel nanosecond pulsed plasma power in water. IEEE Trans. Plasma Sci. 40: 63-67 (2012).

86. Ai S, Wang Q, Li H, Jin L. Study on production of free hydroxyl radical and its reaction with salicylic acid at lead dioxide electrode. J. Electroanal. Chem. 578: 223-229 (2005).

87. Milne L, Stewart I, Bremner DH. Comparison of hydroxyl radical formation in aqueous solutions at different ultrasound frequencies and powers using the salicylic acid dosimeter. Ultrason. Sonochem. 20: 984-989 (2013).

88. Martínez-Tarifa A, Arrojo S, Ávila-Marín AL, Pérez-Jiménez JA, Sáez V, Ruiz-Lorenzo ML. Salicylic acid dosimetry applied for the statistical determination of significant parameters in a sonochemical reactor. Chem. Eng. J. 157: 420-426 (2010).

89. Shimizu N, Ogino C, Dadjour MF, Ninomiya K, Fujihira A, Sakiyama K. Sonocatalytic facilitation of hydroxyl radical generation in the presence of TiO_2. Ultrason. Sonochem. 15: 988-994 (2008).

90. Amin LP, Gogate PR, Burgess AE, Bremner DH. Optimization of a hydrodynamic cavitation reactor using salicylic acid dosimetry. Chem. Eng. J. 156: 165-169 (2010).

91. Arrojo S, Nerín C, Benito Y. Application of salicylic acid dosimetry to evaluate hydrodynamic cavitation as an advanced oxidation process. Ultrason. Sonochem. 14: 343-349 (2007).

92. Rabaaoui N, Allagui MS. Anodic oxidation of salicylic acid on BDD electrode: Variable effects and mechanisms of degradation. J. Hazard. Mater. 243: 187-192 (2012).

93. Peralta E, Roa G, Hernandez-Servin JA, Romero R, Balderas P, Natividad R. Hydroxyl radicals quantification by UV spectrophotometry. Electrochim. Acta 129: 137-141 (2014).

94. Chen XM, da Silva DR, Martínez-Huitle CA. Application of advanced oxidation processes for removing salicylic acid from synthetic wastewaters. Chin. Chem. Let. 21: 101-104 (2010).

95. Goi A, Veressinina Y, Trapido M. Degradation of salicylic acid by Fenton and modified Fenton treatment. Chem. Eng. J. 143: 1-9 (2008).

96. Adán C, Coronado JM, Bellod R, Soria J, Yamaoka H. Photochemical and photocatalytic degradation of salicylic acid with hydrogen peroxide over TiO_2/SiO_2 fibres. Appl. Catal. A-Gen. 303: 199-206 (2006).

97. Westerhoff P, Mezyk SP, Cooper WJ, Minakata D. Electron pulse radiolysis determination of hydroxyl radical rate constants with suwannee river fulvic acid and other dissolved organic matter isolates. Environ. Sci. Technol. 41: 4640-4646 (2007).

98. Bubacz K, Kusiak-Nejman E, Tryba B, Morawski AW. Investigation of OH radicals formation on the surface of TiO_2/N photocatalyst at the presence of terephthalic acid solution. estimation of optimal conditions. J. Photochem. Photobiol. A 261: 7-11 (2013).

99. Page SE, Arnold WA, McNeill K. Terephthalate as a probe for photochemically generated hydroxyl radical. J. Environ. Monitor. 12: 1658-1665 (2010).

100. Charbouillot T, Brigante M, Mailhot G, Maddigapu PR, Minero C, Vione D. Performance and selectivity of the terephthalic acid probe for ·OH as a function of temperature, pH and composition of atmospherically relevant aqueous media. J. Photochem. Photobiol. A 222: 70-76 (2011).

101. Ishibashi K-, Fujishima A, Watanabe T, Hashimoto K. Quantum yields of active oxidative species formed on TiO_2 photocatalyst. J. Photochem. Photobiol. A 134: 139-142 (2000).

102. Villeneuve L, Alberti L, Steghens J, Lancelin J, Mestas J. Assay of hydroxyl radicals generated by focused ultrasound. Ultrason. Sonochem. 16: 339-344 (2009).

103. Linxiang L, Abe Y, Nagasawa Y, Kudo R, Usui N, Imai K, Mashino T, Mochizuki M, Miyata N. An HPLC assay of hydroxyl radicals by the hydroxylation reaction of terephthalic acid. Biomed. Chromatogr. 18: 470-474 (2004).

104. Hirakawa T, Yawata K, Nosaka Y. Photocatalytic reactivity for O_2·- and OH· radical formation in anatase and rutile TiO_2 suspension as the effect of H_2O_2 addition. Appl. Catal. A-Gen. 325: 105-111 (2007).

105. Hirakawa T, Nosaka Y. Properties of O_2·- and OH· formed in TiO_2 aqueous suspensions by photocatalytic reaction and the influence of H2O2 and some ions. Langmuir 18: 3247-3254 (2002).

106. Ishibashi K, Fujishima A, Watanabe T, Hashimoto K. Detection of active oxidative species in TiO_2 photocatalysis using the fluorescence technique. Electrochem. Commun. 2: 207-210 (2000).

107. Tang B, Zhang L, Geng Y. Determination of the antioxidant capacity of different food natural products with a new developed flow injection spectrofluorimetry detecting hydroxyl radicals. Talanta 65: 769-775 (2005).

108. Shafaei A, Nikazar M, Arami M. Photocatalytic degradation of terephthalic acid using titania and zinc oxide photocatalysts: Comparative study. Desalination 252 :8-16 (2010).

109. Kwon BG, Kim J, Kwon J. An advanced kinetic method for HO_2·/O_2-· determination by using terephthalate in the aqueous solution. Environ. Eng. Res. 17: 205-210 (2012).

110. Kwon BG. Characterization of the hydroperoxyl/superoxide anion radical (HO_2·/O_2-·) formed from the photolysis of immobilized TiO_2 in a continuous flow. J. Photochem. Photobiol. A 199: 112-118 (2008).

111. Kwon BG, Lee JH. A kinetic method for HO_2·/O_2-· determination in advanced oxidation processes. Anal. Chem. 76: 6359-6364 (2004).

112. Heller MI, Croot PL. Application of a superoxide (O_2-) thermal source (SOTS-1) for the determination and calibration of O_2- fluxes in seawater. Anal. Chim. Acta 667: 1-13 (2010).

113. Rose AL, Waite TD. Chemiluminescence of luminol in the presence of iron(II) and oxygen: Oxidation mechanism and implications for its analytical use. Anal. Chem. 73: 5909-5920 (2001).

114. Nosaka Y, Takahashi S, Sakamoto H, Nosaka AY. Reaction mechanism of Cu(II)-grafted visible-light responsive TiO_2 and WO_3 photocatalysts studied by means of ESR spectroscopy and chemiluminescence photometry. J. Phys. Chem. C 115: 21283-21290 (2011).

115. Hirakawa T, Nosaka Y. Selective production of superoxide ions and hydrogen peroxide over nitrogen- and sulfur-doped TiO_2 photocatalysts with visible light in aqueous suspension systems. J. Phys. Chem. C 112: 15818-15823 (2008).

116. Wu X-, Lingyue M, Akiyama K. Chemiluminescence study of active oxygen species produced by TiO_2 photocatalytic reaction. Luminescence 20: 36-40 (2005).

117. Hirakawa T, Kominami H, Ohtani B, Nosaka Y. Mechanism of photocatalytic production of active oxygens on highly crystalline TiO_2 particles by means of chemiluminescent probing and ESR spectroscopy. J. Phys. Chem. B 105: 6993-6999 (2001).

118. Nosaka Y, Yamashita Y, Fukuyama H. Application of chemiluminescent probe to monitoring superoxide radicals and hydrogen peroxide in TiO_2 photocatalysis. J. Phys. Chem. B 101: 5822-5827 (1997).

119. Ishibashi K-, Fujishima A, Watanabe T, Hashimoto K. Generation and deactivation processes of superoxide formed on TiO_2 film illuminated by very weak UV light in air or water. J. Phys. Chem. B 104: 4934-4938 (2000).

120. Xu X, Duan X, Yi Z, Zhou Z, Fan X, Wang Y. Photocatalytic production of superoxide ion in the aqueous suspensions of two kinds of ZnO under simulated solar light. Catal. Commun. 12: 169-172 (2010).

121. Goto H, Hanada Y, Ohno T, Matsumura M. Quantitative analysis of superoxide ion and hydrogen peroxide produced from molecular oxygen on photoirradiated TiO_2 particles. J. Catal. 225: 223-229 (2004).

122. You MX, Wang YX, Wang H, Yang RH. Fluorescent detection of singlet oxygen: Amplifying signal transduction and improving sensitivity based on intramolecular FRET of anthryl appended porphyrins. Chin. Sci. Bull. 56: 3253-3259 (2011).

123. Daimon T, Nosaka Y. Formation and behavior of singlet molecular oxygen in TiO_2 photocatalysis studied by detection of near-infrared phosphorescence. J. Phys. Chem. C 111: 4420-4424 (2007).

124. Daimon T, Hirakawa T, Nosaka Y. Monitoring the formation and decay of singlet molecular oxygen in TiO_2 photocatalytic systems and the reaction with organic molecules. Electrochem. 76: 136-139 (2008).

125. Daimon T, Hirakawa T, Kitazawa M, Suetake J, Nosaka Y. Formation of singlet molecular oxygen associated with the formation of superoxide radicals in aqueous suspensions of TiO_2 photocatalysts. Appl. Catal. A-Gen. 340: 169-175 (2008).

126. Tanaka K, Miura T, Umezawa N, Urano Y, Kikuchi K, Higuchi T, Nagano T. Rational design of fluorescein-based fluorescence probes. mechanism-based design of a maximum fluorescence probe for singlet oxygen. J. Am. Chem. Soc. 123: 2530-2536 (2001).

127. Umezawa N, Tanaka K, Urano Y, Kikuchi K, Higuchi T, Nagano T. Novel fluorescent probes for singlet oxygen. Ange. Chem. Int. Edit. 38: 2899-2901 (1999).

128. Haag WR, Holgne J. Singlet oxygen in surface waters. 3. photochemical formation and steady-state concentrations in various types of waters. Environ. Sci. Technol. 20: 341-348 (1986).

129. Song B, Wang G, Tan M, Yuan J. A europium(III) complex as an efficient singlet oxygen luminescence probe. J. Am. Chem. Soc. 128: 13442-13450 (2006).

130. Ruiz-González R, Zanocco R, Gidi Y, Zanocco AL, Nonell S, Lemp E. Naphthoxazole-based singlet oxygen fluorescent probes. Photochem. Photobiol. 89: 1427-1432 (2013).

131. Tan M, Song B, Wang G, Yuan J. A new terbium(III) chelate as an efficient singlet oxygen fluorescence probe. Free Radical Biol. Med. 40: 1644-1653 (2006).

132. Liu Y, Wang K. Visible-light-excited singlet-oxygen luminescence probe based on $Re(CO)_3Cl$(aeip). Eur. J. Inorg. Chem. 2008: 5214-5219 (2008).

133. Lin H, Shen Y, Chen D, Lin L, Wilson BC, Li B, Xie S. Feasibility study on quantitative measurements of singlet oxygen generation using singlet oxygen sensor green. J. Fluoresc. 23: 41-47 (2013).

134. MacManus-Spencer LA, Latch DE, Kroncke KM, McNeill K. Stable dioxetane precursors as selective trap-and-trigger chemiluminescent probes for singlet oxygen. Anal. Chem. 77: 1200-1205 (2005).

135. Li X, Zhang G, Ma H, Zhang D, Li J, Zhu D. 4,5-dimethylthio-4'-[2-(9-anthryloxy)ethylthio]tetrathiafulvalene, a highly selective and sensitive chemiluminescence probe for singlet oxygen. J. Am. Chem. Soc. 126: 11543-11548 (2004).

136. Zheng X, Sun S, Zhang D, Ma H, Zhu D. A new chemiluminescence probe for singlet oxygen based on tetrathiafulvalene-anthracene dyad capable of performing detection in water/alcohol solution. Anal. Chim. Acta 575: 62-67 (2006).

137. Urtiaga A, Fernandez-Castro P, Gómez P, Ortiz I. Remediation of wastewaters containing tetrahydrofuran. study of the electrochemical mineralization on BDD electrodes. Chem. Eng. J. 239: 341-350 (2014).

138. Buxton GV, Greenstock CL, Helman WP, Ross AB. Critical review of rate constants for reactions of hydrated electrons, hydrogen atoms and hydroxyl radicals (·OH/·O−) in aqueous solution. J. Phys. Chem. Ref. Data 17: 513-886 (1988).

139. Vallejo M, San Román MF, Irabien A, Ortiz I. Comparative study of the destruction of polychlorinated dibenzo-p-dioxins and dibenzofurans during Fenton and electrochemical oxidation of landfill leachates. Chemosphere 90: 132-138 (2013).

140. Vallejo M, San Román MF, Ortiz I. Quantitative assessment of the formation of polychlorinated derivatives, PCDD/Fs, in the electrochemical oxidation of 2-chlorophenol as function of the electrolyte type. Environ. Sci. Technol. 47: 12400-12408 (2013).

141. Boye B, Brillas E, Marselli B, Michaud P, Comninellis C, Farnia G, Sandonà G. Electrochemical incineration of chloromethylphenoxy herbicides in acid medium by anodic oxidation with boron-doped diamond electrode. Electrochim. Acta 51: 2872-2880 (2006).

About the author

Pablo Fernández Castro (Santander, 1988) is Chemical Engineer (2006-2012) and Master in Chemical Engineer (2012-2013) by the University of Cantabria (Santander, Spain). After his Bachelor Degree, he joined to the Chemical and Biomolecular Engineering Department as researcher under the supervision of Prof. Ana Urtiaga and Prof. Inmaculada Ortiz. Afterwards, he was granted with a Personnel Research Training Program of the Spanish Ministry of Economy and Competitiveness to develop his Ph.D. studies, which were supervised by Prof. Inmaculada Ortiz and Dr. Mª Fresnedo San Román.

In the framework of his Ph.D studies, he performed a short research stay at Murdoch University in the *Fire Safety & Combustion Kinetics Lab* under the supervision of Prof. Bogdan Dlugogorski and Dr. Mohammednoor Altarawneh.

Currently, he is the author of 4 scientific articles in indexed journals as well as 5 contributions in international conferences.

During the last few decades, different pollutants recalcitrant to conventional biological and chemical processes have emerged and pose a big social concern. At the same time, legislation has become stricter due to the adverse effect of part of these contaminants. Among this group, the presence in aquatic streams of priority pollutants such as dioxins and furans (PCDD/Fs) is of special concern because they affect the environment and living organisms.

Advanced oxidations processes (AOPs) have arisen as feasible technologies to treat wastewaters, which are characterized by the presence of chemically stable and of low biodegradability contaminants, through the generation of powerful oxidants. However, when some organochlorinated compounds, such as chlorophenols, are the target of AOPs, the oxidation products can lead to the uncontrolled generation of the more dangerous pollutants PCDD/Fs.

This thesis progress on the study of the reactivity of the advanced oxidation media by monitoring the generation of reactive oxygen species and on the evaluation of the potential formation of PCDD/Fs during the Fenton oxidation of aqueous solutions containing 2-chlorophenol

UC UNIVERSIDAD DE CANTABRIA

osprocan SASP Advanced Separation Processes